This is to certify that the
dissertation entitled

MODIFIED BIOBASED MATERIALS FROM POLYHYDROXYALKANOATES FOR PACKAGING AND ENGINEERING APPLICATIONS

presented by

Yashodhan S. Parulekar

has been accepted towards fulfillment
of the requirements for the

Doctoral degree in School of Packaging

Amar Kumar Mohanty
Major Professor's Signature

05-05-2007
Date

MODIFIED BIOBASED MATERIALS FROM POLYHYDROXYALKANOATES FOR PACKAGING AND ENGINEERING APPLICATIONS

VOLUME I

By

Yashodhan S. Parulekar

A DISSERTATION

Submitted to
Michigan State University
in partial fulfillment of the requirements
for the degree of

DOCTOR OF PHILOSOPHY

School of Packaging

2007

ABSTRACT

MODIFIED BIOBASED MATERIALS FROM POLYHYDROXYALKANOATES FOR PACKAGING AND ENGINEERING APPLICATIONS

By

Yashodhan S. Parulekar

This work relates to the development of new biobased and biodegradable blends, composites and nanocomposites from polyhydroxyalkanoates (PHAs). PHAs are the renewable-resource-based biodegradable thermoplastic biopolyesters synthesized by bacteria. This dissertation focuses on two members of the PHA family; polyhydroxybutyrate (PHB) and polyhydroxybutyrate-co-valerate (PHBV). Renewable-resource-based polymers are a strategic option to meet the growing need for sustainable materials for the next generation owing to the depletion of global oil reserves, increase in fossil-fuel based resin prices and environmental concerns.

The main goal of this dissertation is to focus on a renewable-resource-based biodegradable polymer and modify as well as develop it so as to make the resulting biobased materials comparable or even better than conventional polymers in properties. In the first part of this work, novel toughened PHB-based green materials were successfully developed through reactive extrusion of PHB and functionalized natural rubber in presence of a compatibilizer followed by injection molding. Maleated polybutadiene with high grafting and low molecular weight was determined to be an efficient compatibilizer for the PHB-rubber blend system thereby improving the toughness of PHB by 440%. The resultant toughened PHB exhibited impact strength (124 J/m) superior to specific toughened conventional polymers. Montmorillonite clay treated with neopentyl (diallyl)oxy tri(dioctyl) pyrophosphato titanate was used as a

reinforcement for toughened PHB in order to develop novel biodegradable nanocomposites. The titanate-based surface modified clay, PHB, toughening partner and specific compatibilizer were processed by extrusion followed by injection molding. The novel aspect of the titanate-based modification was that the nanocomposites still maintained nearly the same impact strength value as that of toughened PHB yet improved the modulus. The diffraction patterns suggest exfoliation of the organically modified clays and this was further supported by transmission electron microscopy and melt rheological analysis coupled with theoretical modeling. Toughened and compatibilized PHB showed significantly lower biodegradation rate than virgin PHB however titanate-modified clay-nanocomposites regained the biodegradation rate.

The second part of this dissertation involved the reactive blending of a plasticized biobased polymer with PHBV matrix in order to get a novel and flexible biodegradable material. A thermoplastic starch (TPS) system was developed by blending of corn starch, glycerol (byproduct of soy-based biodiesel industries) and poly-(butylene adipate-co-terephthalate) (PBAT). Following optimization by structure-property-processing correlation, this thermoplastic starch system was blended with PHBV to obtain a biodegradable flexible polymer blend and further reinforced with talc and processed into cast films. The incorporation of talc promoted disruptive mixing, homogeneity and subsequently reduced the droplet size of the components ultimately giving improvement in physical properties. The talc-filled films showed remarkable improvement in barrier properties and this was ascertained to be because of a combination of the tortuosity effect and the nucleating effect of the talc and the improved mixing. The ability of PHBV-TPS system as well as the talc-filled composites to resist ageing was also established.

To my parents, my family and friends, and to Aishwarya

ACKNOWLEDGEMENTS

*"Somehow I can't believe that there are any heights that can't be scaled by a man who knows the secrets of making dreams come true. This special secret, it seems to me, can be summarized in four C s. They are curiosity, confidence, courage, and constancy, and the greatest of all is confidence. When you believe in a thing, believe in it all the way, implicitly and unquestionable": A*uthor: Walt Disney (1901-1966).

The realization of a dream is truly rewarding in itself yet is nothing without the people that have made it possible. I am deeply indebted to Dr. Amar Mohanty, my advisor, for embarking with me on this thesis journey. I could not have wished for a better mentor. Your contributions, detailed comments and insight have been of great value to me. I am also thankful to Dr. Manjusri Misra, a constant support and guide in my doctoral work. I have to thank the excellent atmosphere both of you have created in our research group that developed me not only as a researcher but more importantly as a thinking individual and part of the scientific community.

I would like to express my most grateful thanks to my committee members Dr. Bruce Harte, Dr. Gary Burgess and Dr. Larry Drzal, whose suggestions and inputs helped shape this dissertation. I am also thankful to the United States Environmental Protection Agency's STAR grant number 8309040, Michigan State University's seed funding to Dr. Mohanty, CFPPR, the School of Packaging, and the graduate school's dissertation completion fellowship for funding for this research.

I am extremely grateful to the following people who contributed immensely to my work: Rahul Bhardwaj and Sanjeev Singh who helped me in many experiments and were always available to engage in discussions on research (amongst many more topics); Per

Askeland, Mike Rich, Brian Rook, Alicia Pastor and Bob Hurwitz for assistance in processing and characterization techniques; Ed Drown, Hiroaki Miyagawa and Qiangxian Wu for aiding and helping me in my research; Linda, Colleen, Jean and Kristin for their support and ever-present assistance; Abhishek, Dhiraj, Kumar, Dinesh, Vijoya and other members of Dr. Mohanty's Research group; and colleagues, co-workers and friends in CMSC, the School of Packaging and Michigan State University.

I would like to thank my parents for instilling in me the values of education and character and for supporting and encouraging me throughout my life. My very special thanks to the one person whom I owe everything I am today, my wife, Aishwarya. Her unwavering faith and confidence in my abilities and in me is what has shaped me to be the person I am today. Thank you for standing by me through thick and thin and thank you for everything. And lastly, a thank you to Duncan just for being himself.

Yashodhan S. Parulekar

East Lansing, MI

May 2007

TABLE OF CONTENTS

LIST OF TABLES

LIST OF FIGURES

KEY TO SYMBOLS OR ABBREVATIONS

Symbols	*Key*
±	Standard deviation
®	Registered
°C	Degrees Celcius
°F	Degrees Fahrenheit
°K	Degrees Kelvin
Å	Angstrom
a,K	Mark-Houwink-Sakudra parameters
CA	Cellulose acetate
CAB	Cellulose acetate butyrate
CAP	Cellulose acetate propionate
cc	cubic centimetre
DMA	Dynamic mechanical analysis
DSC	Differential scanning calorimetry
EML	Epoxidized methyl linseedate
EPA	Environmental Protection Agency
G	Gibbs free energy
GPa	Gigapascal
HDPE	High-density polyethylene
HIPS	High-impact Polystyrene
Hz	Hertz

J	Joules
LDPE	Low-density polyethylene
LLDPE	Linear low-density polyethylene
m	metre
MPa	Megapascal
NA	Not Available
Pa	Pascal
PBAT	Polybutylene adipate-co-terephthalate
PBS	Poly(butylene succinate)
PBSA	Poly(buylene succinate-co-buylene adipate)
PBT	Poly (butylene terephthalate)
PCL	Poly(ε-caprolactone)
PE	Polyethylene
PEA	Polyesteramide
PEO	Polyethylene Oxide
PET	Poly (ethylene terephthalate)
PHA	Polyhydroxyalkanoate
PHB	Polyhydroxybutyrate
PHBV	Polyhydroxybutyrate-co-valerate
PHV	Polyhydroxyvalerate
PLA	Polylactic Acid
PTT	Poly (trimethylene terephthalate)
PU	Polyurethanes

PVA	Poly(vinyl acetate)
PVOH	Poly(vinyl alcohol)
T	Temperature
T_g	Glass Transition Temperature
TGA	Thermogravimetric Analysis
T_m	Melting Temperature
TMA	Thermomechanical Analysis
TPO	Thermoplastic olefin
TPS	Thermoplastic starch
™	Trademark
UK	United Kingdom
US	United States
α	Alpha
β	Beta
Δ	Change
δ	difference
ε	Epsilon
Π	Pi
ρ	Density
Σ	Summation
φ	Volume fraction
χ	Crystallinity

1. INTRODUCTION

1.1 Dissertation Goal and Objectives

Plant/crop-based renewable resources are a strategic option to meet the growing need for sustainable materials for the next century. Polymers based on renewable resources are emerging as a strategic alternative to petroleum based polymers owing to the depletion of global oil reserves and subsequent increase in fossil-fuel based resin prices[1-3]. Also, the exponential growth of the use of polymeric materials in everyday life has led to the accumulation of huge amounts of non-degradable waste materials across our planet[4]. These growing threats of petroleum depletion and disposal problems have led to widespread research in biodegradable as well as biobased materials.

Biodegradable and biobased polymeric materials can be a solution to these problems yet are not used on a large scale primarily due to cost issues and property limitations. The main goal of this dissertation is to focus on a renewable-resource-based biodegradable polymer and modify and develop it so as to make the resulting material comparable or even better than conventional polymers in properties.

Polyhydroxyalkanoates (PHAs) are a class of such biodegradable and renewable-resource based polymers. PHAs were discovered at the Pasteur Institute in France with the first PHA identified as polyhydroxybutyrate (PHB) [5, 6]. These polymers are created intracellularly by bacteria. Bacteria, when subjected to imbalanced conditions of limited growth coupled with excess carbon supply, create PHAs inside the cell. PHAs are

produced from a variety of commercial plants like corn and even from non-conventional agricultural resources like switch-grass and this presents exciting opportunities for economic and agricultural development [6]. The renewable-resource based origin combined with the environmental advantage of PHA's due to their biodegradability has led to active research and development of these materials as future sustainable and 'green' packaging materials.

There is a growing need to develop new applications for these promising PHAs. Demanding applications will allow large scale production which will result in reducing the cost of PHAs significantly. Hence the main goal of this research is to develop PHA based novel materials for varied applications including packaging. These materials because of their special characteristics and broad applications have an extremely promising future.

This dissertation focuses on two members of the PHA family; polyhydroxybutyrate (PHB) and polyhydroxybutyrate-co-valerate (PHBV). In this study, various mechanisms were investigated to modify these selected PHAs and develop PHA based polymeric materials; primarily categorized as:

1. Elastomeric modification followed by nanoclay incorporation.
2. Blending with plasticized biobased polymer followed by reinforcement

The first objective of this study was to toughen PHB using an elastomeric component. The effects of processing conditions, various types and content of elastomers on the performance of toughened PHB were evaluated. Significant differences in the melt

viscosity of PHB and the rubber phase established the need for a compatibilizer to improve the toughness. Theoretical modeling of the blend behavior by Takayanagi models also ascertained the positive effect of a compatibilizer. A suitable compatibilizer was investigated for the PHB-rubber system accompanied by morphological, mechanical, thermal and chemical characterization. Following successful toughening, montmorillonite nanoclay platelets modified with organic surface modifiers were introduced into the toughened blend system with an objective of regaining stiffness and modulus that was lost by the elastomeric modification. Pristine clay is hydrophilic by nature and is difficult to disperse into the organic polymer matrix. Hence the surface of the clay needs to be modified to make it organophilic and compatible with the polymer. Commercially available organoclays and pristine clay treated with a titanate-based coupling agent were investigated. The aim was to achieve chemical modification of pristine montmorillonite with an alkyl-titanate complex. The hydroxyl functionality on the surface of the clay platelet is substituted by alkyl-titanate group from the titianate modifier making the surface organophilic. This clay was incorporated into the toughened bioplastic-elastomer blend by melt compounding and injection molded into testing specimens. The properties of the nanocomposites were correlated with theoretical model predictions for mechanical behavior.

The second part of this dissertation involved the reactive blending of a plasticized biobased polymer with polyhydroxybutyrate-co-valerate (PHBV) matrix in order to get a novel and flexible biodegradable material. A thermoplastic starch (TPS) system was developed by blending of corn starch, glycerol (plasticizer) and poly-(butylene adipate-co-terephthalate) (PBAT). Process engineering was done using screening experiments in

a microcompounder extruder followed by scaling up onto a pilot-scale extruder. The destructurized and plasticized starch was blended in a microcompounder with PHA and Poly (butylene adipate-co-terephthalate) (PBAT) followed by injection molding and characterization. The optimum sequence of addition as well as composition was determined by extensive process engineering and structure-property-processing correlation. The PHBV-TPS systems were reinforced with 2.5 and 5 wt. % of talc and further extruded into films using cast film processing. The ageing and thermal behavior of the composite films, as well as their mechanical properties were studied by means of tensile tests, dynamic mechanical analysis (DMA), differential scanning calorimetry (DSC) and gas barrier experiments. The incorporation of talc promoted disruptive mixing, homogeneity and ultimately reduced the droplet size of the components ultimately giving improvement in physical properties. The talc-filled films showed remarkable improvement in barrier properties and this was ascertained to be because of a combination of the tortuosity effect of the talc, the nucleating effect of the filler and the improved mixing. Theoretical approximation of the effect of the talc aspect ratio on the barrier properties of the composites was undertaken using Cussler's equation. Results indicated the barrier improvement was not only due to the talc geometry but more a combined influence of the nucleation, tortuosity and disruptive mixing. Specifically designed DMA, tensile and DSC experiments established the ability of PHBV-TPS system as well as the talc-filled composites to resist ageing. This resistance to ageing was attributed to be a combined effect of the hydrophobicity of the PHBV, the ability of talc to inhibit plasticizer leaching, and interference of the TPS in the secondary crystallinity of the PHBV phase. Biodegradation rates of the PHBV-TPS system as well as their

composites were in accordance with mandated standards[7]. The developed materials showed are 70% biobased yet show excellent potential as flexible packaging materials with multiple likely benefits such as creating value-added application of glycerol and starch and reducing the cost of PHAs.

1.2. Organization of Dissertation

The first part of this dissertation is an in-depth literature review of the current state of science in this area of research. This part starts of with a review of biopolymers followed by concentrating on the subject of this work, polyhydroxyalkanoates. Literature on structure, production, properties and blends of polyhydroxyalkanoates is reviewed. The next sub-section is on toughening mechanisms such as elastomeric modification and blending followed by reviews of nanocomposites, flexible packaging, starch and finally theoretical models.

The next chapter of this dissertation describes the materials used in this work starting with polyhydroxyalkanoates all the way to chemicals and solvents used. The fourth and fifth chapters explain the processing methods used and the characterization techniques used respectively. Results and pertaining discussions are presented in the next chapter followed by conclusions. The final chapter is comprised of the appendices listing calibration curves and calculations used in this work.

1.3 References

1. A. J. Ragauskas, C. K. Williams, B. H. Davison, G. Britovsek, J. Cairney, C. A. Eckert, W. J. Frederick, Jr., J. P. Hallett, D. J. Leak, C. L. Liotta, J. R. Mielenz, R. Murphy, R. Templer, and T. Tschaplinski, *The Path Forward for Biofuels and Biomaterials*, Science, 2006. 311, 484-489

2. Esposito, F., *Soaring resin prices help out bio-plastics*, 2005, Plastics News, 17, 38, http://www.plasticsnews.com/subscriber/printer.html?id=05112100901, Accessed on March 12, 2007

3. R. A. Gross, B. Karla, *Biodegradable Polymers for the Environment*, Science, 2002. 297, 803-807

4. Duncan, M., *U.S. Federal Initiatives to Support Biomass Research and Development*, Journal of Industrial Ecology, 2003. 7, 193-201

5. Lemoigne, M., Bull. Soc. Chim. Biol, 1927. 9, 446

6. R. W. Lenz, R. H. Marchessault, *Bacterial Polyesters: Biosynthesis, Biodegradable Plastics and Biotechnology*, Biomacromolecules, 2005. 6, 1-8

7. Standard, American Society for Testing and Materials (ASTM International), *ASTM D 5338 Standard Test Method for Determining Aerobic Biodegradation of Plastic Materials under Controlled Composting Conditions.*, 2003

2. LITERATURE REVIEW

2.1 Introduction

Polymers are a part of every aspect of our lives; from the clothes we wear to the automobiles we drive. These omnipresent materials have come up over the years due to mainly their durability and resistance to natural phenomena such as rusting or rotting. But these very characteristics of polymers have made them a bane to the environment. The inane ability of most polymers to resist degradation, over a significant period of time, leads to their persistence in the environment. One striking example of this is the large amount of polymers used for packaging. Plastics began its amazing ascent in the packaging field in the 1980s through major usage in the food and beverage packaging industry. The first use of plastics in food packaging was in the 1920s when bread was packaged using cellophane[1]. Carbonated soft drinks further continued this trend and currently plastic packaging materials touch almost every part of our daily lives[2]. The American plastics council reported that 29% of the plastics used in the United States in 2005 went towards packaging[3]. The majority of these packaging plastics end up in the waste stream upon completion of their useful life and go on to become a disposal issue. The plastics that are not disposed can harm animal and marine life that may ingest them. The plastic that is disposed still is difficult to totally eliminate from the environment; it is either put in landfills or incinerated. Land filling is declining as a disposal option due to the lack of space in most developed countries as well as issues with ground-water

pollution. Incineration is also not a totally environmentally friendly option because of greenhouse gases generation and issues related to global warming.

The viable answer to the above issues is plastic materials that are degradable after the end of their useful life and also can be degraded in a timely manner. Degradation can be defined as "a change in the chemical structure of a plastic involving a deleterious change in properties"[4]. This degradation can be of different types such as photo-degradation, thermal degradation, etc. but the most prevalent one is biodegradation. Biodegradation is basically defined as the natural process of decomposition facilitated by biochemical mechanisms[5]. Such polymers that undergo degradation by biochemical means in a specific time frame are termed as biodegradable polymers and are rapidly rising in appeal to the public as well as industries that are looking to solve the problems associated with non-degradable polymers.

Another class of materials that are generating tremendous interest is biobased polymers. These polymers are made from natural resources that are renewable such as agricultural feedstock and biomass. Such polymers based on renewable resources are emerging as a strategic alternative to petroleum based polymers owing to the depletion of global oil reserves and subsequent increase in fossil-fuel based resin prices[6]. Polymer product manufacturers are significantly affected by fluctuating resin prices and these costs are passed on to the consumer. Petroleum-based resins used in plastic packaging have increased in price by 30% in the year 2005[7]. The majority of the world's oil supply is held by a small but highly unstable group of countries that dictate crude oil prices and consequently such policies control the prices of the polymers that are synthesized from

crude oil. Plastics form a key part of a country's economy and it is thus very beneficial, both for the current scenario as well as for long-term stability, to disengage the connection of plastics with an unstable resource like petroleum. This independence can be achieved by slowly yet steadily increasing the biobased content of materials we use in our everyday lives. With this target in mind, many countries are formulating laws to increase biobased materials usage as well as pushing initiatives for the use of such products. For example, the US government has enacted the 'Biomass Research and Development Act of 2000 (US Public Law 106-224), presidential executive orders 13134 (calling for tripling America's use of biobased products by 2010) and 13101 (greening the Govt. through recycling and waste prevention) and the 2003 Farm Bill (encourages use of biobased materials as a replacement of petroleum-based materials)[8, 9].

Such societal and economic stimuli have initiated widespread research in renewable-resource based materials looking to develop them as alternatives to conventional non-biodegradable petroleum-based polymers [9].

However, polymers from renewable resource do have their own specific cost problem based on economies of scale. Renewable-resource based polymers lack a large market share and hence are generally synthesized on a batch-scale. This batch-scale production cannot economically compete with the continuous production of conventional polymers. Thus one of the ways to decrease the cost of renewable-resource based polymers is to create applications for them thus increasing usage and consequently shift production from batch to continuous ways. This increased market-vale can also be achieved by improving the properties of the renewable-resource based polymers thus

making them more attractive than conventional polymers. This research targets this pathway of enhancing the properties of some specific renewable-resource based polymers by novel technology. The conversion of batch-scale to continuous scale production is the long-term goal in such renewable-resource based polymers but is beyond the scope of this work; hence the near-term goal of cost reduction is targeted by giving more value to the materials via property enhancement or by incorporating inexpensive biobased polymers and fillers into the comparatively expensive matrix.

Thus, biodegradable and biobased polymeric materials can be a solution to the problems of dwindling petroleum reserves and disposal. But these as yet are not used on a large scale primarily due to cost issues and property limitations. This chapter presents an in-depth literature review of the current state of science in the area of biodegradable and biobased polymeric materials.

2.2 Biopolymers

The term "Biopolymers" applies to a broad range of polymers that have at least one of the attributes of being completely made from renewable resources or being biodegradable or being partially made from renewable resources. These attributes are used to classify biopolymers into the three previously-mentioned classes as denoted in Figure 2.1:

1. Renewable-Resource-based Polymers

2. Petroleum-based Biodegradable Polymers

3. Polymers from Mixed Sources (Renewable and Petroleum)

The above classification is based on the current state of scientific literature. However it is to be noted that some polymers may change from one classification to another as developments in synthesis or other specific characteristics are discovered. One

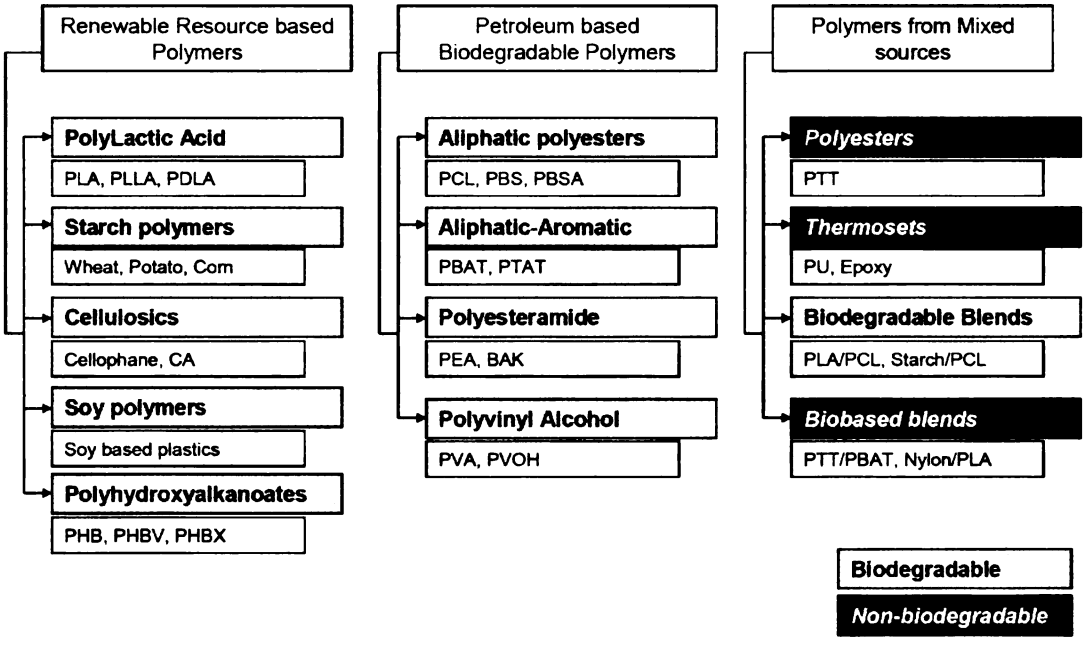

Figure 2.1: Classification of Biopolymers (abbreviations are explained in subsequent section)

such example is the family of petroleum-based biodegradable polymers called poly (alkylene dicarboxylates). These are currently commercially produced from petroleum-based resources by Showa High Polymers ltd., Japan under the trade mark "Bionolle" by the condensation polymerization of 1, 4-butanediol with aliphatic dicarboxylic acids like adipic acid or succinic acid. Mitsubishi Chemical Company, Japan in collaboration with

Ajinomoto Chemical Company is planning to make poly (alkylene dicarboxylates) using succinic acid from plant materials such as vegetable starch [10]. This technology will make poly (alkylene dicarboxylates) partially biobased as well as biodegradable thus changing it's classification from being a petroleum-based biodegradable to mixed-source biodegradable polymer.

2.2.1 Renewable Resource based Polymers

2.2.1.1 Polylactic Acid

Polylactic acid (PLA) is a biopolymer that falls under the renewable-resource based polymers classification as it is made from biomass like corn and sugar beets. PLA is linear and aliphatic in nature and is produced by poly-condensation of lactic acid or by the catalytic ring opening of the lactide group. PLA is a stiff, rigid thermoplastic with a

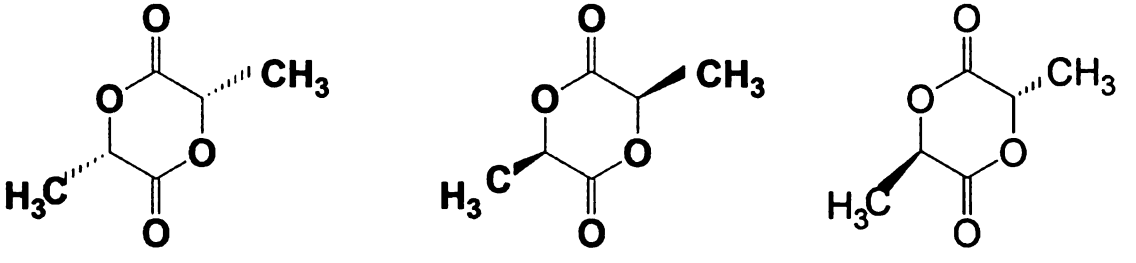

L-Lactide D-Lactide Meso-Lactide

Figure 2.2: Lactide Stereo-isomers

semi crystalline nature. The stereochemistry of the polymer backbone dictates the final properties with Poly L-lactic acid (2-hydroxy propionic acid) being the common form of this polymer[11-13]. D-lactic acid monomers are incorporated in the PLA backbone to gain flexibility and reduce crystallinity (Figure 2.2). Carothers first synthesized PLA by heating Lactic Acid under vacuum in 1932 followed by developments by Dupont and Ethicon of medical-grade PLA, but the high production costs limited the large-scale development of PLA till the 90's. In the synthesis of PLA, the first step is the production of lactide by the depolymerization of low molecular weight PLA under reduced pressure to give a mixture of L-lactide, D-lactide, or meso-lactide. These stereo-isomers of lactide, as shown in scheme 2.1, undergo further cationic ring-opening to yeild high-molecular-

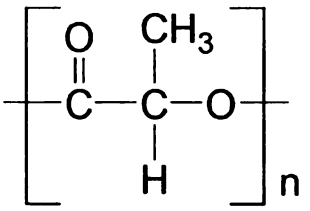

Figure 2.3: Poly (Lactic Acid) Structure

-833E-D46AA3CAA1DC}&link=N"

sulfonic acid (triflic acid) and methyl trifluoromethanesulfonic acid (methyl triflate) are the only cationic initiators to polymerize lactide[14]. The structure of PLA is shown in Figure 2.3.

Cargill Inc. investigated and developed PLA production technology from 1987, and began production of pilot plant quantities in 1992. In 1997, Cargill formed a collaboration with Dow Chemical Company, Inc., creating Cargill Dow Polymers LLC (CDP) and launched Nature Works™ PLA technology in 2001. Dow withdrew its support in 2005 and Natureworks is currently owned totally by Cargill. Natureworks has

a manufacturing facility in Blair, Nebraska, USA, capable of producing 300 million pounds of polymer per year[15].

PLA has a melting point (T_m) range of 130 – 230°C depending on the structure, with PLLA having T_m of 180°C with an enthalpy of fusion of 40-50 J/g and glass transition point (T_g) of about 58°C[15-17]. The pure crystalline PLLA has an estimated density range of 1.37 – 1.49 g/cc, however the solid amorphous PLA has a density of about 1.25 g/cc. The incorporation of L-, D- and meso lactide monomers into natural PLA affects the stereo chemistry and crystallization and consequently the related properties although T_g being least affected. Using such monomer incorporation, branching, molecular weight distribution and isomer contents, it is possible to make a wide variety of PLA resins for specific applications such as films, injection molded and blow molded articles, fiber spinning, etc[17].

PLA has excellent oil and grease barrier, very good barrier for aroma and flavor, excellent low-temperature sealability, good crease retention and crimp properties and thus makes an excellent choice for many packaging related applications[16]. PLA also has very high tensile strength and young's modulus, with modulus in the range of 3.4 to 4.2 GPa and strength of 45-60 MPa depending upon orientation and crystallinity [14]. PLA also possesses good water vapor barrier and relatively good oxygen barrier and this makes PLA as one of the most favorable food packaging materials among biodegradable plastics. PLA is degraded primarily by simple hydrolysis and does not require microbial attack for biodegradation thus further enhancing its value. But PLA has inherently low

elongation owing to its high crystallinity thus limiting its applications in flexible packaging[16].

2.2.1.2 Starch

Starch is an inexpensive, annually renewable material derived from plants. Starch is a polysaccharide and can be isolated from plants such as corn, wheat, potato, cassava, pea etc. All starches contain amylose and amylopectin at ratios that vary with the starch source and this variation provides a natural mechanism for regulating starch material properties. Amylose is the linear portion of starch (Figure 2.4) and is a D-glucose α 1,4-

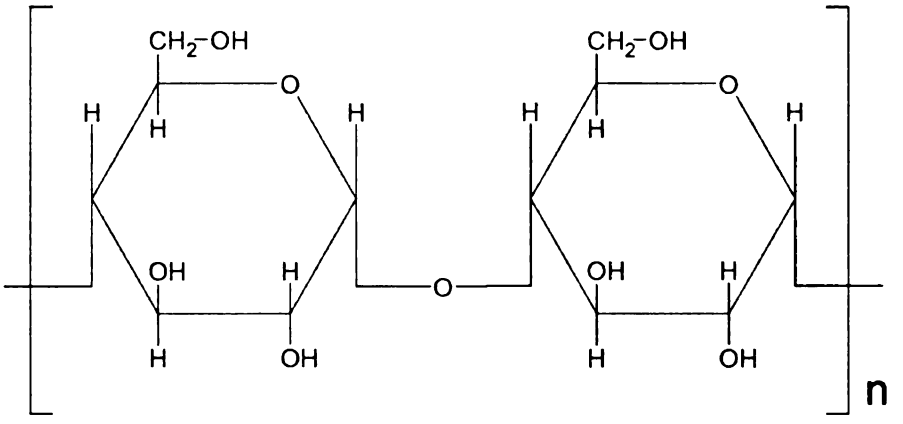

Figure 2.4: Amylose Structure

glucosidic linkage having molecular weight between 2,000 – 150,000[18]. Amylose content varies from 17% (root and tuber) to 30% (cereal starches). Amylopectin is the branched portion of starch (Figure 2.5) and is a D-glucose α-1,6-glucosidic linkage having molecular weight between 65-500 million[18]. Starch exhibits a unique property called gelatinization that involves breaking of the hydrogen bonding by heat, in presence

of water at high temperature, and allowing water to enter. This water disturbs the granular organization of the starch molecules and makes new H-bonds with amylose and amylopectin forming a gel-like structure[18]. Starch is available in 3 main types: cereal starches such as corn, wheat, rice, oat, barley, and rye; root starches such as cassava, tapioca and potato; and tree starches such as sago palm tree, arrowroot and milo. The amylopectin in starch inhibits gelation and hence the amylopectin content dictates the final properties and applications of different starches. Native starches are altered by physical or chemical means to obtain modified starches such as pregelatinized starches, thin-boiling starches, oxidized starches, cross-linked starches and starch phosphates[18].

In the plastics area, unplasticized or un-gelatinized native starch by itself is only

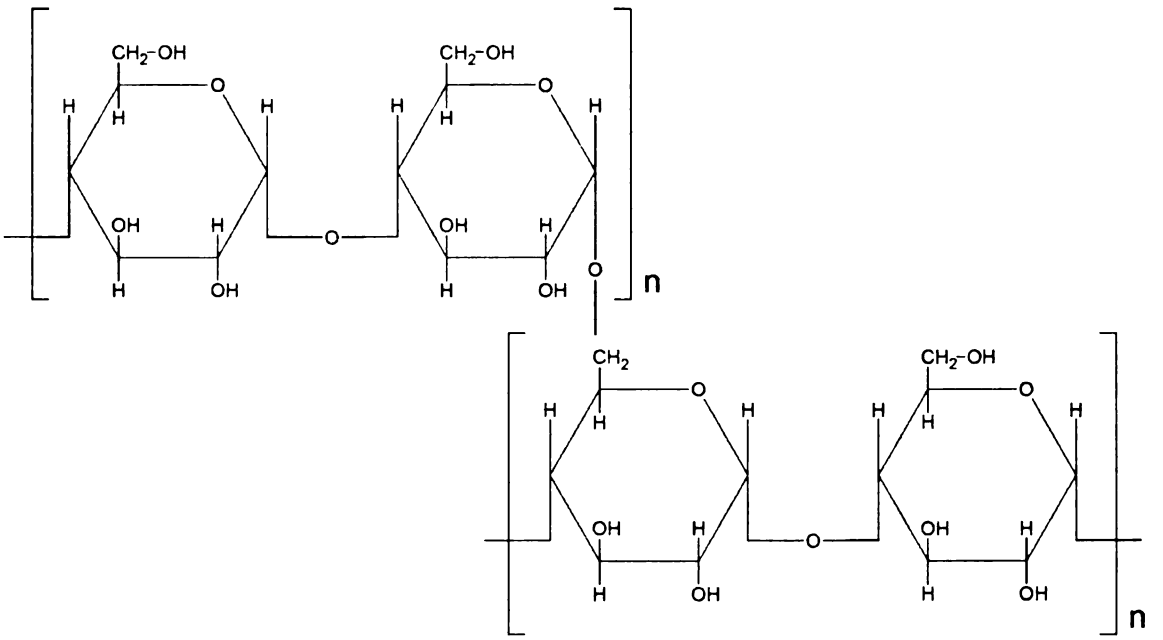

Figure 2.5: Amylopectin Structure

used as a filler and in order to use starch as a plastic material, it needs to be destructurized and plasticized. This is generally done using water and/or a non-volatile

plasticizer such as glycerol or other polyols[19]. Such destructurized starches are termed as "Plasticized Starch" or "Starch Plastic" (PS) and were first reported in the late 80s [20-23]. Plasticized starch in its most general form is a combination of starch, a high-boiling and non-volatile plasticizer and water that has undergone thermo-mechanical treatment such as extrusion processing.

2.2.1.3 Cellulosics

Cellulose is the most abundant renewable-resource based material in the biosphere. It is a linear polymer consisting of β(1–4) linked D-glucose synthesized by plants and bacteria (Figure 2.6). Celluosics are semicrystalline in nature and primarily used as reinforcements in polymer composites. Cellulose can be made into a thermoplastic material by modification via acetylation. This modified cellulose is called cellulose ester and includes cellulose acetate (CA), cellulose acetate propionate (CAP), and cellulose acetate butyrate (CAB)[24, 25]. Cellulosic plastics are commercially

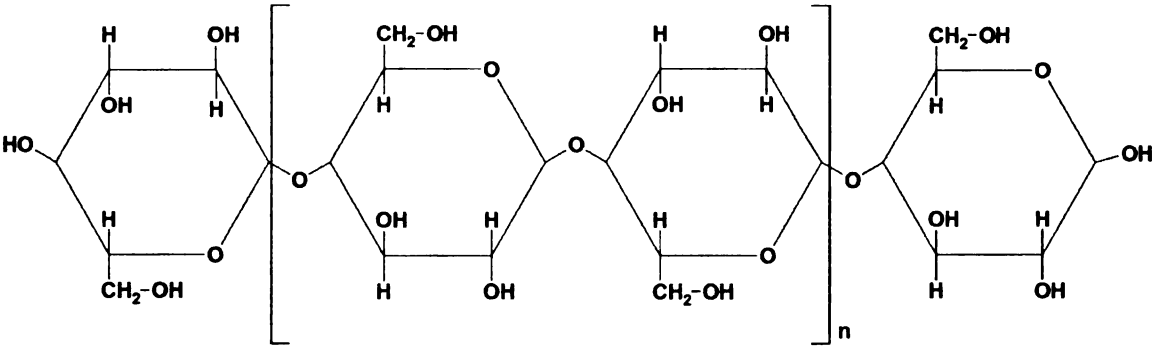

Figure 2.6: Cellulose Structure

manufactured by Eastman Chemical Company and are now used in a variety of plastic applications such as premium toothbrush handles and screwdriver handles[25].

2.2.1.4 Soy Plastics

Soybean is a good candidate for manufacturing a large number of chemicals, including biodegradable plastics, as it is abundantly available and cheap. It is composed of 18-20% oil, 40-45% protein, 25-30% carbohydrate, and 3% other material[26]. Commercially available soy protein products include soy flour, soy concentrate, and soy isolate and these can be compounded with synthetic biodegradable plastics such as poly (ε-caprolactone) or poly (lactic acid) to make molded products or edible films[26]. Henry Ford in the 1930s and 1940s was one of the pioneers of soy-based materials when he mixed cellulose with a resin binder made of soybean and other plant products to produce automobile body parts[27]. Brother and Mckinney in 1940 also reported making plastics by using soy protein and various cross-linking agents[28]. Films from soy protein have also been reported using plasticizers [29]. But plastics made from molding of soy protein have a major drawback that they display swelling after submersion in water.

2.2.1.5 Polyhydroxyalkanoates

Polyhydroxyalkanoates (PHAs) are a class of biodegradable and renewable-resource based polymers. PHAs were discovered at the Pasteur Institute in France with the first PHA identified as polyhydroxybutyrate (PHB)[30]. In 1927 Lemoigne, the director of the Pasteur Institute, described an isolation of lipid-like inclusions seen in cells of *Bacillus megaterium* as 3-hydroxybutyric acid. Lemoigne and co-workers reported on their PHB studies in numerous publications from 1923 to 1951, but it was not until the late 1950s that the significance of Lemoigne's earlier discoveries was

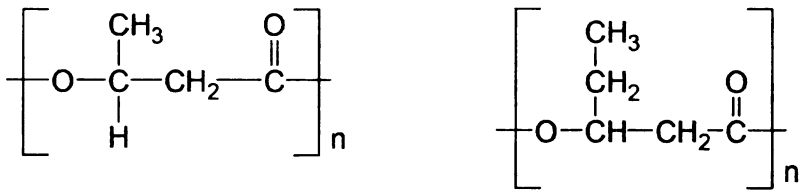

Figure 2.7: Poly(hydroxybutyrate) (left) and Poly(hydroxyvalerate) (right) Structures

recognized[31]. PHAs possess highly attractive qualities for applications, but have not yet fully entered commercial markets due to high production costs. PHAs, like PLA, are produced from renewable feedstock by fermentation. However PHAs are produced in a direct manner via fermentation of carbon substrate within bacterial microorganisms while PLA production is a two-stage process (first step of fermentation of low molecular weight PLA to lactide monomer followed by second step of polymerization). PHAs are created as intracellular inclusions for bacteria and are created as a result of imbalanced conditions caused by supplying excess carbon and limiting growth of the bacteria. PHAs are produced from a variety of commercial plants like corn and even from non-conventional agricultural resources like switch-grass and this presents exciting

opportunities for economic and agricultural development[32]. All these factors combined with the environmental advantage of PHAs due to their biodegradability has led to active research and development of these materials as future sustainable and 'green' packaging materials.

The main members of the PHA family are the homopolymers poly(hydroxybutyrate), (PHB) and poly(hydroxyvalerate), (PHV) (Figure 2.7). Copolymers of PHAs are also commercially available varying by type and proportion of monomers, and are typically random in sequence. Poly(3-hydroxybutyrate–co-3-hydroxyvalerate) is one such copolymer with random units of butyrate and valerate along the backbone and another example is the polyhydroxyhexanoate family of copolymers having structure as poly(3-hydroxybutyrate-co-3-hydroxyhexanoate) with chain length from C7 up to C19 [33]. PHAs are covered in more detail in section 2.3 of this dissertation.

2.2.2 Petroleum-based Biodegradable Polymers

2.2.2.1 Aliphatic Polyesters

A major classification in petroleum based biodegradable polymers is the family of aliphatic polyesters and copolyesters obtained by the combination of diols, such as 1,2-ethanediol, 1,3-propanediol, or 1,4-butadenediol, and dicarboxylic acids such as adipic, sebacic, or succinic acid or by ring opening polymerization.

Poly(ε-caprolactone) (PCL): A large number of biodegradable aliphatic polyesters are based on petroleum resources obtained chemically from synthetic monomers. Poly(ε-caprolactone) (PCL) is one of the most popular examples of this class (Figure 2.8). PCL is obtained by ring opening polymerization of ε-caprolactone using

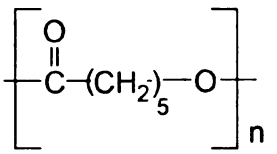

Figure 2.8: Poly(ε-caprolactone) Structure

aluminum isopropoxide as catalyst[34]. Different commercial grades are produced by Union Carbide (now part of the Dow Chemical Company) (Trade name: Tone®), by Solvay (Trade name: CAPA®), and by Daicel (Trade name: Celgreen®)[19]. PCL shows a low melting point (65°C) and a very low Tg (-61°C) which limits its usage in some applications. Therefore, PCL is generally blended or modified by copolymerization or crosslinked to create a more versatile material[35].

Poly(butylene succinate) (PBS) and Poly(buylene succinate-co-buylene adipate) (PBSA): PBS and PBSA are part of the poly (alkylene dicarboxylates) family of aliphatic polyesters (Figure 2.9). These are currently commercially produced from petroleum-

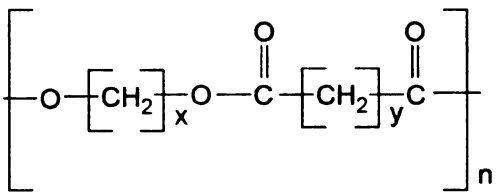

Figure 2.9: Poly (alkylene dicarboxylate) structure, Poly (butylene succinate):- x = 4 and y = 2; Poly (buylene succinate-co-buylene adipate):- x = 4 and y = 2, 4

based resources by Showa High Polymers ltd., Japan under the trade mark Bionolle® by the condensation polymerization of 1, 4-butanediol with aliphatic dicarboxylic acids like adipic acid or succinic acid. Enpol® from Ire Chemicals, Korea and Skygreen® from SK Chemicals, Korea are similar polymers[19]. Mitsubishi Chemical Company, Japan in collaboration with Ajinomoto Chemical Company is planning to make poly(alkylene dicarboxylates) using succinic acid from plant materials such as vegetable starch[10]. Poly(alkylene dicarboxylate)s have appealing properties such as ease in melt processing and biodegradability ideal for flexible packaging applications.

2.2.2.2 Aliphatic-Aromatic Co-polyesters

Compared with totally aliphatic copolyesters, aromatic copolyesters are often based on terephthalic acid. Eastar Bio® from Eastman Chemicals (now produced by

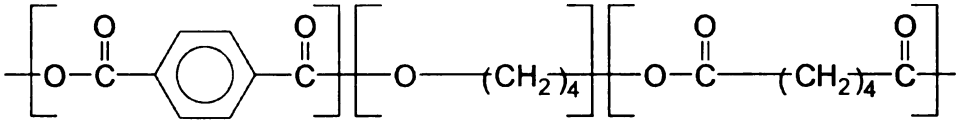

Figure 2.10: Chemical Structure of Poly-(butylene adipate-co-terephthalate) (PBAT)

Novamont), Ecoflex® from BASF and Biomax® from Dupont are the three prime examples of this type of biopolymers[36-38]. Ecoflex®, whose chemical name is Poly-(butylene adipate-co-terephthalate) (PBAT) (Figure 2.10), is a thermoplastic aliphatic-aromatic co-polyester, produced by condensation of 1,4-butanediol with 1,4-benzenedicarboxylic acid (terephthalic acid) and hexanedioic acid (adipic acid)[36]. It is a

biodegradable flexible polymer that is very popular in blown-film applications. PBAT has properties similar to LDPE due to their long chained molecular structure. It can undergo biodegradation by microorganisms and has been accepted as biodegradable by European as well as US Standards. It has very good compatibility with other biopolymers like PLA, other bio polyesters and starch. According to the supplier (BASF), this material can replace many petroleum-based polymers in conventional film applications as well as in packaging applications. It is hydrophobic and has relatively good water vapor barrier properties that make this ideal for moisture-sensitive applications and it is approved for the food contact applications [36]. PBAT has a semi-crystalline nature with melting point in the range of 110 – 120 °C and density in the range of 1.25–1.27 g/cc. It possesses high ultimate break elongation (560 % to 710%) and is thermally stable up to 230°C[36].

Eastar Bio® and Biomax® have fairly similar mechanical properties to Ecoflex® but have slight proprietary variations in the chemical structure such as different terephthalic acid content which modifies some properties such as the melting temperature (200° C) for Biomax®[19].

2.2.2.3 Polyesteramides

Polyesteramides (PEA) (Figure 2.11) are synthesized by the statistical copolycondensation of polyamide (PA 6 or PA 6-6) monomers and adipic acid[39]. Bayer had developed and launched different commercial grades of PEA under BAK® trademark but their production stopped in 2001. This polymer is a highly polar material

and shows excellent compatibility with other polar products such as starches. However it

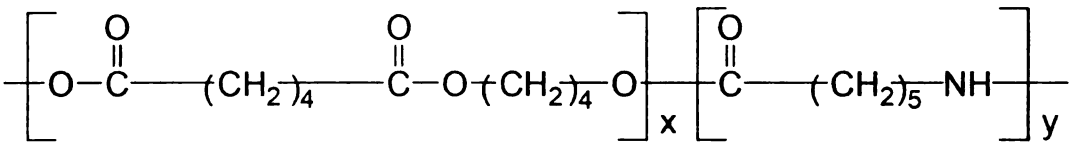

Figure 2.11: Polyesteramide Structure

has extremely low water vapor barrier. PEA is biodegradable but researchers have reported negative eco-toxicological impacts of these materials on compost and hence the environmental impact of this copolymer is still open to discussion [40, 41].

2.2.2.4 Poly(Vinyl Alcohol)

Poly(vinyl alcohol), (PVOH) (Figure 2.12) is synthesized by the reaction of poly(vinyl acetate) in alcohol, with sodium hydroxide[42]. PVOH is also termed as PVA in some publications however PVA classically refers to poly(vinyl acetate). The hydrolysis of PVA to PVOH gives a product with a variable percentage of residual acetate groups that affect its solubility and biodegradability. PVOH has been well recognized and reported by researchers as a biodegradable polymer[43]. PVOH is water-

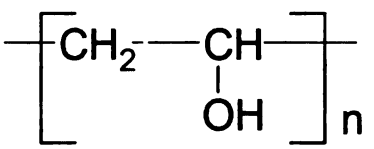

Figure 2.12: Polyvinyl Alcohol Structure

soluble and is an excellent barrier to aroma, flavors, oils and fat and thus has multiple applications in packaging.

2.2.3 Mixed Sources (Renewable and Petroleum) Sources

2.2.3.1 Polyesters

Apart from PLA and PHAs, a number of other polyesters are being produced or have shown the potential to be produced from renewable feedstock. One such example is the polymer poly (trimethylene terephthalate) (PTT) that is made under the tradename Sorona™ by Dupont and Corterra® by Shell chemicals. PTT is a 3-carbon glycol terephthalate that is a condensation polymer of 1,3-propanediol and terephthalic acid (Figure 2.13).

PTT combines the desirable physical properties of poly(ethylene terephthalate): strength, stiffness, toughness and heat resistance with the processing advantages of poly(butylene terephthalate): low melt and mold temperatures, rapid crystallization and faster cycle times; while retaining the general benefits of linear aromatic polyesters: dimensional stability, electrical insulation and chemical resistance[44].

DuPont has demonstrated the capability to produce the propanediol monomer of PTT from corn sugar, a renewable resource, and hence PTT has drawn considerable attention for having a biobased origin yet having the properties of an engineering plastic.

Dupont won the 2003 Presidential Green Chemistry Award for the successful development of 1,3-propane diol (PDO) from a biological source[45].

Poly(butylene terephthalate) can also be partially made from renewable resources in theory as it also utilizes the propanediol monomer as PTT but there does not exist as yet any commercial biobased PBT[33]. It should be noted that though PTT as well as PBT come under the partially biobased polymer class, both of these are not biodegradable.

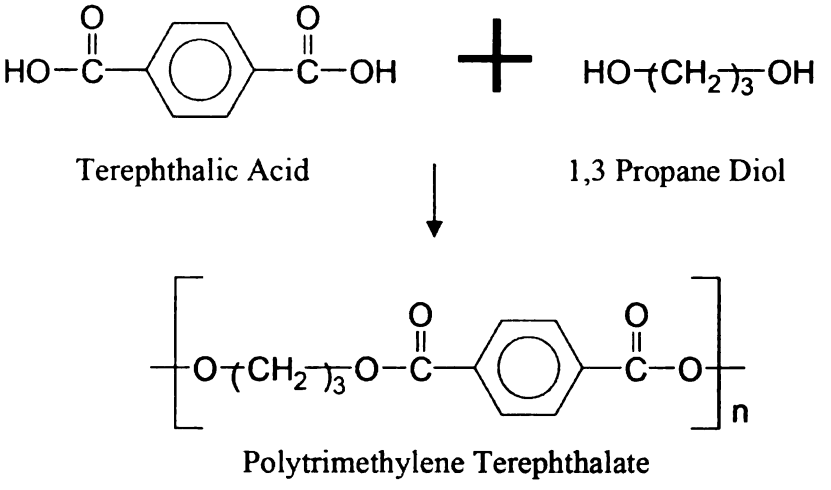

Figure 2.13: Polytrimethylene Terephthalate Synthesis and Structure

2.2.3.2 Thermosets

Thermoset resins are a class of polymers that are capable of being irreversibly cured from a liquid to a solid state when subjected to appropriate conditions. These are further classified into polyester resins, epoxy resins and urethane resins depending on the functional unit present in the polymer backbone. The terminology biobased thermoset

resin refers to thermosets in which one of the components is produced from renewable resources.

Polyester resins are the most widely used resin system especially in the marine industry. These resins are comprised of a glycol and an unsaturated or saturated acid. Biobased polyester materials have been reported that contain up to 25 wt % epoxidized methyl linseedate (EML)[46]. Similarly, unsaturated polyester resin with derivatized vegetable oil has been reported as a matrix for composite materials for use in housing applications[47].

Polyurethanes (PU) are another class of thermosets that are manufactured by the reaction of an isocyanate and a polyol. Some grades of polyurethanes are thermoplastic in nature but thermoset PUs are more commonly used. The isocyanate component is always derived from petroleum resources but the polyol component can be potentially developed from bioresouces. For example, vegetable oil based polyols can be synthesizd from castor, soy, linseed, sunflower, rapeseed, etc.[48] Biobased polyols are also possible from wood, lignin, carbohydrates among other biomass.

Biobased epoxy resins are the third class of thermosets and these too follow the same principle as the ones mentioned above in the sense that some part of the petroleum-based epoxy resin is substituted with epoxidized biobased oil prior to polymerization such as epoxidized linseed oil or epoxidized soy oil[49].

2.2.3.3 Biodegradable Blends

Polymer blends are mixtures of at least two macromolecular species, polymers and/or copolymers. The blending of biodegradable polymers is a route to reduce the overall cost of the material and offers a way of modifying the properties as well as in some cases the biodegradation rates.

Starch based blends: Starch is inherently brittle in absence of plasticizers as well as hydrophilic in nature. Starch also shows deterioration of mechanical properties upon exposure to environmental conditions and hence starch needs to be blended with flexible polymers to eliminate these disadvantages. However, most of the candidate partner polymers are hydrophobic and thermodynamically immiscible with hydrophilic starch leading to incompatibility and poor mechanical properties, especially if starch is present over a threshold loading. Below this critical level, (for example this level is approximately 25–30 wt% in starch–polyester composites) the deterioration in properties has been found to be insignificant[50]. Large-scale research in the area of starch belnds was started with the concept of "biodegradable" polyolefin blends. These were very popular in the last decade and were made by incorporating starch into polyethylene. The thought process for this was that the starch would initiate biodegradation of the polyethylene chains over time. But these materials did not prove to be as quickly biodegradable as expected and were thus withdrawn from commercial usage in a very short time[51]. These blends only showed biodegradability at more than 10% starch content but this detrimentally reduced the mechanical and barrier performance[52]. The main supplier of such starch-polyethylene blends was the St. Lawrence Starch company

that sold these materials under the trade name EcoStarPlus. Later varieties of starch-plastic blends contained higher amounts of starch (as high as 50%) with polypropylene, polystyrene, polyurethane and polyethylene as the blending partners[51, 53]. These materials are not considered biodegradable but have been named bio-fragmentable[19].

The next development in this field addressed the issue of biodegradability by using synthetic biodegradable polymers such as PCL as the blending partners. Starch-PCL blends were first reported by Tokiwa et al. and have been well researched and documented[19, 22, 52, 54-58]. Starch has also been blended with agro-polymers[59] but most of the research is focused on blending with biodegradable polyesters such as PHBV [60, 61], PEA[62], PBAT[63], PBSA [19, 63, 64] or PLA [65].

These materials have also achieved fairly good commercial success; for example the Mater-Bi ranges of products as marketed by Novamont are starch-PCL or starch-PVOH systems. Applications include packaging, disposable cutlery, gardening, leisure, hygiene etc[35].

PLA based blends: PLA, as explained in the earlier part of this section, is a highly brittle material with exceptional strength and modulus but very poor flexibility. Most PLA-based blends aim at overcoming this lack of elongation in order to fabricate flexible films from PLA based materials. McCarthy's group at the University of Massachusetts at Lowell have studied and reported a number of PLA based blends with biodegradable polyesters such as PBAT, PBSA, PCL, Poly(glycolic-acid) (PGA) etc[66-68]. Similar studies on PLA-biopolyester blends have been done by Chidambarakumar[69], Sahu et al[70] and Jiang et al[71]. BASF has quite recently launched a line of resins based on

PBAT-PLA blends named Ecovio® that are intended to be used in flexible packaging applications[72].

PHA based blends: Polyhydroxyalkanoates, specifically poly(3-hydroxy)butyrate (PHB) and poly(3-hydroxybutyrate-hydroxyvalerate) (PHBV) have the desirable characteristics of biodegradability and biocompatibility as well as are biobased in origin. However, their costs and performances need to be adjusted by blending with suitable polymers. Polyhydroxyalkanoate-based blends have been extensively researched with a range of polymers such as PCL, PLA, Polyethylene Oxide (PEO), PBAT, PBS, Starch, etc. The subsequent section on PHAs will elaborate more on this topic.

2.2.3.4 Biobased Blends

Federal initiatives and orders have called for increased biobased content in materials used by the government as well as public sector industries[8, 9]. One of the solutions to achieve such mandates is to blend biobased materials with synthetic materials so as to achieve the desired bio-content. But this research is still in its infancy and needs significant fundamental studies before it can be commercialized.

2.3 Polyhydroxyalkanoates

2.3.1 Polyhydroxyalkanoate History

Amongst all the biopolymers described above, the polymers selected for this dissertation are polyhydroxyalkanoates (PHAs). PHAs are completely biodegradable and made from renewable resources. Lemoigne first synthesized PHAs by polycondensation of an insoluble lipid-like component that was identified as R-3-hydroxybutyric acid. Lemoigne proposed this natural material to have a polyester structure with formula $(C_4H_6O_2)_n$ and he also recorded its optical rotation to establish the chiral properties. Lemoigne and co-workers reported on their polyhydroxybutyrate studies in numerous publications from 1923 to 1951, but it was not until the late 1950s that the significance of Lemoigne's earlier discoveries was recognized[31, 32, 73-75]. PHB was for the most part of its earlier existence known only to microbiologists. Academic collaborations between microbiologists and polymer researchers around 1961 at Syracuse University and at the State University of New York led to recognition of PHB as a polymer further comparing polyhydroxybutyrate to isotactic polypropylene based on isotacticity and helical crystalline conformation. This group further used X-ray diffraction, lamellar single crystal texture, intrinsic viscosity, absolute molecular weight measurements and electron microscopy to demonstrate the thermoplastic nature of polyhydroxybutyrate[31, 76, 77].

This work was followed by research on the structure, biosynthesis and enzymatic degradation processes by researchers in the UK and US. The potential of PHB being an useful material especially for commercial packaging applications was realized and implemented in the early 1960s by W. R. Grace and Co[77-79]. However the first full-scale

production of PHB occurred only in 1982 when ICI started to produce and sell copolymers of PHB under the trade name Biopol®[80, 81]. ICI later split into ICI and Zeneca with Zeneca continuing the PHA related work. In 1996, Monsanto purchased the PHA-related patents and technology from ICI/Zeneca but continued its production only till 1999[77, 82]. Metabolix, an US based company, further bought out this technology from Monsanto and started production of PHAs in 2004. Metabolix has a number of new patents on genetic engineering of plants to give PHAs that resulted in Metabolix receiving the 2005 Presidential Green Chemistry Challenge Award (small business category)[83]. Metabolix recently announced plans to construct a commercial manufacturing facility designed to produce 110 million pounds of PHAs in a joint venture agreement with Archer Daniels Midland Company[84]. Procter and Gamble (P&G) also started commercial-size research in PHAs and launched the Nodax™ brand of PHA copolymers in 2003 and announced commercial production in 2004. However, P&G stepped back from this venture in 2005 and their technology is currently for sale[85]. In Europe, Biomer of Germany produces PHB on an industrial scale[86]. PHB Industrial S/A from Brazil produces PHAs from sugarcane while two different companies in China; Tianjin Tianlu Co. Ltd (Tianjin, China) and Tianan Biologic Material Co., Ltd. (Ningbo, China) also mass-produce PHA homopolymers and copolymers[87, 88]

2.3.2 Polyhydroxyalkanoate Production

Polyhydroxyalkanoates are basically obtained as intracellular inclusions for bacteria and are created as a result of imbalanced conditions caused by supplying excess

carbon and limiting growth of the bacteria. PHAs are synthesized by many gram-positive and gram-negative bacteria from at least 75 different types[75]. The majority of bacteria accumulate these PHAs in response to the above conditions coupled with nitrogen deficiency. These polymers are accumulated intracellularly by these bacteria to levels as

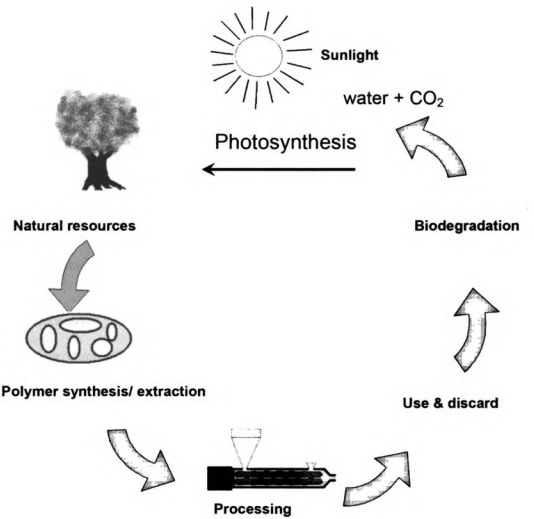

Figure 2.14: Life cycle of biodegradable polymers (Redrawn after Ref. 89).

high as 90% of the cell dry weight and act as a carbon and energy reserve for the bacteria. Observations on polyhydroxybutyrate in the microbiological literature indicate that it is a primary product of carbon assimilation similar to starch and glycogen[32, 73-75, 77]. The

monomer units vary according to the parent bacteria and this creates a possibility for producing a range of biodegradable polymers with an extensive array of properties. The molecular weight of PHAs is in the range of 50,000–1,000,000 Daltons and varies with the PHA supplier[73, 75].

The entire production process of biobased polymers like Polyhydroxyalkanoates can be termed as a cyclic process (Figure 2.14)[89]. The first step is photosynthesis of carbon dioxide from the atmosphere by plants using sunlight which is accumulated in the plant cells. This accumulated carbon is converted to carbohydrates which subsequently becomes a food source for the bacteria that ultimately synthesize PHB. The synthesized PHA is extracted and purified to get PHA plastic that is further converted into products. The products, upon disposal, biodegrade under specific conditions to release carbon dioxide back into the atmosphere thus completing the cycle.

PHAs are synthesized by four primary methods: biosynthesis; production in organisms; production by recombinant bacteria; and by metabolic engineering.

PHB is biosynthesized by using a set of enzymatic reactions catalyzed using three different enzymes; *β-ketoacyl-CoA thiolase, acetoacetyl-CoA dehydrogenase* and P(3HB) polymerase. In the first enzymatic reaction, two *acetyl coenzyme A (acetyl-CoA)* molecules undergo condensation in presence of *β-ketoacyl-CoA* to form *acetoacetyl-CoA*. The second reaction involves the reduction of *acetoacetyl-CoA* to *(R)-3-hydroxybutyryl-CoA* by the *acetoacetyl-CoA dehydrogenase*. Finally, the *(R)-3-hydroxybutyryl-CoA* monomers are polymerized by P(3HB) polymerase to give poly(3-hydroxybutyrate) as the final product[13, 32, 73-75]. The initial step of this process is prefermentation in which

bacteria cells are grown in a mineral medium with a carbon-source. Following prefermentation, the cells are allowed to multiply in order to increase cell density till a dry cell mass of 80% PHB is obtained. This is followed by the final step of isolation in which cell walls are destroyed mechanically or using enzymes and then the polymer is dissolved in chloroform or another solvent and separated by centrifugation and filtration[75].

Production of PHA's in natural organisms was developed mainly by ICI in the early 1970's during its foray into large-scale production of PHA's. This research identified and evaluated several bacterial species as potential production organisms such as methylotrophic bacteria, *azotobacter* and *Ralstonia eutropha*[76]. The methylotropic bacteria did not produce sufficient polymer per cell as well as the molecular weight was too low. The azotobacter strains were recognized as unstable as well as secreted undesirable byproducts such as polysaccharides. The *ralstonia eutropha* was selected as the bacteria of choice as it produced high-molecular-weight PHA and was used extensively by ICI for production of PHB and PHBV copolymers. Several other investigators have also studied PHA production from organic waste by natural isolates of species such as *Agrobacterium, Sphaerotilus, Rhodobacter, Actinobacillus, and Azotobacter*[73, 81, 90].

Although *R. eutropha* has reported to be an excellent producer of PHB, this bacterium has certain limitations such as slow growth rate and difficulty in lysing that prevent it from being useful for the commercial production of PHB[32]. The genetic characterization of *R. eutropa* is also incomplete thus constricting further manipulation

for improved industrial performance. Hence recombinant bacteria strains have been developed using genetic and metabolic engineering to overcome these shortcomings such as recombinant *E. coli*[32, 73].

2.3.3 Polyhydroxyalkanoate Structural Variations

Polyhydroxyalkanoates are classified according to the substitutent present on the 3-β carbon group in the repeat unit of the polymer backbone. The generic formula for PHA is given by Figure 2.15. In this figure, x is the length of the backbone unit which is generally between 1 and 3 CH_2 units long and R is the substitutent group. The chain length (i.e. methyl, propyl, etc.) of this group dictates the final properties of the polymer. The most generic form of polyhydroxyalkanoates is polyhydroxybutyrate in which R is a methyl group and x =1. Polyhydroxyvalerate has R as an ethyl (C_2H_5) group while a specific group of PHAs synthesized by P&G under the trade name Nodax™ has a propyl group (C_3H_7) as the substitutent R group and are chemically called polyhydroxyhexanoates[33, 85].

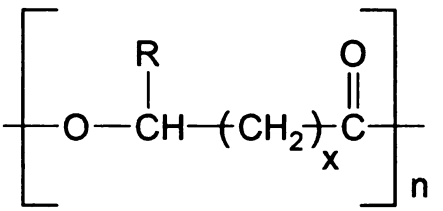

Figure 2.15: General Structure for PHA

2.3.4 Polyhydroxyalkanoate Properties

The main focus polymers of this dissertation are the homopolymer polyhydroxybutyrate and the copolymer poly(hydroxybutyrate-co-valerate) and so this section will primarily concentrate on PHB and PHBV properties with properties of other PHAs discussed to a lesser degree.

PHB is an enantiomerically pure polymer (molecular weight of repeat unit: 86.09)[91] with a methyl substituent present regularly along the backbone adjacent to the methylene group. This structure is comparable with isotactic polypropylene (PP) and hence it has many similar properties with that of PP[92]. The majority of PHB prepared by bacterial fermentation is 100% isotactic. Some partially sydiotactic PHB genres are possible if an optically active catalyst is used but are not commercially made[91]. The isotacticity combined with the linear nature of the chain results in a highly crystalline material with very attractive strength at room temperature and under moderate rates of deformation. The percent crystallinity of PHB varies from 30 to 86% depending on the purification, drying and annealing conditions with the solution precipitation technique followed by vacuum drying and annealing at 160°C for 24 hours giving the highest crystallinity of 86%[91, 93]. The heat of fusion of this highly crystalline PHB is 12.5 kJ/mol with a density of 1.177 g/cc. The density of PHB varies from 1.177 to 1.262 g/cc again depending on processing conditions. PHB shows excellent solubility in many organic solvents such as chloroform, trichloroethylene, dimethyformamide, ethylacetoacetate, methylene chloride, 2,2,2-trifluoroethanol, triolein, comphor, glacial acetic acid, 0.5N

aqueous phenol, N-NaOH, N-hyamine hydroxide, 1,1,2,2-tetrachloroethane, glycerol triacetate, dichloroacetic acid, propylene carbonate and 1,2-dichloroethane[91, 94]. The Mark-Houwink-Sakudra parameters for PHB are a = 0.82 and K = 7700 ml/g for chloroform at 30 °C[95].

PHB has been widely reported to exhibit ageing on storage at room temperature which consequently increases the degree of brittleness[96]. This embrittlement has been uniquely attributed by different authors to be a result of progressive reduction of the amorphous content in the partially crystalline polymer and to the development of secondary crystallization. The small crystallites produced during the secondary crystallization reduce the mobility of the chain segments thus increasing stiffness and embrittling the material. Spherulites are a type of crystal structure that occur in polymers and similar melts and are characterized by radial growth from a nucleating point leading to spherical symmetry. PHB however forms fairly unique spiral spherulites during crystallization. This has been attributed to helicoidally twisting crystallites growing at a constant angle to the plane of the crystallizing polymer melt[97]. The secondary crystallization of PHB, and its subsequent embrittlement, may be limited by annealing or by creating specific crystallization conditions to limit spherulite growth[98]. Bloembergen et al. observed that the rate of crystallization could be significantly increased by the addition of nucleating agents and consequently reduce spherulite size and thus reduce brittleness and increase elongation at break[99]. Barham and coworkers have also extensively studied the melt and nucleation behavior of PHB with emphasis on spherulite growth inhibition[93].

The physical properties of PHB are listed below (Table 2.1). It is evident that PHB has excellent mechanical properties but is impeded by its crystallization behavior as the ageing of PHB detrimentally reduces its mechanical properties[96]. Also, PHB is thermally unstable during processing and the trend of thermal decomposition has been well documented[100]. But the most important property of PHB is that it is water insoluble and relatively resistant to hydrolytic degradation. This differentiates PHB from most other currently available biobased biodegradable plastics, which are either moisture sensitive and/or water soluble. PHB shows good oxygen permeability and ultra-violet resistance. PHB has been widely established to be biocompatible and nontoxic and hence is suitable for medical applications.

Table 2.1: Physical Properties of Polyhydroxybutyrate

Property	**Value**	**Reference**
Tensile Modulus	1.4-2.2 GPa	[91, 93]
Tensile Strength	40-60 GPa	[77, 81, 91, 98]
Young's Modulus	3.5 GPa	[77, 81, 91]
Extension at break	6-8 %	[81, 91, 101, 102]
Notched Izod Impact	35-50 J/m	[81, 91]
Glass Transition temperature (T_g)	-10 to 10 °C	[81, 93]
Melting Temperature (T_m)	170-179 °C	[81, 91]

The biodegradability of PHB has been reported in various environments such as seawater (350 weeks at 15°C), soil (75 weeks at 25°C), aerobic sewage (60 weeks), anaerobic sewage (6 weeks) and compost (few weeks at 50-65°C)[86, 103].

2.3.5 Polyhydroxyalkanoate Copolymers and Blends

The main strategy to improve physical properties of PHB is the incorporation of other hydroxyalkanoate units to form PHA copolymers. Random copolymers of PHB with other hydroxyalkanoate units having different chain lengths (3-14 carbon atoms) have been reported such as poly(hydroxybutyrate-co-valerate) and poly(hydroxybutyrate-co-hexanoate) to name a few. Table 2.2 shows the properties of typical PHA copolymers with variation in valerate content[77, 81]. It is evident that the properties of PHB improve considerably with addition of valerate component in the polymer chain. This is however a costly technique and reportedly raises the cost of the copolymers significantly[33]. Hence a more economical and consequently more popular approach is blending.

Polymer blends of PHB with biodegradable polymers have also been investigated primarily to regulate the physical properties of PHB. Blends can be defined as physical mixtures of structurally different polymers which may exist as a single phase (miscible blends) or distinct phases (immiscible blends). The physical properties of blends are strongly dependent on this miscibility and hence most work on PHB based blends is concentrated in achieving miscibility.

Table 2.2: Physical properties of Polyhydroxyalkanoate copolymers [77, 81]

Valerate content (%)	T_g (°C)	T_m (°C)	Tensile strength (MPa)	Young's modulus (GPa)	Notched Izod impact (J/m)
0	10	179	40	3.5	50
3	8	170	38	2.9	60
9	6	162	37	1.9	95
14	4	150	35	1.5	120
20	-1	145	32	1.2	200
25	-6	137	30	0.7	400

Thermodynamically miscible blends of PHB have been reported with poly (vinyl alcohol)[104], poly (ethylene oxide)[105, 106], poly (lactide)[107, 108], poly (butylene succinate-co-butylene adipate)[109], poly (ε-caprolactone-co-lactide)[110], poly (butylene succinate-co-ε-caprolactone)[109], cellulose acetate butyrate[111], poly (ethylene-co-vinyl acetate)[112], poly (vinylidene chloride-co-acrylonitrile)[113]. Compatible blends of PHB have been obtained with poly (ε-caprolactone)[114, 115] and polysaccharides[116]. Miscible blends of PHB have been formed with non-biodegradable polymers such as poly (epichlorohydrin)[117] and partly miscible blends are formed with poly (methylmethacrylate)[118], ethylene-propylene rubber [119] and poly (butylacrylate) [120].

2.4 Toughening of Semi-crystalline Materials

Semi-crystalline polymers such as PHAs, the primary matrix polymer of this work, exhibit excellent mechanical properties at room temperature and under moderate rates of deformation. However, if such materials are exposed to high rate of deformation such as impact or low-temperature stress, these materials show drastic failure. These are mainly attributed to the presence of large crystalline spherulites in the polymer. Such spherulites are perfect crystals and undergo brittle fracture when exposed to stress. Also, an initiated crack propagates easily through larger spherulites owing to the absence of pathways to mitigate the crack velocity and hence the entire material fails in a fairly fast and brittle manner. Hence there have been numerous studies on the toughening of semi-crystalline materials and the primary techniques that have come forth from these investigations are elastomeric toughening, plasticization and blending.

2.4.1 Elastomeric Systems

The incorporation of rubber particles into a brittle thermoplastic matrix is known to improve the impact properties and the toughness of the polymer. Under proper conditions and using appropriate compatibilizers, synergistic effects arise to create high impact toughened blends[121-123]. The effectiveness of this toughening mechanism highly depends on the mechanical properties of the matrix, the elastomeric modifier, the dispersion of the modifier, and the interfacial adhesion among the different phases[124-127]. Another critical factor is the particle diameter of the elastomeric phase. Modification to

an optimum diameter improves the impact strength. If the concentration remains constant, the impact strength vs. particle diameter behavior follows a bell-shaped curve and can be used to determine the optimum particle diameter and the elastomer effectiveness but this dependence can be used only as a general guide[128]. Rubber toughening mechanisms developed on conventional thermoplastics have been successfully applied to biopolymers. One such study on polylactic acid (PLA) toughened using rubber prepared from trimethyl carbonate reported 250% improvement in impact properties[129].

2.4.2 Blending

Developing a completely new material by chemical synthesis and characterizing it is a long and uneconomical process. Desired properties can be achieved more economically and easily by blending two or more existing polymers than synthesizing a totally new polymer. Polymer blends are defined as mixtures of two or more polymers and/or copolymers. Blending initially was looked upon as an extension of the process of mixing of additives into a polymer resin. Most equipment intended for that process is the basis for present-day compounding devices.

Blending of two or more polymers results in the production of polymeric composites and polymer alloys. The difference between these lies in the compatibility of the constituents; polymeric alloys contain compatible constituents while polymeric composites consist of incompatible matrix in which the other constituent is embedded. In

both cases the properties of the blend are different from the constituents and this is the main reason for commercial blending. Blending has been looked upon primarily as a process to forcibly melt and mix polymers and additives[130]. Conventional blending processes create blends by breaking up the components using high shear mixer and complex flow fields. This often leads to droplet morphologies. Generally, simple blends of immiscible polymers exhibit coarse unstable phase morphologies that give poor mechanical properties due to lack of interfacial adhesion[131]. The extent to which the initially segregated components are made to break up into smaller parts and disperse amongst themseves is generally considered a measure of how successfully blending and compatibilization have been achieved. The primary goal of blending thus is dispersing minor phase components into a major phase[132].

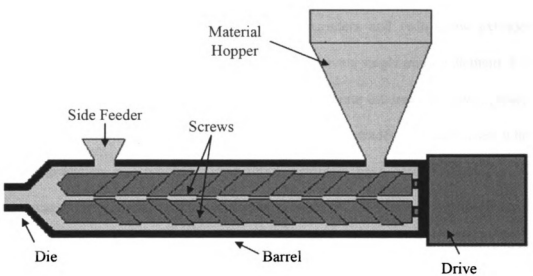

Figure 2.16: Components of a Twin-screw extruder

The primary equipment used for mixing can be classified into mixers and extruders. Mixers consist of plodders, paddle mixers and ribbon blenders used primarily for dry blending. Multishaft mixers were developed to overcome deficiencies in the single shaft mixers like the tendency of the mixture to stick to the rotor and vortex formation[133].

The most extensively used equipment for mixing is the extruder shown in Figure 2.16. It is a device that by the action of one or two rotating screws in a barrel melts and mixes two or more components and at the same time propels them in the forward direction. The components are generally in the form of powders or granules initially and are converted into melts due to the shearing action of the screw and externally applied heat. These melt streams intermingle in the barrel of the extruder and exit through a shaping die.

Extruders are classified as single screw extruders and twin-screw extruders. Single screw extruders, as the name suggests, usually have a single mixing element. Even though a conventional single screw extruder cannot generate intersecting flows, pressure gradients or stress loading of a comparable twin-screw extruder, it is still used where thermal degradation is a problem. Twin-screw extruders have counter-rotating or co-rotating screws, which may or may not be intermeshing. Twin-screw extruders are the most preferred since the melt is dragged an additional distance along the periphery in one revolution thus leading to efficient phase re-orientation[133].

Blending theory indicates that, to achieve a specific property of one component of the blend i.e. toughness, that particular phase has to be continuous[134, 135]. But the

component phases may be vastly different in their rheological properties. Hence for the desired phase to be continuous it either has to be added in large amounts or a compatibilizer needs to be introduced to increase interfacial adhesion. The compatibilizer also reduces the interfacial tension that is responsible for phase separation[136]. Studies on blends of scrap rubber and linear low-density polyethylene (LLDPE) reported the use of maleated LLDPE and epoxidized natural rubber (ENR) as dual compatibilizer which vastly improved the interfacial adhesion[137]. Incompatible binary blend of polylactic acid and starch has been reported to be successfully compatibilized by maleic anhydride[138].

Blends can be termed as miscible or immiscible depending on the sign (positive or negative) of the free energy of mixing of the components. However even for blends termed as miscible, total polymer/polymer miscibility does not exist. The observed miscibility is always limited to a range of independent variables such as temperature, molecular weight distribution, composition, molecular weight, molecular conformation and configuration, pressure etc[128].

The morphology of immiscible blend depends on many factors, primary among these being the interfacial properties and the rheological properties. Many polymer blends are incompatible because the interface between the phases is weak and hence they usually need external compatibilization. This is done to reduce the interfacial tension and thus facilitating dispersion and distribution, stabilize the resulting blend morphology, and to improve interphase adhesion in the solid state[128, 132].

Two techniques to achieve compatibilization have been developed by researchers: addition of a extra component that either is miscible with both phases such as a block

copolymer whose one block is miscible with one component of the blend and the other block with the other component, or a core-shell copolymer that behaves like a multipurpose compatibilizer-cum-impact modifier; and secondly reactive compatibilization that creates interactions between the component phases[128].

Each of these above techniques can give different blends, with different specific properties. The addition of a small amount of block copolymer mainly targets the interfacial tension coefficient, and thus the size of dispersion while the addition of comparatively large quantities of core-shell copolymer targets impact-modification of blends of two brittle, immiscible polymers [132]. Both these techniques involve addition of a third component that needs to be capable of enhancing adhesion between the phases by lowering the interfacial energy and improving dispersion. An example of such a material is a block copolymer, where one block must be miscible in one component polymer but immiscible in the other, and vice versa. The third method is known as reactive compatibilization. This technique aims to create a thick interphase, capable of remaining stable under high stress and strain. Reactive compatibilization works by creating conditions for chemical reactions between the two component polymers in the molten state. This is achieved by introducing a reactive third component with appropriate functional groups or a catalyst in the system during blending.

Reactive compatibilization consists of a series of steps such chain cleavage, end group reaction, formation of bonds and cross-linking. These steps occur during the compounding or processing stage and need to be capable of in-situ compatibilizing the system by generating sufficient amounts of interfacial agents[128]. Reactive compatibilization can be termed as a combination of polymer chemistry with polymer processing.

2.5 Nanocomposites

2.5.1 Polymer-Clay Nanocomposites

The science that enables the understanding and manipulation of matter at a scale of 1 to 100 nanometers is termed as Nanotechnology[139]. This nano-length scale imparts unique characteristics to the materials that are generally absent in the macro-scale and hence nanomaterials and their nanocomposites exhibit distinctive phenomena and consequently have unique applications. In recent years, nanoscale fillers in polymers have generated enormous interest in academia as well as industry because they exhibit improvements in material properties at small loading levels[140-147]. Montmorillonite clay is one such commonly used filler of polymer nanocomposites because layered silicate platelets of the clay can exfoliate as nanoparticles. Dispersion of clay in organic matrices and polymers has been well established in the early 1950's however it was only after the publication of research on polyamide/montmorillonite composites with impressive materials properties in the early 90's that these polymer nanocomposites attracted strong interest[148, 149]. This was augmented by Giannelis et al. that reported melt mixing of polymers with clays without the use of organic solvents[150]. Since these breakthroughs, the hunger for industrial applications has motivated vigorous research, which yielded nanocomposites with improvement of many physical properties when compared with virgin polymers or conventional composites. Nanocomposites also exhibited flame-retardancy and dramatic improvements in barrier properties that could not be realized by conventional fillers[140-147].

Nanotechnology research is a very lucrative and well-funded area, especially in developed countries. The United States government has over a billion dollars of federal funds invested in nanotechnology research in 2005 with non-federal funding estimated to be double of this amount. Similarly, the European Union and Japan have significant funds in nanotechnology research[151]. The polymer-clay nanocomposite market is currently estimated to be $75 million with a predicted growth of 25 % per year growth consequently touching $250 million in 2008[152].

Polymer nanocomposite technology has taken great strides to enter the commercialization stage and a few examples are:

- Automotive giant General Motors (GM) in 2002 initiated use of polymer-clay nanocomposites in automotive parts in some of the models. Montell North America, GM and Southern Clay have jointly developed Thermoplastic polyolefin (TPO) based nanocomposites for use in the molding of body-side claddings and step assist parts for specific models of vans[153]. GM also introduced nanocomposite body side molding in the 2004 Chevrolet Impala and some parts of the 2005 GM Hummer[154].
- Other automotive manufacturers have also started use of nanocomposites in their vehicles. Honda Motors have used polypropylene nanocomposite in seat backs of the 2004 Acura TL and with likely further usage for interior center consoles in other models[155]. Mitsubishi Motors has collaborated with Unitika Co. of Japan to develop Nylon 6 nanocomposites to be used in engine cover on its GDI models.

Nylon-clay nanocomposites have also been used by Toyota Motor Company for manufacturing the timing-belt cover on the Toyota Camry[156].

- Materials compounders such as PolyOne and Colormatrix have successfully launched nanocomposite masterbatch formulations[155].
- An estimated 5 million lb of nanocomposite materials will be used in packaging in the next five years with beer packaging leading the way (3 million lbs.) followed by meat packaging and carbonated soft drinks. This is expected to exponentially increase to almost 100 million pounds by 2011. Nylon-nanoclay nanocomposites are already used commercially in Europe for alcoholic beverage bottles with limited success in the US market[152].

The above examples are just the preview of technology to come to the market and a more elaborate list of nanocomposite suppliers and the targeted markets is given in Table 2.3. [154, 157]

Table 2.3: Polymer nanocomposite suppliers and applications[154, 157]

Supplier	Tradename	Nanoparticle	Base Polymer	Application
Bayer	*Durethan*	Organo-clay	*Nylon 6*	Packaging
Clariant		Organo-clay	*PP*	Packaging
Creanova	*Vestamid*	Nanotubes	*Nylon 12*	Electronics
Elementis	*Bentone*	Organoclay	-	Modified Clay
Foster Corp.	*Nanomed*	Organo-clay	*Nylon 12*	Medical
GE plastics	*Noryl GTX*	Nanotubes	*PPO/Nylon*	Automotive
Honeywell	*Aegis*	Organo-clay	*Nylon 6*	Packaging
Hyperion		Nanotubes	*PETG, PP, PC, PBT, PPS*	Electronics
Kabelwerk Eupen		Organo-clay	*EVA*	Wires/ cables
Nanocor	*Iperm*	Organo-clay	*Nylon 6, PP*	Packaging
Nycoa	*NanoTUFF*	Organo-clay	*Nylon 6*	Automotive
Polymeric Supply		Organo-clay	*UPE*	Marine
RTP		Organo-clay	*Nylon 6, PP*	Electronic
Showa Denko	*Systemer*	Clay, mica	*Nylon 6, Acetal*	Flame retardant
Southern Clay	*Cloisite*	Organoclay	-	Modified clays
Ube	*Ecobesta*	Organo-clay	*Nylon 6, 66, 12*	Automotive
Unitika		Organo-clay	*Nylon 6*	Multi-purpose
Yantai Haili		Organo-clay	*UHMWPE*	

2.5.2 Clay

Owing to their natural abundance, smectite clays have been incorporated as fillers in many engineering and commodity polymers and have also been used in extensive fundamental studies for nanocomposites[140]. Nanoclays are sheet unit aggregated silicate particles with length dimensions that vary from 300 A° to several microns depending on the particular clay and 1 nm thickness for each individual clay sheet[141, 147]. In a 2:1 layered silicate, the sheets have three layers: an inner octahedral layer of alumina sandwiched between outer tetrahedral layers of silica[158]. These layers, due to van der Waals forces, organize themselves in a parallel fashion to form stacks with a regular spacing between them, called interlayer or gallery. The intercalation of polymer chains into this gallery to exfoliate the individual clay platelets is the focus of most research on clay-based polymer nanocomposites.

Clay used in polymer-clay nanocomposites is predominantly montmorillonite. Montmorillonite is part of the smectite family of minerals obtained from bentonite rock. Bentonite is abundant in nature and is formed due to mechanical and chemical weathering of volcanic rock in alkaline environment. Bentonite comprises of many sheet-like minerals such as saponite, hectorite, montmorillonite etc. witm montmorillonite being predominantly used due to its high aspect ratio, cation exchange capacity and layered structure[158, 159].

Montmorillonite structurally is an octahedral sheet of aluminum/magnesium hydroxide sandwiched by 2 tetrahedral silicate sheets (Figure 2.17)[160]. This arrangement is called as a 2:1 layered silicate structure. Montmorillonite is chemically represented as [$M_x(Al_{4-x}Mg_x)(Si_8)O_{20}(OH)_4$] where M stands for monovalent cation and x is the degree of isomorphous substitution (between 0.3-1.3)[159]. The aluminum or magnesium ions in the clay gallery are capable of isomorphic substitution. The Al^{+3} or Mg^{+2} are isomorphically substituted in these structures by cations having lesser positive charge (Mg^{+2},Fe^{+2}or Li^{+1}) thus generating a negative charge. This negative charge is counterbalanced by alkali or alkaline earth cations in the clay structure. These cations can be exchanged with cationic surfactants or similar organic species to modify the clay. This capability to exchange cations is termed as the cation-exchange capacity (CEC) of the clay. It is a measure of the ability of the clay to accept surface modifications and is expressed in mequiv/100 g of clay. For example, Montmorillonite has a CEC of 110 mequiv/100g and Saponite has a CEC of 86.6 mequiv/100g[140, 159].

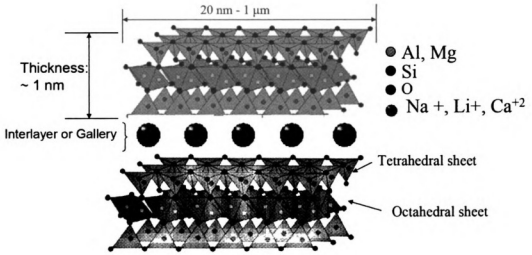

Figure 2.17: Structure of Montmorillonite Clay (Redrawn after Ref. 160)

2.5.3 *Modification of Clay*

The surface of the silicate clay platelets is inherently hydrophilic and thus it must be modified by surface treatments to make the platelet compatible with the organic polymer[158]. Earlier studies in clay-polymer systems used unmodified clay and reported not significant improvement in properties of the resulting composites even at 50 wt % loadings[159]. The research group at Toyota that pioneered polymer-clay nanocomposites initiated the use of surface modified clay in polymers that led to development of high-performance materials[148, 149, 159].

There are different ways to modify clay surfaces; adsorption, ion exchange with inorganic cations and cationic complexes, ion exchange with organic cations, edge-binding of inorganic and organic anions, grafting of organic compounds, reaction with acids, polymerization, dehydroxylation and calcination, delamination and reaggregation, and physical treatments such as lyophilisation, ultrasound, and plasma[161-170].

The most popular and commercially used method of surface modification of layered silicates is ion exchange. Weiss in 1963 reported the modification of montmorillonite clays by ion exchange of the clay cations with n-alkylammonium ions[171]. He reported the increase in basal spacing of montmorillonite as a function of the length of the alkyl chains on the n-alkylammonium ions. The methodology adopted for modification has not changed much in principle over time with changes being in the different modifiers used. The inorganic clay particles are mixed with a solvent (for the modifier) to create a fairly stable suspension following which the modifier is added to this suspension and the reaction is carried out for determined time(Figure 2.18). The

slurry is washed with the same solvent a number of times, decanted and then dried to remove excess solvent as well as unreacted modifier. Surface ions are de-adsorbed from the inorganic material and the "exchanged" modifier molecules adsorb onto the clay surface. Large organic cations almost stoichiometrically replace inorganic ions thus giving organically modified clay[158].

Another popular method of surface modification is edge grafting that targets the hydroxyl functionality on the clay surface for modification. Most commonly used modifiers are organo-silanes and their derivatives and the reaction methodology is similar to ion exchange wherein the modifier is added to a suspension of the inorganic particles in a solvent and after the reaction is complete, excess modifier is washed off and solvent is dried off. The organic species are adsorbed to the outer surfaces and bound to the edges of the clay via condensation with edge hydroxyl groups[172]. In some cases, edge functionalization is used to twice-functionalize clay meaning a clay already primarily

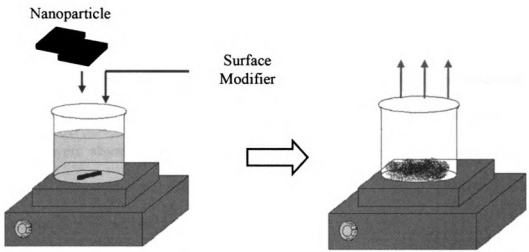

Figure 2.18: Surface Modification Technique

functionalized using ion exchange of alkyl-metal compounds is further functionalized by using edge modifiers[173].

Another less common method of clay modification is acidification with hot mineral acid in order to impart surface acidity to the clay to achieve increased adsorption and catalytic properties. In this method, the interlayer cations are replaced with H+ ions followed by dissolution of certain ions in octahedral and silicon tetrahedral sheets. The acid concentration determines the modification as low acid concentration affects octahedral sheet while high acid concentration affects tetrahedral sheet[174].

Clay is also modified by pillaring by exchanging cations between the clay layers with large inorganic metal hydroxycations. These hydroxycations are oligomeric and are formed by hydrolysis of metal oxides or salts and undergo calcination to be decomposed into oxide pillars. These pillars keep the clay layers apart and create interlayer and interpillar spaces, thereby exposing the internal surfaces of the clay layers[175].

Monomer intercalation is also a type of surface modification but is more generally considered as a type of nanocomposite processing method than a pure modification method. In this method, monomer and inorganic particles are mixed thoroughly and monomer layers absorb onto the inorganic particle surface and in between adjacent layers. The monomer is polymerized using surface groups of the clay as part of the reaction and thus increasing the inter-particle spacing[148, 149].

2.5.4 Processing of Polymer Nanocomposites

The best properties of polymer nanocomposites can be achieved primarily if the following factors act synergistically: nanoparticle-matrix interaction and dispersion/distribution of the nanoparticles in the polymeric matrix. The first factor is dependant on the formulation and chemistry of the surface and the polymer matrix while the second is affected by the preparation technique used for fabricating the polymer nanocomposites. Before reviewing the processing techniques, it is necessary to understand the different morphologies possible in polymer nanocomposites. The three main possible structures in polymer nanocomposites are: Agglomerated, Intercalated and Exfoliated (Figure 2.19). If the nanomaterial tends to agglomerate and not disperse at all in the polymeric matrix, it is termed as agglomerated or immiscible morphology. This may be due to lack of interaction between polymer and the nanoparticle surface or improper processing. Such structures tend to give poor properties as the true nanoscale nature of the nano-filler is not realized and it behaves like a macro-filler. For example, in

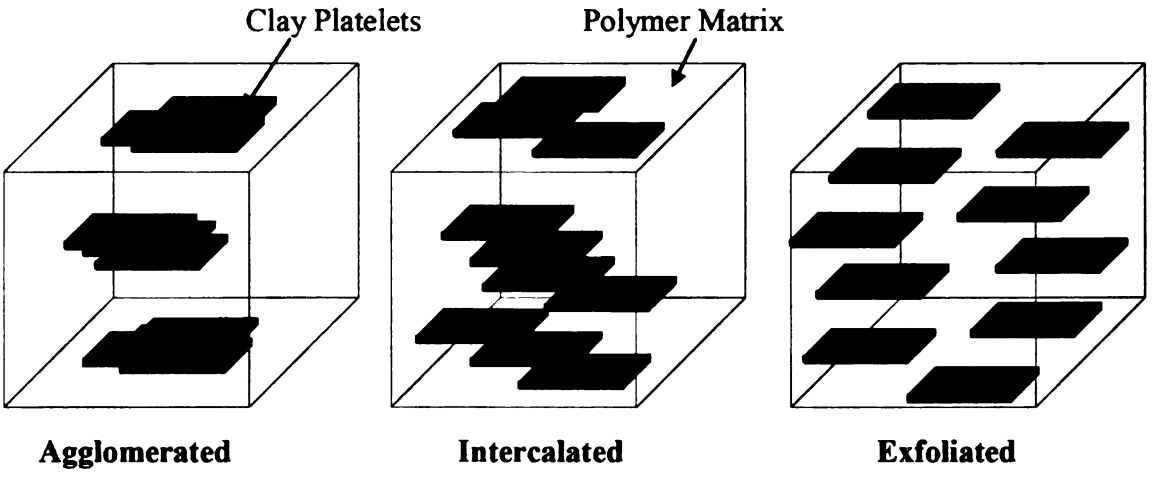

Figure 2.19: Different types of possible morphologies in PolymerNanocomposites

the early work on clay-polymer composites, unmodified silicate clay minerals were added to a polymeric matrix and they tended to agglomerate and acted as macro-sized fillers and could not show any improvement in properties even at loadings as high as 50 wt %. But these very clays, when appropriately modified, get dispersed as nanoscale-level reinforcements and thus show dramatic improvement in properties even at only 2-7 wt % loading[159].

The second possible morphology is called the intercalated structure. In this, the polymer chains penetrate or intercalate in between the nanoparticle layers thus causing individual layers to be separated out. This mechanism gives an intimate contact between individual nanoparticles and the polymer matrix as well as distributes and disperses the nanoparticles. This morphology can to a great extent give the high-performance properties due to its ability to significantly separate out individual nanoparticle layers.

The third and the most desired structure is called the exfoliated morphology. In this, each individual nanoparticle is separated as well as distributed relatively far apart from one another thus giving a perfect dispersion. The resulting nanocomposites will potentially have the best properties owing to the high surface area available for nanoparticle-matrix interaction in each nanoparticle. For example, a few grams of montmorillonite clay platelets have the equivalent area of an entire football field if each platelet is completely exfoliated[176].

Several strategies have been considered to prepare polymer-layered silicate nanocomposites and they include the following three main processes: In-situ Polymerization, Solution processing and Melt Intercalation.

2.5.4.1 In-situ Polymerization

The first polymer-clay nanocomposites, created by group in Toyota, used this method of fabrication[148, 149]. In this method, the monomer and organically modified nanoclay are mixed together intimately. The monomer enters into the interlayer gallery of the clay and swells the clay resulting in a well dispersed and intercalated suspension. Following this intercalation of the monomer, the polymerization process is carried out which causes the clays to further separate out. The completely polymerized material gives a well exfoliated morphology. In some cases, the surface modifier on the clay is used as the initiator for the polymerization reaction. Polymerization of ε-Caprolactam, the monomer for Nylon-6, in presence of clay modified with ω-amino acid follows this methodology. The ε-Caprolactam monomer enters the modified clay gallery and pushes the clay platelets apart. The ω-amino acid modifier on the clay surface acts as a catalyst and opens the ε-Caprolactam ring that further undergoes polymerization to give Nylon-6. The Nylon-6 polymer chains are obviously longer in length and thus push the clay platelets further apart as they polymerize thus giving an extremely well-exfoliated morphology of the final nanocomposites[148].

Monomer intercalation generally yields the best-exfoliated morphology in nanocomposites but it has drawbacks. Not all polymers can be easily polymerized from their monomers and hence the possible polymer matrices are limited. For example polyethylene is synthesized from gaseous state using catalysts and this process cannot be recreated in ambient conditions nor can the clay be added at any stage. Also this is a

process that can only be done by the polymer manufacturer and then sold as masterbatches to the convertor and hence has limited flexibility in terms of formulations and process changes if desired by the user. This method is frequently used for processing of thermoset polymer based nanocomposites.

2.5.4.2 Solution Technique

The solution technique, as the name suggests, involves dissolving the polymer matrix and adding a suspension of the clay to this solution followed by evaporation of the solvent. The solvent system is so chosen such that it can dissolve the polymer as well as can swell the clay silicate layers. The organically modified clay is first dispersed in the solvent and the solvent enters into the inter-clay gallery and swells the clay leading to a well-distributed suspension. Sometimes the dispersion is also sonicated using ultrasound waves that further separate out individual clay layers. The matrix polymer is dissolved in same solvent in separate vessel (generally 1 to 5 % by weight solution) and then the polymer solution and the layered silicate solutions are mixed. The dissolved and mobile polymer chains intercalate into the clay gallery and displace the solvent. The final step is the removal of solvent and casting the resulting nanocomposites into desired shape. An example of this technique is the casting of polyimide-clay nanocomposite films. One such work reported nanocomposite fabricated by dissolving polyamic acid and organoclay were in dimethylacetamide (DMAC) followed by solution casting. The DMAC was removed to obtain polyimide-clay nanocomposites that exhibited significant improvement in certain barrier properties[148].

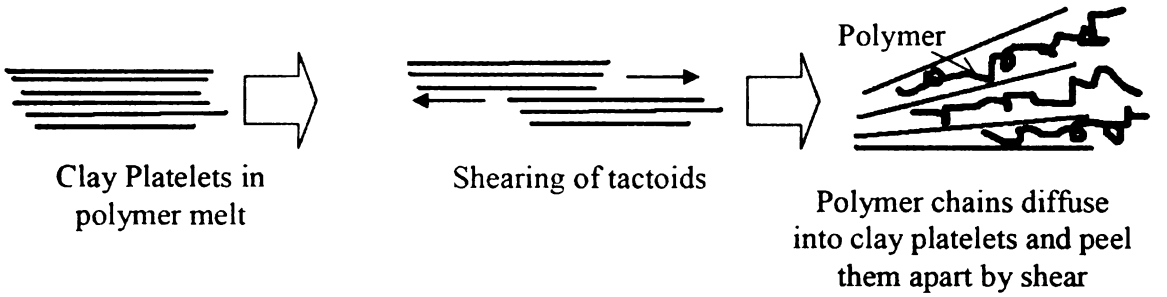

Figure 2.20: Effect of shear in melt intercalation processing of nanocomposites

(Redrawn after Ref. 178)

The positive aspect of this method is the excellent dispersion owing to the swelling of the clay in the solvent. The dissolved polymer chains also can move freely into the clay gallery and hence intercalation is achieved. This method is generally used for laboratory-scale experiments owing to the solvent removal and subsequent disposal issues. Also the solvent removal is time-consuming and is not economical on a commercial scale.

2.5.4.3 Melt Intercalation

This is by far the most popular method of polymer nanocomposite fabrication. Polymer is melted in a melt compounding instruments, such as an extruder, and the organoclay platelets are introduced into the molten polymer.

The shear forces induced by the movement of the polymer break up the clay tactoids into individual platelets[177, 178].

The tactoids peel apart by a combined diffusion/ shear process that ultimately gives a well exfoliated and dispersed nanocomposite (Figure 2.20)[178]. This nanocomposite material is extruded, pelletized and further processed into the desired products. This process is favored for commercial use primarily due to absence of organic solvents as well as its compatibility with current instruments. Numerous instruments can be used for melt intercalation such as single-screw extruder, brabender plasticorder, etc. but studies have reported the best morphologies are generated when a counter-rotating

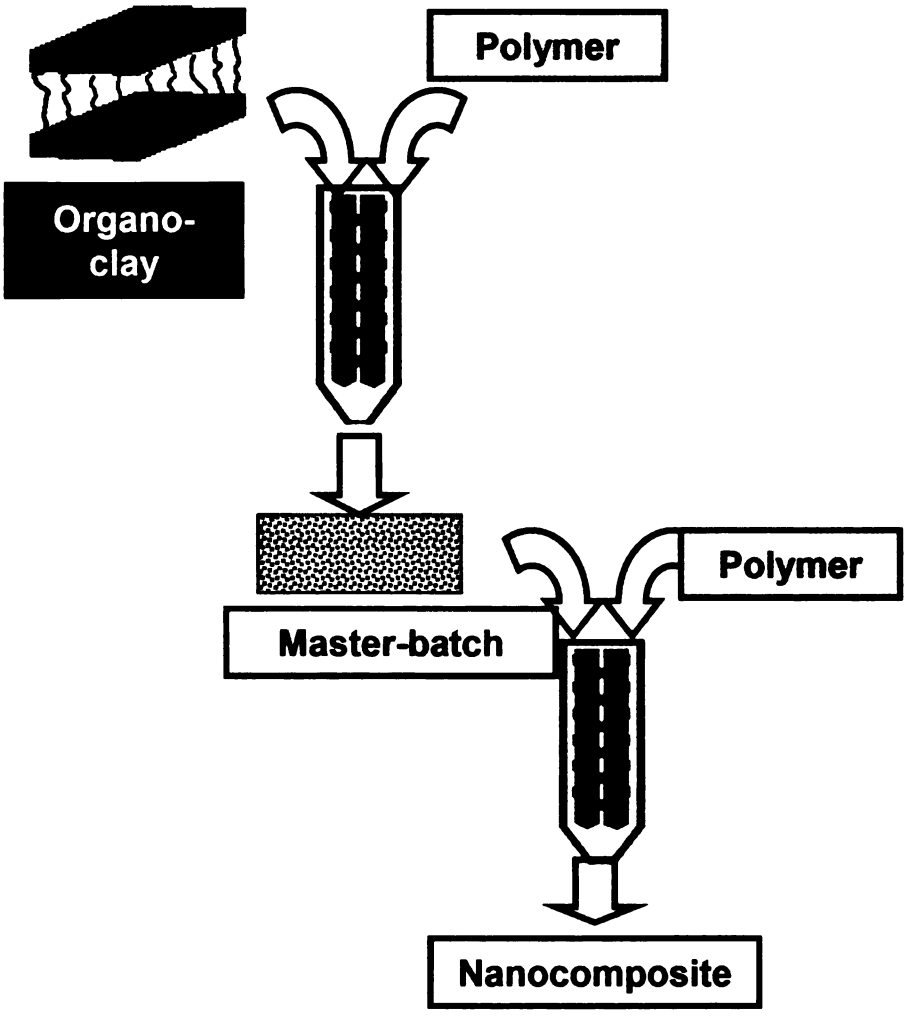

Figure 2.21: Masterbatch method of Nanocomposite Fabrication

non-intermeshing twin-screw extruder is used[177].

Nanocomposite fabrication by melt intercalation can be done by two ways: direct blending or masterbatch blending. In direct blending, clay is introduced into molten polymer directly at the desired composition level in a one-step method. In masterbatch blending, first a high-load masterbatch is prepared (~20-30 wt % nanoclay in polymer) which is let-down into final composition (2~5%) by adding polymer again in a second step (Figure 2.21). This method promotes addition mixing and subsequent exfoliation of the clay platelets due to the increased mechanical shearing. This masterbatch method is especially useful for adding other additives such as maleated compatibilizers[179].

2.5.5 Properties and Applications of Polymer-clay Nanocomposites

Polymer-clay nanocomposites primarily show improvement in mechanical properties and gas barrier properties with some reports of additional improvements in related properties such as thermal stability and biodegradability.

Okada et al of Toyota Research Laboratories reported the first successful polymer-clay nanocomposites in 1990[149]. They were able to achieve 41 % improvement in tensile strength, 83% improvement in tensile modulus and 99° improvement in heat deflection temperature over un-reinforced Nylon 6 in their nanocomposites containing only 5.3 wt.% of modified clay[149]. Current commercially available Nylon 6 nanocomposites containing 2 - 6 wt % clay as supplied by Nanocor, Honeywell plastics and Bayer AG reportedly show similar trends for mechanical and thermal properties

improvements as compared to virgin nylon 6. Nanocor also has reported 3 times reduction in gas permeability for the same materials at 6 wt. % clay loading. They claim that oxygen barrier of their proprietary Nylon MXD6 nanocomposites improved by 80% as compared to neat Nylon MXD6 and carbon-dioxide barrier improved by 60%[180, 181]. Foster Corporation, a materials company, supplies a line of specialty Nylon 12 resins reinforced with nanoclay. These materials reportedly exhibit 65% increase in flexural modulus and 30% increase in HDT at 10% nanoclay loading[182].

Polyolefin based nanocomposites such as polypropylene (PP)-montmorillonite nanocomposites have been reported to exhibit 75-95% improvement in mechanical properties and 30% improvement in HDT combined with gas permeability reduction by 25-50% and water vapor transmission reduction by 10-15%[181]. Comparison of PP-clay nanocomposites containing approximately 4 wt % clay with PP-talc composites (20–40 wt % talc) showed that mechanical properties for the nanocomposites improved by 20% over virgin PP and were comparable with talc-filled PP and yet had lower density[183]. Owing to the nonpolar nature of PP, nanocomposites of PP generally utilize maleated PP as a compatiblizer[179]. One such study using 20% PP-g-MA as compatibizer showed 126% improvement in mechanical properties over neat PP as compared to only 34% for nanocomposites without compatibilizer[184]. PP-clay nanocomposites have been widely commercialized and are used for many diverse applications such as automotive components, packaging etc. Polyone Corporation manufactures the Nanoblend® brand of nanocomposites that have 30-40% weight loadings of nanoclay from clay supplier Nanocor in a polypropylene matrix. These are supplied to manufacturers that utilize them

after letdown to 4% clay loading and have shown significant improvement in flexural properties and HDT[185].

Polyethylene (PE) nanocomposites have been studied by many researchers mainly targeting thermal and mechanical property improvement. Wei and coworkers have reported 107% improvement in tensile modulus of PE reinfoced with 5.43 wt% clay[186]. Researchers at University of Science and Technology of China have shown that the heat release rate (HRR) is reduced by 32% in PE-nanocomposites with low silicate loading (5 wt.%)[187]. Clay supplier Nanocor has reported PE-nanocomposites with 6% wt clay which showed 72% improvement in flexural modulus and 22% reduction in oxygen transmission rate[181].

Scientists at the National Institute of Standards and Technology have determined successfully that nanocomposites behave like novel flame retardants. Nylon-6 nanocomposites with 5% clay loading showed 63% reduction in heat release rate. These nanocomposites also showed improved physical properties and slowed the escape of volatile products which were generated by decomposition[188].

Numerous studies on nanocomposites of biopolymers have been reported in literature with matrices such as PLA, PHB, PHBV, Starch, PCL, PBAT etc. with noteworthy achievements in improvement of mechanical, thermal and barrier properties[189, 190]. The most interesting result as related to biodegradable-polymer based nanocomposites is the increase in rate of biodegradation due to presence of nanoclay as observed by some researchers. Ray et al at Toyota Technological Institute in 2002 studied nanocomposites of PLA and octadecylammonium cation modified

montmorillonite with α,ω,-Hydroxy-terminated oligomer of PCL as compatiblizer. They observed that the nanocomposits exhibited significantly increased degradation rates than virgin PLA under the same conditions. The authors hypothesized that the terminal hydroxylated edge groups of the silicate layers started heterogeneous hydrolysis of the PLA matrix after absorbing water from compost thus increasing the biodegradability[191]. An earlier publication by this group describes this preparation and characterization of a novel porous ceramic material via the burning of the PLA nanocomposite while yet another study reports the ability to enhance the rate of biodegradation of PLA by choice of organically modified layered silicate[192, 193].

2.6 Composites

Composites by definition are a combination of two or more materials that create one new material which shows better or superior properties than the parent constituents especially in terms of economic values and mechanical properties. Composites are primarily made up of two main components: the matrix or the binder; and the reinforcement or the filler. The matrix can be glue, polymer resin etc. while examples of reinforcements are fibers, inorganic fillers etc. One such popular organic filler is Talc.

2.6.1 Talc

Talc is a benign naturally occurring mineral used as filler in plastics industry to improve the performance and cost reduction of final product[194, 195]. Talc is a hydrated magnesium silicate with the chemical formula $Mg_3Si_4O_{10}(OH)_2$ and is hydrophobic and extremely resin compatible[194]. Talc platelets possess a layered structure with the middle layers of MgO and $Mg(OH)_2$ sandwiched between two silicate layers (Figure 2.22)[196]. This layered structure is very similar to clay however talc has lower aspect ratio than clay (5-20 for talc Vs 100-150 for montmorillonite clay)[197].

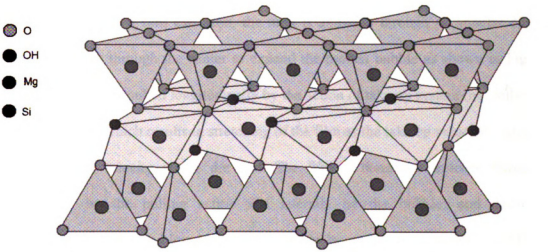

Figure 2.22: Talc Structure (Redrawn after Ref.196)

2.7 Flexible Packaging

2.7.1 Polymer Films

Of the over 27 billion pounds of polymers were processed into flexible packaging in 2004 and the United States had a 24.2 % share of that market[198]. The majority of this flexible packaging market is polymer films. Polymer films are primarily produced by blown film extrusion or by chill-roll-casting depending on the processing parameters of the constituents or on desired properties.

In blown film extrusion, the melt is extruded through an annular die in which air is blown through the center to expand the molten bubble as shown in Figure 2.23. This extrudate is pulled longitudinally by the action of take up system (nip rolls and collapsible guides) which results in stretching of the film as the take up velocity is greater than the average velocity at the die exit. The film is therefore stretched biaxially (longitudinally by the pulling action and laterally by the bubble) and develops orientation. Cooling air is blown along the bubble by an air ring placed around the outside of the die. The solidified film is then taken up on a roller and either slit to make flat film or sealed and cut to make bags[133].

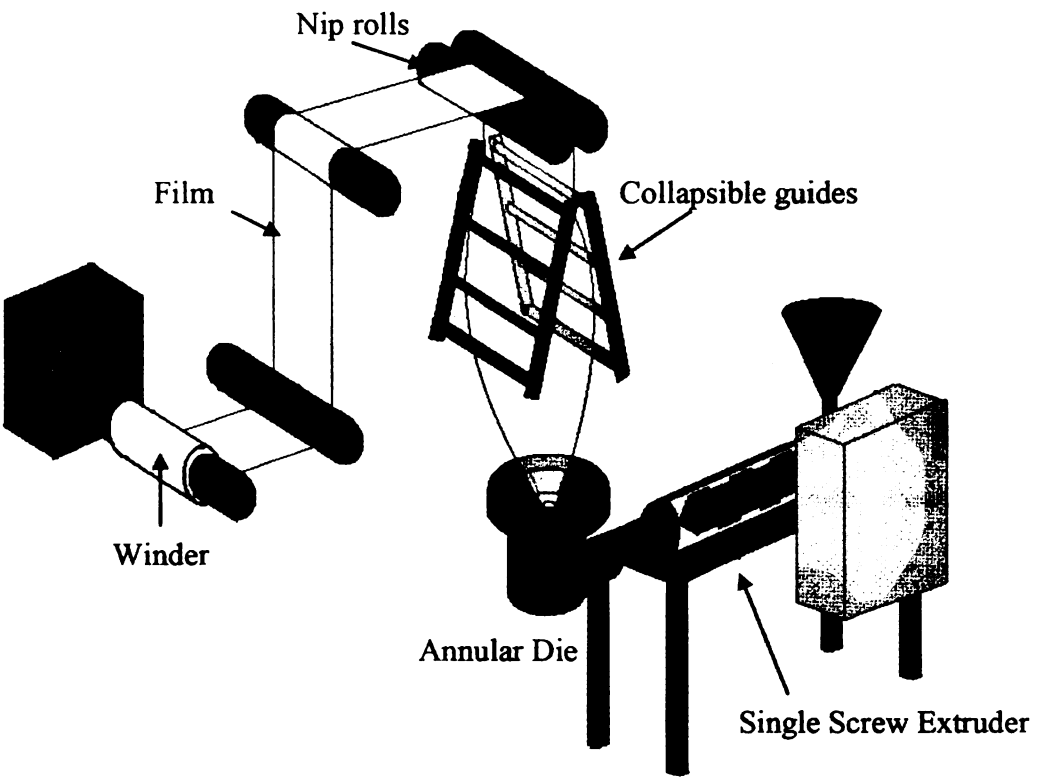

Figure 2.23 Blown Film Extrusion

Extrusion of the melt through a narrow slit die onto a chill roll is another process to make films and is called casting as shown in Figure 2.24. The film can be drawn to required thickness in the melt state and cast, i.e., cooled below solidification temperature on a large diameter chill roll. The production rate of casting processes is very high as the cooling is faster than in a blown film process. This also has the advantage of casting thicker films or sheets than blown film extrusion. The die used is a coat hanger die unlike the annular die used in blown film extrusion[133].

Flexible polymer packaging is dominated by polyethylene, PET, PVC, EVOH and their multilayer films and thus primarily non-biodegradable polymers and hence these are disposed by incineration or in landfills. Hence there is a need to develop

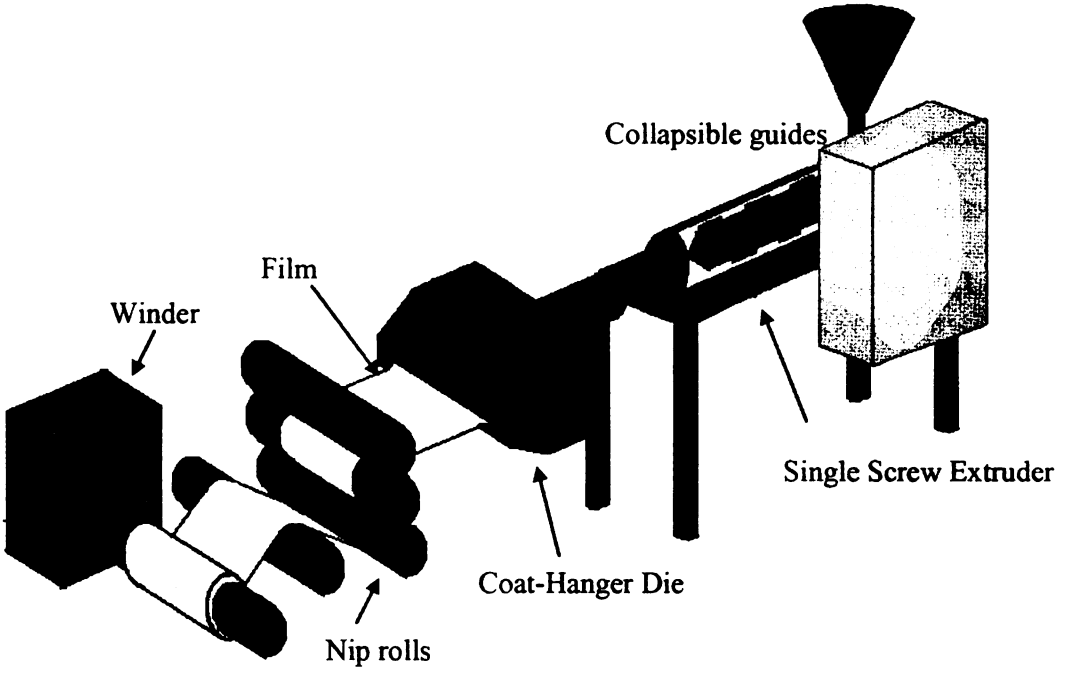

Figure 2.24: Cast Film Extrusion

biodegradable as well as biobased flexible packaging as sustainable and eco-friendly alternatives.

2.7.2 Biodegradable Polymer Films

Even though biodegradable flexible packaging is a very promising option, only a few amongst all the biopolymers discussed in section 2.2 are used for flexible packaging. The prime examples of this are the biodegradable polyesters (PCL, PBS) and copolyesters (PBAT, PTAT, PBSA) that are used for flexible packaging. BASF, Showa, Eastman and other suppliers have launched successful lines of biodegradable packaging products based on such materials[11, 25, 36]. But all these polymers are still non-renewable

resource based and not biobased. All the biobased biopolymers such as polysaccharides, PLA, PHAs etc. lack the toughness and elongation required of flexible packaging and hence cannot be used unless they are significantly modified or blended with some of the non-biobased biodegradable polymers. Examples of such blends are the Ecovio® line of PBAT-PLA blends from BASF and numerous starch-based blends such as PCL-starch, PBAT-starch, PTAT-starch[35, 52, 72].

2.7.3 Barrier

Many foods and perishables are subject to deterioration in quality and ultimate spoilage by exposure to oxygen and moisture. Plastics, which are the most widely used packaging material, are susceptible to oxygen and water vapor permeation. A barrier material is defined as having an acceptably low permeability to gas transfer over the shelf life of the package contents. The permeability P of a material can be quantified by the equation:

$$P = Q\,L / t\,A\,\Delta p \qquad (2.1)$$

where Q is the amount of gas transmitted in the given interval of time,t ,and A is the area of the film exposed to the diffusing gas, Δp is the difference in pressure across the film surfaces and L is the film thickness. Permeability has many different units among which the more generally used are (cc-mm/m^2-day-atm) and (cc-mil/100in^2-day-atm)[199]. The permeability P, diffusivity D and the solubility S of the permeant are interlinked by equation 2.2.

$$P = DS \qquad (2.2)$$

Equation 2.2 provides much of the basis for barrier design and is used extensively. Substances are adsorbed by contact with the surface of the material and this depends on the solubility coefficient which is in turn defined by the morphology and chemical nature of the material and also the temperature. Permeation is thereby the transport of substance through a substrate involving adsorption and condensation on one surface, solution into the substrate, diffusion to the other surface and dissolution on the other side. Because of limited polymer chain mobility, penetrant molecular size and shape are important parameters in determining the diffusion coefficient. Crystallinity affects the mechanical and barrier properties of a polymer significantly and a good barrier material should have low permeability to penetrants. A crystalline region is a perfect barrier and is assumed to have zero permeability. Thus all the diffusion in a polymer occurs in the amorphous regions. Hence the actual permeability P_a of a polymer can be related to the theoretical permeability P of the polymer by a generic relation:

$$P_a = P\,(1-\chi_c) \qquad (2.3)$$

Where χ_c is the crystalline fraction or the percent crystallinity of the polymer. Hence it is seen that the permeability of the polymer will decrease with increased crystallinity[199].

Barrier films commonly use three strategies to reduce gas permeation. First, they can be made of organic or inorganic polymers like cellulose which are highly impermeable to the solutes of interest. Low permeability can be achieved by a low solution coefficient which excludes target solutes. Low permeability can also result from

a small diffusion coefficient due to a highly crystalline polymer film. Where increased barriers are necessary, it is more economical to incorporate a thin layer of highly efficient barrier between other structural polymer layers than to simply increase the thickness of the monolayer. For example, to equal the oxygen barrier of 1 mil of a high barrier material like polyvinylidiene chloride, it would require 2500 mils of polypropylene or 50 mils of polyethylene terpthalate or 10 mils of Nylon 6[200]. In such cases a multilayered composite is preferred in spite of the high equipment cost. The second strategy for reduced gas transport is to add impermeable flakes to a polymer matrix. When these flakes are oriented perpendicular to the film surface, the effect is small, comparable with the small effects of impermeable spheres. However, when the flakes are oriented parallel to the film surface, the amount of gas transport can be reduced ten times or more because diffusion now follows a tortuous path[201].

The third strategy for reducing permeability is to incorporate reactive groups within the films. Studies of this mechanism, which began in pharmacy, include reversible and irreversible reactions. They include catalysts and non-linear adsorbents. In almost all cases, gas transport is found to be reduced in unsteady state, often dramatically[202].

A barrier material should be capable of giving low permeability and at the same time it should have good mechanical strength, insensitivity to UV degradation, be impervious to crazing and cracking and also be cheap and easily processable[199]. All these properties are not available in a single material and hence manufacturers combine layers of different materials, each possessing a unique property, to create good barrier materials. This has limitations due to the individual processability and properties of the

constituent polymers. Out of the three strategies explained above, the second one concerning distribution of flake-like additives oriented parallel to the film surface is of interest in this study.

2.8 Thermoplastic Starch

2.8.1 Starch

Starch, as explained earlier in the section 2.2 on different biopolymers, is an inexpensive, annually renewable material derived from plants. Starch is a very commonly used ingredient of edible films and this section looks at the film-forming properties of starch. The linear amylose portion of starch determines its ability to form networks and consequently its thermoplasticity. The branched Amylopectin inhibits gelation and hence limits the thermoplasticity of starch.

2.8.2 Plasticized Starch

All starches contain amylose and amylopectin, at ratios that vary with the starch source and this variation provides a natural mechanism for regulating starch material properties. Amylose is the linear portion of starch (Scheme 2.3) while Amylopectin is the branched portion of starch (Scheme 2.4). Amylose content varies from 17% (root and tuber) to 30% (cereal starches). Higher amylose content generally gives better films due

to the ability of the linear chains to form gel-like structures[18]. However, high amylose starches are comparatively costlier and used more as films than filler materials.

Starch exhibits a unique property called gelatinization that involves breaking of the hydrogen bonding by heat and allowing water or a non-volatile plasticizer such as glycerol or other polyols to enter[19]. This plasticizer disturbs the granular organization of the starch molecules and makes new H-bonds with amylose and amylopectin forming a gel-like structure[18]. This is termed as plasticized starch and in its most general form is a combination of starch, a high-boiling and non-volatile plasticizer and water that has undergone thermo-mechanical treatment such as extrusion processing. One of the most commonly used plasticizers for starch is glycerol or glycerine. Currently, the upcoming biodiesel industry is widely promoting alternative uses of glycerol that is a byproduct of biodiesel production. Rising petroleum-based fuel costs are driving up the demand for biodeisel and as biodiesel production increases, consequently the production of glycerol increases. Federal agencies have identified the need for this glycerol to be used or it may drive up the price of biodiesel[203]. Hence utilization of glycerol in plasticization of starch is considered to be benefiting society by supporting the biodiesel industry.

Plasticized starch is a very commonly used material in edible films but its use as a biodegradable packaging material is limited by its poor physical properties. These poor physical properties are mainly due to the high hydrophilicity of plasticized starch; it actually dissolves in contact with water. The solution for this has been well investigated and there exist many references for blends of plasticized starch with biodegradable polymers such as PCL as the blending partners. Starch-PCL blends were first reported by

Koenig and Huang in 1995 followed by wide-spread resrach and commercialization in this area[19, 22, 52, 54-57]. Narayan et al have successfully chemically modified starch materials such as cationized starch, propoxylated starch, starch containing charged and uncharged functions and bioengineered starches with altered patterns of branching (amylopectin and phytoglycogen) into thermoplastic starch[52, 204-206]. The Mater-Bi range of products as sold by Novamont of Italy are starch-PCL or starch-PVOH systems[35]. TPS based blends are also very popular as mulch bags owing to their excellent biodegradability.

2.9 Biodegradation

Biodegradation, as defined earlier, is the natural process of decomposition facilitated by biochemical mechanisms. Biodegradability of any material requires some parameter or set of parameters that can be measured and related to the rate and extent of biodegradation of the material being tested. Under aerobic conditions, biodegradation of an organic substrate can be expressed as following an iterative reaction:

$$C_{substrate} + O_2 \text{ --------> } CO_2 + C_{cell\ biomass}$$

$$C_{cell\ biomass} + O_2 \text{ --------> } CO_2 + C_{cell\ biomass}$$

If the experiment to measure biodegradability continues over many generations, cell biomass is metabolized by the bacteria species, and as the substrate is depleted and predation

continues, the carbon originally present in the substrate will be largely mineralized to carbon dioxide[4].

These above reactions occurring during degradation have been used to develop test methods to quantify the percent biodegradation of test material. The American Society for Testing and Materials (ASTM) has developed the key standard ASTM D5338-93 for determining aerobic biodegradation of plastic materials under controlled composting conditions[207]. In this method, the polymer material to be tested is introduced into stabilized and mature compost kept in a sealed chamber with inlet and outlet for streaming air. The net production of carbon dioxide is recorded relative to a control or blank chamber containing only the mature compost. After determining the carbon content of the test substance (using elemental analysis techniques), the percentage biodegradation can be calculated as the percentage of solid carbon of the test substance which has been converted to gaseous carbon in the form of carbondioxide. In addition to carbon conversion, disintegration and weight loss may also be evaluated. To meet the ASTM D5338-93 standard, 60% of single polymer materials must mineralize in six months[207].

2.10 Theoretical Models

A theory is considered as the framework by which physical results can be predicted and such proposed theory is further validated by performing experiments to establish the relationship between connected parameters [208]. The iterative and cyclic procedure of understanding of the behavior of materials is illustrated in Figure 2.25[208].

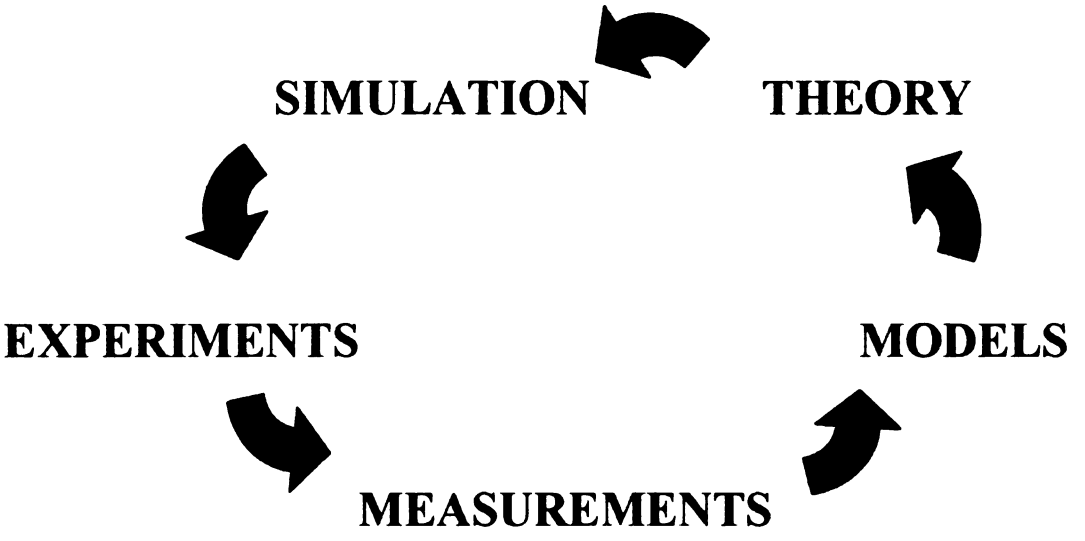

Figure 2.25: Illustration of the interdependence of methods and validation (Redrawn after Ref. 208)

The first step in the process of understanding behavior of materials is through observation via experiments. Such measurements of observed data are subsequently analyzed and used for the development of models that predict the observed behavior under the specific experimental conditions. The subsequently developed models are essential to develop the theory that will provide basis for comparison of predicted behavior to experiments via simulation. These correlations serve to either validate the theory, or to give an iterative feedback cycle to improve the theory.

2.10.1 Blend Models

Blending physics dictates that for a binary blend (Phase 1 and Phase 2), the lower viscosity phase tends to be continuous. This is quantified by equation 2.4 which gives the relation between volume fraction (V) and melt viscosity (η) as[134]:

$$X = V_1 \eta_2 / V_2 \eta_1 \qquad (2.4)$$

The value of X determines the continuous phase. In case of a blend of a semi-crystalline polymer, like PHB, and an elastomer, the elastomer ideally needs to be continuous to achieve the intended toughness.

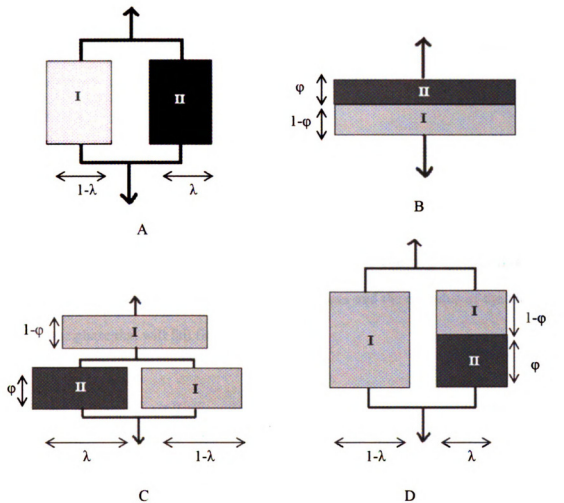

Figure 2.26: Takayanagi Model systems for a binary blend

The compatibility of a binary blend can also be established by using the Takayanagi model that predicts the blend moduli of phase separated systems[209]. These models give a lower bound and upper bound estimate of the modulus of a binary blend system based on the morphology of the blend components. Let us consider a binary blend

of an elastomer (minor component) and a polymer (major component) (Figure 2.13). In all the models E is the elastic modulus and the quantities λ and φ or their products are the volume fractions of the minor phase. For example in equation 2.7 and 2.8 the volume fraction of the minor phase is given by the product $\lambda\ \varphi$.

The upper bound value of the modulus of the blend is given by equation 2.5 which represents an iso-strain system with both minor and major phases continuous (Figure 2.26 A).

$$E_{max} = (1 - \lambda)\ E_{major} + \lambda\ E_{minor} \qquad (2.5)$$

The lower bound value of the modulus is given by equation 2.6 which is for a blend system wherein neither the phases are continuous and the modulus of the blend is nearer to the phase that will fail first (Figure 2.26 B).

$$E_{min} = [(\varphi/E_{minor}) + (1 - \varphi/E_{major})]^{-1} \qquad (2.6)$$

The intermediate values are for a continuous major phase with a discontinuous minor phase and are dependant on the morphologies of the blends and are given by equations 2.7 and 2.8. Equation 2.8 has a major continuous phase in series with a parallel connection of the discontinuous minor phase and another major phase (Figure 2.26 C):

$$E = [\ [\varphi/(\lambda E_{minor} + (1-\lambda)E_{major})] + [(1-\varphi)/E_{major}]\ ]^{-1} \qquad (2.7)$$

Equation 2.8 assumes the continuous major phase in parallel with a series connection of the discontinuous minor phase and another major phase (Figure 2.26 D):

$$E = \lambda[(\varphi/E_{minor}) + ((1-\varphi)/E_{major})]^{-1} + (1-\lambda)E_{major} \qquad (2.8)$$

2.10.2 Nanocomposite Models

In order to predict behavior of nanocomposites to enhance the development of nanostructured materials systems, it is necessary to primarily consider the structure-property relationships. These relationships relate the fundamental structure of the material to the desired performance. Table 2.4[208] gives a list of these structure-property relationships for polymers and polymer/nanoparticle composites according to corresponding scales.

Table 2.4: Scale-based relationships for polymers and polymer/ nanoparticle composites (adapted from Ref.[208])

STRUCTURE			PROPERTY
Molecular		Meso	Macro
Nano	Micro	Mini	
Inter-molecular forces	Molecular weight	Composition (Volume fraction)	Strength, modulus, viscosity, Toughness
Bond type, rotation, bond strength	Cross link density	Orientation	Strength, modulus, viscosity
Bond Strength	Crystallinity	Dispersion, nucleation	Glass transition Temperature, barrier
Aspect ratio	Polymer-nanoparticle interaction	Exfoliation, intercalation	CLTE, Viscosity

Thus, many mechanical, physical, and chemical factors could potentially influence the properties of polymer nanocomposites, and the better understanding of their relative contributions is necessary. .

A high aspect ratio of nanoclays and resulting extraordinary properties provide the ultimate reinforcement for the next generation of advanced composite materials. However, the resultant physical/mechanical behavior imparted by such incorporation has been, to date, difficult to predict owing mainly to fact that the majority of these models were developed for composites with macro-sized fillers at high concentrations. In case of

nanocomposites, because the fillers are nanoscopic in size as well as present at low concentrations, often it is difficult to predict the performance of the nanocomposites using the conventional theories of polymer composites.

These selected models, in most cases, may be effectively applied to model/predict other mechanical properties with specific modifications for the property in mind. The basic assumptions of the models studied are:

1. The system is a two-phase composite (matrix and reinforcement)
2. Matrix is isotropically thermoelastic
3. Reinforcements are isotropically thermoelastic
4. Reinforcements have identical shape and size
5. Reinforcements are perfectly bonded to the matrix

2.10.2.1 Rule of Mixtures

Rules of Mixtures are empirical mathematical expressions which give the specific property of the composite in terms of the properties, arrangement and quantity of its constituents. It is the simplest approximation for the prediction of the mechanical properties. The reinforcement is assumed geometrically to be a spherical rigid particle with perfect bonding between the filler and the matrix and consequently all the applied load is efficiently transferred from matrix to the filler. For simplification, let us consider the system shown in Figure 2.14. A load applied in direction 1 is shared between filler and matrix to give the following equation:

$$E_i = E_f V_f + E_m (1\text{-}V_f) \qquad (2.9)$$

Where E_i is the modulus and V_i is the volume fraction of the *i* component. This equation gives the upper bound value of the modulus. For the lower bound modulus, the load is considered to be applied in the direction given by arrow 2 in Figure 2.27 For this scenario, it is assumed that the stress is the same in each component ($\sigma_2 = \sigma_f = \sigma_m$) but the strains ε are different in each component. Substituting these conditions, the final equation that is derived is:

$$1/E_2 = V_f / E_f + (1\text{-}V_f) / E_m \qquad (2.10)$$

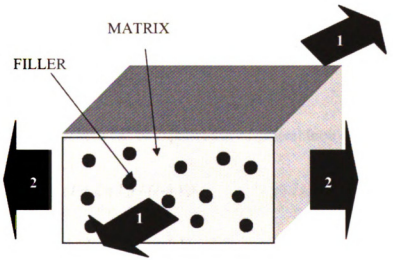

Figure 2.27: Polymer-filler system for Rule of Mixtures

Equation 2.10 gives the lower bound value of the modulus. These sets of equations give a very rough prediction of the range of the values and the reason behind this lack of accuracy is that filler geometry, matrix-filler interaction, filler dispersion, orientation etc. are not considered.

2.10.2.2 Halpin-Tsai

To overcome the shortcomings of the rule of mixtures, Halpin and Tsai in 1969 developed and presented a theory that incorporated aspect ratio of the filler and thus provided a more accurate solution to the problem of prediction of composite properties[210]. The basics of this theory are developed from the "self-consistent method" developed by Hill that modeled a composite as a single fiber, encased in a cylinder of matrix. Both the cylinder and the filler are considered to be embedded in an unbounded homogeneous medium which is "macroscopically indistinguishable" from the composite[211]. Hermans had earlier used Hill's model to propose a solution and Halpin and Tsai further reduced Hermans' model to a simpler analytical form and extended its use to a wide variety of filler geometries[212].

The Halpin-tsai equations can be expressed in its general form as:

$$E = E_m (1 + \zeta \eta V_f) / (1-\eta V_f) \qquad (2.11)$$

where E and E_m represent the Young's modulus of the composite and matrix, respectively, ζ is a shape parameter dependent upon filler geometry, V_f is the volume fraction of filler, and η is expressed as:

$$\eta = [(E_f / E_m)-1] / [(E_f / E_m) + \zeta] \qquad (2.12)$$

The shape parameter, ζ, is dependant on the aspect ratio of the filler and this has been studied extensively by many researchers in order to get closer and closer correlation

between predictions and experiments. Halpin-tsai and Ashton used a value of 2(L/D) for this parameter (L being the length and D the width or thickness of the filler particle as shown in Figure 2.28) while Van-Es has proposed 2/3 (L/D) as being more accurate for nanocomposites with platelet-shaped fillers[213, 214].

An interesting observation is that as ζ=0, equation 2.11 reduces to:

$$1/E = V_f/E_f + (1-V_f)/E_m$$

which is the lower-bound rule of mixtures and, conversely, when $\zeta = 1$, the theory reduces to the rule of mixtures (upper bound), i.e.

$$E = E_f V_f + E_m (1-V_f)$$

2.10.2.3 *Mori- Tanaka* and *Tandon-Weng*

The Mori–Tanaka theory has been well reviewed and used by researchers in the field of composites[215]. This theory was derived on the principles of Eshelby's inclusion model for calculating an elastic stress field in and around an ellipsoidal particle present in

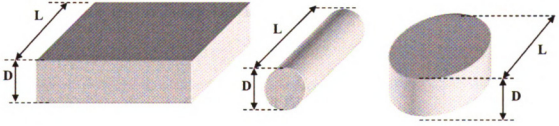

Figure 2.28: Aspect ratio considerations for different filler geometries

an infinite matrix[216]. Tandon and Weng further refined this theory by assuming many identical spheroidal particles and went on to propose solutions for the elastic modulus of an isotropic matrix having aligned spheroidal fillers[217]. The Tandon-weng equations for longitudinal elastic modulus can be expressed as:

$$E = E_m A / [A + V_f (A_1 + 2 \upsilon_m A_2)] \qquad (2.13)$$

And for transverse elastic modulus, the expression is:

$$E = E_m 2A / [2A + V_f (-2 \upsilon_o A_3 + (1 - \upsilon_m) A_4 + (1 + \upsilon_m) A_5 A)] \qquad (2.14)$$

where υ_0 is the Poisson's ratio of the matrix, V_f is the volume fraction of filler, and A_1; A_2; A_3; A_4; A_5; and A are functions of the Eshelby's tensor, Poisson's ratio, filler concentration, filler aspect ratio and Young's modulus; complete details of these equations are given in the original publication[217].

2.10.2.4 *Kerner's* Equation

Kerner in 1956 has derived a theory to predict effective modulus of composites with moderate filler content[218]. This theory is called Kerner's equation and Nielsen further modified this to incorporate low filler content and proposed the following equation[219]:

$$E = E_m (1 + A B V_f) / (1 - B \psi V_f) \qquad (2.15)$$

Where A is the contribution of the interfacial interaction and filler geometry effect, B represents the relative stiffness of the two components. The factor ψ was incorporated by Nielsen and is a constant representing the filler packing and is given as:

$$\psi = 1 + [(1-V_m)/V_m^2]V_f \qquad (2.16)$$

with the usual notations and V_m being the volume fraction of the matrix. Equations 2.15 and 2.16 were quite successful in calculating the modulii of diverse composite systems even where phase inversion occurred.

2.10.3 Barrier Models

In the diffusion process through a nanocomposite, the impregnable regions require penetrant migration around them which increases the average path length relative to the normal dimensions of the membrane. This effect is called the tortuosity factor τ and is given by equation 2.17 where L is the actual migration path length and L_0 is the nominal film sample thickness[201]

$$\tau = L/L_0 \qquad (2.17)$$

This effect is more visible in case of diffusion across a membrane with a random array of impermeable additives like clay platelets. For such a membrane containing impermeable flakes or discs oriented perpendicular to the diffusion direction, the simplest solution is equation 2.18 where α is the aspect ratio of the flake[220].

$$D_0/D = 1 + [(\alpha^2\Phi^2) / (1-\Phi)] \qquad (2.18)$$

Further studies on this system led to inclusion of other factors like the distance *s* between flakes and the slit size σ. Another model by Aris[221] uses an idealized membrane with flakes *2d* wide, *a* thick and separated by distance *b* and the diffusion is given by equation 2.19 where $\alpha = d/a$, $\Phi = 2da / [(d+s)(a+b)]$, and $\sigma = s/a$.

$$D_0/D = 1 + [(\alpha^2\Phi^2) / (1-\Phi)] + [\alpha\Phi/\sigma] + [4\,(\alpha\Phi)/\,\Pi\,(1-\Phi)]\,\ln\,[\,\Pi\,\alpha^2\Phi/\sigma\,(1-\Phi)] \qquad (2.19)$$

The second term in equation 2.19 represents the resistance to diffusion along the tortuous path, the third term is the slit resistance and the fourth term represents the constriction of the solute to pass into and out of the narrow slits.

2.11 Summary

As seen in this literature review section, biodegradable and biobased polymeric materials can be a solution to the problems of dwindling petroleum reserves and disposal. But these are as yet not used on a large scale primarily due to cost issues and property limitations. Renewable-resource based polymers lack a large market share and hence are synthesized on a batch-scale. This batch-scale production cannot economically compete with the continuous production of conventional polymers. Thus one of the ways to decrease the cost of renewable-resource based polymers is to create applications for them thus increasing usage and consequently shift production from batch to continuous ways.

This increased market-value can also be achieved by improving the properties of the renewable-resource based polymers thus making them more attractive than conventional polymers. This research targets this pathway of enhancing the properties of some specific renewable-resource based polymers by blending and composite technology. The conversion of batch-scale to continuous scale production is the long-term goal in such renewable-resource based polymers but is beyond the scope of this work; hence the near-term goal of cost reduction is targeted by incorporating inexpensive biobased polymers and fillers into the comparatively expensive PHA matrix.

The need of the moment is to develop and modify biobased materials using unique and novel techniques in order to create high-performance materials that can not only justify the cost difference but also be considered as long-term alternatives to non-biodegradable and non-renewable-resource-based materials. Toughening of PHAs by elastomeric modification or blending followed by nanoreinforcement is seen to be as yet an unexplored and unique area of research that promises high dividends if successfully achieved. Even the approach of using glycerol, a by-product of the burgeoning biodiesel industry, in plasticizing starch aims to give widespread socio-economic benefits. The developed materials also necessitate intense characterization and evaluation against theoretical models.

2.12 References

1. Kirk, A. G., *Film, Plastic* in *The Wiley Encyclopedia of Packaging Technology*, 1997, Wiley, pp. 423-427

2. Griff, A.L., *Carbonated Beverage Packaging* in *The Wiley Encyclopedia of Packaging Technology*, 1997, Wiley, pp. 158-161

3. *Percentage Distribution of Resin Sales & Captive Use By Major Market*, 2005, http://www.americanplasticscouncil.org/s_apc/docs/1100/1017.pdf, Accessed on: December 18, 2006

4. Andrady, A.L., *Assessment of environmental biodegradation of synthetic polymers*, Journal of Material Science – Rev Macromol Chem Phys, 1994 C34 25-76

5. A. Calmon-Decriaud, V. Bellon-Maurel, F. Silvestre, *Standard Methods for Testing the Aerobic Biodegradation of Polymeric Materials.Review and Perspectives*, Advances in Polymer Science, 1998, 135, 208-224

6. *Biomass As Feedstock For A Bioenergy And Bioproducts Industry: The Technical Feasibility Of A Billion-Ton Annual Supply*, 2005, http://www1.eere.energy.gov/biomass/pdfs/final_billionton_vision_report2.pdf, Accessed on: December 14, 2006

7. Staff, Purchasing, *Analysts see plastics packaging rising soon*, 2005, Purchasing, March 14, 2005, http://www.purchasing.com/article/CA510418.html?industryid=2148, Accessed on March 12, 2007

8. *The Technology Roadmap for Plant/Crop-based Renewable Resources 2020*, 1999, http://www.eere.energy.gov/biomass/pdfs/technology_roadmap.pdf, Accessed on: December 14, 2006

9. Duncan, M., *U.S. Federal Initiatives to Support Biomass Research and Development*, Journal of Industrial Ecology, 2003, 7, 193-201

10. Wood, A., *Mitsubishi Enters Biodegradables Market; Links with Ajinomoto*, 2003, Chemical Week, April 9, 2003, http://www.chemweek.com/inc/articles/t/2003/04/09/009.html, Accessed on April 12, 2007

11. R. A. Gross, B. Karla, *Biodegradable Polymers for the Environment*, Science, 2002, 297, 803-807

12. C. H. Holten, A. Miiller, D. Rehbinder, *Lactic Acid: Property and Chemistry of Lactic Acid and Derivatives*, Verlag Chemie, 1971, 221-231

13. Lowe, C.E., *Preparation of High Molecular Weight Polyhydroxyacetic ester,* 1954, US Patent no. 2,668,162,

14. Garlotta, Donald, *A Literature Review of Poly(Lactic Acid)*, Journal of Polymers and the Environment, 2001, 9, 63-84

15. Natureworks, *Natureworks Company Information*, 2006, http://www.natureworksllc.com/About-NatureWorks-LLC/Who-are-we.aspx Accessed on: December 26, 2006

16. Auras, R., *Investigation of Polylactide as Packaging Material*, 2004, Ph.D. Thesis, School of Packaging, Michigan State University, East Lansing

17. Natureworks, *Natureworks Company Information*, 2006, http://www.natureworksllc.com/Product-and-Applications/NatureWorks-Polymer/Technical-Resources.aspx, Accessed on: April 23, 2007

18. McWilliams, M., *Foods, Experimental Perspectives*. 5th ed. 2005: Pearson Prentice Hall.

19. Avérous, L., *Biodegradable Multiphase Systems Based on Plasticized Starch: A Review*, Journal of Macromolecular Science—Part C, Polymer Reviews, 2004, C44, 231-274

20. Russel, P.L., *Gelatinisation of starches of different amylose/ amylopectin content. A study by differential scanning calorimetry*, Journal of Cereal Science, 1987, 6, 133-145

21. B. Dobler, I. Tomka, R. F.T. Stepto, *Process for Making Destructurized Starch,* 1988, European Patent no. EP 282 451

22. C. Bastioli, R. Lombi, G. Del Tredici, I. Guanella, *Method for the preparation of destructured-starch-based compositions and compositions produced therby,* 1995, US Patent no. 5,462,982,

23. R. Stepto, I. Tomka, *Injection molding of natural hydrophilic polymers in the presence of water*, Chimia, 1987, 41, 76-81

24. Wilkinson, S. L., *Nature's Pantry is open for Business*, 2001, Chemical Engineering News, 79, 4, 61-62, January 22, 2001, http://pubs.acs.org/isubscribe/journals/cen/79/i04/html/7904sci2.html, Accessed on April 28, 2007

25. A. K. Mohanty, M. Misra and L.T. Drzal, *Sustainable Bio-Composites from Renewable Resources: Opportunities and Challenges in the Green Materials World*, Journal of Polymers and the Environment, 2002, 10, 19-26

26. S. N. Swain, S. M. Biswal, P. K. Nanda, and P. L Nayak, *Biodegradable Soy-Based Plastics: Opportunities and Challenges*, Journal of Polymers and the Environment, 2004, 12, 35-42

27. Anonymous, *Plastic Ford Unveiled*, 1941, Time, 38, 8, 63, http://www.time.com/time/magazine/article/0,9171,766014,00.html, Accessed on March 12, 2007

28. G. H. Brother, L. L. McKinney, *Protein Plastics from Soybean Products*, Industrial and Engineering Chemistry, 1940, 32,

29. Guilbert, S., *Food Packaging and Preservation. Theory and Practice*, ed. M. Mathouthi. 1986, London: Elsevier Applied Science.

30. Lemoigne, M., Bull. Soc. Chim. Biol, 1927, 9, 446

31. R. W. Lenz, R. H. Marchessault, *Bacterial Polyesters: Biosynthesis, Biodegradable Plastics and Biotechnology*, Biomacromolecules, 2005, 6, 1-8

32. L. Madison, G. W. Huisman, *Metabolic Engineering of Poly (3-Hydroxyalkanoates): From DNA to Plastic*, Microbiology And Molecular Biology Reviews, 1999, 63, 21-53

33. O. Wolf, M. Crank, M. Patel, F. Marscheider-Weidemann , J. Schleich, B. Hüsing, G. Angerer *Techno-economic Feasibility of Large-scale Production of Bio-based Polymers in Europe*, 2005, European Commission Joint Research Centre, http://www.biomatnet.org/publications/1944rep.pdf, Accessed on: March 12, 2007

34. Okada, M., *Chemical syntheses of biodegradable polymers*, Progress in Polymer Science, 2002, 27, 87-133

35. Bastioli, C., *Properties and Applications of Mater-Bi starch-based materials*, Polymer Degradation and Stability, 1998, 59, 263-272

36. M. Yamamoto, U. Witt, G. Skupin, D. Beimborn, R. Muller *Biodegradable aliphatic-aromatic polyesters "Ecoflex"*, in *Biopolymers, Polyesters III: Applications and Commercial Products*, Y. Doi A. Steinbuchel Editor. 2002, Wiley-VCH: Weinheim.

37. *DuPont Biomax*, 2006, http://www2.dupont.com/Biomax/en_US/, Accessed on: December 28, 2006

38. Bastioli, C., *Biodegradable materials - Present situation and future perspectives*, Macromolecular Symposia, 1998, 135, 193-204

39. E. Grigat , R. Koch, R. Timmermann, *BAK 1095 and BAK 2195: completely biodegradable synthetic thermoplastics*, Polymer Degradation and Stability, 1998, 59, 223-226

40. Fritz, J., *Ecotoxicity of Biogenic Materials During and After Their Biodegradation*, 1999, Ph.D. Thesis, University of Agriculture, Vienna

41. C. Bruns, R. Gottschall, B. de Wilde, *Ecotoxicological Trials with BAK 1095 (Bayer AG, Leverkusen) according to DIN V 54900*, Organic Recovery and Biotreatment (ORBIT) Journal, 2001, 1,

42. M. Biswas, A. Mazumdar, P. Mitra, *Vinyl Ether Polymers* in *Encyclopedia of Polymer Science and Engineering*, 1989, J. Wiley and Sons, New York, Vol. **17**, pp.

43. E. Chiellini, A. Corti, R. Solaro *Biodegradation of poly(vinyl alcohol) based blown films under different environmental conditions*, Polymer Degradation and Stability, 1999, 64, 305-312

44. Kurian, J. V., *Sorona Polymer: Present Status and Future Perspectives*, in *Natural Fibers, Biopolymers, and Biocomposites*, M. Misra and L. T. Drzal A. K. Mohanty, Editor. 2005, CRC Press. pp. 497-526.

45. Agency, U.S. Enviromental Protection, *2003 Greener Reaction Conditions Award*, 2003, http://www.epa.gov/greenchemistry/pubs/pgcc/winners/grca03.html, Accessed on: March 2, 2007

46. H. Miyagawa, A. K. Mohanty, R. Burgueño, L. T. Drzal, and M. Misra, , *Development of Biobased Unsaturated Polyester Containing Functionalized Linseed Oil*, Industrial & Engineering Chemistry Research, 2006, 45, 1014-1018

47. G. Mehta, A. K. Mohanty, M. Misra and L. T. Drzal, *Biobased resin as a toughening agent for biocomposites*, Green Chemistry, 2004, 6,

48. J. P. Latere Dwan'Isa, A. K. Mohanty, M. Misra and L. T. Drzal, *Biobased Polyurethanes and Their Composites: Present Status and Future Perspective*, in *Natural Fibers, Biopolymers, and Biocomposites*, M. Misra and L. T. Drzal A. K. Mohanty, Editor. 2005, CRC Press. pp. 775-806.

49. H. Miyagawa, M. Misra, L.T. Drzal, and A.K. Mohanty, *Fracture Toughness and Impact Strength of Anhydride -cured Biobased Epoxy*, Polymer Engineering and Science, 2005, 45, 487-495

50. S. Kalambur, S.S.H. Rizvi *Biodegradable and Functionally Superior Starch–Polyester Nanocomposites from Reactive Extrusion*, Journal of Applied Polymer Science, 2005, 96, 1072-1082

51. Selke, S.E., ed. *Biodegradation and Packaging*. 2nd ed. PIRA International Reviews of Packaging. 1996, Pira.

52. Narayan, R., *Starch Based Plastics*, in *Polymers from Biobased Materials*, H. L. Chum, Editor. 1991, Noyes Data Corporation: New Jersey. pp. 90-114.

53. N. Gontard, S. Guilbert, *Technology and properties of agricultural biopolymers based packaging*, 8th IAPRI World Conference on Packaging, Sao Paulo, Brazil, 1993.

54. M. F. Koenig, S. J. Huang, *Biodegradable blends and composites of polycaprolactone and starch derivatives*, Polymer Degradation and Stability, 1995, 36, 1877-1882

55. H. Pranamuda, Y. Tokiwa, K. Tanaka, *Physical properties and biodegradability of blends containing poly(ε-caprolactone) and tropical starches*, Journal of Environmental Polymer Degradation, 1996, 4, 1-7

56. L. Avérous , L. Moro, P. Dole , C. Fringant *Properties of thermoplastics blends: starch-polycaprolactone*, Polymer, 2000, 41, 4157-4167

57. P. Matzinos, V. Tserki , A. Kontoyiannis, C. Panayiotou *Processing and characterization of starch/polycaprolactone products*, Polymer Degradation and Stability, 2002, 77, 17-24

58. Y. Tokiwa, M. Koyoma, S. Takagi, *Starch-containing biodegradable plastic and method of producing same,* 1993, European Patent no. EP0535994,

59. Arvanitoyannis, I. S., *Totally and partially biodegradable polymer blends based on natural and synthetic macromolecules: preparation, physical properties, and potential as food packaging materials*, Journal of Macromolecular Science(Part C):Reviews in Macromolecular Chemistry and Physics, 1999, 39, 205-271

60. B. A. Ramsay, V. Langlade, P.J. Carreau, J. A. Ramsay, *Biodegradability and mechanical properties of poly(hydroxybutyrate-co-hydroxyvalerate)-starch blends*, Applied Environmental Microbiology, 1993, 59, 1242-1246

61. H. Verhoogt, N. St-Pierre, F. S. Truchon, B. A. Ramsay, B.D. Favis, J. A. Ramsay, *Blends containing poly(hydroxybutyrate-co-B-hydroxyvalerate) and thermoplastic starch*, Canadian Journal of Microbiology, 1995, 41, 323-328

62. L. Avérous , N. Fauconnier, L. Moro, C. Fringant, *Blends of thermoplastic starch and polyesteramide: processing and properties*, Journal of Applied Polymer Science, 2000, 76, 1117-1128

63. L. Avérous, C. Fringant, *Association between plasticized starch and polyesters: processing and performances of injected biodegradable systems*, Polymer Engineering and Science, 2001, 41, 727-734

64. J.A. Ratto, P.J. Stenhouse, M. Auerbach, J. Mitchell, R. Farrell, *Processing, performance and biodegradability of a thermoplastic aliphatic polyester/starch system*, Polymer, 1999, 40, 6777-6788

65. O. Martin, L. Avérous, *Poly(lactic acid): plasticization and properties of biodegradable multiphase systems*, Polymer, 2001, 42, 6237-6247

66. S. P. McCarthy, R. Gross, W. Ma, *Polylactic Acid-Based Blends,* 1999, US Patent no. 5,883,199,

67. G. V. Laverde, S. P. McCarthy, *Analysis of the Mechanical Properties of Biodegradable Films Made From Blends of Polylactic Acid (PLA) and Polyesters by Blown Film Extrusion*, Annual Technical Conference, Atlanta, GA, 1998.

68. W. Ma, S. P. McCarthy, *Biodegradable Polymer Blends of Polylactic Acid (PLA) and Polybutylene Succinate*, Annual Technical Conference, Atlanta, GA, 1998.

69. Chidambarakumar, Mariappan, *Development of Polylactic Acid (LA) Based Blends and Their Nanocomposites for Packaging Applications.* , 2005, M.S. Thesis, School of Packaging, Michigan State University, East Lansing

70. L. K. Sahu, K. Britten, N. A. D'Souza, *The Effect Of Addition Of PCL On The Mechanical Properties And Thermal Transitions Of PLA*, Annual Technical Conference, Charlotte, NC, 2006.

71. L. Jiang, J. Qian, M.P. Wolcott, J. Zhang, *Investigation of Toughening of Poly (lactic acid) by Poly (butylene adipate-co-terephthalate)*, Polymeric Materials: Science and Engineering, 2005, 93, 397-398

72. BASF, *Lending nature a helping hand*, 2005, http://www2.basf.de/basf2/html/plastics/englisch/pages/presse/05_538.htm, Accessed on: January 4, 2007

73. A J. Anderson, E. A. Dawes, *Occurrence, Metabolism, Metabolic Role, and Industrial Uses of Bacterial Polyhydroxyalkanoates*, Microbiological Reviews, 1990, 54, 450-472

74. C.S.K. Reddy, R. Ghai, Rashmi, V.C. Kalia, *Polyhydroxyalkanoates: an overview*, Bioresource Technology, 2003, 87, 137-146

75. K. Sudesh, H. Abe, Y. Doi, *Synthesis, structure and properties of polyhydroxyalkanoates: biological polyesters*, Progress in Polymer Science, 2000, 25, 1503-1555

76. D. C. Lundgren, R. Alper, C. Schnaitman, R.H. Marchessault, *Characterization of poly-b-hydroxybutyrate extracted from different bacteria*, Journal of Bacteriology, 1965, 89, 245-251

77. R. H. Marchessault, G. Yu *Crystallization and Material Properties of Polyhydroxyalkanoates*, in *Biopolymers* Y. Doi A. Steinbüchel, Editor. 2001, Wiley-VCH: Weinheim. pp. 157-200.

78. Baptist, J. N., *Isolation of Bacteria,* 1963, US Patent no. 3,072,538,

79. J.N. Baptist, Laurel, F.X. Werber, *Molded Product containing Polyhydroxybutyric acid and method of making,* 1963, US Patent no. 3,107,172,

80. Holmes, P.A., *Applications of PHB-a microbially produced biodegradable thermoplastic*, Phys. Technol., 1985, 16, 32-36

81. Holmes, P. A., *Biologically produced PHA polymers and copolymers*, in *Developments in Crystalline Polymers*, D. C. Basset, Editor. 1988, Elsevier: London. pp. 1-65.

82. Sykes, K., *Plastics You Could Eat - Recyling*, 2001, http://www.firstscience.com/site/articles/sykes.asp, Accessed on: 5 February, 2007

83. Metabolix, *Metabolix's Natural Plastics win Presidential Green Chemistry Challenge Award*, 2005, http://ir.metabolix.com/releasedetail.cfm?ReleaseID=211090, Accessed on: 5 February, 2007

84. Metabolix, *Metabolix, Inc. Announces Commencement of Construction of Commercial Manufacturing Facility for Biodegradable Natural Plastic*, 2006, http://metabolix.com/publications/pressreleases/PR20061211_2.html, Accessed on: 5 February, 2007

85. Gamble, Procter &, *Fully Biodegradable Plastic Resins from Renewable Sources*, 2007, http://pg.t2h.yet2.com/t2h/page/techpak?keyword=&id=38101&qid=0&sid=50&cargs=3%25091%25090%2509%2509%2509%2509%2509245200, Accessed on: 5 February, 2007

86. Biomer, *Remarks on biodegradation*, 2007, http://biomer.de/BioabbauE.html, Accessed on: February 4, 2007

87. Chen, X., *Industrialization of PHBV in China,*, BEPS International Degradable Plastics Symposium: Status Of Biobased And Synthetic Polymer Technology., Chicago, IL, 2006.

88. L. Velho, P. Velho, *The Development of a sugar-based plastic in Brazil: The Role of Government Schemes in Fostering Public Sector Research-Industry Relations, 2006 Technology Transfer Society Conference*, 2006. Atlanta, Georgia, USA, http://www.cherry.gatech.edu/t2s2006/papers/velho-1004-T.pdf, Accessed on April 12, 2007

89. A. K. Mohanty, M.M. Misra, L.T Drzal, S.E. Selke, B.R. Harte, G. Hinrichsen, *Natural Fibers, Biopolymers and Biocomposites: An Introduction*, in *Natural Fibers, Biopolymers and Biocomposites*, M.M. Misra A. K. Mohanty, L.T Drzal, Editor. 2005, CRC Press: Boca Raton, FL. pp. 1-57.

90. A. Steinbuchel, H.E. Valentin, *Diversity of bacterial polyhydroxyalkanoic acids*, FEMS Microbiol Lett, 1995, 128, 219-228

91. I. Noda, R. H. Marchessault, M. Terada, *Poly(hydroxybutyrate)*, in *Polymer Data Handbook*. 1999, Oxford University Press: New York. pp. 586-597.

92. S. Y. Lee, J. Choi, S.H. Lee, *Production of polyhydroxyalkanoates by fermentation of bacteria*, Macromol Symposia, 2000, 159,

93. P. J. Barham, A. Keller, E. L. Otun, P. A. Holmes, *Crystallization and morphology of a bacterial thermoplastic: poly-3-hydroxybutyrate*, Journal of Material Science, 1984, 19, 2781-2794

94. E.A. Dawes, P. J. Senior, *The role and regulation of energy reserve polymers in micro-organisms*, Advances in Microbial Physiology, 1973, 10,

95. R. H. Marchessault, K. Okamura, C. J. Su. , *Physical Properties of Poly(hydroxy butyrate) II:Conformational Aspects in Solution*, Macromolecules, 1970, 3, 735-740

96. F. Biddlestone, A. Harris, J. N. Hay, T. Hammond, *The Physical Ageing of Amorphous Poly(hydroxybutyrate)*, Polymer International, 1996, 39, 221-229

97. J. K. Hobbs, D. R. Binger, A. Keller, P. J. Barham, *Spiralling Optical Morphologies in Spherulites of Poly(hydroxybutyrate)*, Journal of Polymer Science, Part B: Polymer Physics, 2000, 38, 1575-1583

98. P. J. Barham, A. Keller, *The Relationship between Microstructure and Mode of Fracture in Polyhydroxybutyrate*, Journal of Polymer Science: Polymer Physics Edition, 1986, 24, 69-77

99. S. Bloembergen, D. A. Holden, G. K. Hamer, T. L. Bluhm, R. H. Marchessault. , *Studies of composition and crystallinity of bacterial poly(P-hydroxybutyrate-co-p-hydroxyvalerate)*, Macromolecules, 1986, 19, 2865-2871

100. N. Grassie, E. J. Murray, P. A. Holmes, *The thermal degradation of poly(β-hydroxybutyric acid): Part 2—Changes in molecular weight*, Polymer Degradation and Stability, 1984, 6, 95-103

101. H. Brandle, R. A. Gross, R. W. Lenz, R. C. Fuller, *Plastics from bacteria and for bacteria: Poly(β-hydroxyalkanoates) as natural, biocompatible, and biodegradable polyesters*, Advances in Biochemical Engineering/ Biotechnology, 1990, 41, 77-93

102. Howells, E. R., *Opportunities in biotechnology for the chemical industry*, Chemistry & Industry, 1982, 15, 508-511

103. Winton, J. M., 1985, Chemical Week, 28, 55-57, August 28, NA, Accessed on NA

104. Y. Azuma, N. Yoshie, M. Sakurai, Y. Inoue, R. Chujo, *Thermal behavior and miscibility of poly(3-hydroxybutyrate)/poly(vinyl alcohol) blends.* , Polymer, 1992, 33, 4763-4767

105. M. Avella, E. Martuscelli, *Poly-(3-hydroxybutyrate)/poly(ethyleneoxide) blends: phase diagram, thermal and crystallization behavior*, Polymer, 1988, 29, 1731-1737

106. M. Avella, E. Martuscelli, P. Greco, *Crystallization behavior of poly(ethylene oxide) from poly(3-hydroxybutyrate)/poly(ethylene oxide) blends: phase structuring, morphology and thermal behavior.* , Polymer, 1991, 32, 1647-1653

107. E. Blümm, A.J. Owen *Miscibility, crystallization and melting of poly(3-hydroxybutyrate)/poly(L-lactide) blends*, Polymer, 1995, 36, 4077-4081

108. N. Koyama, Y. Doi, *Miscibility of binary blends of poly[(R)-3-hydroxybutyric acid] and poly[(S)-lactic acid].* Polymer, 1997, 38, 1589-1593

109. Y. He, T. Masuda, A. Cao, N. Yoshie, Y. Doi, Y. Inoue, *Thermal, crystallization, and biodegradation behavior of poly(3-hydroxybutyrate) blends with poly(butylene succinate-co-butylene adipate) and poly(butylene succinate-co-ε-caprolactone).* , Polymer Journal, 1993, 184-192

110. N. Koyama, Y. Doi, *Miscibility, thermal properties, and enzymatic degradability of binary blends of poly[(R)-3-hydroxybutyric acid] with poly(ε-caprolactone-co-lactide)*, Macromolecules, 1996, 29, 5843-5851

111. T. Wang, G. Cheng, S. Ma, Z. Cai, L. Zhang, *Crystallization Behavior, Mechanical Properties, and Environmental Biodegradability of Poly(hydroxybutyrate)/Cellulose Acetate Butyrate Blends*, Journal of Applied Polymer Science, 2003, 89, 2116-2122

112. J. Yoon , S.Oh, M. Kim, *Compatibility of poly(3-hydroxybutyrate)/ poly(ethylene-co-vinyl acetate) blends*, Polymer, 1998, 39, 2479-2487

113. A. Gonzalez, M. Iriarte, P.J. Iriondo, J.J. Iruin, *Miscibility and carbon dioxide transport properties of blends of bacterial poly(3-hydroxybutyrate) and a poly(vinylidene chloride-co-acrylonitrile) copolymer*, Polymer, 2002, 43, 6205-6211

114. Y. Kumagai, Y. Doi, *Enzymatic degradation and morphologies of binary blends of microbial poly(3-hydroxybutyrate) with poly(ε-caprolactone), poly(1,4-*

butylene adipate) and poly(vinyl acetate). Polymer Degradation and Stability, 1992, 36, 241-248

115. F. Gassner, A.J. Owen, *Physical properties of poly(β-hydroxybutyrate)-poly(ε-caprolactone) blends*, Polymer, 1994, 35, 2233-2236

116. I. Koller, A. J. Owen, *Starch-Filled PHB and PHB/HV copolymer*, Polymer International, 1996, 39, 175-181

117. E. Dubini Paglia, P. L. Beltrame, M. Canetti, A. Seves, B. Marcandalli, E. Martuscelli, *Crystallization and thermal behaviour of poly (3-hydroxybutyrate)/poly(epichlorohydrin) blends*, Polymer, 1993, 34,

118. J.C. Yoon, C.S. Choi, S. J. Maing, H. J. Choi, H. Lee, S. J. Choi, *Miscibility of poly-image(−)(3-hydroxybutyrate) in poly(ethylene oxide) and poly(methyl methacrylate)*, European Polymer Journal, 1993, 29, 1359-1364

119. P. Greco, E. Martuscelli, *Crystallization and thermal behaviour of poly(3-hydroxybutyrate)-based blends*, Polymer, 1989, 30, 1475-1483

120. M. Avella, B. Immirzi, M. Malinconico, E. Martuscelli, G. Orsello, A. Pudia, G. Ragosta, *Poly(butyl acrylate) inclusive polymerization in the presence of bacterial polyesters, 1. Synthesis and preliminary mechanical and morphological characterization* Die Angewandte Makromolekulare Chemie, 1993, 205, 151-160

121. Z. Bartczak, A. S. Argon, R. E. Cohen and M. Weinberg, *Toughness mechanism in semi-crystalline polymer blends: I. High-density polyethylene toughened with rubbers*, Polymer, 1999, 40, 2331-2346

122. Z. Bartczak, A. S. Argon, R. E. Cohen and M. Weinberg, *Toughness mechanism in semi-crystalline polymer blends: II. High-density polyethylene toughened with calcium carbonate filler particles*, Polymer, 1999, 40, 2347–2365

123. J. Lu, G.Wei, H. Sue and J. Chu *Toughening Mechanisms in Commercial Thermoplastic Polyolefin Blends*, Journal of Applied Polymer Science, 2000, 76, 311-319

124. A. van der Wal, R. Nijhof and R. J. Gaymans, *Polypropylene Rubber Blends 1: The effect of matrix properties on the impact behaviour*, Polymer, 1998, 39, 6781-6787

125. A. van der Wal, R. Nijhof and R. J. Gaymans, *Polypropylene–rubber blends: 2. The effect of the rubber content on the deformation and impact behaviour*, Polymer, 1999, 40, 6031-6044.

126. Gaymans, A. van der Wal and R. J., *Polypropylene–rubber blends: 3. The effect of the test speed on the fracture behaviour*, Polymer, 1999, 40, 6045-6055

127. A. van der Wal, A. J. J. Verheul and R. J. Gaymans *Polypropylene–rubber blends: 4. The effect of the rubber particle size on the fracture behaviour at low and high test speed*, Polymer, 1999, 40, 6057-6065

128. L.A.Utracki, A.Abdellah *Interphase and Compatibilization of Polymer Blends*, Polymer engineering and science, 1996, 1574-1585

129. D. W. Grijpma, R. D. A. Van Hofslot, H. Supèr, A. J. Nijenhuis, A. J. Pennings *Rubber toughening of poly(lactide) by blending and block copolymerization*, Polymer Engineering and Science, 1994, 34, 1674-1684

130. Zumbrunnen, D. A., *Smart Blending: A Means to Obtain Fibers and Plastic Products with Tailored Properties*, Journal of The Textile Institute: Part 3, 2000, 91, 92-104

131. C.C. Chen, J. L. White, *Compatibilizing agents in polymer blends : interfacial tension, phase morphology, and mechanical properties*, Polymer Engineering and Science, 1993, 33 923-930

132. Utracki, L. A., *Polymer Alloys and Blends*. 1989, Munich: Hanser

133. D. G. Baird, D. I. Collias, *Polymer Processing Principles and Design*. 1995, New York: Butterworth-Heineman.

134. D. R. Paul, J. W. Barlow, *Polymer blends (or alloys)*, Journal of Macromolecular Science, Part C - Reviews in Macromolecular Chemistry, 1980, C18,

135. J. W. Barlow, D.R. Paul, *Polymer Alloys*, Annual Reviews Material Science, 1981, 11, 299-319

136. Matsen, R. B. Thompson and M. W., *Effective interaction between monolayers of block copolymer compatiblizer in a polymer blend*, Journal of Chemical Physics, 2000, 112, 6863-6872

137. B. Guo, Y. Cao, D. Jia, Q. Qiu, *Thermoplastic Elastomers Derived from Scrap Rubber Powder/LLDPE Blend with LLDPE-graft-(Epoxidized Natural Rubber) Dual Compatibilizer*, Macromolecular Materials and Engineering, 2004, 289, 360-367

138. J. Zhang, X.Sun, *Mechanical Properties of Poly(lactic acid)/Starch Composites Compatibilized by Maleic Anhydride*, Biomacromolecules, 2004, 5, 1446-1451

139. National Science and Technology Council:Committee on Technology:Subcommittee on Nanoscale Science, Engineering and Technology, *National Nanotechnology Initiative: The Initiative and its Implementation Plan*, 2000, Washington D. C., Accessed on:

140. S. S. Ray, M. Okamoto, *Polymer/layered silicate nanocomposites: a review from preparation to processing*, Progress in Polymer Science, 2003, 28, 1539-1641

141. Giannelis, E. P., *Polymer Layered Silicate Nanocomposites*, Advanced Materials, 1996, 8, 29-35

142. E. P. Giannelis, R. Krishnamoorti, E. Manias, *Polymer-Silicate Nanocomposites: Model Systems for Confined Polymers and Polymer Brushes*, Advances in Polymer Science, 1999, 138, 107-147

143. Giannelis, E. P., *Polymer-Layered Silicate Nanocomposites: Synthesis, Properties and Applications*, Applied Organometallic Chemistry, 1998, 12, 675-680

144. M. Biswas, S.S. Ray, *Recent Progress in Synthesis and Evaluation of Polymer-Montmorillonite Nanocomposites*, Advances in Polymer Science, 2001, 155, 167-221

145. Fischer, H., *Polymer nanocomposites: from fundamental research to specific applications*, Materials Science and Engineering, 2003 C 23, 763-772

146. Q.H. Zeng, A.B. Yu, G.Q. Lu, D.R. Paul, *Clay-Based Polymer Nanocomposites: Research and Commercial Development*, Journal of Nanoscience and Nanotechnology, 2005, 5, 1574-1592

147. M. Alexandre, P. Dubois, *Polymer-layered silicate nanocomposites: preparation, properties and uses of a new class of materials*, Materials Science and Engineering: Reports, 2000, 28, 1-63

148. K. Yano, A. Usuki, A. Okada, T. Kurauchi, O. Kamigaito, *Synthesis and Properties of Polyimide-Clay Hybrid*, Journal of Polymer Science, Part A: Polymer Chemistry, 1993, 31, 2493-2498

149. O. Okada, M. Kawasumi, A. Usuki, T. Kurauchi, O. Kamigaito, *Synthesis and properties of nylon-6/clay hybrids*, Materials Research Society Symposia, Pittsburgh, 1990.

150. P. B. Messersmith, E. P. Giannelis, *Synthesis and Characterization of Layered Silicate-Epoxy Nanocomposites*, Chemistry of Materials, 1994, 6, 1719-1725

151. Technology, President's Council of Advisors on Science and, *The National Nanotechnology Initiative at Five Years: Assessment and Recommendations of the National Nanotechnology Advisory Panel*, 2005, http://www.nano.gov/html/res/FINAL_PCAST_NANO_REPORT.pdf Accessed on: April 2, 2007

152. Partners, Principia, *Nanocomposites: Enhancing Value in the Global Plastics Industry 2005*, 2005, Exton, PA, NA, Accessed on: NA

153. R. Ottaviani, W. Rodgers, P. Fasulo, T. Pietrzyk, C. Buehler, Global SPE TPO Conference, Troy, 1999.

154. Leaversuch, R., *Nanocomposites Broaden Role in Automotive, Barrier Packaging*, 2001, Plastics Technology, 64-69, October http://www.ptonline.com/articles/200110fa3.html, Accessed on March 12, 2007

155. Sherman, L. M., *Chasing Nanotechnology*, 2004, Plastics Technology, 50, 11, November, http://www.ptonline.com/articles/200411fa2.html, Accessed on March 12, 2007

156. J. M. Garcés, D. J. Moll, J. Bicerano, R. Fibiger, D. G. McLeod, *Polymeric Nanocomposites for Automotive Applications*, Advanced Materials, 2000, 12, 1835-1839

157. Associates, Bins &, *Nanocomposite Market Opportunities*, 2001, Sheboygan, WI, NA, Accessed on: NA

158. C.J. Vanoss, R. F.Giese, *Surface modification of clays and related materials*, Journal of Dispersion Science and Technology, 2003, 24, 363-376

159. Okamoto, M., *Polymer/Clay Nanocomposites* in *Encyclopedia of Nanoscience and Nanotechnology*, 2004, American Scientific Publishers, Valencia, CA, Vol. **8**, pp. 791-843

160. Grim, R.E., *Applied Clay Mineralogy*. 1962, New York: McGraw-Hill.

161. F. Bergaya, G. Lagaly, *Surface modification of clay minerals*, Applied Clay Science, 2001, 19, 1-3

162. J. C. Dai, J.T. Huang, *Surface modification of clays and clay–rubber composite*, Applied Clay Science, 1999, 15, 51-65

163. Lagaly, G., *Introduction: from clay mineral–polymer interactions to clay mineral–polymer nanocomposites*, Applied Clay Science, 1999, 15, 1-9

164. R. A.Vaia, G. Price, P.N. Ruth, H.T. Nguyen, J. Lichtenhan, *Polymer/ layered silicate nanocomposites as high performance ablative materials*, Applied Clay Science, 1999, 15, 67-92

165. P.C. LeBaron, Z.Wang, T.J. Pinnavaia, *Polymer-layered silicate nanocomposites: an overview*, Applied Clay Science, 1999, 15, 11-29

166. Z. Klapyta, T. Fujita, N. Iyi, *Adsorption of dodecyl- and octadecyltrimethylammonium ions on a smectite and synthetic micas*, Applied Clay Science, 2001, 19, 5-10

167. Moraru, V. N., *Structure formation of alkylammonium montmorillonites in organic media*, Applied Clay Science, 2001, 19, 11-26

168. T. Lan, T.J. Pinnavaia, *Clay-Reinforced Epoxy Nanocomposites*, Chemistry of Materials, 1994, 6, 2216-2219

169. N.N. Herrera, J. Letoffe, J.Putaux, L.David, E. Bourgeat-Lami, *Aqueous Dispersions of Silane-Functionalized Laponite Clay Platelets. A First Step toward the Elaboration of Water-Based Polymer/Clay Nanocomposites*, Langmuir, 2004, 20, 1564-1571

170. S. Lee, J.J. Kim, *Surface Modification of Clay and Its Effect on the Intercalation Behavior of the Polymer/Clay Nanocomposites*, Journal of Polymer Science, Part B: Polymer Physics, 2004, 42, 2367-2372

171. Weiss, A., *Organic Derivatives of Mica-Type Layer-Silicates*, Angewandte Chemie International Edition, 1963, 2, 134-144

172. Y. Parulekar, A.K. Mohanty, *Effect of Titanate-based Surfaces on Hydrophilicity and Interlayer spacing of Montmorillonote Clay for Polymer Nanocomposites*, Journal of Nanoscience and Nanotechnology, 2005, 5, 2138-2143

173. G. Chen, J. Yoon, *Nanocomposites of poly[(butylene succinate)-co-(butylene adipate)] (PBSA) and twice-functionalized organoclay*, Polymer International, 2005, 54, 939 - 945

174. B. Tyagi, C D. Chudasama, R.V. Jasra, *Determination of structural modification in acid activated montmorillonite clay by FT-IR spectroscopy*, Spectrochimica Acta Part A, 2006, 64, 273-278

175. N.N. Binitha, S. Sugunan, *Preparation, characterization and catalytic activity of titania pillared montmorillonite clays*, Microporous and Mesoporous Materials, 2006, 93, 82-89

176. Pottish, Nancy, *Nanoparticles, Nanotubes and Nanocomposites*, 2005, Composites Technology, April, http://www.compositesworld.com/ct/issues/2005/April/809, Accessed on March 12, 2007

177. H. R. Dennis, D. L. Hunter, D. Chang, S. Kim, J. L. White, J. W. Cho, D. R. Paul, *Effect of melt processing conditions on the extent of exfoliation in organoclay-based nanocomposites*, Polymer, 2001, 42, 9513-9522

178. T. D. Fornes, P. J. Yoon, H. Keskkula, D. R. Paul, *Nylon 6 nanocomposites: the effect of matrix molecular weight*, Polymer, 2001, 42, 9929-9940

179. M. Kawasumi, N. Hasegawa, M. Kato, A. Usuki, A. Okada, *Preparation and Mechanical Properties of Polypropylene-Clay Hybrids*, Macromolecules, 1997, 30, 6333-6338

180. Y. Liang, S.Omachinski, J. Logsdon, J.Cho, T. Lan, *Nano Effect in In-Situ Nylon 6 Nanocomposites*, ANTEC, Dallas, TX, 2001.

181. T. Lan, J. Cho, Y. Liang, G. Qian, P. Maul, *Applications of Nanomer in Nanocomposites: From concept to Reality*, Nanocomposites, Chicago, 2001.

182. Corporation, Foster, *Nanomed® Nanocomposite Formulations*, 2007, http://www.fostercomp.com/_Site/productsnf.php, Accessed on: 10 February, 2007

183. T.S. Ellis, J.S. D'Angelo, *Thermal and Mechanical Properties of a Polypropylene Nanocomposites*, Journal of Applied Polymer Science, 2003, 90, 1639-1647

184. P.Reichert, H. Nitz, S. Klinke, R. Brandsch, R. Thomann, R. Mülhaupt, *Poly(propylene)/organoclay nanocomposite formation: Influence of compatibilizer functionality and organoclay modification*, Macromolecular Materials and Engineering, 2000, 275, 8-17

185. Corporation, Polyone, *Nanoblend Compounds*, 2007, http://www.polyone.com/prod/trade/trade_info.asp?ID={A8704A0F-CBCC-4B54-833E-D46AA3CAA1DC}&link=N, Accessed on: 10 February, 2007

186. L. Wei, T. Tang, B. Huang, *Synthesis and characterization of polyethylene/clay-silica nanocomposites: A montmorillonite/silica-hybrid-supported catalyst and in situ polymerization*, Journal of Polymer Science, Part A: Polymer Chemistry, 2004, 42, 941-949

187. S. Wang, Y. Hu, Q. Zhongkai, Z. Wang, Z. Chen and W. Fan, *Preparation and flammability properties of polyethylene/clay nanocomposites by melt intercalation method from Na+ montmorillonite*, Materials Letters, 2003, 57, 2675-2678

188. J. W. Gilman, T. Kashiwagi, J.D. Lichtenhan *Nanocomposites: a revolutionary new flame retardant approach*, 42nd International SAMPE Symposium, Anaheim, CA, 1997.

189. J. K. Pandey, P. A. Kumar, A. K. Mohanty, M. Misra, L. T. Drzal, R. P. Singh, *Recent Advances in Biodegradable Nanocomposites*, Journal of Nanoscience and Nanotechnology, 2005, 5, 497-526

190. J. K. Pandey, R. Reddy, P.A. Kumar, R. P. Singh, *An overview on the degradability of polymer nanocomposites*, Polymer Degradation and Stability, 2005, 88, 234-250

191. S. S. Ray, P. Maiti, M. Okamoto, K. Yamada, K. Ueda, *New Polylactide/Layered Silicate Nanocomposites. 1. Preparation, Characterization, and Properties*, Macromolecules, 2002, 35,

192. S.S. Ray, K. Yamada, M. Okamoto,K. Ueda, *Control of Biodegradability of Polylactide via Nanocomposite Technology*, Macromolecular Materials and Engineering, 2003, 288, 203-208

193. P. Maiti, K. Yamada, M. Okamoto, K.Ueda, K. Okamoto, *New Polylactide/Layered Silicate Nanocomposites: Role of Organoclays*, Chemistry of Materials, 2002, 14, 4654-4661

194. Keating, J. Z., *The role of talc and mica in natural fiber composites*, The Global Outlook for Natural Fiber and Advanced Wood Composites 2001.

195. Pukanszky, B., *Particulate filled polypropylene: structure and properties*, in *Polypropylene: structure, blends and composites.*, J. Karger-Kocsis, Editor. 1995, Chapman and Hall: London. pp. 1-70.

196. Minerals, Mondo, *Technical Bulletin 1301: Talc in Plastics*, 2007, http://www.mondominerals.com/pdf/plastics.pdf Accessed on: March 2, 2007

197. Toensmeier, P. A., *Nanotechnology Is Extending the Range of Additive and Polymer Performance*, 2006, Society of Plastics Engineers, http://www.4spe.org/htmlemail/techfocus/supportingdocs/0608_industry.pdf, Accessed on: April 2, 2007

198. *Plastics News FYI: Global Market for Flexible Packaging*, 2005, Plastics News, November 28, 2005, http://www.plasticsnews.com/subscriber/fyi.html?id=1132774806, Accessed on March 12, 2007

199. S.E. Selke, J. D. Cutler, R. Hernandez, *Plastics Packaging: Properties, Processing, Applications, And Regulations*. 2nd ed. 2004, Munich: Carl Hanser Verlag.

200. Risch, S. J., *New Developments in packaging materials*, in *Food Packaging: Testing methods and applications*, S. J. Risch, Editor. 2000, American Chemical Society: Washington, DC. pp. 1-8.

201. Rogers, C.E., *Permeation of Gases and Vapours in Polymers*, in *Polymer Permeability*, J. Comyn, Editor. 1985, Elsevier Applied Science: New York. pp. 11-74.

202. E. L. Cussler, S. E. Hughes, W.J. Ward, R. Aris, *Barrier membranes*, Journal of Membrane Science, 1988, 38, 161-174

203. D.Coltrain, *Biodiesel: Is It Worth Considering?, Risk and Profit Conference*, 2002. Manhattan, Kansas, http://www.agmrc.org/NR/rdonlyres/513C6A14-28DE-4B54-A57E-EA7FE052E399/0/bdconsider.pdf, Accessed on April 17, 2007

204. P. Dubois, M. Krishnan, R. Narayan, *Aliphatic polyester grafted Polysaccharide-like composites by in situ ring-opening polymerization*, Polymer, 1999, 40, 3091-3100

205. D. Rutot, P. Degee, R. Narayan, P. Dubois, *Aliphatic polyester-grafted starch composites by in situ ring opening polymerization*, Composite Interfaces, 2000, 7, 215-225

206. P. Dubois, R. Narayan, *Biodegradable compositions by reactive processing of aliphatic polyester/polysaccharide blends*, Macromolecular Symposia, 2003, 198, 233-244

207. Standard, American Society for Testing and Materials (ASTM International), *ASTM D 5338 Standard Test Method for Determining Aerobic Biodegradation of Plastic Materials under Controlled Composting Conditions.*, 2003

208. T. S. Gates, J.A. Hinkley, *Computational Materials: Modeling and Simulation of Nanostructured Materials and Systems*, 2003, National Aeronautics and Space Administration, Hampton, Virginia, http://techreports.larc.nasa.gov/ltrs/PDF/2003/tm/NASA-2003-tm212163.pdf, Accessed on: April 28, 2007

209. Takayanagi, M., *Mem. Fac. Eng. Kyushu Univ.*, 1963, 23

210. Halpin, J. C., *Stiffness and expansion estimates for oriented short-fiber composites*, Journal of Composite Materials, 1969, 3, 732-734

211. Hill, R., *Theory of mechanical properties of fiber-strengthened materials: I Elastic behaviour*, Journal of the Mechanics and Physics of Solids, 1964, 12, 199-212

212. Hermans, J.J., *The elastic properties of fiber reinforced materials when the fibers are aligned*, Proc Kon Ned Akad v Wetensch, 1967, B 65, 1-9

213. Es, M. Van, *Polymer-clay nanocomposites*, 2002, Ph.D. Thesis, Technical University of Delft, Delft

214. J. E. Ashton, J.C. Halpin, P.H. Petit, *Primer on Composite Materials: Analysis*, 1969, Techomic Pub. Co, Stamford, Conn, NA, Accessed on: NA

215. T. Mori, K. Tanaka *Average stress in matrix and average elastic energy of materials with misfitting inclusions*, Acta Metallica, 1973, 21, 571-574

216. Eshelby, J.D., *The Determination of the Elastic Field of an Ellipsoidal Inclusion, and Related Problems*, Royal Society of London. Series A, Mathematical and Physical Sciences, 1957.

217. G.P. Tandon, G.J. Weng *The effect of aspect ratio of inclusions on the elastic properties of undirectionally aligned composites*, Polymer Composites, 1984, 5, 327-333

218. Kerner, E. H., *Elastic and Thermoelastic Properties of Composite Media*, Proceedings Physics Society, 1956, B69, 808-813

219. Nielsen, L. E., *Generalized Equation for the Elastic Moduli of Composite Materials*, Journal of Applied Physics, 1970, 41, 4626-4627

220. E. L. Cussler, M. Mulski, W.R. Falla, *Estimating diffusion through flake-filled membranes*, Journal of Membrane Science, 1996, 119, 129-138

221. Aris, R., *On a Problem in Hindered Diffusion*, Archive for Rational Mechanics and Analysis, 1986, 95, 83-91

3. MATERIALS

3.1 Polyhydroxyalkanoates

Polyhydroxybutyrate (PHB) (Scheme 3.1) was supplied by Biomer (Germany). This polymer is sold under the trade name Biomer® P226 and is available in pelletized form[1]. The pellets contained proprietary amounts of plasticizer and nucleating agent [2]. P226 pellets used in this work were from lot number 16M236/99/1404.

Polyhydroxybutyrate-co-valerate (PHBV) (Figure 3.1) was obtained from Monsanto as Biopol®. This was donated to Michigan State University by The Dow Chemical Company. The specific PHBV used in this study was plasticizer-free and from lot number 6L600N19 having 14% valerate content[3].

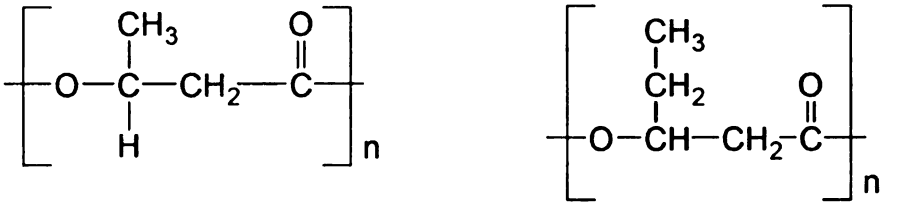

Figure 3.1: Structure of Poly(hydroxybutyrate) (left) and Poly(hydroxyvalerate) (right)

3.2 Elastomers

The rubber used (Figure 3.2) was a high quality, clean (ash content <0.50 %, dirt content <0.02%, Nitrogen <0.6%) latex grade natural rubber (Standard Malaysian Rubber SMR CV 60) supplied by Centrotrade (Akron, OH). Epoxidized natural rubber (ENR 25) with 25 % epoxidization was used as the functionalized rubber (Figure 3.3).

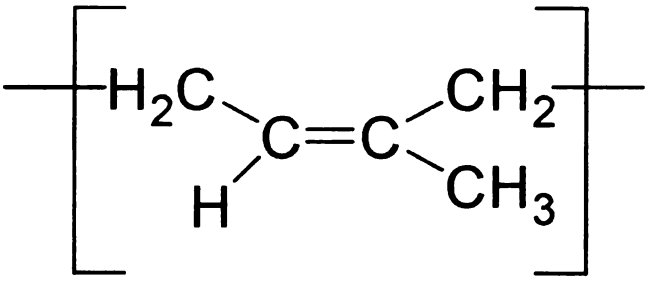

Figure 3.2: Chemical Structure of Natural Rubber

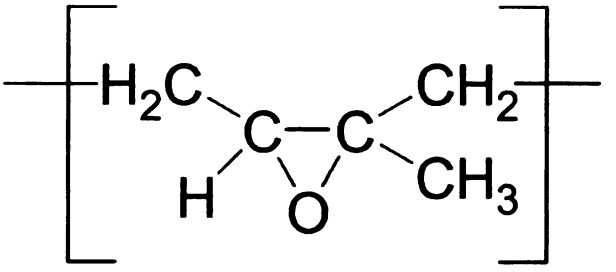

Figure 3.3: Chemical Structure of Epoxidized Natural Rubber

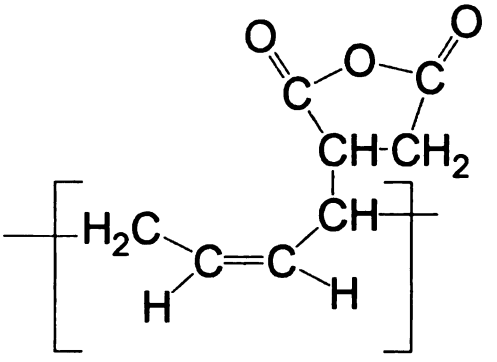

Figure 3.4: Chemical Structure of Maleated Polybutadiene

3.3 Compatibilizers

The maleated rubber compatibizers (RI 130 MA20 and RI 131MA5) (Figure 3.4) were provided by Sartomer (Exton, PA). RI 130 MA20 has molecular weight of 3100 and 6 maleic anhydride groups/chain while RI 131 MA5 has molecular weight of 4700 and 2 maleic anhydride groups/chain[4].

3.4 Clay

Pristine montmorillonite clay was purchased from Nanocor (Nanocor, IL). The specific clay used in the study is called PGV with a specific gravity of 2.6, cation exchange capacity of 145 meq/100 g and aspect ratio of 150-200[5]. Organically modified montmorillonite (OMMT) clays in the powder form were supplied by Southern Clay

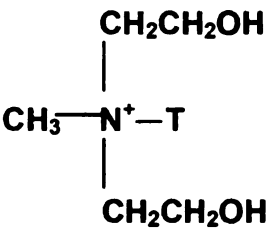

Figure 3.5: Chemical structure of organic modifier of Cloisite® 30B.

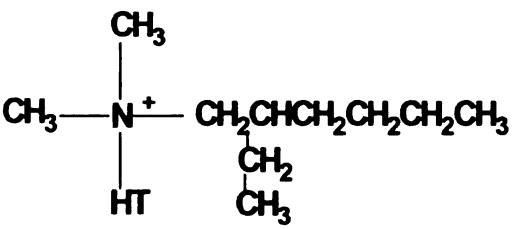

Figure 3.6: Chemical structure of organic modifier on Cloisite® 25A

Products Inc. (Gonzales, TX) under the trade names of Cloisite®30B (Figure 3.5) and Cloisite®25A (Figure 3.6). The "T" in the structures stands for tallow which is a mixture of long-chain alkyl molecules (~65% C18; ~30% C16; ~5% C14)[6]

3.5 Talc

Unmodified talc was purchased from Luzenac (Centennial,CO) and is available under the trade name Jetfil® 700C. This specific talc has a small median particle size (1.5 microns) and hence was selected for this work.

3.6 Surface Modifiers

The surface modifier used is *neopentyl (diallyl)oxy tri(dioctyl) pyrophosphato titanate* (Figure 3.7)[7] which was provided by Kenrich Petrochemicals, Inc. (Bayonne, NJ) as Ken-react® LICA-38 and was used as received.

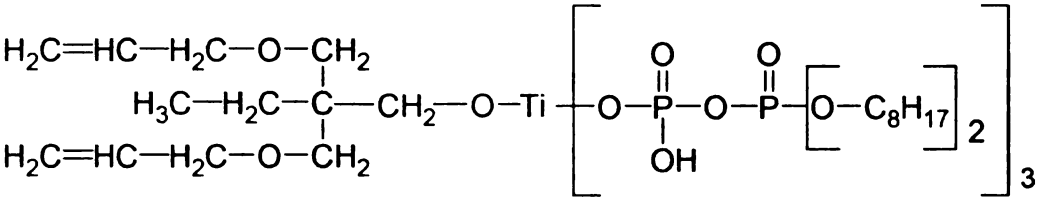

Figure 3.7: Neopentyl (diallyl)oxy tri(dioctyl) pyrophosphato titanate

3.7 Polymer Blend Partners

Poly-(butylene adipate-co-terephthalate) (PBAT) (Figure 3.8), film grade pellets were supplied by BASF AG, Germany under the trade name of Ecoflex® F (BX7011). Poly-(tetramethylene adipate-co-terephthalate) (PTAT), pellets were supplied by Eastman, USA under the trade name of EastarBio GP Copolyester. Poly(ε-caprolactone) (PCL) was supplied by Union Carbide as Tone®787. Thermoplastic polyolefin (TPO) was obtained from Basell Polyolefins as research sample and High Impact Polystyrene (HIPS) samples (Styron 421 and Styron 482) were requested as samples from the Dow Chemical Company.

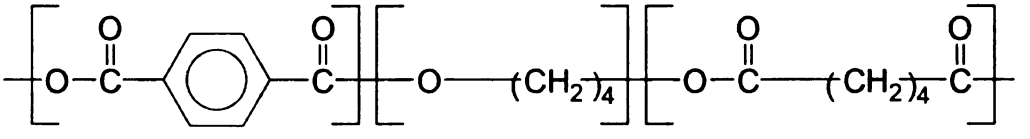

Figure 3.8: Chemical Structure of Poly-(butylene adipate-co-terephthalate) (PBAT)

3.8 Starch

The starch used was an unmodified high amylose corn starch from National Starch Company. This starch is sold under the trade name HYLON® VII and has approximately 70% amylose content[8]. The specific batch number for the starch is JE9730 and material code 0560902-905.

3.9 Chemicals and Solvents

Toluene, hexane and deionized water of scientific grade were obtained from Aldrich and used as received. The non-aromatic solvent was purchased from Ashland Chemicals as Kwik-dri™ aliphatic hydrocarbon. This has CAS number 8052-41-3 and is also called Stoddard Solvent.

Table 3.1: Physical properties of polymers used

	Density g/cc	Tm °C *	Tg °C *	Characteristic
PHB (P226)[1]	1.25	180	5	Plasticized
PHBV[9]	1.25	155	4	14 % valerate
Rubber (NR/ ENR)	0.93	145	-70	25% Epoxidation
PBAT[10]	1.25	110	-30	Film grade
PCL[9]	1.25	65	-61	Pulverized/ pellets
Starch (Corn)[8]	1.5	220	43	70% amylose
HIPS (Styron 421)[11]	1.04	270	100	High stiffness grade
HIPS (Styron 482)[11]	1.04	270	100	High flow grade

Note: '' indicates data from characterization; other data is from corresponding references.*

Table 3.2: Physical properties of additives used[5, 6]

	Pristine Clay	Cloisite® 30B	Cloisite® 25A	Talc	Ti-modified clay
Density (g/cc)	2.6	1.98	1.87	2.7	-
Bulk Density (lbs/ft^3)	12.45	14.25	12.08	40-50	-
Modifier type	-	methyl, tallow, bis-2-hydroxyethyl, quaternary ammonium	dimethyl, dehydrogenated tallow, 2-ethylhexyl quaternary ammonium	-	neopentyl (diallyl)oxy tri(dioctyl) pyro-phosphato titanate
Modifier conc. (wt.%)	-	30	34	-	11.4
CEC (mequiv/ 100g)		90	95	-	-
d – spacing (A)		18.5	18.6		

3.10 References

1. Biomer, *Biomer Biodegradable Polyesters*, 2007, http://biomer.de/IndexE.html, Accessed on: March 12, 2007

2. Hanggi, U. J., Biomer, *E-mail Correspondence*, Y. Parulekar, 2006

3. R. Bhardwaj, A.K. Mohanty, *C-NMR analysis of PHBV*, Unpublished Work, 2006, Michigan State University

4. Sartomer, *Maleinized Polybutadiene: Functionalized Polybutadiene Resins*, 2007, http://sartomer.com/prodsubgroup.asp?plid=8&sgid=47, Accessed on: 18 February, 2007

5. Nanocor, *Polymer Grade Montmorillonites*, 2006, http://nanocor.com/tech_sheets/G105.pdf, Accessed on: March 12, 2007

6. *Cloisite Additives: Nanoscale Additives for Reinforced Plastics*, 2007, http://nanoclay.com/product_bulletins.asp, Accessed on: March 1, 2007

7. Monte, S. J., *Kenrich Petrochemicals Reference manual and product literature*, 2007

8. Starch, National, *HYLON VII Technical Service Bulletin*, 2006

9. Avérous, L., *Biodegradable Multiphase Systems Based on Plasticized Starch: A Review*, Journal of Macromolecular Science—Part C, Polymer Reviews, 2004, C44, 231-274

10. M. Yamamoto, U. Witt, G. Skupin, D. Beimborn, R. Muller *Biodegradable aliphatic-aromatic polyesters "Ecoflex"*, in *Biopolymers, Polyesters III: Applications and Commercial Products*, Y. Doi A. Steinbuchel Editor. 2002, Wiley-VCH: Weinheim.

11. Dow, *Styron 421 and 482*, 2005, http://plastics.dow.com/ap/prod/polystyrene/index.htm, Accessed on: May 5, 2005

4. MATERIALS PREPARATION

4.1 Processing Equipment

4.1.1 Microcompounding

Melt compounding was carried out in a micro twin-screw extruder with injection molder system (TS/I-02, DSM, Netherlands). The mini extruder (Figure 4.1) is equipped with co-rotating screws having length 150 mm, with L/D 18 and net capacity 15 cc and an attached injection molding unit capable of 140 psi injection force (Figure 4.2). Material components were weighed as per calculated compositions and mixed together in cups and fed to the extruder barrel. Liquid additives were injected inside the barrel via the feed port using disposable syringes midway through the experimental residence time. The materials were melt compounded for specific processing conditions of residence time and speed and after extrusion the melted materials were transferred through a preheated cylinder to the mini injection molder (pre-set at desired mold temperature) to obtain the desired specimen samples for various measurements and analysis

The injection molder has the following molds that were used for sample preparation.

1. Disc Mold (1.5 mm thickness, 25 mm diameter)
2. Tensile coupon mold (90 mm length, 1.5 mm thickness, 32 mm gauge length, 5 mm gauge width)
3. Izod Impact coupon mold (63.5 mm length, 4 mm thickness, 12.8 mm width)
4. Flexural coupon mold (65 mm length, 3 mm thickness, 12.5 mm width)

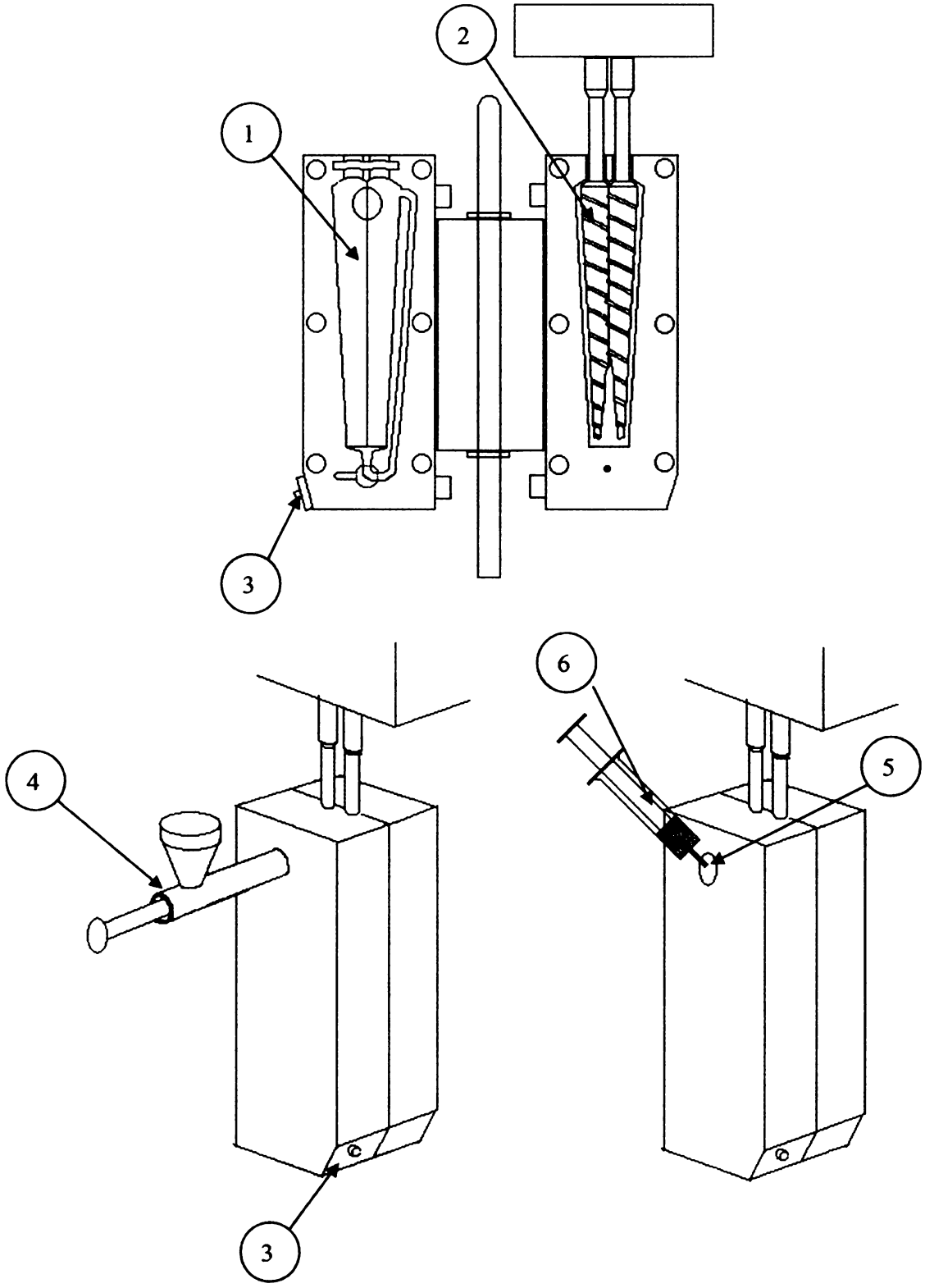

Figure 4.1: DSM Microcompounder with (1) Barrel; (2) Screws; (3) Exit port; (4) Feeder; (5) Feeder port; (6) Liquid additive Injector

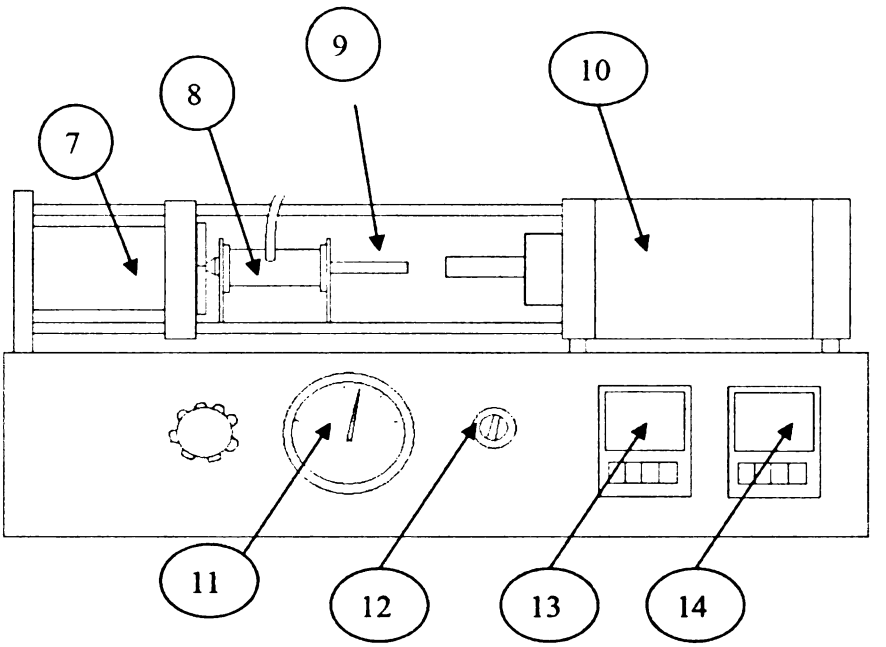

Figure 4.2: DSM Injection Molding Unit with (7) Mold and mold heater; (8) Transfer cylinder ;(9) Piston; (10) Pneumatic piston; (11) Pressure gauge; (12) Piston control knob; (13) Mold temperature controller; (14)Transfer Cylinder temperature controller

4.1.2 Extrusion Compounding

Pilot scale melt compounding was done in co-rotating twin screw extruder with metered feeders: CX Century Extruder (Model OX-30) was used for full-scale melt compounding of PHB-PBAT blends and their nanocomposites while for the Starch-PHBV work, a ZSK-30 extruder with venting ports was used.

The CX Century is a co-rotating twin screw extruder with a 30 mm screw diameter and 40:1 L/D ratio and attached with metered feeders. Small feeding screws were used to control the feed rate for resin and clay. The materials were melted and

mixed in the extruder section and forced through the die as strands. These melt compounded strands were then collected, dried and then pelletized.

The extruder used for the starch-PHBV work is a Werner-Pfleiderer ZSK 30 Twin Screw Extruder with co-rotating screws having 30 mm diameter and 30:1 L/D ratio outfitted with 3 vent ports. The screw configuration is shown in detail in Figure 4.3[1]. The compounded materials were collected on non-stick sheets, air cooled and then granulated using a regrinder.

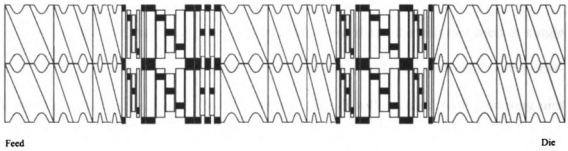

Figure 4.3: Screw configuration for the ZSK-30 extruder (Ref. 1)

4.1.3 Compression Molding

Compression molding of specimens into films for barrier testing was done using a carver press. A sandwich assembly comprising of two high-polish steel plates with non-stick sheets in between was used for compression molding. Disc specimens from injection molding or virgin pellets were placed in this sandwich assembly and the entire system was put in the pre-heated carver plates and compressed followed by water cooling.

4.1.4 Blown Film Extrusion

Blown film extrusion is a continuous process in which the polymer pellets are melted in the extruder and converted into film. A single screw extruder having 1 ¼ inch screw diameter and 24:1 L/D ratio attached with a blown film die was used for this process. The extruder was started up and the desired temperature profile was set following which the machine was allowed to stabilize for 3 hours. The feed zone was water cooled using external water to avoid pellet-choking during processing.

4.1.5 Cast Film Extrusion

The cast film extrusion process uses a slit die to shape the polymer melt. A single screw extruder having 1 ¼ inch screw diameter and 24:1 L/D ratio attached with a coat-hanger cast film die was used for this process. A chill roll attached with a cooling unit was used for winding the fabricated film. The extruder was started up and the desired temperature profile was set following which the machine was allowed to stabilize for 3 hours. The feed zone was water cooled using external water to avoid pellet-choking during processing.

4.2 Elastomeric Modification

4.2.1 Microcompounding

The PHB and PHBV pellets and the clays were dried in convection oven for 3 hours at 80 °C prior to processing. The optimized processing conditions (speed, temperature and residence time) were determined from analysis of extensive experiments

with variations in parameters. The natural rubber or epoxidized natural rubber is available as slabs and were cut into granules by hand prior to processing. Optimized Processing conditions for the materials in the microcompounder are listed in Table 4.1. The acronym TPO stands for thermoplastic olefin (rubberized polypropylene from Bassel) and HIPS stands for high-impact polystyrene (Styron from Dow).

Table 4.1: Processing conditions for micro-compounder

Material System	Temperature (°C)				Residence time (Minutes)	Speed (rpm)	Mold Temperature (°C)
	Top	Mid	Bot	Cyl			
PHB P226	190	185	172	180	2	200	50
P226-Rubber	190	185	172	180	3	200	50
TPO	190	190	190	190	2	200	60
HIPS	250	250	250	250	2	200	60

4.3 Compatibilizer Incorporation

4.3.1 Maleated Polybutadiene

Microcompounder: Maleated polybutadienes exist as high-viscous liquids at ambient temperature. These were incorporated into the PHB: natural rubber and PHB: epoxidized natural rubber systems via injection directly into the molten materials. The polymer and rubber were first charged into the microcompounder barrel and exactly

midway through the experimental residence time, the liquid compatibilizer system was injected inside the barrel using a disposable syringe. The variations in composition that were experimented in order to get the optimized combination are shown in the grid below (Table 4.2). The remaining component weight percentage in the "C" boxes is the amount of compatibilizer. E.g. the 70/25 box with C notation denotes that there is 100-70-25=5 weight % compatibilizer in the system.

Table 4.2: Elastomeric modification compositions

Rubber ↓ wt% →											
50											**X**
45										**X**	
40									**X**		**C**
35								**X**	**C**		
30							**X**		**C**		**C**
25						**X**	**C**		**C**		
20					**X**		**C**		**C**		
15				**X**	**C**						
10			**X**								
5		**X**									
0	**X**										
PHB wt% →	100	95	90	85	80	75	70	65	60	55	50

*Note: **X** denotes PHB/rubber and **C** denoted PHB/rubber/compatibilizer combination*

The processing conditions followed for all the compatibilized systems are given in Table 4.3

Table 4.3: Processing conditions for compatiblized systems

Material System	Temperature (°C)				Residence time (Minutes)	Speed (rpm)	Mold Temperature (°C)
	Top	Mid	Bot	Cyl			
PHB P226 + rubber + compatibilizer	190	185	172	180	2	200	50

4.4 Surface Modification of Clay

4.4.1 Toluene Based

The surface modification of pristine clay was done by edge modification. The reaction was carried out in toluene. The proposed reaction of the hydroxyl group from the clay with the titanate-coupling agent is represented in Figure 4.4[2]. Similar type of mechanism for the reaction of titanate coupling agent with inorganic substrate has also been reported by Monte[3]. Pristine monmorillonite clay (50g) was first suspended in the organic medium (300 ml), and the calculated amount of neopentyl (diallyl)oxy tri(dioctyl) pyrophosphato titanate was introduced in the reaction vessel and stirred for 2

hours at ambient temperature. Two levels of surface treatment were achieved by varying the amount of modifier; modified clay MC1 having titanate modifier corresponding to 3.8

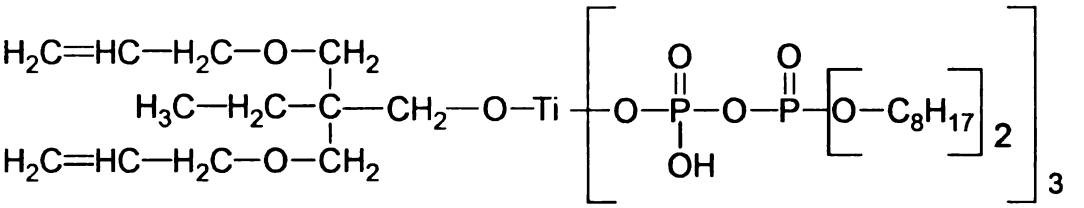

Neopentyl (dially)oxy tri (dioctyl) pyro-phospato titanante

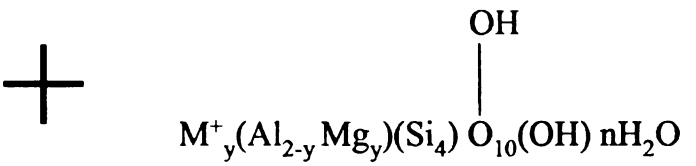

$M^{+}_{y}(Al_{2-y}Mg_{y})(Si_4)O_{10}(OH)\,nH_2O$

Montmorillonite

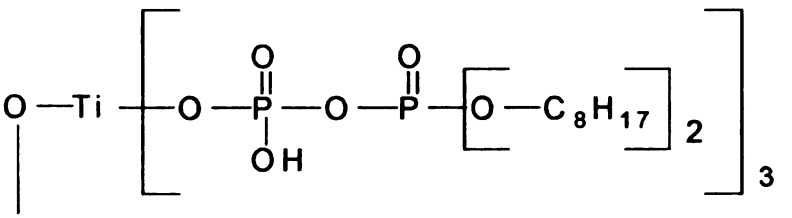

$M^{+}_{y}(Al_{2-y}Mg_{y})(Si_4)O_{10}(OH)\,nH_2O$

Modified clay with organo-titanate layer

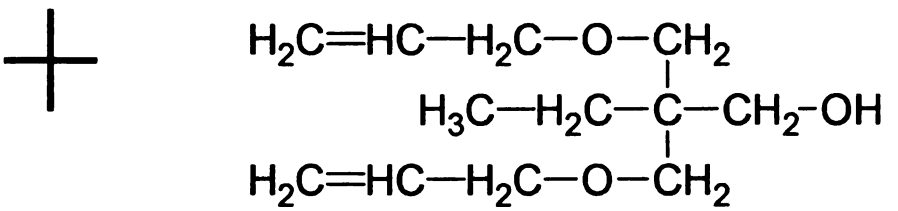

By-product

Figure 4.4: Schematic representation of the surface modification reaction (Ref. 2)

% of clay weight and MC2 corresponding to 11.4 % of clay weight. The modified clay was washed thrice with toluene in order to remove the modifier in excess and byproducts and dried at 55 °C in a vacuum oven for 5 hours before use.

4.4.2 Non-Aromatic Solvent Based

Toluene is an ideal medium for the above reaction owing to its ability to dissolve the titanate-based coupling agent. However toluene, being an aromatic hydrocarbon, is environmentally harmful and the large amount of waste toluene generated in the modification step was a reason of concern. The 5th Principle of Green Chemistry advocates the minimal use of auxiliary substances (e.g., solvents, separation agents, etc.) wherever possible and innocuous when used[4]. Hence such a solvent was investigated for the modification of the clay. This solvent is an aliphatic hydrocarbon sold under the trade-name Kwik-Dri by Ashland chemicals and it showed similar affinity and solubility for the titanate-based modifier. The modification technique is similar to the toluene-based modification.

4.5 Nanoclay Incorporation

In direct blending, clay is introduced into molten polymer directly at the desired composition level in a one-step method. In masterbatch blending, first a high-load masterbatch is prepared (~20-30 wt % nanoclay in polymer) which is let-down into final composition (2~5%) by adding polymer again in a second step. This technique was used for the PHB-rubber nanocomposites and the process conditions are given in Table 4.4. A

masterbatch was initially made having 20 weight % clay in PHB and this was the let down in the final nanocomposite to have 3, 5 or 7 weight % clay. This technique was also used for the materials made in the brabender as well as the two-roll mill.

Table 4.4: Processing conditions for nanocomposites

Material System	Temperature (°C)				Residence time (Minutes)	Speed (rpm)	Mold Temperature (°C)
	Top	Mid	Bot	Cyl			
PHB P226 + clay	190	185	172	-	2	200	-
PHB P226 + rubber + compatiblizer + clay	190	185	172	180	3	200	50

4.6 Starch Plasticization

The starch and glycerol were premixed in a kitchen mixer and allowed to set overnight in order to achieve impregnation. The starch to glycerol ratio was varied as 70:30, 65:35, 60: 40 and 55:45. These mixtures were extruded as per conditions given in

Table 4.5 and collected on non-stick sheets and then pelletized. These systems are denoted as plasticized starch (PS) from this point forth.

Table 4.5: Processing conditions for twin-screw extruder

Material name	Zone 1 (°C)	Zone 2 (°C)	Zone 3 (°C)	Zone 4 (°C)	Zone 5 (°C)	Die (°C)	Speed (rpm)	Torque (%)
Starch-Glycerol	125	130	135	140	150	140	125	50

4.7 Thermoplastic Starch and Polyhydroxyalkanoate Blending

4.7.1 Microcompounding

The optimum sequence of addition and blending of PHB, plasticized starch and PCL was investigated. In the first system, the plasticized starch was blended with PCL followed by addition of the PHBV in a second stage. In the second system, PHB and plasticized starch were blended followed by addition of the PCL in a second step. The third system consisted of adding all the components in one step. The composition variations included substituting PHB with PHBV and PCL with PBAT. The processing conditions for these experiments are presented in Table 4.6

Table 4.6: Processing conditions for micro-compounder

Material System	Temperature (°C)				Residence time (Minutes)	Speed (rpm)	Mold Temperature (°C)
	Top	Mid	Bot	Cyl			
PHB	165	160	155	160	3	100	55
PS-PCL	165	160	155	-	2	100	-
PS-PHB	165	160	155	-	2	100	-
(PS-PCL)-PHB	165	160	155	160	3	100	55
(PS-PHB)-PCL	165	160	155	160	3	100	55
(PS-PCL-PHB)	165	160	155	160	3	100	55
(PS-PCL-PHBV)	165	160	155	160	3	100	55
(PS-PBAT-PHB)	165	160	155	160	3	100	55
(PS-PBAT-PHBV)	165	160	155	160	3	100	55

4.7.2 Large-scale Compounding

The extruder used for the starch-PHBV work is the ZSK 30 Twin Screw Extruder. For the composites and nanocomposites, a masterbatch technique was followed. A 20% by weight masterbatch of talc or nanoclay in PBAT was prepared first and then let down using the other components so as to achieve the final composite or nanocomposite containing the desired additive concentrations. The talc or nanoclay feeding was done using a side feeder. For the blends as well as the composites and nanocomposites, the pelletized masterbatch and/or plasticized starch were thoroughly mixed with the PBAT and PHBV pellets by hand and this mixture was fed to the extruder via the main feeder. Process conditions are provided in Table 4.7. The compounded materials were collected on non-stick sheets, air cooled and then granulated using a regrinder.

Table 4.7: Processing conditions for twin-screw extruder for PHBV-TPS

Material name	Zone 1 (°C)	Zone 2 (°C)	Zone 3 (°C)	Zone 4 (°C)	Zone 5 (°C)	Die (°C)	Speed (rpm)	Torque (%)
PHBV-PBAT-PS	130	150	170	160	160	150	125	60
PBAT-clay/talc	130	150	170	160	160	150	125	80
PHBV-PBAT-PS-clay/talc	130	150	170	160	160	150	125	60

4.7.3 Cast Film Extrusion

The pelletized materials were processed into cast films using the single-screw cast film extruder. The chill roll was set at 0°C with an actual temperature of 10°C. The process parameters followed in cast film making are shown in Table 4.8.

Table 4.8: Processing conditions used in the Cast Film Extruder

Zone	**PHBV/PS/PBAT blends**	**PHBV/PS/PBAT blends with clay or talc**
	Temperature (°C)	**Temperature (°C)**
zone 1	170	170
zone 2	170	170
zone 3	170	170
Adaptor	160	160
Die	155	155
Screw speed (machine value)	50	50
Winding Speed (machine value)	1.3	1.3

4.8 References

1. Werner-Pfleidderer, *ZSK 30 Twin Screw Extruder manual*, 1994

2. Y. Parulekar, A.K. Mohanty, *Effect of Titanate-based Surfaces on Hydrophilicity and Interlayer spacing of Montmorillonote Clay for Polymer Nanocomposites*, Journal of Nanoscience and Nanotechnology, 2005, 5, 2138-2143

3. Monte, S. J., *Kenrich Petrochemicals Reference manual and product literature*, 2007

4. P. T. Anastas, J.C. Warner, *Green Chemistry: Theory and Practice*. 1998, New York, : Oxford University Press.

MODIFIED BIOBASED MATERIALS FROM POLYHYDROXYALKANOATES FOR PACKAGING AND ENGINEERING APPLICATIONS

VOLUME II

By

Yashodhan S. Parulekar

A DISSERTATION

Submitted to
Michigan State University
in partial fulfillment of the requirements
for the degree of

DOCTOR OF PHILOSOPHY

School of Packaging

2007

5. MATERIALS CHARACTERIZATION

5.1 Thermal

5.1.1 Differential Scanning Calorimetry

A differential scanning calorimeter (DSC Q100, TA Instruments, DE) was used to determine the thermal transitions of the materials as well as the developed blends and nanocomposites as per ASTM D-3418[1]. These experiments were performed at a ramp rate of 10°C/min from –40°C to 200°C using hermetically-sealed aluminum pans.

5.1.2 Thermogravimetric Analysis

A thermogravimetric analyzer (TGA 2950, TA Instruments, DE) was used to determine the weight change of the materials as a function of temperature. These experiments were performed in platinum pans at a ramp rate of 10°C/min under nitrogen purge flow (90ml/min) from room temperature to 600°C.

5.1.3 Dynamic Mechanical Analysis

Storage modulus of the materials was measured using a Dynamic Mechanical Analyzer (2980 DMA, TA Instruments, DE). For the injection molded samples, the DMA was run in the dual cantilever mode over a temperature range of –50°C to 150°C at a scanning rate of 5°C per minute and using a frequency of 1 Hz and amplitude of 15μm as per ASTM D-5023[2]. For the film samples, the DMA was run in a film tension mode over a temperature range of -90°C to 150°C at a scanning rate of 5°C per minute using a

frequency of 1 Hz and amplitude of 5 μm as per ASTM D-5026[3]. Storage modulus values were noted at 30°C.

5.1.4 Thermo Mechanical Analysis

The coefficient of linear thermal expansion was measured using a Thermo-Mechanical Anaylzer (2900 series TMA, TA Instruments, DE). Injection molded materials were cut into cubes with 3 mm dimensions and these were analyzed using standard probe over a temperature of 30°C to 150°C.

5.1.5 Heat Deflection Temperature

Heat deflection temperature (HDT) is denoted as the maximum temperature at which the material can be used in rigid applications. This was evaluated on the DMA apparatus in controlled force mode according to ASTM D 648 standard[4]. This procedure defined the heat deflection temperature as the temperature at which the sample deflects by 250 μm under an applied load of 0.455 N/mm^2.

5.2 Optical

5.2.1 Polarized Light Microscopy

For crystallinity studies, materials were compression molded into films and these films were studied using polarized optical microscopy (Olympus BH-2, Olympus, NY). The films were heated using a Mettler hot stage (Mettler FP-90, Mettler, OH) to above the melting temperature of the material and cooled at 5°C per minute to the crystallization

temperature and held isothermally. The crystallization and spherulite growth were observed using a polarized lens.

5.3 Morphological

5.3.1 Sample Preparation

Scanning Electron Microscopy and Environmental Scanning electron microscopy require the material be conductive for observations. The fracture surfaces (Izod impact fracture or tensile fracture) were coated with gold sputtering.

Transmission electron microscopy can be used to observe ultra-thin films only. Hence the bulk specimens were sectioned using microtoming to get samples having thickness of 100 nm. The microtoming was carried out at –130°C using diamond blade on a RMC cryomicrotome station.

Atomic Force microscopy samples were cut from the bulk injection molded specimens using a diamond cutter and then polished to high smoothness using an abrasive sander.

5.3.2 Environmental Scanning Electron Microscopy

An Environmental Scanning Electron Microscope equipped with both secondary electron detectors and backscattered electron detectors was used to observe the fracture surface of the samples at current of 1.85A and 15 kV beam voltage.

5.3.3 Scanning Electron Microscopy

A JOEL 6300F with field emission (Oxford EDS) SEM microscope was used to observe the gold-sputter-coated samples at beam voltage of 15 kV and current of 1.83 A.

5.3.4 Transmission Electron Microscopy

A JOEL 100 CXII TEM microscope was used to analyze the morphology of nanocomposites at an acceleration voltage of 100 kV in bright field operating mode.

5.3.5 Atomic Force Microscopy

AFM studies of polished samples were done using an AFM microscope (Digital Instrument MultiMode SPM with Nanoscope IV controller, Digital Instruments, NY) in the force modulation mode.

5.3.6 X-ray Diffraction

X-ray powder diffraction patterns were obtained using a Rigaku 200B X-ray diffractometer (45 kV, 100 mA) equipped with CuKα radiation (λ= 1.541 nm) and a curved graphite crystal monochromator at a scanning rate of 0.5 °/min. The d_{001} basal spacings were calculated from the 2θ values using *Braggs'* Equation[5].

5.4 Spectroscopy

5.4.1 Fourier Transform Infra Red Spectroscopy

Infrared (IR) spectra were obtained on a Fourier Transform IR instrument (Spectrum One, Perkin-Elmer, MA) in the attenuated total reflectance mode.

5.4.2 X-ray Photoelectron Spectroscopy

Surface elemental analysis was performed on an X-ray photoelectron spectrometer (XPS). XPS measurements were performed using a Physical Electronics PHI-5400 ESCA workstation. X-Ray photons were generated from a polychromatic Magnesium anode (1254 eV). The analyzer was operated in the fixed energy mode employing a pass energy of 89.45 eV for survey scans and 17.9 eV for utility scans. Clay samples were affixed to the specimen holder with double-sided tape. Semi-quantitative information was obtained by measuring the C 1s and O 1s peak areas and applying the appropriate sensitivity factors[6]. The C 1s spectral envelope was fitted using a non-linear least-squares curve fitting routine. Goodness of fit was tested with a simple materials balance by comparing the O/C atomic ratio estimated from the deconvolution to the actual value.

5.4.3 C-H-N Analysis

Carbon-Hydrogen-Nitrogen analysis of milled samples was done on a Perkin-Elmer CHN 2400 Series II CHNS/O analyzer.

5.5 Surface Characterization

5.5.1 Capillary Wicking

The water contact angles for the clays were measured on a CAHN 322 microbalance (ThermoCahn, WI) in the wicking mode using a modified Washburn equation. The Washburn equation[7, 8] is given in its original form as equation 5.1.

$$h^2 = \frac{tr\gamma_L Cos\theta}{2\eta} \qquad (5.1)$$

In this equation, the height, h, of the probe liquid uptake is measured at time, t, and the contact angle, θ, is calculated from the effective interstitial pore radius, r, the viscosity, η, and the surface tension of the probe liquid, γ_L. Measuring the height uptake is difficult and error-prone and so the equation is modified based on the density of the liquid and the mass increase. The modified Washburn equation 5.2 calculates the contact angle based on the liquid mass uptake by the solid [9]:

$$m^2 = \frac{tc\rho^2\sigma Cos\theta}{\eta} \qquad (5.2)$$

In this equation, the mass (m) of the probe liquid uptake is measured at time (t) and the contact angle (θ) is calculated from the material constant (c), the viscosity (η), the density (ρ), and the surface energy (σ), of the probe liquid. The material constant is calculated for a powder-capillary pair using a liquid that spreads completely over the surface (hexane, Cos θ = 1) and this value is used for the water contact angle calculations. The clay samples were filled in sealed PTFE capillaries of 0.0066 inch diameter and 1 inch length. These capillaries were then packed on a universal testing machine (UTS SFM-20, United Calibration Systems, CA) in the compression mode (Figure 5.1 a). The capillaries were held in a metallic holder on the compression fixture and a thin metal piston was used to pack the clay at a rate of 0.1 inch per minute to a force of 5 lbs and then 0.05 inch per minute to a force of 5 lbs. This method ensured all the capillaries were packed uniformly

with the same force and with minimal voids. These packed capillaries were suspended in the microbalance (Figure 5.1 b) and bought in contact with hexane for three minutes

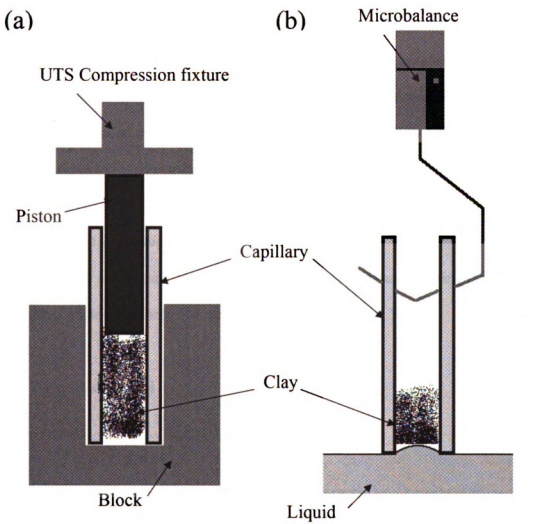

Figure 5.1: Schematic representation of contact angle measurement setup by wicking. (a) Capillary packing, (b) wicking in microbalance

(hexane: Cos $\theta = 1$, $\eta = 0.33$ centipoise (cP), $\rho = 0.661$ mg/mm^3, $\sigma = 18.4$ mN/m). The mass uptake was measured as a function of time and then the corresponding graphs of square of mass absorbed against time were plotted. The slopes of these plots were used to

calculate the material constants for the modified Washburn equation 5.2. The hexane-exposed capillaries were dried in vacuum oven at 50°C for 8 hours to remove the absorbed hexane. These dried capillaries were then suspended in the microbalance and bought in contact with deionized water for three minutes (deionized water: η = 0.89 cP, ρ = 1 mg/mm^3, σ = 72.3 mN/m). The corresponding plots of square of mass absorbed against time were used to obtain the slopes and these values were substituted in equation 5.2 along with material constant values to calculate the contact angle for the pristine and modified clays.

5.5.2 Goniometry

The water contact angles of the bulk materials were measured using a Rame-Hart NRL contact angle goniometer (Model 100-00-115, Rame-Hart, NJ).

5.6 Mechanical

5.6.1 Tensile

Universal Tester (Instron) model 5565 was used for measuring tensile strength, modulus of elasticity and the percent elongation of the films following the ASTM standard D 882 [10]. The sample width of 1 inch and the gauge length of 1 inches with a grip separation speed of 2 in/min were used. The tensile properties of the injection-molded materials were measured with the United Testing System SFM-20 according to ASTM D 638[11].

5.6.2 Impact

Izod notched impact properties of the materials were measured on an Izod Impact Tester (TMI Model 43-02, TMI, NY) as per ASTM D256[12] for notched Izod impact testing with 5 lb-f pendulum. The samples were notched up to prescribed depth using a mechanical notcher (TMI Model 22-05, TMI, NY) and then conditioned for 48 hours at 50% RH and 23°C. Ten specimens were tested for each sample material.

5.6.3 Flexural

The flexural properties of the injection-molded materials were measured with a United Testing System SFM-20 according to ASTM D 790 standard[13].

5.7 Rheological

5.7.1 Parallel Plate

Rheology experiments on the blended materials and their nanocomposites were carried out in a parallel rheometer (ARES, TA Instruments, DE). Dynamic frequency sweep experiments were performed at 170 °C using 25 mm parallel plates in the linear viscoelastic region of the materials.

5.8 Mass Transfer

5.8.1 Oxygen Transmission

The Oxygen transmission tester (OXTRAN) model 2/21 from Mocon Instruments, MN was used to measure the oxygen permeability of the films as per ASTM D 3985[14]. Samples were cut from the films and then mounted onto the cells. The samples were tested at 23°C, 0%RH and 740 mmHg.

5.8.2 Water Vapor Transmission

The Water Vapor transmission tester (PERMATRAN) model W3/31 from Mocon was used to determine the water vapor permeability of film samples as per ASTM E-96[15]. Samples were cut from the films and then mounted onto the cells. The films were tested at 37.8°C, 100%RH and 740 mmHg.

5.8.3 Leaching

Leaching of plasticizer from the fabricated thermoplastic starch-PHBV-PBAT blends was investigated using two methods: weight change and dynamic mechanical analysis. For both these tests the samples were conditioned at 30°C and 50 % relative humidity in a controlled environmental chamber for the duration of the study (30 days from day of fabrication). Samples were tested every alternate day for the above two tests as well as for mechanical and DSC testing. For the weight change experiments, samples were wiped with paper towels to absorb the plasticizer that may have leached out to the surface of the samples and then weighed. For the DMA, the samples were tested as per conditions described in section 5.6.3 and the shift of the Tan delta peak was observed. Similar observations were done for the percent crystallinity as calculated from the melting endotherm in the DSC curves.

5.9 Biodegradation

5.9.1 Biodegradation by Respirometry

Sample Preparation: Samples were milled to fine consitency (average particle size is 25 μm) using a hammer mill under liquid nitrogen environment. These milled samples were analyzed for initial carbon content using an automatic Carbon/hydrogen/nitrogen analyzer. .

Respirometry: these experiments were done in collaboration with United States Department of Agriculture's Bioproduct Chemistry and Engineering Research, Western Regional Research Center, Agricultural Research Service at their facilities. About 0.2 g of each sample of known carbon content was mixed with 20 g of compost under appropriate conditions. These sample-soil mixtures were kept in seperate 250-mL sample chambers of a fully computerized, closed-circuit Micro-Oxymax Respirometer System (Columbus Instruments, Inc., Columbus, OH) equipped with an expansion interface, a condenser, and a water bath. The sample chamber was placed in a water bath controlled at 25° C and 50% RH and connected to the Micro-Oxymax Respirometer. Experiments were carried out over a period of 105 days. CO_2 evolution from each sample was measured every 8 hours.

The total available carbon in the starting material (0.2 g) of each sample was calculated from the predetermined percent carbon values. The values for the total accumulated CO_2 volume during biodegradation for a sample in a reaction chamber were obtained through respirometry. These volume V data were used in the equation of state of

the ideal gas law; PV = nRT, to determine the moles (n) of carbon converted into CO_2 as a result of microbial processes in a compost, where the molar gas constant R= 0.082055 L-atm/K-mol; T = 298 Kelvin (25° C), and pressure P = 1 atm.

The percent biodegradation was obtained from the sum of net moles of CO_2 released in a sample chamber divided by the moles of CO_2 present in the original sample and multiplied by 100.

5.9.2 Aerobic Biodegradation

Sample Preparation: Samples were grinded to a fine particle size using a granulator with a 2 mm screen. The compost was obtained from the Michigan State University composting facility (East Lansing, MI). The compost pile had initial composition of cow manure, wood shaving and waste and was matured for 3 months. The initial temperature of the compost was 65 ± 5° C with relative humidity of 63 ± 5%, and pH of 8.5 ± 0.5 as given by the provider. This was altered by drying under vacuum to get 50± 1 % relative humidity. The compost as received was filtered through a wire mesh having 5 mm hole size in order to get an uniformly sized material devoid of large chips. 15 g of each polymeric material that is to be tested was mixed with 180 g of compost having 50% moisture in order to get a testing material to compost dry solids ratio of 1:6. These mixed samples were introduced into the testing chambers set at 60°C for testing.

Testing: The experimental setup was designed as per ASTM D 5338[16] and is shown in Figure 5.2. As per Figure 5.2, the external air is scrubbed of carbon dioxide by bubbling it through sodium hydroxide solution (10 N strength). This carbon dioxide-free air is then fed through distilled water to appropriately moisten the air stream and this is

then divided to each biodegradation chamber. Fifteen chambers were prepared having compositions given in Table 5.1. The above air stream passes through the biodegradation

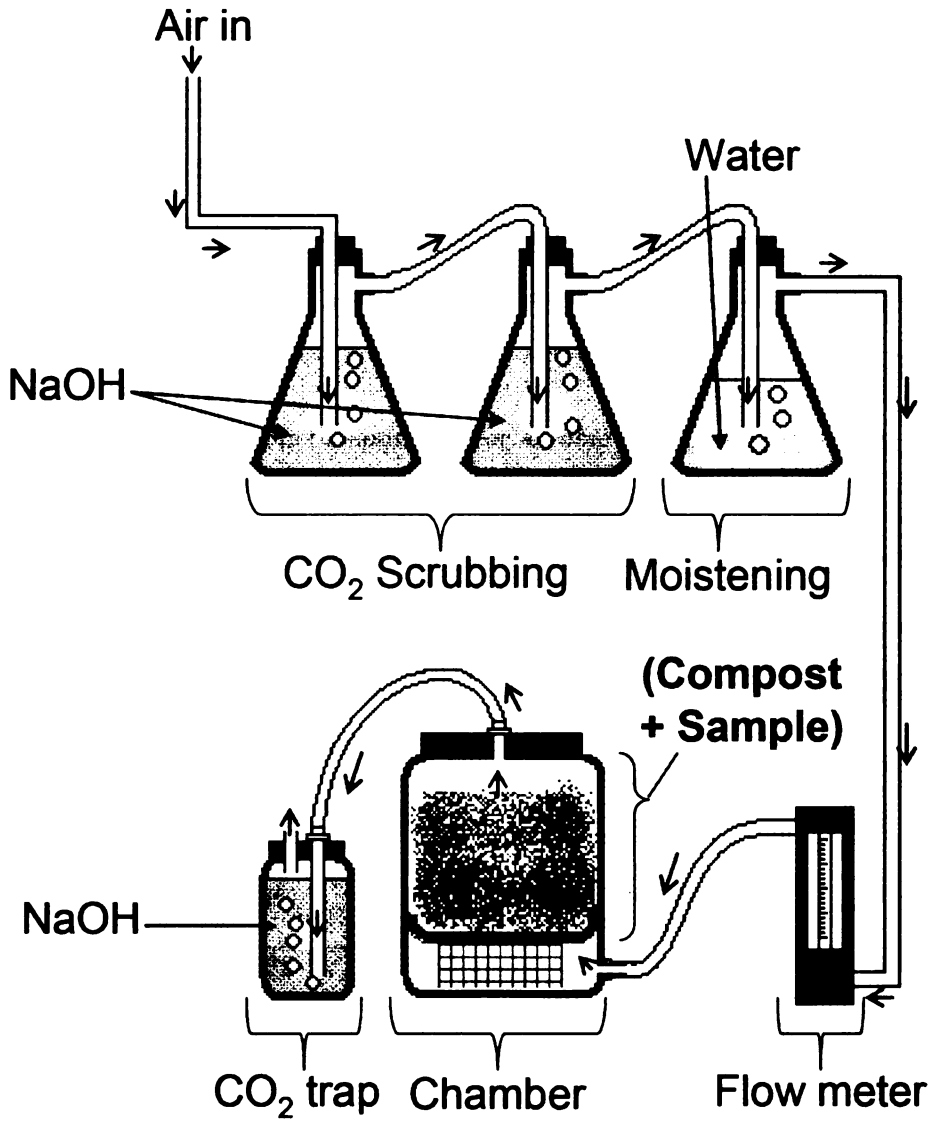

Figure 5.2: Schematic representation of aerobic biodegradation setup

chamber and is then fed to individual bottles containing sodium hydroxide (0.25 N). This sodium hydroxide reacts with the carbon dioxide released from the biodegradation

reaction present in the air and forms sodium carbonate. This solution of sodium carbonate and unreacted sodium hydroxide was titrated over specific time intervals against hydrochloric acid (0.5 N) to determine the carbon dioxide released by aerobic biodegradation. The entire biodegradation setup was installed in a controlled environmental chamber maintained at 60 °C and 50% relative humidity for the duration of the experiment. The system was allowed to stabilize overnight and then the air stream was introduced into the chambers. The air was controlled by the individual flow meters on the chambers so as to achieve a bubble rate of approximately one per second.

Table 5.1: Sample Compositions for Aerobic Biodegradation studies

Sample	**Composition**	**Chamber numbers**	**Sample weight (g)**	**Compost dry weight (g)**	**Compost Weight (g)**
Blank	-	1,2,3	-	90	180
Positive control	Corn Starch	4,5,6	15	90	180
A	PHBV+ TPS	7,8,9	15	90	180
C	PHBV+ TPS + 5% talc	10,11,12	15	90	180
D	PHBV	13,14,15	15	90	180

5.10 References

1. Standard, American Society for Testing and Materials (ASTM International), *ASTM D3418 Standard Test Method for Transition Temperatures and Enthalpies of Fusion and Crystallization of Polymers by Differential Scanning Calorimetry*, 2003

2. Standard, American Society for Testing and Materials (ASTM International), *ASTM D5023 Standard Test Method for Measuring the Dynamic Mechanical Properties: In Flexure (Three-Point Bending)*, 2001

3. Standard, American Society for Testing and Materials (ASTM International), *ASTM D5026 Standard Test Method for Plastics: Dynamic Mechanical Properties: In Tension*, 2006

4. Standards, American Society for Testing and Materials (ASTM International), *ASTM D648: Standard Test Method for Deflection Temperature of Plastics Under Flexural Load in the Edgewise Position*, 2006

5. W.H. Bragg, W.L. Bragg, *The Reflection of X-rays by Crystals*, Proceedings of the Royal Society of London, 1913.

6. Sherwood, P. M. A., in *Practical Surface Analysis by Auger and X-ray Photoelectron Spectroscopy* and M.P. Seah D. Briggs, Editor. 1990, Wiley.

7. R. E. Ayala, E. Z. Casassa, G. D. Parfitt, *A study of the applicability of the capillary rise of aqueous solutions in the measurement of contact angles in powder systems*, Powder Techology, 1987, 51, 3-14

8. Washburn, E., *The Dynamics of Capillary Flow* Physical Review, 1921, 17, 273-283

9. G. Berendsen, L. De Galan, *Preparation and chromatographi properties of some chemically bonded phases for reversed-phase chromatography*, Journal of Liquid Chromatography, 1978, 1, 561-569

10. Standard, American Society for Testing and Materials (ASTM International), *ASTM D882 Standard Test Method for Tensile Properties of Thin Plastic Sheeting*, 2002

11. Standard, American Society for Testing and Materials (ASTM International), *ASTM D638 Standard Test Method for Tensile Properties of Plastics*, 2003

12. Standard, American Society for Testing and Materials (ASTM International), *ASTM D256 Standard Test Methods for Determining the Izod Pendulum Impact Resistance of Plastics*, 2006

13. Standard, American Society for Testing and Materials (ASTM International), *ASTM D790 Standard Test Methods for Flexural Properties of Unreinforced and Reinforced Plastics and Electrical Insulating Materials*, 2003

14. Standard, American Society for Testing and Materials (ASTM International), *ASTM D3985 Standard Test Method for Oxygen Gas Transmission Rate Through Plastic Film and Sheeting Using a Coulometric Sensor*, 2005

15. Standard, American Society for Testing and Materials (ASTM International), *ASTM E96/E96M Standard Test Methods for Water Vapor Transmission of Materials*, 2005

16. Standard, American Society for Testing and Materials (ASTM International), *ASTM D 5338 Standard Test Method for Determining Aerobic Biodegradation of Plastic Materials under Controlled Composting Conditions.*, 2003

6. RESULTS AND DISCUSSION

The major goal of this work is to overcome the inherent brittleness of Polyhydroxyalkanoates and hence considerable emphasis has been placed on mechanical properties coupled with morphological analyses as a measure of effective toughening.

The first part of this section covers elastomer-toughened PHB and their nanocomposites followed by analysis of the thermoplastic starch based PHBV systems and their composites.

6.1 Elastomeric Toughening

6.1.1 Polyhydroxybutyrate - Natural Rubber System

The incorporation of rubber particles into a brittle thermoplastic matrix is a widely followed technique to improve the impact properties and the toughness of the polymer. One well-known example of this is high-impact polystyrene (HIPS) in which an elastomer (polybutadiene) is mixed with the styrene monomer and polymerized[1]. Under optimal conditions and using appropriate compatibilizers, synergistic effects arise to create high impact toughened blends[2-4]. The effectiveness of this elastomer-based toughening mechanism highly depends on the mechanical properties of the matrix, the elastomeric modifier, the dispersion of the modifier, and the interfacial adhesion among the different phases[4, 5].

Keeping with the focus on renewable resources in this work, the elastomer-based toughening experiments were started with using pure natural rubber as the toughening agent. However, natural rubber and semi-crystalline polymers similar to PHB form an immiscible blend, which has been widely reported in literature[5-11]. This is primarily due to the significant difference in melt behavior of the materials that translates to poor properties in the solid state. PHB is a linear polymer with no side-chains and hence there is minimal entanglement[12, 13]. This causes the chains to slip and move among themselves easily at elevated temperatures. Because of this effect, PHB exhibits pseudoplastic behavior; highlighted by a drastic drop in viscosity with increase in temperature. In comparison, the viscosity of the specific rubber used is very high. The reason for this is that the viscosity of rubber is a function of its purity and quality and the qualitatively best rubber has been reported to have the highest initial viscosity[14]. This study used a high purity grade rubber and hence the viscosity values were expected to be much higher than those of PHB at similar conditions. These melt viscosities of the virgin materials were determined by doing parallel-plate rheological studies. This instrument can provide the viscosity curves as a function of shear rate and mimics conditions that the material may be subjected to in the actual processing stages. The primary mode of processing of the toughened PHB in this work is the microcompounder. The microcompounder has conical co-rotating screws whose diameters decrease from feed port to the outlet. The microcompounder barrel was opened and the minimum (0.1 cm) and maximum (0.35 cm) clearances between the screws and the barrel walls were measured using micrometer calipers. Using the processing speed (200 rpm), the shear rate in the micro-extruder was calculated. These values gave the shear rate window of the microcompounder to be

between 8.42 s^{-1} to 230 s^{-1}. These shear rate conditions were simulated in the parallel plate rheometer at the desired processing temperature and the corresponding melt viscosity values were obtained for PHB and rubber (Figure 6.1). Thus it was determined that rubber is 20-50 times more viscous than PHB at the processing temperature used (170° C).

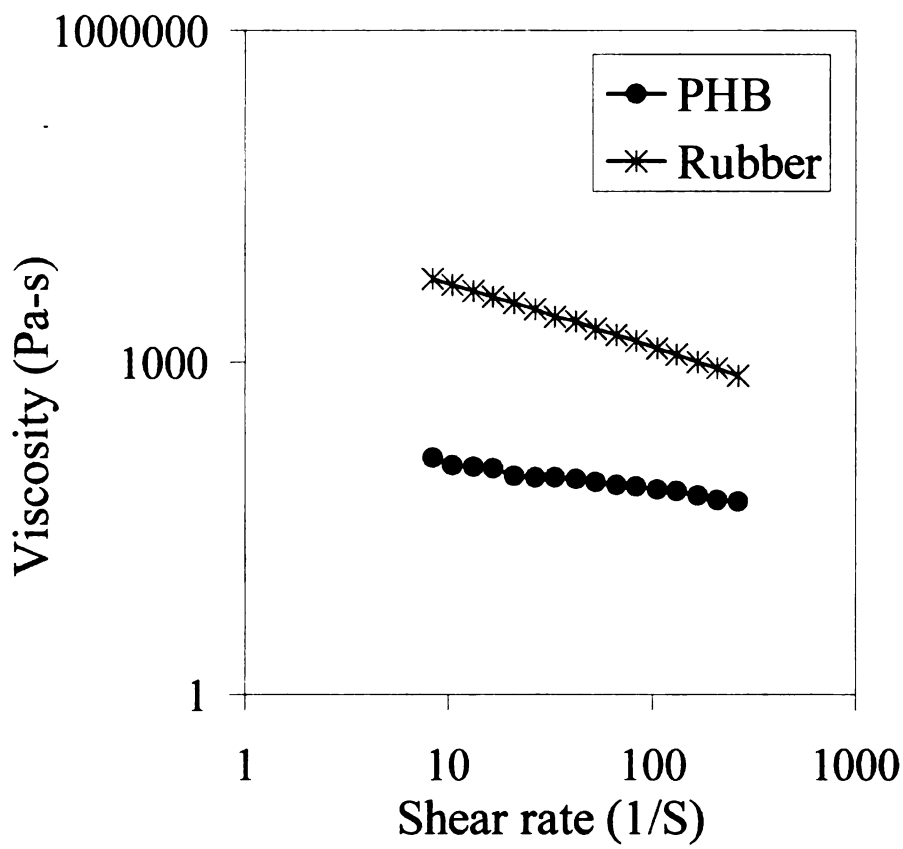

Figure 6.1: Melt viscosity values of PHB and Rubber for the shear rate range in the microextruder.

The melt viscosity ratio x, of the dispersed rubber phase to the PHB matrix is known to control the rubber particle coalescence and breakup during processing and consequently the ultimate rubber particle size[15]. This is quantified by equation 6.1 which gives the relation between volume fraction (V) and melt viscosity (η) as:

$$X = V_{PHB}\eta_{rubber} / V_{rubber}\eta_{PHB} \qquad (6.1)$$

The value of X determines the continuous phase. The PHB phase is continuous if X>1 whereas at X≈1, phase inversion occurs and the rubber phase will become continuous. The particle size reaches a minimum value at the value of X approaches 1 and this imparts maximum toughness to the material.

The high viscosity of the rubber component in comparison with PHB results in PHB remaining the continuous phase over the processing window of the blend. This can be overcome by using large quantities of rubber in relation to PHB or using a low molecular weight rubber that can give lower viscosity or by using compatibilizers. The first two methods are not feasible as they will compromise the structural integrity of the blend and hence the compatibilizer technique was selected to improve the blend properties.

The incompatibility of PHB and rubber in absence of compatibilizer was also established by using the *Takayanagi* models that predicts the blend moduli of phase

separated systems[16]. These models give a lower bound and upper bound estimate of the modulus of a binary blend system based on the morphology of the blend components. In all the models E is the elastic modulus and the quantities λ and φ or their products are the volume fractions of rubber phase. For example in equation 6.4 and 6.5 the volume fraction of the rubber phase is given by the product $\lambda \varphi$.

The upper bound value of the modulus of the blend is given by equation 6.2 which represents an iso-strain system with both rubber and PHB phases continuous.

$$E_{max} = (1 - \lambda) E_{PHB} + \lambda E_{rubber} \qquad (6.2)$$

The lower bound value of the modulus is given by equation 6.3 which is for a blend system wherein neither the PHB nor the rubber phases are continuous and the modulus of the blend is nearer to the phase that will fail first i.e. the rubber phase.

$$E_{min} = [(\varphi/E_{rubber}) + (1 - \varphi/E_{PHB})]^{-1} \qquad (6.3)$$

The storage modulus of PHB was measured as 1600 MPa and the storage modulus of rubber as 1.70 MPa (measured in DMA). The storage modulus measured by DMA relates to the elastic component of the material. These values were equivalent to

tensile modulus values measured earlier for the same materials and hence the DMA modulus values are used in calculations. The volume fraction of rubber in all the systems is 0.25. Substituting these values gave the upper bound value as 1200 MPa and the lower bound value as 6.78 MPa.

The intermediate values are for a continuous PHB phase with a discontinuous rubber phase and are dependant on the morphologies of the blends and are given by equations 6.4 and 6.5. Equation 6.4 has a continuous phase (PHB) in series with a parallel connection of the discontinuous rubber phase and another PHB phase:

$$E= [[\varphi/(\lambda E_{rubber}+(1-\lambda)E_{PHB})] +[(1-\varphi)/E_{PHB}]]^{-1} \qquad (6.4)$$

Equation 6.5 assumes the continuous phase (PHB) in parallel with a series connection of the discontinuous rubber phase and another PHB phase:

$$E= \lambda[(\varphi/E_{rubber}) + ((1-\varphi)/E_{PHB})]^{-1} +(1-\lambda)E_{PHB} \qquad (6.5)$$

The volume fraction of the rubber phase is $\varphi\lambda = 0.25$ and so $\varphi = \lambda = 0.5$. Equation 6.4 predicts the modulus value to be 1067 MPa and this will be possible if the rubber phase is encapsulated by the plastic and also these phases are significantly compatible.

Equation 6.5 predicts the modulus value to be 801 MPa and will be possible if again the

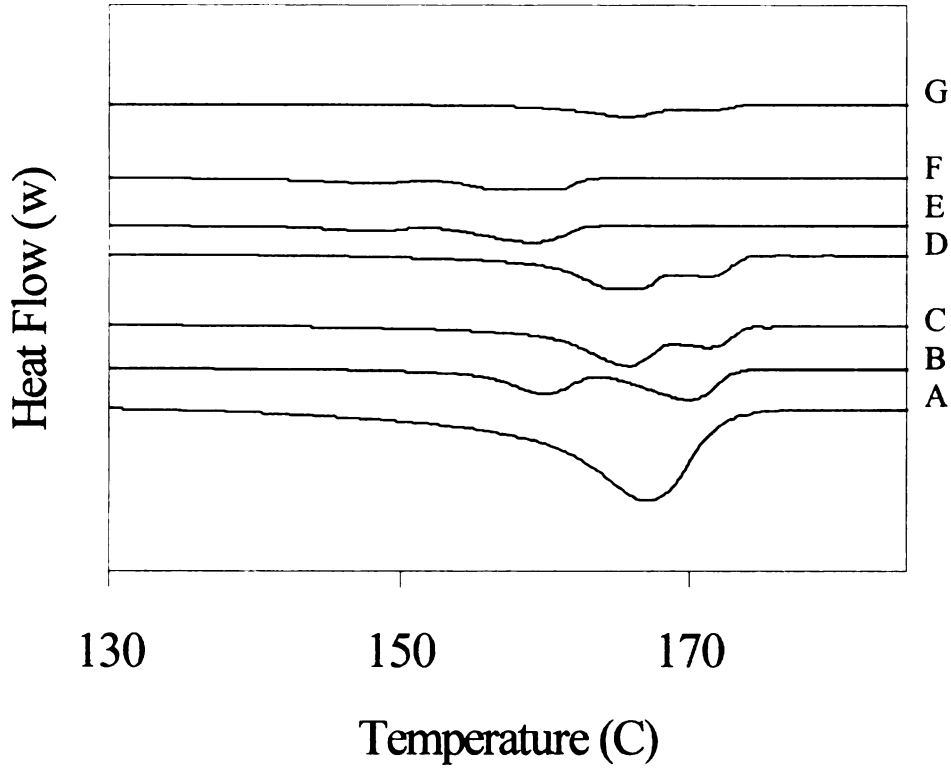

Figure 6.2: DSC curves denoting melting peaks: (A) PHB, (B) PHB + 40% NR, (C) PHB + 10% MR1 + 30% NR, (D) PHB + 10% MR2 + 30% NR, (E) PHB + 40% ENR, (F) PHB + 30 % ENR + 10 % MR1 and (G) PHB + 30 % ENR + 10 % MR2.

NOTE: PHB: Polyhydroxybutyrate, NR: Natural Rubber, MR1: RI131MA5, ENR: Epoxidized Natural Rubber and MR2: RI130MA20.

rubber phase is encapsulated by PHB and these form a well-dispersed yet uncompatibilized blend that gives the lower bound value. The actual value of the PHB-rubber blend modulus was 600 MPa and this is lower than the lower predicted value of the modulus for a blend with a dispersed rubber phase (equation 6.5) thus establishing

that the rubber is unable to be dispersed by shear alone and it needs chemical or physical intervention such as a compatibilizer.

Comparison of DSC thermal transition profiles of PHB and the PHB-natural rubber blend showed that the blend gave two melting peaks (Figure 6.2). Since natural rubber is completely amorphous, this behavior can be explained as being due to the presence of a hybrid type of crystal formed due to some interaction between PHB crystallites and the rubber[17]. When there are two types of crystals such as seen in this system, it is possible for them to have individual melting points. The DSC curves were also used to obtain the melting enthalpies of the PHB phases in the virgin polymer and the blend. For PHB, the melting enthalpy is dependant on the spherulite size and the blend morphology[18, 19]. Hence the rubber and the compatibilizers are expected to significantly affect the melting enthalpy. The melting enthalpy ΔH for PHB and of the PHB phase in the PHB-natural rubber blends are given in Table 6.1 along with their corresponding specific melting enthalpies. These specific melting enthalpies of the PHB phases in all the systems remain relatively unchanged, thus implying that the natural rubber is not interacting with the PHB, nor is it compatible. The polarized light micrographs of PHB (Figure 6.3) and the PHB-natural rubber blends (Figure 6.4) also do not exhibit any change in the size of the spherulites. If the rubber phase were compatible with the PHB, it would interfere with the PHB crystallites and reduce the spherulite size.

Table 6.1: Melting enthalpies and corresponding specific melting enthalpies of PHB and the PHB phase in the toughened blends.

No.	Composition	ΔH (J/g)	W_{PHB}[a]	$\Delta H/W_{PHB}$
1	PHB	81.37	0.9	90.41
2	PHB + 40% NR	49.83	0.54	92.27
3	PHB + 30 % NR + 10% MR1	48.24	0.54	89.33
4	PHB + 30 % NR + 10% MR2	48.21	0.54	89.27
5	PHB + 40% ENR	48.25	0.54	89.35
6	PHB + 30 % ENR + 10 % MR1	47.65	0.54	88.24
7	PHB + 30 % ENR + 10 % MR2	42.96	0.54	79.55

[a] *The PHB in this study has 10% proprietary plasticizer mixed in it as supplied and hence the weight fraction of PHB is 0.9 in case of virgin polymer and corresponding to 0.9 of the PHB content in the blends. PHB: Polyhydroxybutyrate, NR: Natural Rubber, MR1: RI131MA5, ENR: Epoxidized Natural Rubber and MR2: RI130MA20*

The large spherulites of PHB cause it to be brittle under severe conditions of deformation such as low temperature or high strain rates and can undergo a sharp ductile-to-brittle transition. These large spherulites are capable of initiating cracks. A crack can also propagate with little resistance in the brittle regime. The notched Izod impact strength of PHB was measured to be 23 J/m. This value was unaffected by the rubber phase in the PHB-rubber blend (Table 6.2). The modulus of PHB was reduced from 1.6 GPa to 0.6 GPa by addition of the rubber as expected (Table 6.2). The fracture surface from the impact tests was observed in ESEM and SEM to determine the mode of failure and to investigate the morphology. PHB exhibits a clean fracture surface devoid of any tendrils or fibrils due to its high crystallite size (Figures 6.5 and 6.6). The surface of the PHB-natural rubber sample (Figure 6.7) shows that the unbonded rubber phase, as indicated with an arrow in Figure 6.7, has separated from PHB in the blend. All these above observations validated the prediction of the theoretical model and indicated the need for a compatibilizer.

Table 6.2: Notched Izod Impact strength, Modulus and Approximate particle sizes.

No.	Composition	Impact Strength (J/m)	Storage Modulus (GPa) at 23°C	Rubber particle size (μm)
1	PHB	23 ±1.53	1.6 ±0.03	-
2	PHB + 40% NR	24 ±1.53	0.6 ±0.02	25-30
3	PHB + 30 % NR + 10% MR1	22 ±1.61	0.8 ±0.01	15-25
4	PHB + 30 % NR + 10% MR2	28 ±1.57	0.8 ±0.01	15-25
5	PHB + 40% ENR	25 ±2.32	0.5 ±0.02	20-25
6	PHB + 30 % ENR + 10 % MR1	62 ±0.92	0.6 ±0.01	15-25
7	PHB + 30 % ENR + 10 % MR2	124 ±4.64	0.8 ±0.03	1-5
8	Thermoplastic Olefin (TPO)	84 ±1.17	1±0.08	-
9	High impact Polystyrene (HIPS)	70 ±4.98	2.4 ±0.08	-

PHB: Polyhydroxybutyrate, NR: Natural Rubber, MR1: RI131MA5, ENR: Epoxidized Natural Rubber and MR2: RI130MA20, HIPS: Dow Styron 421, TPO: Basell Research grade TPO

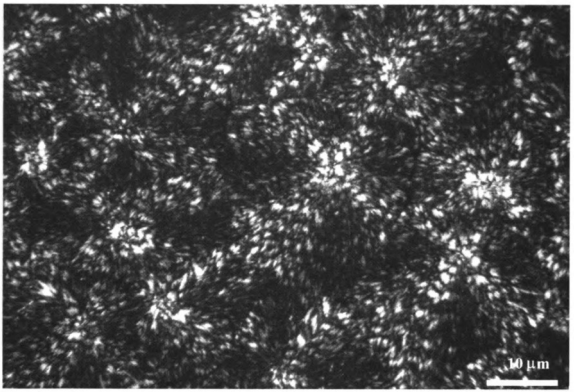

Figure 6.3: Polarized light micrograph denoting spherulites of PHB (Scale bar 10µm)

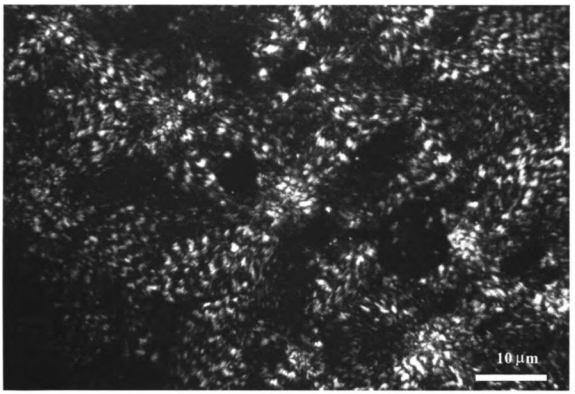

Figure 6.4: Polarized light micrograph of PHB with 40 wt. % Natural rubber (Scale bar 10µm)

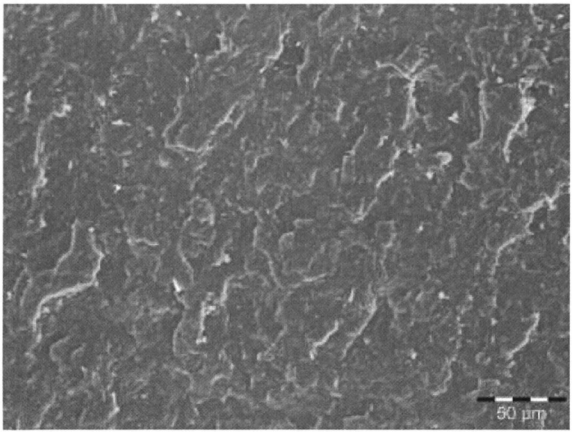

Figure 6.5: Scanning Electron micrograph of PHB (Scale bar 50µm)

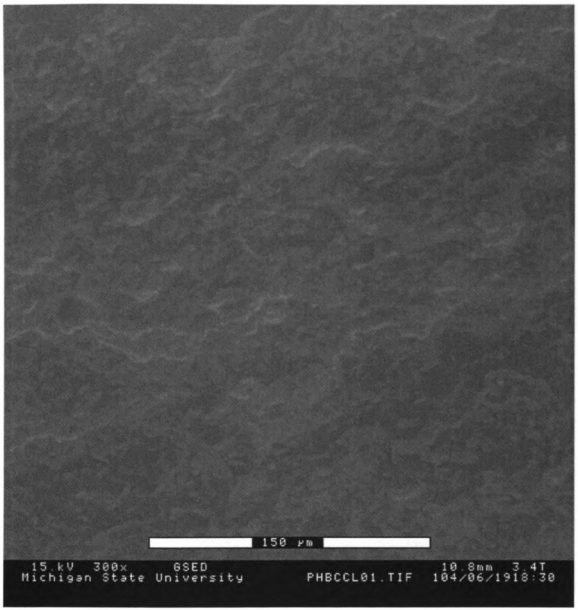

Figure 6.6: ESEM micrograph of PHB (Scale bar 150µm)

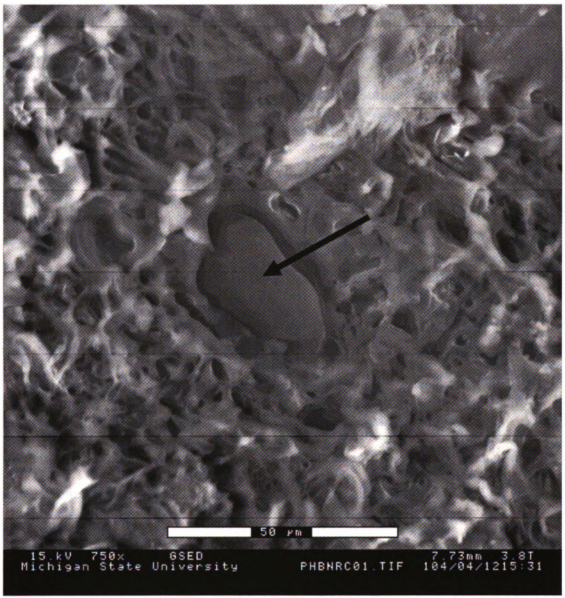

Figure 6.7: ESEM micrograph of PHB with 40% natural rubber (Scale bar 50µm). The arrow denotes the rubber phase.

6.1.2 Polyhydroxybutyrate - Natural Rubber System with Maleated Polybutadiene as Compatibilizer

The blend system can be considered to be a simple binary immiscible blend of a brittle polymer and an elastic polymer. The dominant properties of such blends are dictated by the continuous phase and properties of the continuous phase. The polymer and the elastomeric phases are vastly different in their rheological properties. Hence for the elastomeric phase to be continuous it either has to be added in large amounts or a compatibilizer needs to be introduced to increase interfacial adhesion. The compatibilizer also reduces the interfacial tension that is responsible for phase separation[20]. Studies on blends of scrap rubber and linear low-density polyethylene (LLDPE) reported the use of maleated LLDPE and epoxidized natural rubber (ENR) as dual compatibilizer which vastly improved the interfacial adhesion[21]. Incompatible binary blend of polylactic acid and starch has been reported to be successfully compatibilized by maleic anhydride thus justifying the use of a maleated compatibilizer in this work[22]. Polybutadiene grafted with maleic anhydride is selected as the compatibilizer system. A low maleated-content polybutadiene (named as MR1) with 2 MA groups/chain and having high molecular weight was initially evaluated. This system was not successful in increasing the impact strength of PHB (Table 6.2) and this was attributed to the lack of sufficient reactive groups both on the maleated rubber and the natural rubber. This reasoning was supported by the ESEM micrographs which showed no bonding and a clean fracture surface (Figure 6.8). The polarized light micrographs (Figure 6.9) also did not show evidence of any spherulite size reduction and the amorphous rubber phase was seen distinctly separate from the PHB spherulites. The high molecular weight of the MR1 compatibilizer was

determined to be hindering the penetration of the compatibilizer into the interfacial regions. Researchers have reported that the extent of MA grafting and the molecular weight of the compatibilizer determine the efficiency of compatibilization[23]. Hence lower molecular weight polybutadiene adducted with higher amount of maleic anhydride (6 MA groups/chain) was used as a compatibilizer. The lower molecular weight of this compatibilizer (MR2) than the molecular weight of the maleated rubber used earlier (MR1) meant that it would penetrate and disperse more easily into the blend and hence create an interphase between the phases.

This system too was not successful in increasing the impact strength of PHB (Table 6.2) and was backed by the ESEM micrographs which again showed a clean fracture surface (Figure 6.10). The polarized light micrographs (Figure 6.11) also did not show evidence of any spherulite size reduction and from these observations it was determined that the lack of reactive groups on natural rubber, which are needed for the compatibilizer to bond, was hindering the compatibilization mechanism.

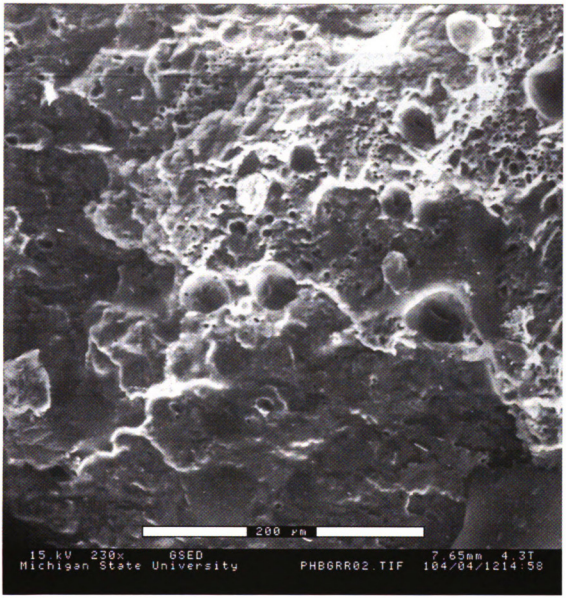

Figure 6.8: ESEM micrograph of PHB with MR1 and natural rubber (Scale bar 200 µm)

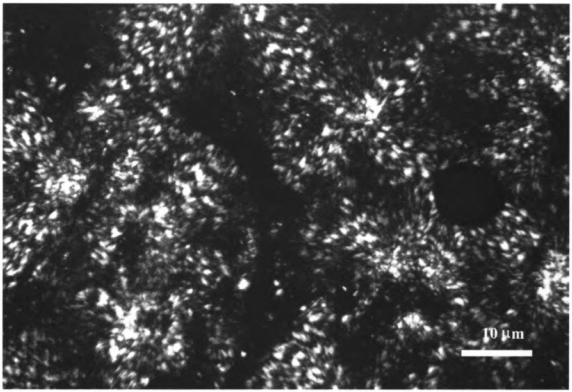

Figure 6.9: Polarized light micrograph of spherulites of PHB with MR1 and natural rubber (Scale bar 10µm)

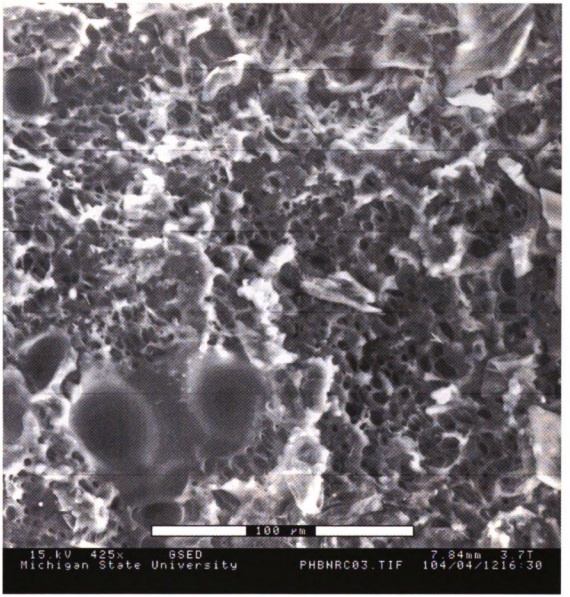

Figure 6.10: ESEM micrograph of PHB with MR2 and natural rubber (Scale bar 100 µm)

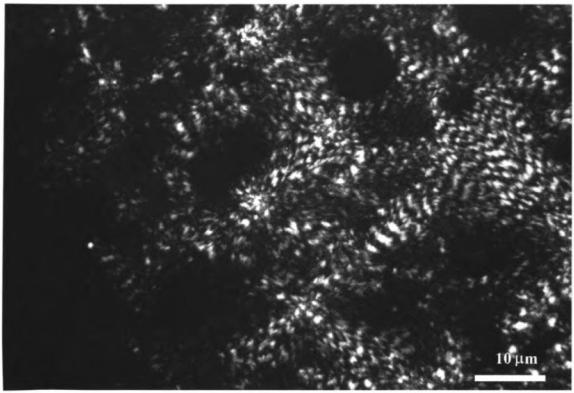

Figure 6.11: Polarized light micrograph of spherulites of PHB with MR2 and natural rubber (Scale bar 10μm)

6.1.3 Polyhydroxybutyrate - Epoxidized Natural Rubber System

Natural rubber was unable to improve the toughness of PHB even in presence of compatibilizers and this was attributed to the lack of reactive groups on the rubber. Epoxidized natural rubber (ENR) is a chemically modified form of natural rubber, with epoxide rings on the main chain. This epoxy linkage is expected to be a reactive site for bonding between the PHB and the rubber chains[11].

The impact strength of PHB was not affected by ENR (Table 6.2). The SEM micrographs (Figure 6.12) and ESEM micrograph (Figure 6.13) showed the lack of interfacial adhesion between the ENR and the PHB phases. The enthalpy values (Table 6.1) also were not affected and the ENR phase did not show any distinct interference with spherulite growth (Figure 6.14) in the PLM micrograph. Hence it was again concluded that a compatibilizer was necessary in this system.

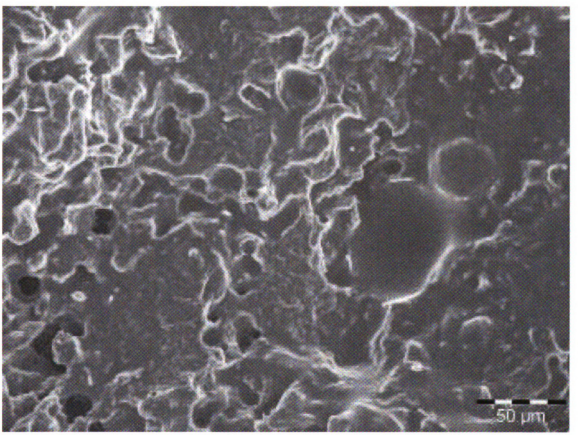

Figure 6.12: SEM micrograph of PHB with 40% epoxidized natural rubber (Scale bar 50 µm)

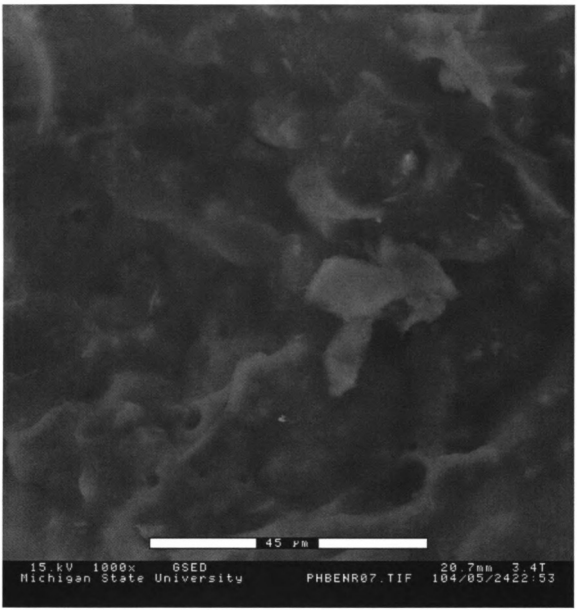

Figure 6.13: ESEM micrograph of PHB with 40% epoxidized natural rubber (Scale bar 45 µm)

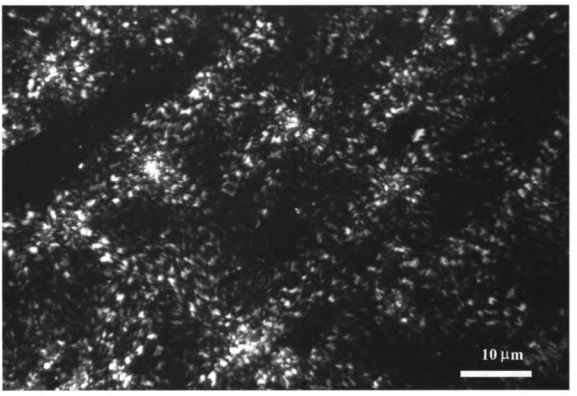

Figure 6.14: Polarized light micrograph of spherulites of PHB with epoxidized natural rubber (Scale bar 10µm)

6.1.4 Polyhydroxybutyrate - Epoxidized Natural Rubber System with Maleated Polybutadiene as Compatibilizer

The MR1 compatibilizer did not significantly improve the mechanical properties of the blend (Table 6.2) as was expected due to the high molecular weight of the compatibilizer which hinders its penetration and dispersion as well as the low number of reactive sites on it. The fracture surface (Figure 6.15) did not show sufficient dispersion and some large MR1 molecules were evident. The PLM micrograph (Figure 6.16) also did not show significant reduction in the spherulite size and thus need for the low molecular weight compatibilizer with higher grafting was established.

The MR2 compatibilizer system significantly improved the toughness of the PHB-ENR as evidenced by the 440% increase in notched Izod impact strength (Table 6.2). This impact strength (124 J/m) is superior to comparable grades of commercial toughened semi-crystalline polymers like high-impact polystyrene (HIPS) (70 J/m) and thermoplastic polyolefin (TPO) (84 J/m). The modulus of PHB reduced by 63% by addition of ENR but only by 50% when MR2 and ENR were added together thus showing the positive effect of the compatibilizer (Table 6.2). This modulus value of 800 MPa agreed with the Takayanagi model prediction of 801 MPa for a well-dispersed compatiblized system.

Morphology analysis of the blends validated these observations and the ESEM micrograph (Figure 6.17) of the compatibilized system showed good dispersion. The

evident droplet morphology and rough fracture surface seen in the SEM micrographs (Figure 6.18) also confirmed strong interactions. The compatibilizer successfully reduced the rubber particle size to about 1 μm thus creating a well dispersed particulate morphology ideal for toughening. The PLM micrographs showed distinct increase in the amorphous content and reduction in spherulites (Figure 6.19). AFM analysis in the force modulation mode was also used to study morphology of the toughened blends. In this mode, the variation in the moduli of the blend components can be observed: the softer rubber phase appears lighter under AFM and the stiffer PHB phase appears darker[24].

In case of the PHB-ENR two-phase system, distinct dark regions and light regions were observed (Figure 6.20) denoting a two-phase uncompatiblilized system with no intermediate regions. But in case of the PHB-ENR-MR system (Figure 6.21), besides the dark PHB and light rubber regions, intermediate regions of medium darkness can also be seen denoting formation of interphases and bonding. These interfacial adhesions led to the dramatic improvement in impact strength yet with acceptable loss in modulus. The moduli of PHB, the uncompatiblized PHB-ENR blend and of the PHB-ENR with MR2 compatiblized blend were studied as a function of temperature (Figure 6.22) in the DMA apparatus. At –50°C, the modulus of PHB reduced by 63% by addition of ENR but only by 50% when maleated rubber and ENR were added together and similar behavior was seen at room temperature 30°C and at 120°C. As seen from the figure, the loss in storage modulus with increasing temperature was less drastic for the blends than PHB, denoting the reduction in brittleness at sub-ambient temperatures. The compatibilized blend gave an intermediate value; low enough to indicate toughness yet high enough to maintain the structural integrity of the material.

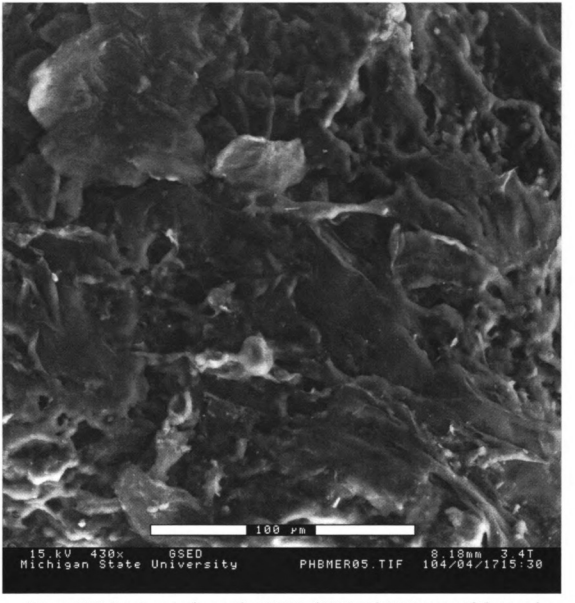

Figure 6.15: Fracture surface under ESEM of PHB with MR1 compatibilizer and epoxidized natural rubber (Scale bar 100µm)

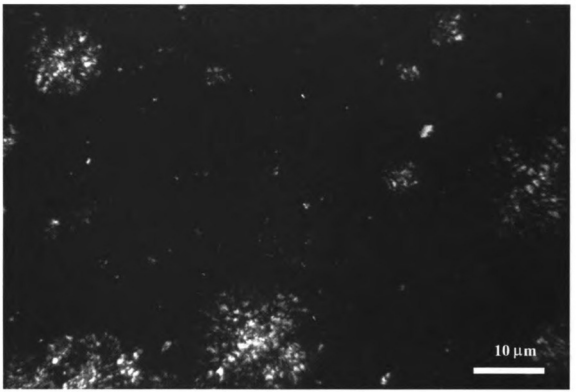

Figure 6.16: Polarized light micrograph of spherulites of PHB with epoxidized natural rubber and MR1 (Scale bar 10µm)

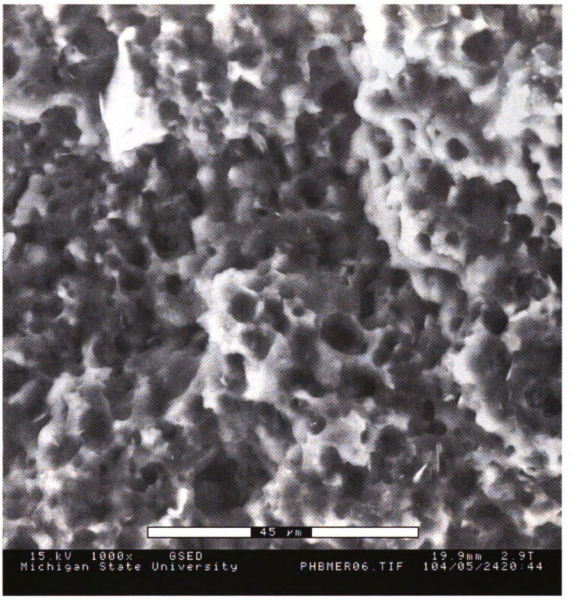

Figure 6.17: Fracture surface under ESEM of PHB with MR2 compatibilizer and epoxidized natural rubber (Scale bar 45 µm)

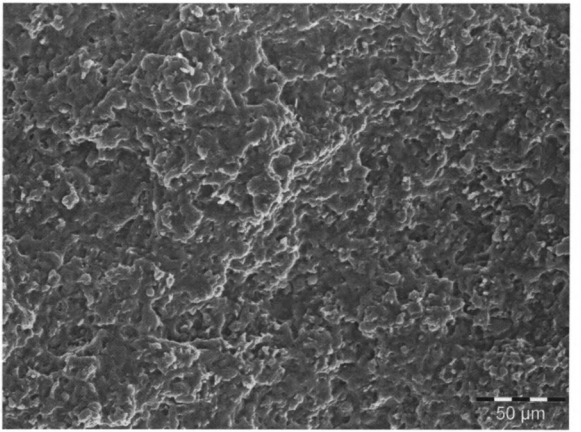

Figure 6.18: SEM micrograph of Fracture surface of PHB with MR2 compatibilizer and epoxidized natural rubber (Scale bar 50µm)

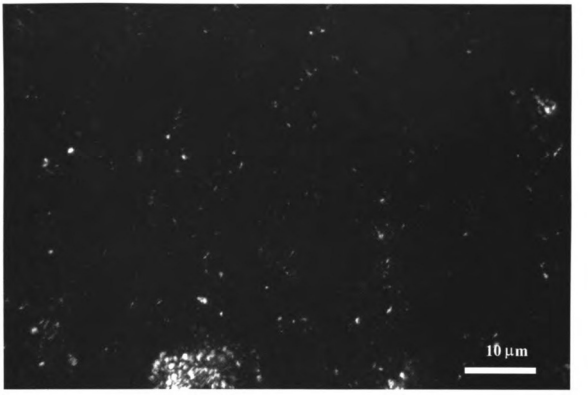

Figure 6.19: Hindered spherulites of PHB with epoxidized natural rubber and MR2 seen under PLM (Scale bar 10µm)

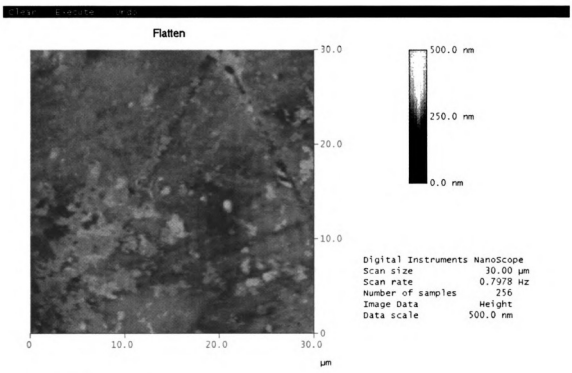

Figure 6.20: AFM micrograph of polished sample surface in force modulation mode of PHB with epoxidized natural rubber (scale bar: 30 µm)

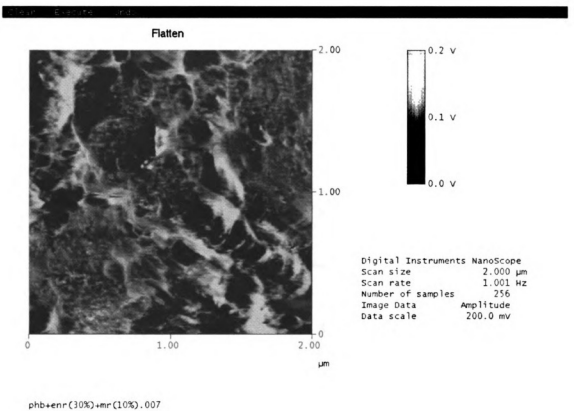

Figure 6.21: AFM micrograph of polished sample surface in force modulation mode of PHB with epoxidized natural rubber and MR2 compatibilizer (scale bar: 2 µm)

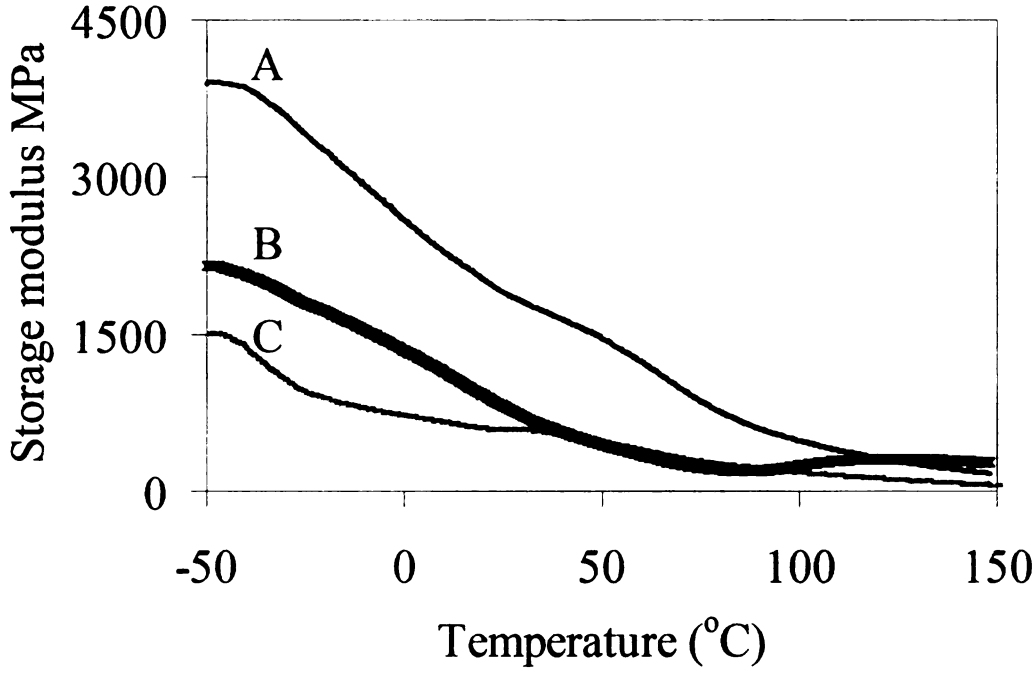

Figure 6.22: Variation of Modulus with temperature for A) PHB, B) PHB-ENR-MR2 and C) PHB-ENR

Thus polyhydroxybutyrate was successfully toughened by reactive extrusion with epoxidized natural rubber and using maleated rubber as the compatibilizer. The maleated rubber having high amount of maleic anhydride (MA) grafting and low molecular weight was found to be an effective compatibilizer. However, impact modification using low-modulus elastomeric components results in lowering the stiffness of the toughened material and this hampers its structural properties. This loss in modulus needed to be overcome to use the material for structural applications and hence generally high-modulus fillers such as talc, natural fibers or glass fibers are incorporated into a toughened matrix to improve its stiffness. But these fillers also act as stress concentrators and result in reducing the impact strength of the matrix. In recent years, the addition of nanoparticulate fillers such as organically modified clay has been shown to be an effective strategy for achieving improved stiffness in thermoplastic olefins without detrimentally affecting the toughness[25, 26]. The following section elaborates on this topic with emphasis on surface modification of clay followed by nanocomposite fabrication.

6.2 Surface Modification of Clay

Clay platelets have a tendency to agglomerate into tactoids held together by long-range attractive forces when dispersed in nonpolar matrices. In order to overcome this trend, the clay was chemically modified using varying amount of an alkyl-titanate complex (Figure 6.23). Qualitative analysis of the surface modification by Fourier

transform infrared (FTIR) spectroscopy confirmed this modification (Figure 6.24). The surface treatment of the pristine clay should render the surface organophilic and show established bonding between the modifier and the clay substrate to validate the modification system. The coupling agent can be attached to clay by chemical bonding, adsorption and coating to form a monomolecular layer on the clay surface. The coating and adsorbing mechanisms on to the clay surface do not affect the IR vibrations of various groups in the clay while only the coupling agent fixed on the clay mineral surface

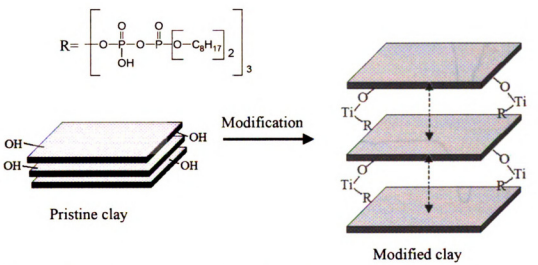

Figure 6.23: Schematic representation of the mechanism to increase interlayer gallery by the surface modification

by chemical bonding will change the IR spectra[27]. The exchange of surface OH group by reaction with the alkyl-titanate group has been considered a typical chemical modification technique. FTIR measurement was conducted before and after the surface modification reaction but did not yield any substantial results as expected. As shown in Figure 6.23; the O – O linkage is formed after grafting of Ti modifier on to the clay surface. The O – O linkage also occurs in the pristine montmorillonite clay. Thus characteristic peak of Ti modified clay cannot be expected in the FTIR spectra.

To gain more insight into the modification process, elemental (XPS) and thermal (TGA) analyses were used to determine surface composition of the clay and the amount of alkyl-titanate molecules chemically anchored on the clay after extensive washing of the un-reacted coupling agent. X-ray photoelectron spectroscopy utilizes emitted photoelectrons from a sample by photo-ionization and energy-dispersive analysis to study

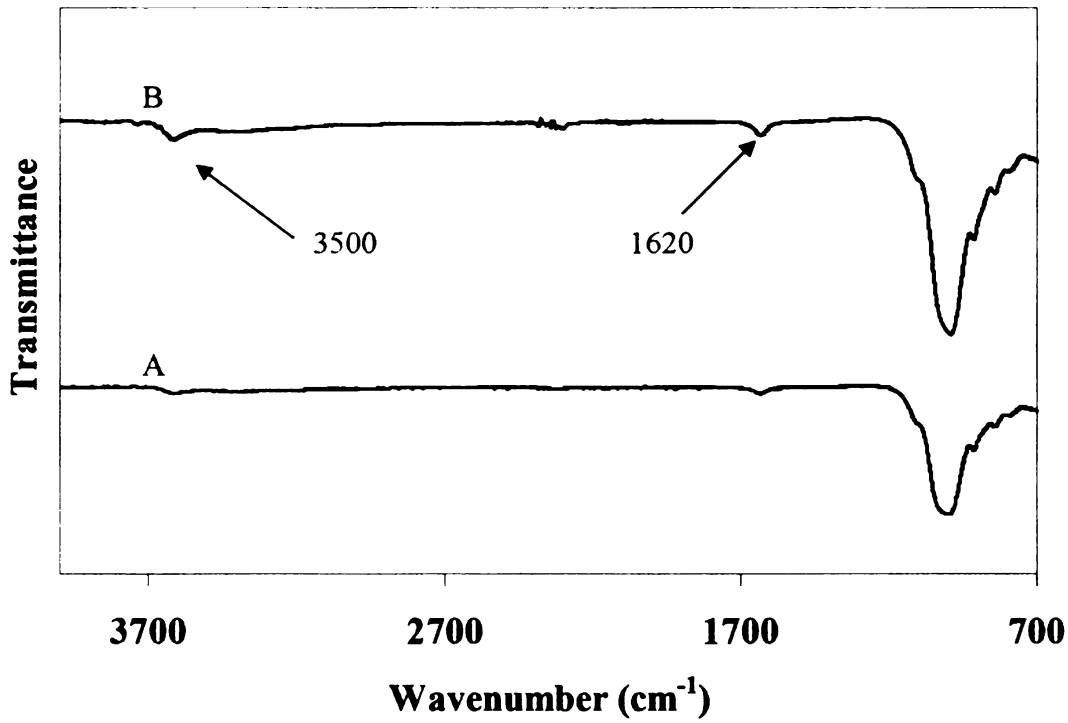

Figure 6.24: FTIR absorption spectra. (A) unmodified montmorillonite, (B) Montmorillonite modified by alkyl-titanate coupling agent.

the composition of the sample surface. The XPS analysis (Figure 6.25) of pristine montmorillonite clay and the two modified clays gave the atomic concentration profiles of the surfaces (Table 6.3). Pristine clay shows the presence of silicon and aluminum atoms that are integral to the clay structure. The high oxygen atom concentration on the surface is attributed to the hydroxyl groups on the hydrophilic surface. These hydroxyl groups are targeted to be reacted with alkyl-titanate complexes from the surface modifier

in the modification reaction. The XPS spectra of the modified clays show significant reduction in the atomic concentration of oxygen thus justifying the modification mechanism. The titanium and phosphorous atoms in the alkyl-titanate complex of the surface modifier that has reacted onto the clay surface are also evident in the atomic profile. The increase in carbon content is due to the alkyl chains and this increases

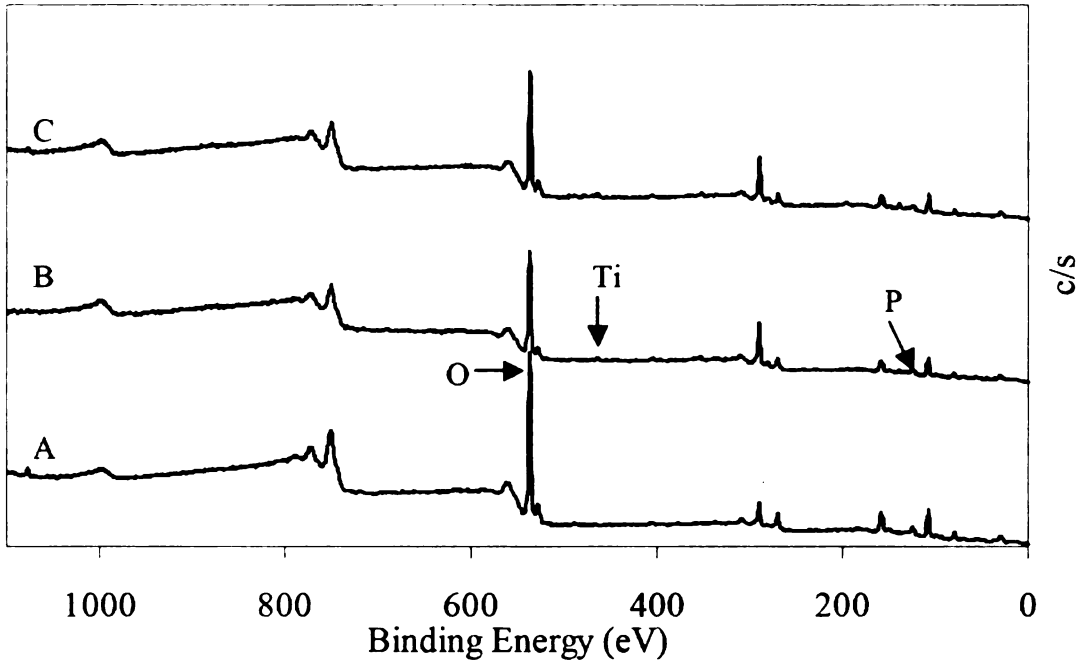

Figure 6.25: XPS spectrographs of pristine and modified clays; (A) Pristine clay, (B) Modifed clay -1, (C) Modifed clay -2

corresponding to the amount of surface modifier added to the clay. The carbon content for MC-1 (with 3.8 wt. % titanate-modifier loading) is 33.07% and this increases to 35.53% for MC-2 clay (with 11.4 wt. % titanate-modifier loading). Another important observation is the reduction in the silicon and aluminum atomic concentrations due to the modifier monolayer covering the surface of the clay.

Table 6.3: Elemental data from XPS spectra of the clay and surface treated clay

	Pristine clay	Modified clay-1	Modified clay-2
Carbon	20.59	33.07	35.53
Nitrogen	0.77	1.05	1.1
Oxygen	53.24	46.33	43.74
Sodium	1.64	0.82	0.87
Aluminum	6.47	5.45	4.52
Silicon	17.29	11.56	11.5
Phosporous	0	1.3	2.03
Titanium	0	0.42	0.71

The amount of surface modifier grafted onto the clay surface (expressed in mequiv of grafted titanate per gram of montmorillonite) was determined from the difference ΔC (wt %) of carbon content after and before modification using equation 6.6[28, 29]

$$\text{Grafted amount (mequiv/g)} = \frac{10^3 \Delta C}{1200 N_c - \Delta C(M - 1)} \qquad (6.6)$$

where N_c and M(g/mol) designate the number of carbon atoms and the molecular weight of the grafted titanate molecule, respectively (N_c = 48 and M = 1273). For MC-1, the grafted amount is calculated to be 0.29 mequiv/g, and for MC-2, the grafted amount is 0.40 mequiv/g thus increasing proportionate to the amount of modifier added to the clay.

Table 6.4 provides the basal spacing of raw and functionalized montmorillonite clays as calculated from the X-ray diffraction (XRD) spectra (Figure 6.26). The initial

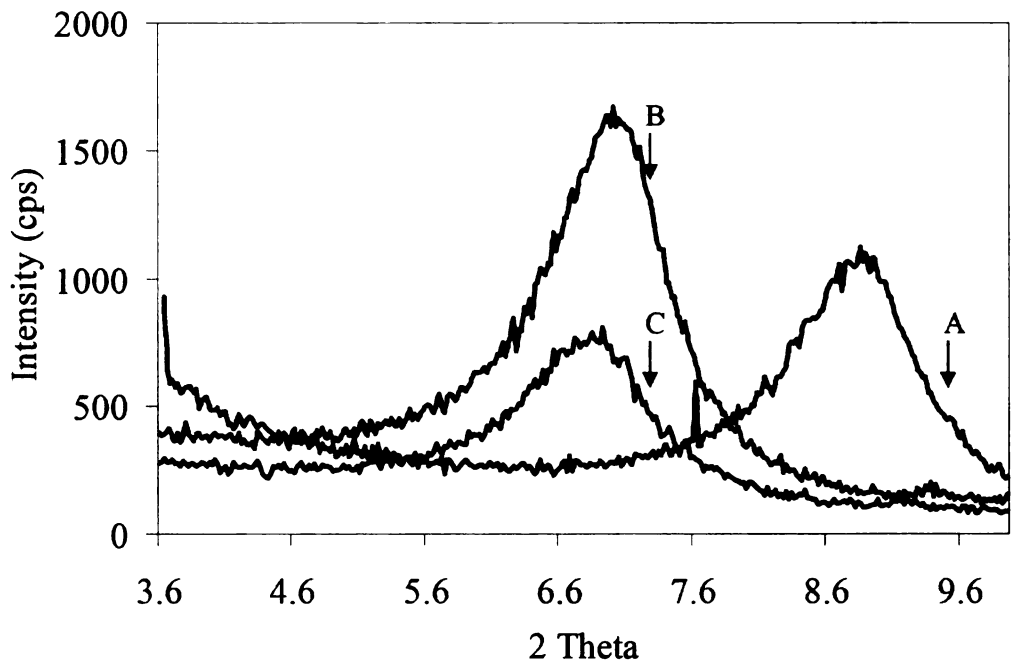

Figure 6.26: X-Ray diffraction pattern of pristine and modified clays; (A) Pristine clay, (B) Modifed clay –1, (C) Modifed clay -2

basal spacing of 9.81 Å corresponding to pristine montmorillonite increased to 12.55 Å for the MC-1 titanate-grafted clay, while the XRD patterns of the MC-2 clay powder indicate nearly no change of the spacing (Figure 6.26). The increase in the basal spacings

suggests that polycondensates are formed in the interlaminate space (Figure 6.23). Similar results have been reported in the literature for the modification of layered polysilicates using various alkyl-silanes[28].

Table 6.4: Basal spacings of pristine and modified montmorillonite clay

Material	2θ °	d spacing (A°)
Pristine clay	8.98	9.81
MC-1	6.96	12.70
MC-2	7.04	12.55

Figure 6.27 shows the TGA curves of the pristine and the modified montmorillonite clays. The weight decomposition curves indicate the presence of surface modification in both the treated clays as indicated by the lesser weight loss till 250°C as compared to the pristine clay.

Modified clay-2 shows more amount of material present as expected for the corresponding more amount of modifier added in the initial reaction. Only the region on the thermograms between 120 and 500 °C, which corresponds to the thermal decomposition of the organic molecule, was considered for quantitative determination of the titanate coverage. The grafted amount was determined using equation 6.7 from the weight loss W between 120 and 500 °C corresponding to alkyl-titanate degradation[28].

$$\text{Grafted amount (mequiv/g)} = \frac{10^3 W_{120} - W_{500}}{100 - (W_{120} - W_{500})M} \qquad (6.7)$$

The grafted amount as calculated from the thermogravimetric analysis is lesser than the corresponding values calculated from the elemental analysis (Table 6.5). The titanate

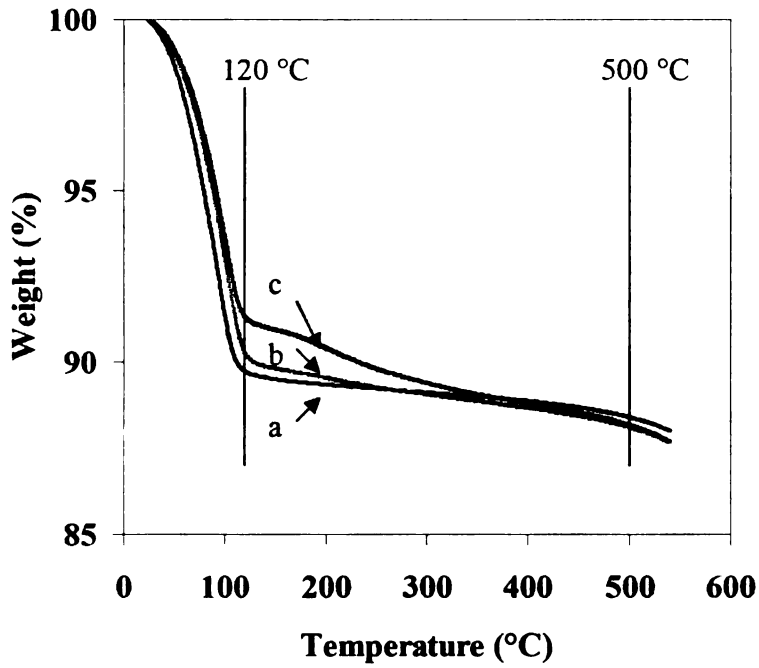

Figure 6.27: Thermogravimetric degradation profiles of (a) pristine montmorillonite, (b) modified clay-1 and (c) modified clay-2

treatment forms a layer on the surface of the substrate, which is at the most a few molecules deep, yet spread over the entire surface[30, 31]. Hence the weight percent grafted onto the substrate in proportion to the entire weight of the clay is much smaller in comparison to the proportion of the entire clay surface area to the modifier-covered surface. This effect results in the difference in the grafted amounts (mequiv/g) as measured by the two techniques. The values are different yet the trend is similar showing grafting proportionate to the amount of modifier added in the reaction.

Table 6.5: Elemental and Thermogravimetric Analyses of pristine and modified montmorillonite clays

	XPS Elemental Analysis			*Thermogravimetric Analysis*	
	Carbon Content (%)	ΔC (%)	Grafted amount (mequiv/g)	Weight loss (%) W_{120}-W_{500}	Grafted amount (mequiv/g)
Pristine MMT	20.59	0	-	-	-
Modified clay-1	33.07	12.48	0.29	2.29	0.018
Modified clay-2	35.53	14.94	0.40	3.24	0.026

The contact angle is typically defined as the angle between a solid substrate and a liquid drop on the surface of the substrate (Figure 6.28). This can be measured fairly easily for solid substrates with regular geometries like large flat surfaces by using a digital camera connected to a software system. However, for solids such as powders with irregular geometries, these techniques are not feasible because of the nanosize surface areas and also the surface roughness tends to give erroneous contact angle values[32]. These materials require special techniques and one such method is capillary wicking based on the capillary rise due to surface tension of a liquid into pores[29, 33]. The surface modification should make the hydrophilic clay surface into organophilic that can be described by an increase in the contact angle for water. Experiments with hexane gave

the material constants for the pristine clay, modified clay 1 and the modified clay 2 (Table 6.6). These values combined with the mass uptake values for water for the same materials gave the contact angles for the untreated and treated clays (Table 6.6). The contact angle for pristine clay is close to zero as is expected for the hydrophilic surface with ample hydroxyl groups capable of interacting with water. For the modified clay, the organic groups in the alkyl-titanate complex increase the surface energy of the clay

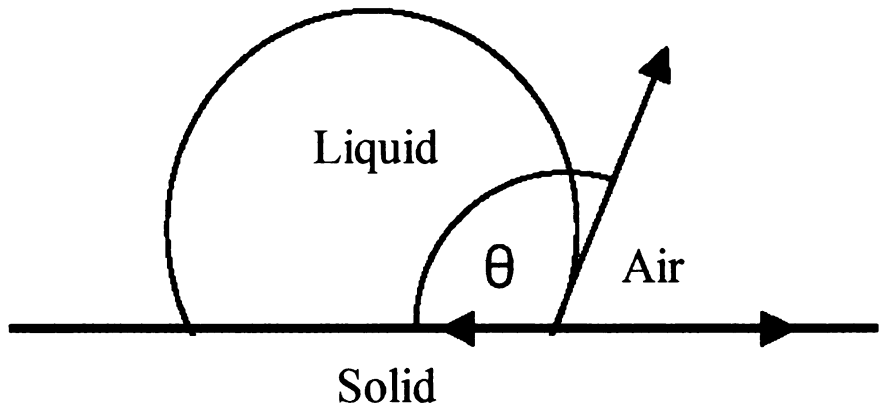

Figure 6.28: Contact angle between solid substrate and sessile liquid droplet on the surface

surface. This increase in the surface energy reflects in decrease in wettability and thus the contact angle increases. The increase in contact angle was seen to be in agreement with the increase in organic modifier content on the clay surface as previously determined from the XPS. Thus the clay surface has successfully been modified to make it organophilic and thus ideal for organic matrices such as PHB and rubber.

The matrix contact angle, as measured by conventional goniometry, increased from 55.8° for PHB to 64.3° for the PHB-ENR-MR blend. The rubber incorporation is

making the matrix more hydrophobic and more similar in nature to the surface of the organically modified nanoclay. This similarity in the surface characteristics of the matrix and filler will increase the matrix-filler adhesion. This characteristic will also exfoliate the clay platelets through transfer of applied shear from the matrix to the clay during the melt processing.

Table 6.6: Contact angles for pristine and modified montmorillonite clays and the matrices

Samples	*Material constant (c)*	*Cos θ*	*θ (Degrees)*
Pristine clay	0.000142	0.9948	6.0
Modifed Clay-1	0.000165	0.8483	31.9
Modified Clay-2	0.000275	0.7168	44.2
PHB	-	-	55.8
PHB-ENR-MR2	-	-	64.3

6.3 Nanocomposites

6.3.1: Nano-reinforcement of Toughened Polyhydroxybutyrate

Optimum clay exfoliation and clay surface chemical modification gives nanocomposites with enhanced properties and has been widely reported in literature[32, 34-37]. Addition of clay not only acts as reinforcement but also leads to breakup of rubber particles due to the following effects. Primarily the clay increases the melt viscosity thereby increasing the stresses on the rubber particles leading to particle size reduction. Secondly, the extremely strong clay platelets as well as agglomerates shear the rubber particles during the melt processing. The accompanying chemical modifiers of the clay also act as interfacial agents and reduce the interfacial tension leading to reduction in the particle size[38]. These effects synergistically combine to reduce the particle size of the rubber consequently increasing the impact strength. The exfoliated nanoclay platelets have the largest dimension in the range of 100-200 nm and hence too small to act as stress concentrators in the matrix. Thus nanoclay is able to improve the modulus without sacrificing the toughness but only if the platelets are successfully exfoliated. This exfoliation is dependant on the surface treatment of the clay and to investigate this effect two different clays were used having different surface modifications. The commercially modified clay (COC) detrimentally affected the impact strength of the toughened PHB (Table 6.7 and Figure 6.29) and this may be attributed to two factors; the lack of interaction between the surface modifier and the matrix and the subsequent inability to exfoliate into the system. These reasons led to the clay forming agglomerates in the

matrix that ultimately acted as stress concentrators during impact loading and negated the effect of the elastomeric impact modification. But in case of the nanocomposites with 5 wt. % titanate modified clay, the impact strength was significantly retained (Table 6.7).

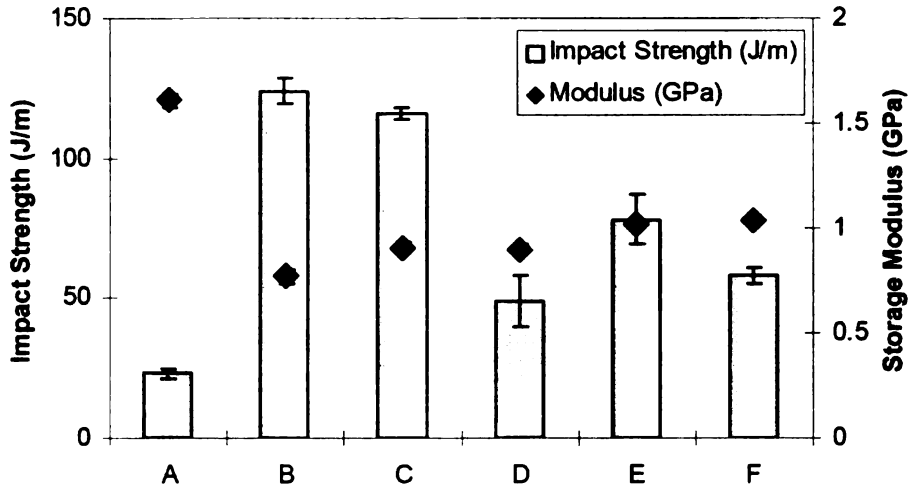

Figure 6.29: Storage Modulus from DMA and Impact Strength of selected materials A) PHB, B) PHB + 30 % ENR + 10 % MR, C) (PHB + 30 % ENR + 10 % MR) + 5% MC, D) (PHB + 30 % ENR + 10 % MR) + 5% COC E) TPO and F)TPO + 5% COC.

NOTE: PHB: Polyhydroxybutyrate, ENR: Epoxidized Natural Rubber, MR: Maleated Rubber, MC: Modified Clay, COC: Commercially Modified Clay and TPO: Thermoplastic Olefin.

The interaction of the surface modifier with the matrix has resulted in better exfoliation of the clay platelets consequently leading to breakup of the rubber particles and ultimately high impact strength. The amount of treated clay affects the impact strength significantly (Table 6.7). For low loadings (2%), the level of the titanate coupling agent is low and it does not affect the impact strength positively. At 5% loading, there is optimum

clay as well as coupling agent present to improve the impact strength. But if we increase the clay loading to 7%, the excessive amount of clay present in the matrix negates the effect of the surface treatment and forms stress concentrators leading to failure on impact.

Table 6.7: Notched Izod Impact Strength and Storage Modulus of the toughened materials and their nanocomposites.

No.	Composition	Impact Strength (J/m)	Storage Modulus (GPa) at 23°C
1	PHB	23 ±1.53	1.61±0.03
2	PHB 60% + ENR 40%	25 ±2.32	0.56±0.02
3	PHB 60% + ENR 30 % + MR 10 %	124 ±4.64	0.77±0.03
4	98% (PHB 60% + ENR 30 % + MR 10 %) + 2% TMC	93 ±10.71	0.78±0.02
5	95% (PHB 60% + ENR 30 % + MR 10 %) + 5% TMC	116 ±2.10	0.91±0.02
6	93% (PHB 60% + ENR 30 % + MR 10 %) + 7% TMC	87 ±1.39	0.85±0.03
7	95% (PHB 60% + ENR 30 % + MR 10 %) + 5% COC	49 ±9.15	0.90±0.02
8	TPO	78 ±8.88	1.02±0.02
9	TPO 95% + COC 5%	58 ±3.14	1.04±0.01

PHB: Polyhydroxybutyrate, ENR: Epoxidized Natural Rubber, MR: Maleated Rubber, TMC: Titanate Modified Clay, COC: Commercially Modified Clay, TPO: Thermoplastic Olefin

The modulus of the toughened PHB reduced to 0.77 GPa from 1.61 GPa of virgin PHB because of the impact modifier (Table 6.7). The titanate-modified clay as well as the COC nanocomposites regained the modulus to 0.9 GPa. The high modulus of the clay has fulfilled its intended role in increasing the stiffness of the matrix and this improvement in modulus from the toughened PHB gives a material with the required stiffness for structural applications.

The TEM images (Figures 6.28 and 6.29) of the titanate-modified clay show well-exfoliated morphology. The mechanism of clay incorporation is also well defined by the images. Initially a master-batch of the clay in PHB was processed. The PHB chains have intercalated into the clay gallery and the PHB chains present inside adjoining clay platelets in the final nanocomposites can be distinguished (Figure 6.30). Subsequently when the master-batch is added to the elastomeric components and the final exfoliated clays can be seen distinctly (Figure 6.31). Rubber-clay nanocomposites are reportedly difficult to characterize by TEM owing to the tendency of the rubber phase to smear the thin sections as well as the limited sectioning possible with such matrices. Hence viscoelastic measurements that are highly sensitive to the nanoscale structure of the nanocomposites materials have been used to investigate the state of exfoliation of the clay[39]. It is well known that particulate fillers increase the melt viscosity of the matrix. But this depends on the structure of the filler inside the polymer; an agglomerated filler will impend the melt flow more and give higher viscosity values while a well-exfoliated filler will have a less profound effect on the viscosity[39]. Figure 6.32 shows this exact behavior for the complex viscosity of PHB-ENR-MR in the presence of COC or TMC. The modified clay is exfoliated to a greater extent in the matrix than the COC and this

gives the viscosity values in between the matrix and the COC nanocomposites. These observations denote the incomplete exfoliation of the COC in comparison with TMC in the toughened PHB matrix.

Figure 6.30: TEM micrograph of modified clay dispersed in the PHB + ENR + MR matrix. (Scale Bar= 100nm). The PHB chains have intercalated into the clay gallery and adhered to the organic treatment on the clay.

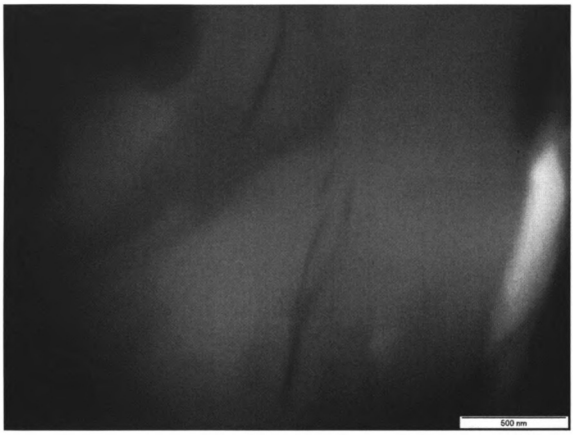

Figure 6.31: TEM micrograph of modified clay dispersed in the PHB + ENR + MR matrix. (Scale Bar= 500nm)

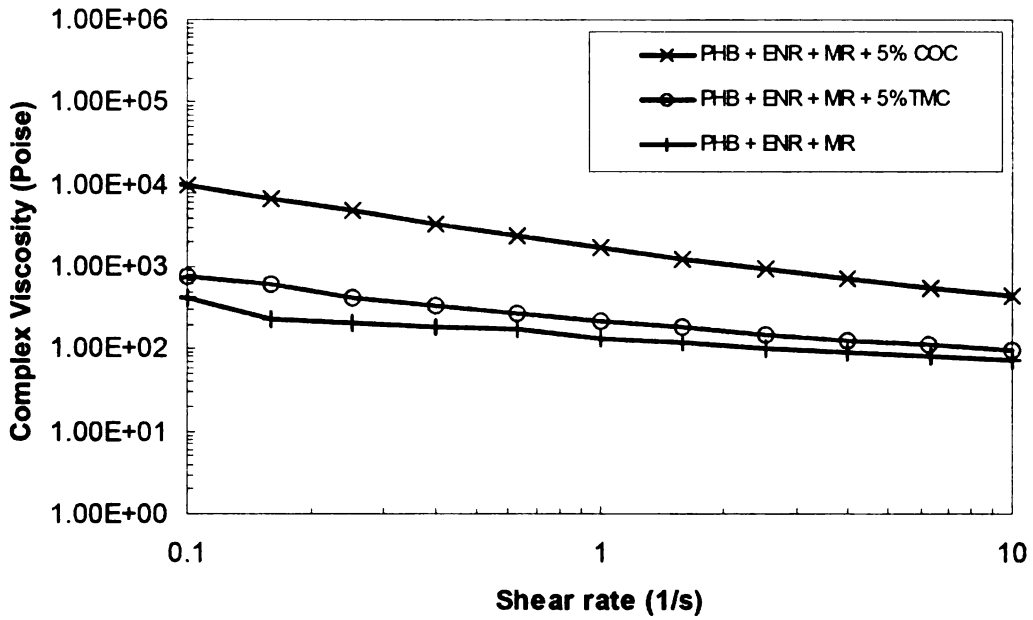

Figure 6.32: Rheological data for PHB-ENR-MR, and PHB-ENR-MR/clay nanocomposites.

6.3.2 *Theoretical nanocomposite model*

A modified *Haplin-Tsai* equation was used to evaluate the reinforcing effect of randomly-oriented clay platelets[40, 41] The elastic modulus of clay is taken to be 170 GPa from literature in these calculations[35]. Experimental values of modulus are 1.6 GPa for PHB and 0.0017 GPa for rubber. Applying the Halpins-Tsai equation to just the

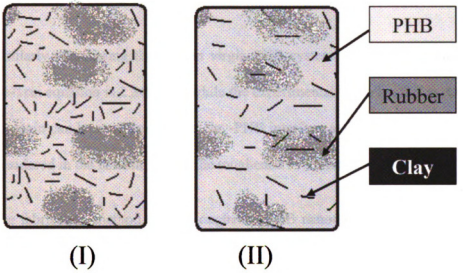

Figure 6.33: Schematic representation of morphology and clay distribution used for modified Halpin-Tsai equation. (I) Case I: all the clay remains in the PHB phase and (II) Case II: The clay is distributed equally into the rubber and PHB regions.

toughened PHB matrix without the nanoclay while considering the rubber particles as the reinforcements in the PHB, the effective predicted modulus is 0.874 GPa. The volume fraction of rubber (V_{rubber}) is 0.25 and the rubber regions are assumed to be spherical droplets with L/D=1. Van-Es has proposed the following parameter[42]: $\xi = 2/3$ (L/D) and $\eta = (E_{reinforcement}-E_{matrix})/(E_{reinforcement}+\xi E_{matrix})$

Comparing this with the experimental modulus value of 0.77 GPa for the same composition, it is seen that the actual modulus is 88.1% of the predicted value. This difference can be attributed to the interface between the PHB and the rubber particles and hence subsequent calculations for the nanocomposite modulus are multiplied by this factor. Also the MR is in liquid form and cannot be characterized for modulus and so is considered to have similar physical properties as ENR in the model and this leads to the difference between the predicted and the actual value.

Similarly considering the clay in virgin PHB system, the predicted modulus by the Halpin-Tsai equation is 2.349 GPa while the experimental value for this system is 1.9 GPa. This again can be attributed to the clay-PHB interface and hence a factor of 80.8% is also considered in the calculations of the toughened PHB nanocomposites.

The fabrication method for the toughened PHB nanocomposites, as explained in the experimental methods section, is by initially making a high loading master-batch of the clay in virgin PHB and subsequently adding the rest of the components. This fabrication technique leads to two boundary scenarios for the clay distribution: case I where all the clay remains in the PHB phase and case II where the clay is distributed equally into the rubber and PHB regions as denoted in Figure 6.33. These two conditions are numerically modeled as function of varying clay aspect ratio (L/D) from 10 to 100 in the nanocomposites. The volume fraction of rubber (V_{rubber}) is 0.25 for all the cases and the rubber or rubber-clay regions are assumed to be spherical droplets with L/D=1.

Case I: The boundary case assumes all the clay remains in the PHB regions and hence the the *Halpin-Tsai* equation was initially applied to the clay-rich PHB phase and equation 6.8 gives the predicted modulus value for these regions as:

$$E_I = E_{PHB}\,(1+\xi\eta V_{clay}) / (1-\eta V_{clay}) \qquad (6.8)$$

The volume fraction of clay (V_{clay}) is 0.0288 for case I and $\eta = (E_{clay}-E_{PHB})/(E_{clay}+\xi E_{PHB})$. Using the value of E_I from the above equation and E_{Rubber} in a combined equation 6.9 gives the modulus of the final nanocomposite:

$$E_{nanocomposite\ (I)} = E_I\,(1+\xi\eta V_{Rubber}) / (1-\eta V_{Rubber}) \qquad (6.9)$$

In this case $\eta = (E_{Rubber}-E_I)/(E_{Rubber}+\xi E_I)$ and the rubber regions are again assumed to be spherical droplets with L/D=1. The final value is multiplied by 0.881 (rubber-PHB interface effect) and 0.808 (clay-PHB interface effect) to get the effective value of the modulus and this is plotted as a function of clay aspect ration in Figure 6.34.

Case II: The lower boundary case assumes equal distribution of the clay in the PHB regions and the rubber regions. Thus the *Halpin-tsai* equation is first applied to the clay-rich PHB phase and equation 6.10 gives the predicted modulus value for these regions as:

$$E_{II} = E_{PHB} (1+\xi\eta V_{clay}) / (1-\eta V_{clay}) \qquad (6.10)$$

The volume fraction of clay (V_{clay}) is 0.0187 for case II for both the regions and $\eta = (E_{clay}-E_{PHB})/(E_{clay}+\xi E_{PHB})$. For the rubber-clay region, the modulus is given by equation 6.11:

$$E_{III} = E_{Rubber} (1+\xi\eta V_{clay}) / (1-\eta V_{clay}) \qquad (6.11)$$

with $\eta = (E_{clay}-E_{Rubber})/(E_{clay}+\xi E_{Rubber})$. Using the value of E_{II} and E_{III} from the above equations in a combined equation 6.12 gives the modulus of the final nanocomposite:

$$E_{nanocomposite\ (II)} = E_{II} (1+\xi\eta V_{III}) / (1-\eta V_{III}) \qquad (6.12)$$

In this case V_{III}= 0.25, $\eta = (E_{III}-E_{II})/(E_{III}+\xi E_{II})$ and the rubber-clay regions are again assumed to be spherical droplets with L/D=1. Again the final value is multiplied by 0.881 (rubber-PHB interface effect) and 0.808 (clay-PHB interface effect) to get the effective value of the modulus and this is plotted as a function of clay aspect ration in Figure 6.34. The experimental value for this system is 0.91 GPa (Table 6.7) and the subsequent TEM images (Figure 6.30 and 6.31) show the aspect ratio for the clay to be 50. The predicted value for this aspect ratio is 0.93 for the equal-distribution model and 1.53 for the model that considers all the clay in the PHB. Thus the experimental value is closely in agreement to the case II model and this suggests that the system is behaving in a manner as to influence the clay to migrate from the PHB to the rubber regions. There is

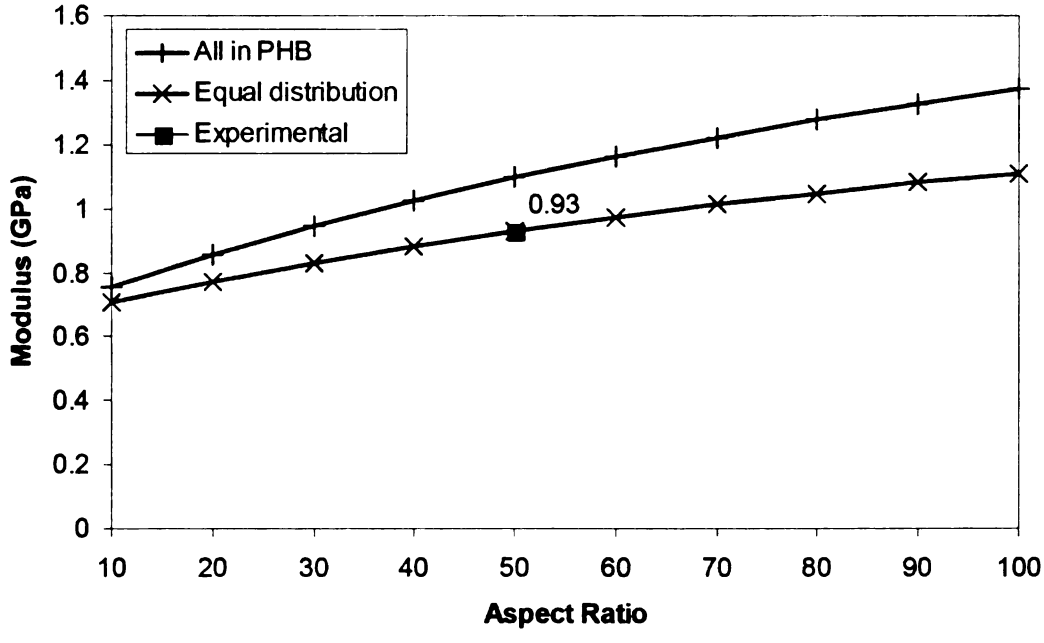

Figure 6.34: Predicted and Experimental values of the modulus of the nanocomposite materials as a function of clay aspect ratio.

also no empirical technique to determine the exact concentration of the clay in the PHB and the rubber regions and hence this distribution and migration cannot be established.

6.3.3 Biodegradation

Polyhydroxybutyrate is degraded by the action of enzymes known as esterases produced by a wide range of microorganisms. Degradation causes polymer hydrolysis, leading to a decrease in its molecular weight as well as weight loss[43]. All tested samples degraded in compost, albeit at different rates and extents (Figure 6.35). From the biodegradation view point, both PHB and PHB-ENR samples appeared to be quite similar, achieving close to 60% degradation by the end of the experiment (2500h). PHB-ENR-MR exhibited the slowest degradation (<10%) among all samples tested. This was hardly surprising, as natural rubber degrades in soil by undergoing oxidative cleavage of the double bond in the backbone, which is a fairly slow process[44]. Thus, addition of rubber component to the PHB matrix would certainly lead to a much slower biodegradation of the polymer matrix. Further addition of the compatibilizer slowed the degradation much more significantly. Addition of fillers and/or compatibilizers could form interphase networks that may restrict enzyme accessibility, impacting both the rate and the extent of matrix biodegradation. This is also evidenced by the scanning electron micrographs shown in Figure 6.17 and 6.18 when compared to Figure 6.5.

However, the addition of small amount of nanoclay in same formulation enhanced the biodegradation several fold (Figure 6.35). In this regard, silicate layers have been shown to significantly improve the biodegradability of biodegradable matrices, especially systems that undergo hydrolysis[45]. The proposed mechanism for this enhancement in biodegradation is that the terminal hydroxylated edge groups of the silicate clay layers could absorb moisture from compost leading to the initiation of the hydrolysis of the

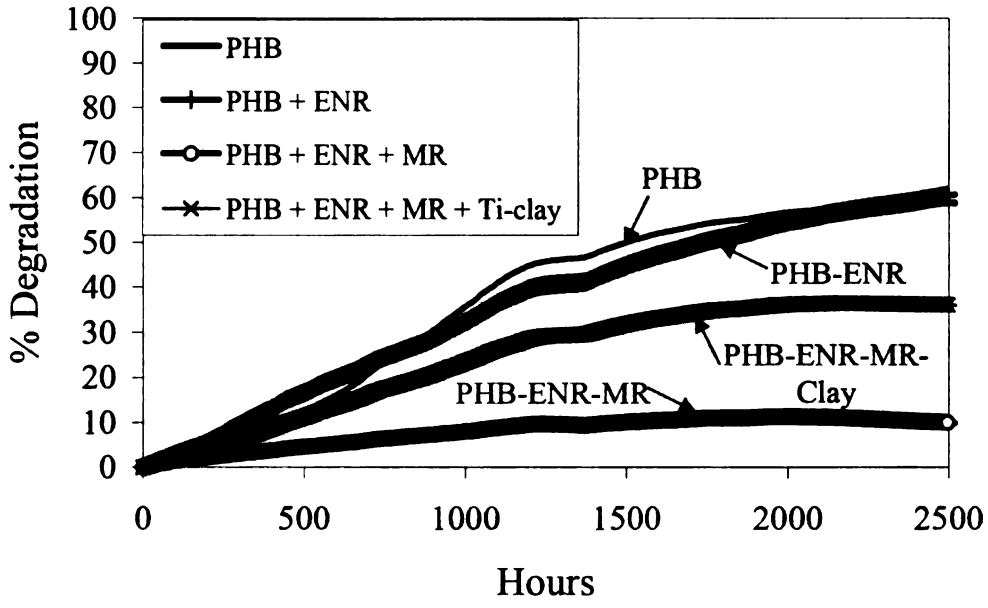

Figure 6.35: Percent biodegradation of the materials as a function of time.

matrix. Additionally, well-dispersed clay particles cause the polymer chains to fragment more rapidly resulting in increased rate of degradation. The biodegradation rate of the toughened and compatibilized PHB nanocomposite was observed to be significantly higher than the matrix. This increased rate is attributed to the presence of the nanoclay layers that cause the above mentioned phenomena of increasing the fragmentation and hydrolysis leading to faster biodegradation of the matrix.

6.4 Thermoplastic Starch-Polyhydroxyalkanoate blends

One of the ways to increase value of renewable-resource based polymers is by improving the properties thus making them more attractive than conventional polymers. This work targets this pathway of enhancing the properties of some specific renewable-resource based polymers by blending and composite technology. The objective of this part of this work is to blend PHAs with a low-cost biodegradable polymer in order to fabricate PHA-based materials intended for flexible packaging applications. PHAs are inherently brittle owing to the presence of large spherulites created during crystallization from melt. The elongation at break of PHB homopolymer is 6-8 % and some PHBV copolymers have reported values as high as 50% with 20% valerate content[46, 47]. However the cost of the material increases significantly with increase in the valerate content. A cost-effective technique is blending with a low-cost flexible polymer. The blending partner selected for this work is thermoplastic starch.

6.4.1 Starch plasticization

Native starch by itself (in an unplasticized or un- gelatinized form) is used in the plastics area generally only as a filler, and in order to use starch as a plastic material, it needs to be destructurized and plasticized. This is generally done using water or a non-volatile plasticizer such as glycerol or other polyols[48]. Starch exhibits a unique property called gelatinization that involves breaking of the hydrogen bonding by heat and allowing water or a non-volatile plasticizer to enter.

Starch plasticization is a well-established science and most publications on such systems have reported the improvement in properties of plasticized starch as being a function of two factors: amylose content and extent of destrurization[48-54]. This work uses a starch that is one of the highest amylose-content starches available with 70% amylose[55]. Amylose is the linear portion of starch while amylopectin is the branched portion of starch and higher amylose content generally gives better films due to the ability of the linear chains to form gel-like structures[48].

The destructurization of starch is determined by the amount of plasticizer that can be incorporated into the starch[56]. This plasticizer also brings down the processing temperature of the system. This is important because native starch melts at 220 °C and begins to thermally degrade at only 5° C above its melting point[48, 56]. Hence this significantly limits the processability of starch. The effect of plasticizer such as glycerol present in the plasticized starch is significant; a 4:1 dry starch to glycerol system has shown a T_g of 8°C that is characteristic to flexible materials[48, 57]. The amount of plasticizer also determines the mechanical properties; percent elongation values of 60% have been reported for a glycerol/starch system containing 35 wt% glycerol and 65 wt% starch. However, the amount of glycerol that can be added successfully to starch is limited to 35 wt % as above this value, the excess glycerol leaches out of the system[48].

Glycerol is a byproduct of the soy-based biodiesel industry. Current rising fossil-fuel costs have turned public attention to plant-based fuels for their needs. This trend has resulted in the tremendous increase in the number of biodiesel production facilities in the US. These facilities have a ready market for the biodiesel but they also generate large

amounts of glycerol. This surplus of glycerol needs to be utilized or the cost of this disposal will add to the biodiesel cost and ultimately will drive the price of biodiesel up. Hence there is a need to develop applications and uses for this glycerol in order to supplement the agro-economy[58-60]. Value-added applications of glycerol are expected to affect the cost of biodiesel ultimately. Hence the aim here is to incorporate maximum possible glycerol into the starch system in order to achieve two goals: improve the mechanical properties, and to create value added applications for glycerol.

The plasticization of starch is a two-stage process; in the first stage the starch and glycerol are dry mixed using a paddle mixer and allowed to set overnight; and in the second stage this mixture is "cooked" or processed at high shear and temperature in an extruder. The overnight setting is necessary for impregnation of the glycerol homogenously into the starch and is obvious on visual inspection of the system.

Corn starch and varying amounts of glycerol (Table 6.8) were mixed in the paddle mixer and allowed to set overnight followed by extrusion as per the conditions given in section 4.6. The processed materials were visually observed for characteristics and leaching behavior.

Table 6.8: Starch plasticization trials

Starch (wt%)	**Glycerol (wt%)**	**Conditioning (hours set)**	**Observation**
70	30	0	Brittle
66	33	0	Brittle
66	33	Overnight	Semi-brittle
60	40	0	Semi-brittle, plastic, leaching
60	40	Overnight	Plastic, minimal leaching
55	45	Overnight	Significant leaching, rubbery

Based on the above observations, the 60:40 starch:glycerol w/w composition was chosen for further work. The rationale was that the system had appropriate plasticizer to yield high elongation yet was still processable with minimal leaching and also the excess plasticizer may be absorbed by the PHA component in the subsequent processing.

6.4.2 Thermoplastic Starch

Thermoplastic starch is defined as a blend of plasticized starch with a flexible blending partner. The rationale for this blending is the poor resistance of plasticized starch to water that degraded the properties of these materials over time as they were exposed to moisture. Thermoplastic starches were developed to overcome this and

popular candidates for partners are poly(ε-caprolactone) (PCL), poly-(butylene adipate-co-terephthalate) (PBAT), poly(tetramethylene adipate-co-terepthalate) (PTAT) and poly(vinly alcohol) (PVOH)[48, 61]. There have been reports of TPS systems with non-biodegradable polymers but these are no longer popular and almost all TPS materials available currently are biodegradable[62]. Two candidate blending partners were chosen for this work; PBAT and PCL. Plasticized starch-PCL is a well-established system and this was chosen for the preliminary experiments on composition and sequence optimization. However PCL has a very low melting point (60°C) that translates to lower temperature for its final usage. Hence PBAT was chosen primarily due to its excellent physical properties but also mainly due to its high melting point and and processing temperature window that is closer to the temperature range for PHA processing.

The TPS fabrication as well as the final PHB/PHBV-TPS system fabrication was seen to be significantly affected by the sequence of addition of the components and this is explained in detail in the subsequent section. Hence optimization of TPS composition is discussed in that section also.

6.4.3 Polyhydroxyalkanoate-Thermoplastic Starch Blend

Polyhydroxyalkanoate based blends with starch have been reported earlier[53, 63]. These findings have all used polyhydroxybutyrate-co-valerate (PHBV) as the matrix owing to two primary reasons: (i) PHBV, owing to the presence of the valerate co-monomer, shows better mechanical properties such as elongation and toughness than pure

PHB and this is very much required for TPS systems and (ii) PHBV generally does not have any plasticizer like PHB that may affect the plasticizer present in the TPS.

PHBV-starch blends with polyethylene oxide (PEO) as compatibilizer have reported about 22 % elongation for 30 wt-% PEO-coated starch in PHBV and 20 % elongation for 50 wt-% PEO-coated starch in PHBV[64]. These values are insufficient for flexible packaging applications and hence cannot be considered as potential systems for this work. Another work blended PHB with three different starch derivatives: natural starch, starch adipate and grafted starch-urethane to improve properties but were unsuccessful and yielded extremely brittle materials[65]. PLA-starch blends have also been extensively studied with limited success in eliminating the inherent brittleness. However, one group has reported excellent properties (more that 200 % elongation) by using maleated PLA as the matrix instead of PLA[66]. Thus it is determined that there is a need for a compatibilizer in the biopolyester-plasticized starch blends.

The compatibilizer may be a chemical compatibilizer, such as maleated compound, or a physical compatibilizer such as a polymer that is compatible with both the plasticized starch and PHB or PHBV. The maleated route was discarded owing to issues with cost (chemicals and compatibilizer processing costs negate the low cost of starch), matrix molecular characteristics (molecular weight decreases owing to maleation) and environment (maleation byproducts disposal). The physical compatibilizer candidates investigated were PCL and PBAT. PBAT's compatibility with plasticized starch has been reported and a system containing 25 wt % PBAT with 75 wt-% of plasticized starch (having 65:35 starch:glycerol w/w) was reported to have ~ 150 % elongation at break[50].

Similarly PHAs and starch have also been reported to be significantly compatible[53]. Thus the main concern here is the compatibility of PHA and PCL or PBAT

The miscibility or compatibility of PBAT and PCL with PHBV or PHB can determined by looking at the Gibb's free energy of mixing given by equation 6.13[67]:

$$\Delta G_m = \Delta H_m - T(\Delta S_m^c + \Delta S_m^e) \qquad (6.13)$$

where ΔH_m, is the heat of mixing, T is the temperature, ΔS_m^c is the combinatorial entropy of mixing, ΔS_m^e is the excess entropy of mixing and ΔG_m is the Gibb's free energy. A miscible polymer blend needs to have the Gibb's free energy value less than zero. Flory gives the value of ΔS_m^c as being dependant on the inverse of the molar volume of the components[67, 68]. This is thus related to the molecular weight and since the materials in question are polymers having significantly large molecular weights, the ΔS_m^c is virtually zero. Consequently, this means that ΔG_m can be less than zero only when ΔHm is less than zero or ΔS_m^e is much greater than zero. The second scenario is rarely possible and hence can be ignored for all practical purposes. The enthalpy of mixing can be estimated using the following equation 6.14[68].

$$\Delta H_m = (\delta_1 - \delta_2)^2 \varphi_1 \varphi_2 \qquad (6.14)$$

where δ_n is the solubility parameter and φ_n is the volume fraction of component *n*. The value of solubility parameter is calculated by using the term $\delta = \rho\Sigma G/M$, where ρ is the density, G is the group molar attraction constant and M is the mer molecular weight. The group molar attraction constants were tabulated by Small and these were used for the structures of PHBV, PHB, PCL and PBAT (Table 6.9) and subsequently Gibb's free

energy of mixing was calculated for the polymer pairs based on the solubility parameters[67, 69].

Table 6.9: Solubility parameter values for polymers

Polymer	G ($cal^{1/2} cm^{3/2}$/mol)	δ ($cal^{1/2} cm^{3/2}$)	Polymer blend pair	ΔG_m cal/gm^3
PHB	768	11.162	PHB-PBAT	1.322
PHBV	1669	11.216	PHBV-PCL	0.623
PBAT	2409	8.65	PHBV-PBAT	1.379
PCL	975	9.49	PHB-PCL	0.585

The PHB-PCL system shows the lowest value of ΔG_m over the composition range (0.58 cal/gm^3) but all the systems had low values thus indicating slight miscibility between the polymers. Initial experiments used PHB as the matrix and the successful results were recreated in PHBV-TPS systems.

The sequential addition of the three components played a significant role in the final properties of the blend. It was previously determined that the starch plasticization needed to be a separate step as the other components interfered with the destructurizing process. Once the plasticized starch was prepared, the optimum sequence of addition and blending of PHB, plasticized starch (PS) and thermoplastic partner (TP) (PCL or PBAT)

was investigated. In the first trial system (I in Table 6.10), the plasticized starch was blended with TP followed by addition of the PHB in a second stage. In the second trial system (II in Table 6.10), PHB and TP were blended followed by addition of the plasticized starch in a second step. The third system (III in Table 6.10) consisted of adding all the components in one step. All the above systems had a composition of 40 wt. % PHB, 36 wt. % PCL, 14.4 wt.% corn starch and 9.6 wt. % glycerol. These materials were compounded on the microcompounder and then injection molded into tensile and DMA coupons. The mechanical properties are listed in table 6.10.

Table 6.10: Tensile properties for sequence optimization trials

System no.	Sample	Tensile Strength (MPa)	Tensile Modulus (GPa)	Percent elongation (%)
I	(PS-TP)-PHB	15 (±1.14)	0.90(±0.09)	47 (±11)
II	(TP-PHB)-PS	18 (±1.15)	1.08 (±0.11)	32 (±5)
III	(PS-TP-PHB)	21 (±1.28)	1.02 (±0.13)	114 (±13)

The first trial of blending of TP with the plasticized starch gave inferior properties (low tensile strength and elongation) owing to the loss of excess glycerol to evaporation at the processing temperature. In the second trial, the PHB underwent processing twice thus leading to poor properties as it is very sensitive to thermal degradation. When all are added together, then the PHB seems to absorbs the excess glycerol (from visual

observations of absence of glycerol fumes during the process) and is plasticized resulting in high elongation as well as has to be processed only once thus retaining its properties and hence all-together processing was determined to be the best under the present experimental conditions.

Following optimization of the sequence, the next stage was determining the most effective composition. The goal here was to obtain a material with appropriate properties for flexible packaging yet have the maximum biobased polymer content (PHA and plasticized starch). The variation in compositions followed the order shown in Table 6.11. The PBAT did not show any significant increase or drop in properties to immediately suggest improvement over PCL however the thermal characteristics mentioned earlier were a deciding factor. Composition 3 replaced the PHB component of composition 1 with PHBV and the valerate comonomer in the PHBV chain effectively reduces the stiffness of the polymer and this is transferred to the modulus of composition 3 as it decreases from 1.02 GPa to 0.45 GPa. The modulus of PHB is 3.5 GPa which reduces to 1.5 GPa with 14% valerate content thus explaining the loss in modulus of the blend[12]. This composition also gave the maximum elongation (405%) but the low value of modulus and strength (resulting from the PCL component which has low tensile strength) eliminated this material for selection. Polyhydroxyalkanoate based blends with starch have been reported earlier[53, 63-65] These findings have all used polyhydroxybutyrate-co-valerate (PHBV) as the matrix owing to two primary reasons: PHBV, owing to the presence of the valerate comonomer, shows better mechanical properties such as elongation and toughness than pure PHB and this is very much required for TPS systems and secondly, PHBV generally does not have any plasticizer

like PHB that may affect the plasticizer present in the TPS. Hence PHBV was selected as the matrix polymer over plasticized PHB. The next composition, number 4, substituted the PHB component of composition 1 with PHBV as well as the PCL component with PBAT. This composition gave ideal balance of elongation and modulus as well as maintained the strength. In composition 5, the components are same as number 4 however the PHBV component weight was increased to 50% and the remaining part is PBAT: plasticized starch at 60:40 w/w ratio. This combination was determined to give sufficient elongation (284%) for the intended flexible packaging purpose. PBAT is a biodegradable polymer synthesized from petroleum products and the aim was to have minimal PBAT content. The biobased content of composition 5 was highest (50 % PHBV + 20 % plasticized starch = 70 % biobased) and PBAT content was kept to 30 wt.%. Hence this system was selected for further investigation.

Table 6.11: Tensile properties for composition variations

No	PHA	TP	Corn Starch	Glyc.	Tensile strength (MPa)	Elongation (%)	Modulus (GPa)
1	40 (PHB)	36 (PCL)	14.4	9.6	21 (±1.28)	114 (±13)	1.02 (±0.13)
2	40 (PHB)	36 (PBAT)	14.4	9.6	17 (±1.84)	114 (±9)	0.87 (±0.16)
3	40 (PHBV)	36 (PCL)	14.4	9.6	15 (±0.68)	405 (±38)	0.45 (±0.09)
4	40 (PHBV)	36 (PBAT)	14.4	9.6	17 (±0.63)	300 (±27)	0.68 (±0.04)
5	50 (PHBV)	30 (PBAT)	12	8	17 (±0.61)	284 (±82)	0.66 (±0.01)

The PHBV-TPS system comprising of 50 wt. % PHBV, 30 wt. % PBAT, 12 wt% Starch and 8 wt. % glycerol was determined to be an excellent material for flexible packaging applications under the present experimental conditions studied and in order to ascertain this, this material was fabricated into films by cast film extrusion. The resulting films showed excellent mechanical properties, tensile strength of 15 MPa, tensile modulus of 0.55 GPa and especially improved elongation (368 %). This improvement in elongation of the cast films over the injection molded samples can be attributed to the

process of cast film extrusion that is making the PBAT phase continuous via elongational distribution. The Gibb's free energy calculations indicated the lack of miscibility between the PHBV and PBAT components. However, more importantly than miscibility, the required property for useful polymer blends is compatibility and phase continuity. Compatible polymers mean the combination of the polymers is useful while miscibility means the polymers are soluble as defined by phase diagrams[70]. This miscibility exists over a set of conditions that may not exist in actual usage. Thus compatibility is more important for describing the usefulness of a polymer blend than miscibility. This phase continuity determines the overall properties of the system as the applied forces are distributed over the continuous phases and are no localized. Such localized forces on the component having poor properties may cause failure of the entire material and hence continuity of the tougher component is highly sought after. This behavior is more evident in the SEM micrographs of the films (Figure 6.36, 6.37 and 6.38). These films were dipped for 30 seconds in liquid nitrogen and fractured. This dipping caused phase separation owing to the different contraction coefficients of the components. Thus the layered yet continuous morphology was very obvious in the films. The discrete phases of the minor component (plasticized starch) are enveloped by the PHBV or PBAT phases. Thus PHBV is fulfilling the intended role of blocking the leaching and PBAT is maintaining the continuity of the system.

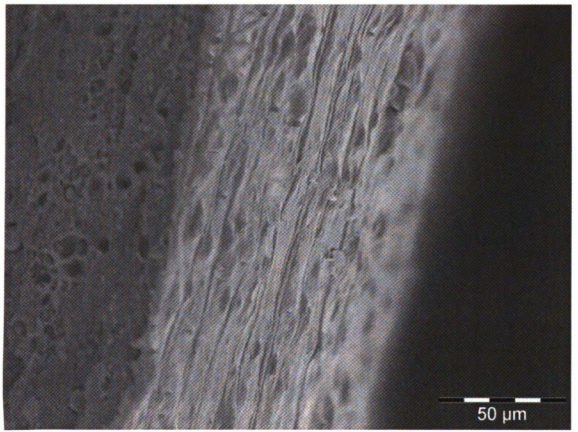

Figure 6.36: SEM image of the cryogenically fractured surface of PHBV-TPS system observed at 550 times magnification (Scale bar: 50 µm)

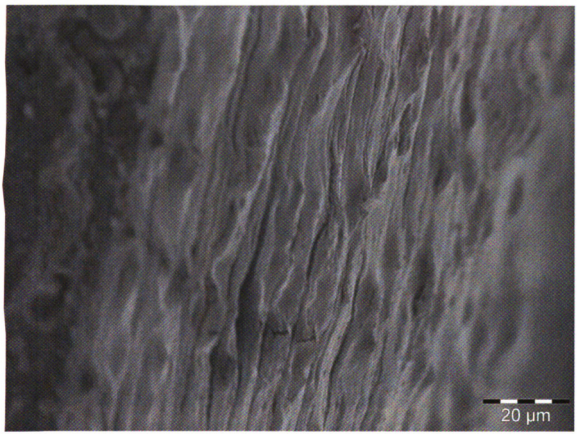

Figure 6.37: SEM image of the cryogenically fractured surface of PHBV-TPS system observed at 950 times magnification (Scale bar: 20 µm)

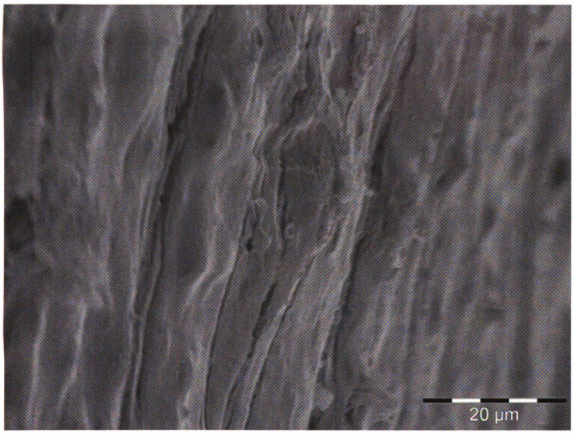

Figure 6.38: SEM image of the cryogenically fractured surface of PHBV-TPS system observed at 1600 times magnification. The minor component is seen to be encapsulated by the major component (Scale bar: 20 µm)

The films were also analyzed by dynamic mechanical analysis to determine the glass transition temperatures of the components. Literature values for the glass transition temperatures (T_g) of the components are: PHBV (5°C), PBAT (-30°C) and plasticized starch (65 wt.% corn starch with 35 wt% glycerol) (-20°C)[48]. The blend showed an α-transition at -13 °C and a β-transition at 22°C (Figure 6.39). The β-transition is intrinsic to the plasticized starch and is seen in generally all TPS systems[48]. However the most notable point was the absence of Tg peaks for the components and a single very sharp peak at -13 °C. Blending science dictates that for a multicomponent blend, the Tg values of the components shift toward each other for even slightly miscible components while a single peak is a sign of complete miscibility[67]. This however contradicts the Gibb's free

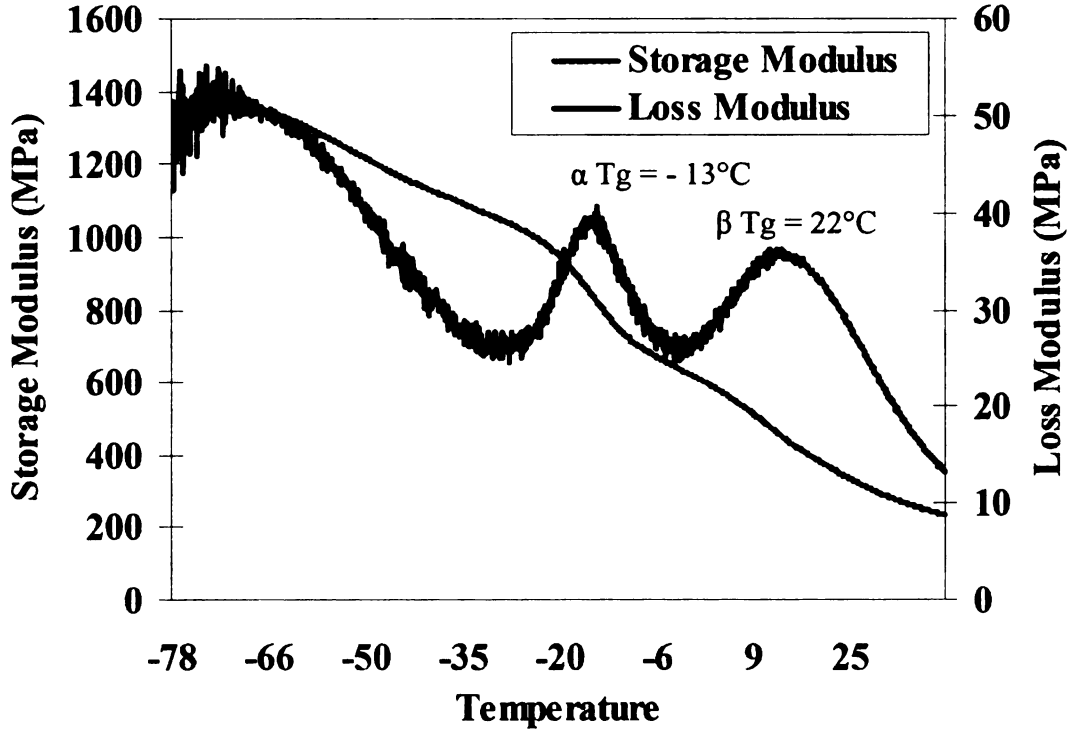

Figure 6.39: Storage modulus and loss modulus of PHBV-TPS film as a function of temperature

energy predictions for the binary PHBV-PBAT system. Thus it can be concurred that the plasticized starch is miscible with both the PHBV and PBAT and is creating a miscible blend. The purpose of adding PBAT was to serve as a compatibilizer for the PHBV-plasticized starch system however in actuality the plasticized starch is acting as the compatibilizer.

6.4.4 Polyhydroxyalkanoate-Thermoplastic Starch Blend based Composites

In-depth studies indicated room for improvement of the PHBV-TPS materials and the inferred route was via composite technique. The objective of this part was to incorporate low-cost fillers into the PHA-TPS to address the following issues:

(i) The morphology observations of the PHA-TPS system indicated that the size of the phases is fairly large and potentially better properties are possible if the phase distribution can be improved. Addition of a filler or reinforcement, at specific levels, increases the viscosity of the polymer and this can lead to better disruptive mixing of the minor component[67].

(ii) Plasticized starch has a tendency to expel excess glycerol out of the system over time and this can be inhibited or maybe even totally stopped by adding filler with platelet-like geometry. This structure may block the plasticizer from leaching out at the surface of the blend.

(iii) Platelet-shaped fillers have been proven to significantly increase the barrier properties of polymers by making the path of penetrant molecules tortuous[71, 72].

(iv) A low-cost filler reduces the overall material cost as well may improve thermo-mechanical properties.

The internal structure of the films, observed after cryogenically fracturing the films, indicates a layered morphology. Even though the system is showing elongation at break of 368%, it can be inferred that there is still room for improvement provided the distribution of the components can be improved. The layered morphology lacks homogeneity and hence is susceptible to failure at regions in the material that have PHBV-rich phases. This can be reduced by achieving more disruptive mixing of the components consequently leading to a droplet and dispersed morphology. One route to improving disruptive mixing is by either increasing the shear forces via increasing the processing torque. But PHAs are susceptible to thermal degradation and increasing the shear further exacerbates this problem[73]. The other route is to change the melt viscosity via incorporating fillers that impede the flow of the polymer chains. This increased viscosity leads to increase of interfacial forces between the phases and ultimately breaks down the layered morphology into the desired droplet morphology[70]. The size of the filler and the amount of filler both are important factors in achieving this behavior. Nano-sized fillers can actually have a reverse effect and decrease the melt viscosity, upto certain weight loadings, and hence were discarded as potential filler candidates[74]. Macro-sized particulate fillers such as talc are ideal candidates owing to their platelet-like geometry and inherent affinity for polymeric matrices.

Unmodified talc was incorporated at 2.5 and 5 wt. % loading into the PHBV-TPS blend by extrusion processing. Talc-filled composites showed remarkable improvement in mechanical properties; especially the elongation at break that increased from 368 to ~650%. (Table 6.12).

Table 6.12: Tensile properties for talc-filled composites

Sample	Tensile Strength (MPa)	Tensile Modulus (GPa)	Percent elongation (%)
PHBV-TPS	15 (±2.07)	0.55 (±0.10)	368 (±60)
PHBV-TPS + 2.5% talc	16 (±2.08)	0.50 (±0.11)	674 (±50)
PHBV-TPS + 5% talc	15 (±0.01)	0.55 (±0.01)	598 (±7)

The SEM images better explained this behavior. Figure 6.40 and 6.41 show the cryogenically fractured surfaces of the PHBV-TPS system with 2.5% talc loading. In comparison with Figure 6.36, 6.37 and 6.37, there is markedly different droplet morphology in the composite than the layered morphology in the blend. The increased viscosity is promoting disruptive mixing and is reducing the size of the minor components. These are well dispersed and completely encapsulated by the major components this giving better phase continuity. Also the composite material is seen to be much more homogeneous than the blend. These factors are combining to bring forth the

maximum properties of the individual components (PBAT has elongation of ~ 800%) in a synergistic sense. Figure 6.42 and 6.43 show the cryogenically fractured surfaces of the PHBV-TPS system with 5% talc loading. These images indicate an even better dispersion, homogeneity and reduced droplet size of the minor component. This explains the remarkably low variation in the values of the mechanical properties observed in Table 6.12. Thus talc is seen to be excellent filler for the PHBV-TPS system due to outstanding mechanical property improvements.

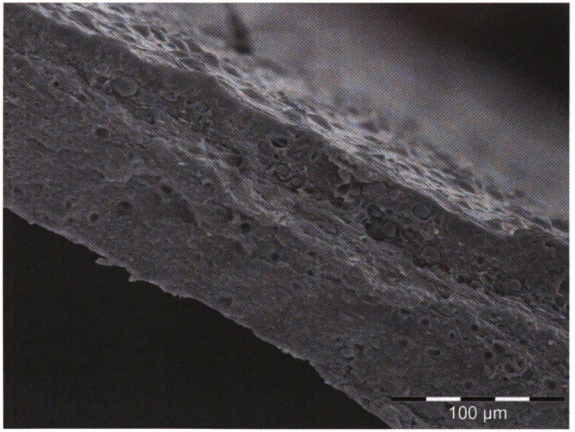

Figure 6.40: SEM image of the cryogenically fractured surface of PHBV-TPS composite with 2.5 wt. % talc observed at 370 times magnification (Scale bar: 100 µm)

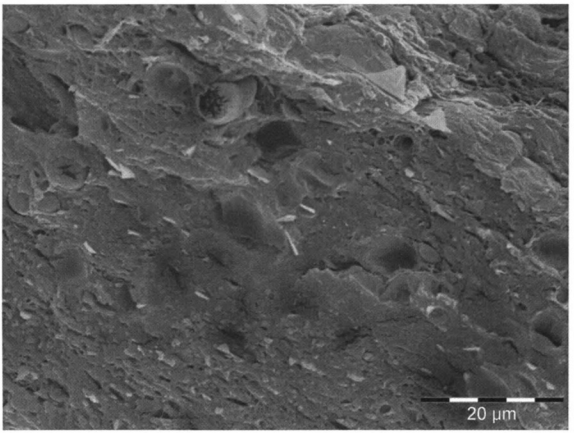

Figure 6.41: SEM image of the cryogenically fractured surface of PHBV-TPS composite with 2.5 wt. % talc observed at 1600 times magnification. The homogeneity of the material is evident (Scale bar: 20 µm)

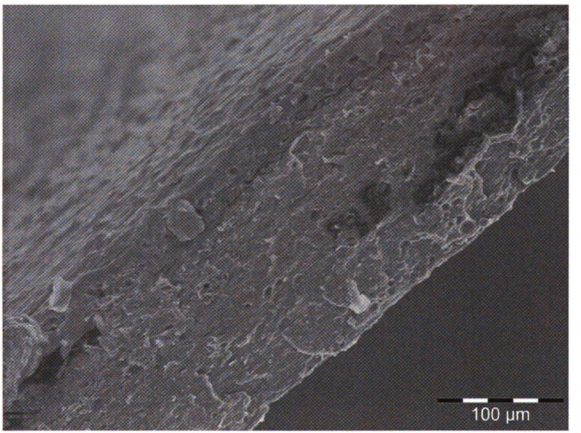

Figure 6.42: SEM image of the cryogenically fractured surface of PHBV-TPS composite with 5 wt. % talc observed at 270 times magnification. (Scale bar: 100 µm)

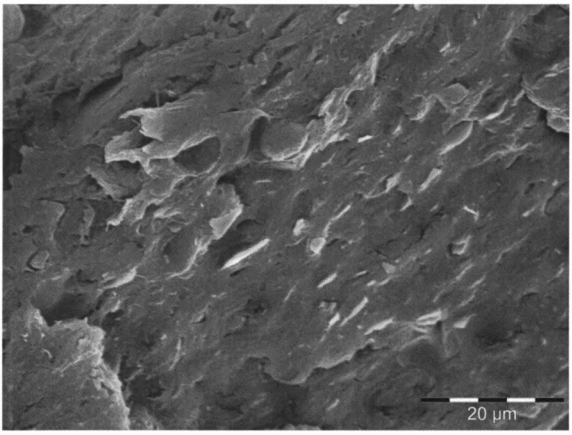

Figure 6.43: SEM image of the cryogenically fractured surface of PHBV-TPS composite with 5 wt. % talc observed at 1600 times magnification. The well dispersed and separated talc platelets are visible (Scale bar: 20 µm)

Another reason behind addition of talc was the expected improvement in barrier. PHBV has excellent barrier to oxygen (25 cc-mil/100 in^2 day-atm) however it cannot be fabricated into films owing to its inherent brittleness. PBAT, however, has high OTR (~ 400 cc-mil/100 in^2 day-atm) or a very low oxygen barrier. The PHBV-TPS blend shows oxygen transmission rate of 46.4 ±0.78 cc-mil/100 in^2 day-atm. The composites show notable further reduction in OTR (Figure 6.44); 2.5% talc is reducing OTR by ~24% and 5% talc is reducing OTR by ~ 44 % over the PHBV-TPS blend. Similar trends are also seen in the Water vapor transmission rates (WVTR) (Figure 6.45). The WVTR of PHBV-TPS decreased by ~ 20 % by incorporation of 2.5% talc and by ~ 42% by incorporation of 5% talc. These reductions are due to a combination of multiple factors explained below; namely the tortuosity effect of the talc, the increase in crystallinity and the improved mixing. The above permeability values compare favorably with some conventional polymers (Table 6.13)[75].

Table 6.13: Permeability values for conventional polymers (adapted from Ref.[75])

Polymer	Oxygen Permeability 25°C (cc-mil/100 in^2-day-atm)	Water Vapor transmission 38°C, 50-100% RH (g-mil/100 in^2-day)
LDPE	500	1.3
PP	250±160	0.5±0.2
PS	330±165	8.5
Nylon 6	2.6	19±3
PET	4.5±1.5	1.2

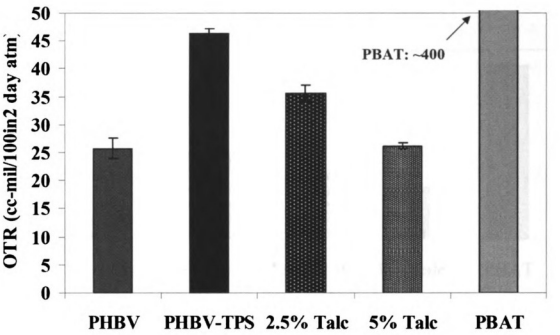

Figure 6.44 Oxygen Barrier properties of PHBV-TPS and their talc-based composites

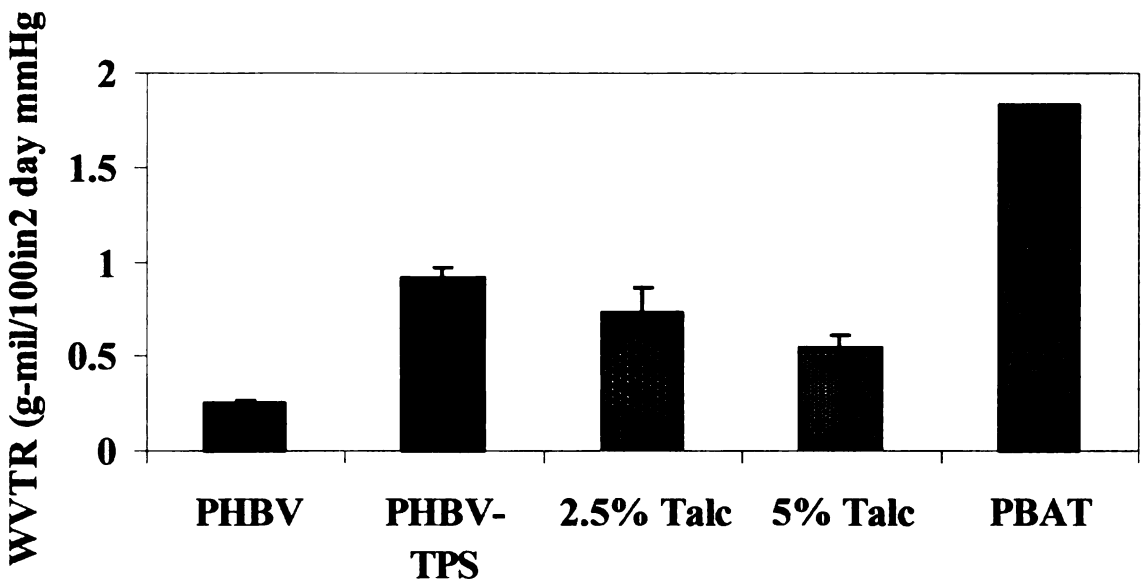

Figure 6.45 Water vapor Barrier properties of PHBV-TPS and their talc-based composites

The talc is effectively a completely impermeable material and a composite having well dispersed talc is making the penetration and diffusion path of the gas molecules tortuous. This tortuosity is reducing the permeation of the composites over the blend. Secondly, the talc is a known to behave as a nucleating agent and increases the crystallinity of the polymer matrix by initiating wide-spread spherulite growth. The PHBV component is highly conducive to crystallize and the incorporation of talc is increasing the percent crystallinity of the PHBV phase. Diffusion of gas molecules in polymers occurs in the free volume and the amorphous regions while the crystalline regions are effective impermeable. Hence increased percent crystallinity of the PHBV phase is reducing the overall permeability of the composite.

Thirdly, the talc is aiding the disruptive mixing of the minor components (PBAT and plasticized starch). These components have lower barrier and hence a more distributed and consequently smaller sized minor component effectively is limiting the areas of poor barrier in the entire system. These poor barrier components exist as dispersed droplets according to the SEM images and hence are not in large areas. Thus the overall barrier of the system improves by addition of the talc. These above trends also explain the improvement in barrier as a function of talc content as each of these factors proportionately increase with the amount of talc present.

A platelet-shaped filler can decrease the permeability of a polymeric matrix significantly by itself and it needs to be ascertained if the other two factors; i.e. the increased crystallinity and the disruptive mixing, did play a role in improving the barrier. The effect of the talc alone can be predicted by using a model proposed by Cussler et al[71]. For such a system of a film containing impermeable flakes or discs oriented

perpendicular to the diffusion direction, the ratio of the permeability P_{blend} of the blend to the permeability of the composite $P_{composite}$ is given by equation 6.15 where α is the aspect ratio of the talc and Φ is the volume fraction of the talc:

$$P_{blend}/P_{composite} = 1 + [(\alpha^2\Phi^2) / (1-\Phi)] \qquad (6.15)$$

Using the value for density of talc as 2.7 g/cc[76] and the density of the PHBV-TPS system as 1.25 g/cc, the volume fraction of talc corresponding to 2.5 wt % is 1.17 vol. % and for 5 wt.%, it is 2.37 vol. %. Figure 6.46 shows the actual and predicted values for the P_{blend} /$P_{composite}$ ratio for water vapor permeability and Figure 6.47 shows the actual and predicted values for the P_{blend} /$P_{composite}$ ratio for oxygen permeability. These values were calculated by substituting the known values in the above model and were plotted as a function of aspect ratio of talc.

The actual and predicted values for WVTR match closely at aspect ratio of 44 for the 2.5 wt. % talc composite and aspect ratio of 36 for the 5 wt. % talc composite. Similarly, the actual and predicted values for OTR matched closely at aspect ratio of 48 for the 2.5 wt. % talc composite and aspect ratio of 38 for the 5 wt. % talc composite But the SEM image (Figure 6.46) for the 2.5 wt. % talc give an approximate aspect ratio of 14 and the SEM image (Figure 6.47) for the 5 wt. % talc composite shows aspect ratio of approximately 16. These values agree with the aspect ratio values reported by the manufacturer[77]. Thus the improvement in barrier cannot be attributed only to the high aspect ratio of the talc forming high-barrier areas but to also other two factors that of

increased crystallinity and disruptive mixing. These factors cannot be measured by empirical techniques or models and hence their effects cannot be quantified individually.

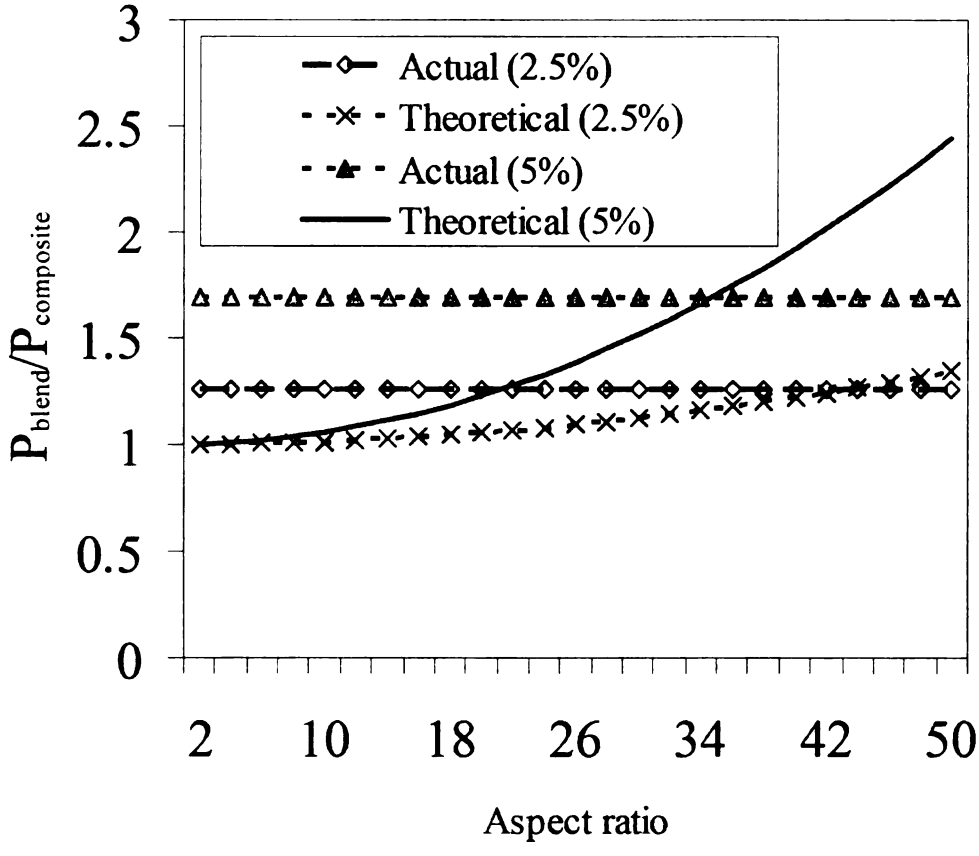

Figure 6.46: Theoretical versus actual behavior for WVTR for the blends and composites

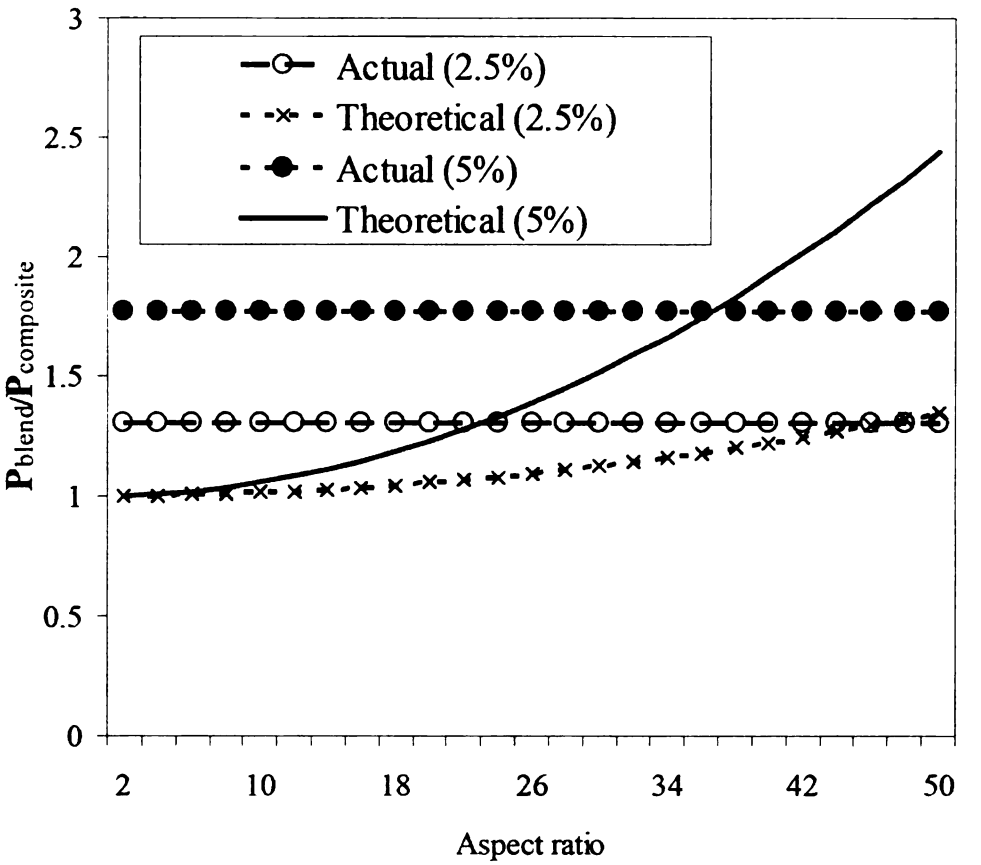

Figure 6.47: Theoretical versus actual behavior for OTR for the blends and composites

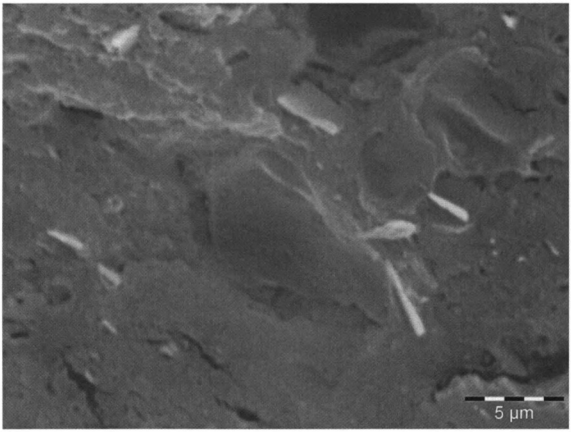

Figure 6.48: Talc platelets visible in PHBV-TPS system with 2.5 wt. % talc content (scale bar 5 um)

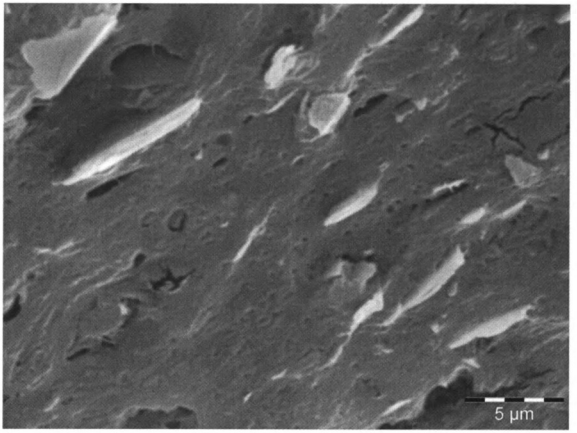

Figure 6.49: Talc platelets observed at 4500 times magnification in PHBV-TPS system with 5 wt. % talc content (scale bar 5 um)

6.4.5 Ageing Behavior

TPS systems and PHA based materials both have independently been reported of showing ageing behavior; i.e. loss of properties as a function of storage time[48, 78]. In case of TPS, this is attributed to two factors: the hydrophilicity of the starch that results in moisture uptake and consequent drop in properties; and the leaching of the plasticizer from the system. In case of PHA-based materials, this ageing is attributed to the secondary crystallinity of the PHA. This embrittlement has been uniquely attributed by different authors to be a result of progressive reduction of the amorphous content in the partially crystalline polymer and to the development of secondary crystallization[78]. The small crystallites produced during the secondary crystallization reduce the mobility of the chain segments thus increasing stiffness and embrittling the material[19].

The developed materials of the above work aimed to overcome these effects by the following means: (i) the high hydrophobicity of the PHBV may reduce the moisture uptake of the starch; (ii) the talc may inhibit the plasticizer leaching; (iii) the disruptive and homogeneous mixing coupled with the discerned miscibility of the components from DMA analysis may restrict the secondary crystallinity of the PHBV component.

Hence to ascertain the above reasoning, a multi-fold ageing experiment was designed. Films were fabricated by cast film extrusion from the blends and composites. These films were cut into samples 10 inches long and 1 inch wide and stored in an environmental chamber maintained at 30 °C and 50% relative humidity for 30 days.

Every alternate day, 5 specimens of each sample (PHBV-TPS, PHBV-TPS with 2.5% talc and PHBV-TPS with 5 % talc) were removed from the chamber and subjected to tensile testing, DMA analysis and DSC analysis. The tensile testing was aimed at demonstrating the loss of plasticizer corresponding to drop in elongation or increase in modulus; the DMA testing aimed to investigate the increase or decrease in T_g ; and the goal of the DSC analysis was to measure the percent crystallinity of the PHBV phase. Simultaneously, three specimens of each sample were weighed initially at day zero and every second day to ascertain the weight change. The samples were wiped with paper towels prior to each weight measurement.

6.4.5.1 Tensile testing

PHBV-TPS films and their composites with talc exhibited remarkable properties as seen in the earlier part of this work and these properties are reported at day zero (day of fabrication). The TPS-PHBV blend does not exhibit discernable ageing behavior in the context of tensile properties. The elongation at break (Figure 6.50) remains nearly the same as that of the initial day-zero material. This signifies that the plasticizer has not leached out of the system and is still very much fulfilling its role of eliminating the brittleness. The tensile strength (Figure 6.51) and modulus data (Figure 6.52) show a slight increase during the initial period that is attributed to the primary crystallinity of the PHBV phase. This effect of crystallinity is more profound in the composites as the talc is acting as nucleating agent and initiating crystallinity via nucleation. Thus the elongation at break drops from ~600-700 % to ~ 175 % in the composites and remains constant after

that. An observation of note here is that this drop is to a large extent similar for the 2.5 wt. % and 5 wt. % composites. This is so because for polymer nucleation, only a very small amount of nucleating agent is required (generally <0.1 vol. %) and any amount of nucleating agent above this value is expelled by the growing spherulites and remains at the crystal boundary. As this value is significantly smaller than the actual volume percent of talc present in both the compositions, the effect is same in both cases and hence the trend of mechanical properties is similar.

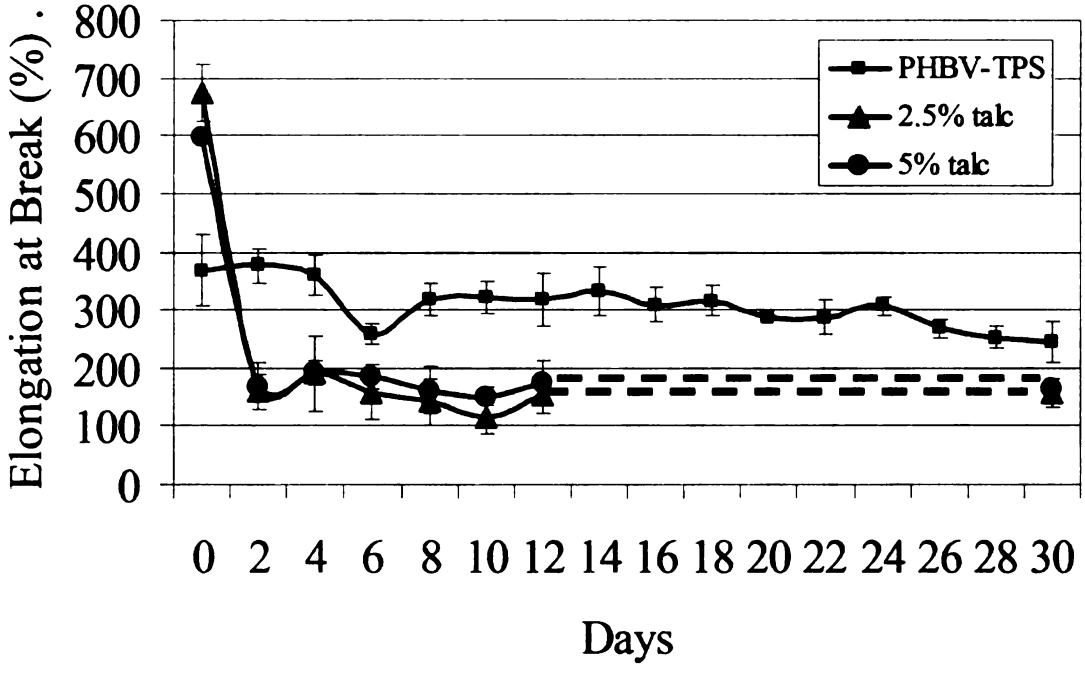

Figure 6.50: Elongation of PHBV-TPS blends and composites as a function of time

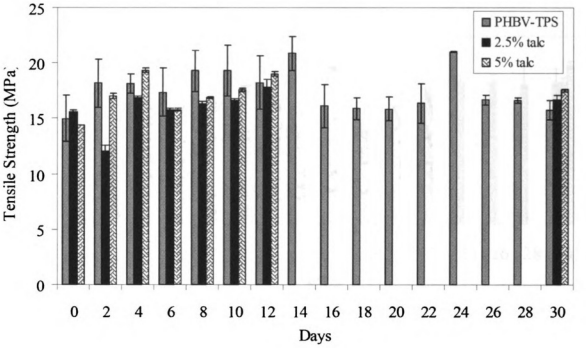

Figure 6.51: Tensile strength of PHBV-TPS blends and composites as a function of time

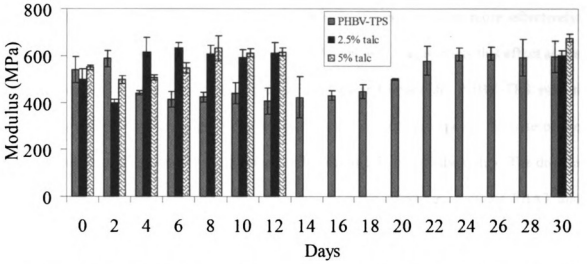

Figure 6.52: Tensile modulus of PHBV-TPS blends and composites as a function of time

6.4.5.2 Thermal Analysis

The glass transition temperature of a material is very sensitive to plasticizer content. Hence even a slight decrease in plasticizer content is reflected in the increase in glass transition temperature. This T_g was measured using the peak values of tan delta curves for the films as measured in DMA (Figure 6.53). The composites are showing decreased T_g values owing to the dispersion of the plasticizer and subsequent penetration into the matrix caused by the disruptive mixing. This improved mixing is due to the increased melt viscosity of the components that transfer the applied shear during processing directly to the minor components thus dispersing them more effectively. However, presence of more amounts of filler (5% versus 2.5%) restricts this effect as the actual amount of plasticizer in the material reduces and hence the PHBV-TPS system with 5% talc shows very slightly higher T_g than the 2.5 wt% composite. In case of the blend, the plasticizer is not well dispersed and hence the T_g is slightly higher. The drop in T_g after day 12 for the blends can be explained by the interference of the PBAT and starch in the secondary crystallization of the PHBV component. The spherulite growth has stopped and consequently also the expelling of the plasticizer by the growing spherulites has stopped and hence translates to a lowered T_g.

The crystallinity of the PHBV phase can be determined from the ratio of the melting enthalpy ΔH_0 for 100% crystalline PHBV, which is 109 J/g from literature[79], to the melting enthalpy ΔH_{sample} of the sample. The absolute crystallinity can be calculated from these values and weight fraction W of PHBV in the blend by using equation 6.16:

$$\chi_c = \frac{\Delta H_{sample}}{\Delta H_0} \times \frac{100}{W_{sample}} \qquad (6.16)$$

The percent crystallinity values of PHBV and of the PHBV phase in the PHBV-TPS blends and their composites are given in Table 6.14. For PHBV, films were made by cast film extrusion according to similar process conditions as the blends in order to have similar thermal history.

Table 6.14: Percent crystallinity of the PHBV component in the PBV-TPS blends and composites

Day	PHBV	PHBV-TPS	PHBV-TPS + 2.5 wt. % talc	PHBV-TPS + 5 wt. % talc
0	42.7	37.8	46.3	44.9
5	43.9	37.6	51.9	63.9
10	49.8	38.7	58.7	67.1
15	55.4	39.9	65.6	70.1

The PHBV component of the PHBV-TPS blend is showing reduced percent crystallinity at day zero and this trend remains for the duration of the testing. Thus the PBAT and plasticized starch have inhibited the secondary crystallization of the PHBV successfully. In case of the composites, the nucleating effect of the talc has increased the primary crystallinity and this explains the drop in elongation for the second day of testing (Figure 6.50). Yet after the initial period, the increase in crystallinity levels off and attains a plateau indicating that the secondary crystallinity has still been hindered.

The weight change experiments (Figure 6.54) show some interesting observations; the PHBV-TPS samples gained maximum weight for day 0-2 from moisture uptake while the composites resisted this uptake owing to the factors explained in the barrier section. All the samples lost weight in the initial period and this is attributed to the plasticizer being expelled by the primary crystallization process. This effect is pronounced in the composites as expected from the crystallinity data and is proportional to the talc loading. After the initial period, the system stabilized and this is reflected in the tensile property measurements.

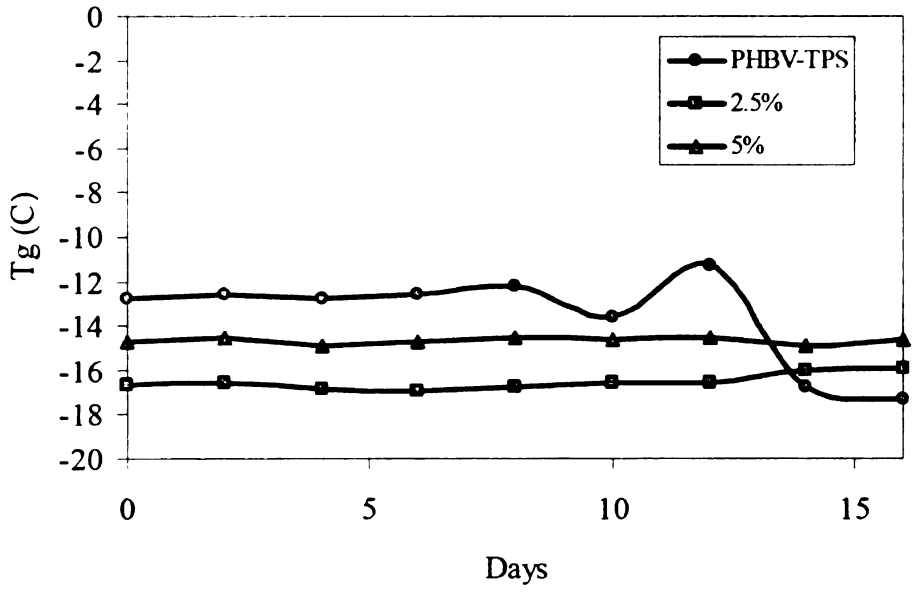

Figure 6.53: Glass transition temperature as function of time

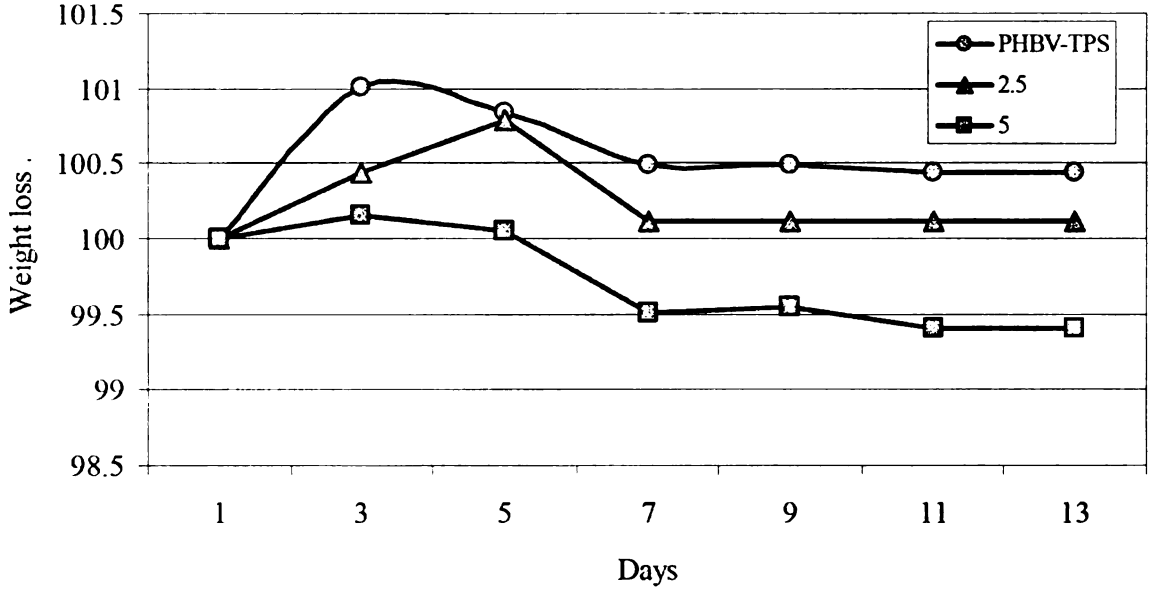

Figure 6.54: Weight change as a function of time for the PHBV-TPS blends and composites

6.5 Biodegradation

Polyhydroxybutyrate is degraded by the action of enzymes known as esterases produced by a wide range of microorganisms. Degradation causes polymer hydrolysis, leading to a decrease in its molecular weight as well as weight loss[43]. All tested samples degraded in compost, albeit at different rates and extents (Figure 6.53). From the biodegradation view point, PHBV-TPS showed the maximum rate of biodegradation. The PHBV component is the slowest to degrade amongst the constituents and this agrees with literature values[47, 80]. The PHBV-TPS-talc composite samples appeared to be quite retarded in biodegradation possibly because of the homogeneous mixing and presence of talc that is limiting the access of the polymer to the compost bacteria. The positive sample (pure starch) showed 60% biodegradation in 60 days indicating the validity of the test. Testing standards mandate 60% biodegradation in 190 days for a system to be considered biodegradable. The initial trends for the PHBV-TPS system as well as the PHBV-TPS-talc composite indicate that this value is being approached well within the required time period.

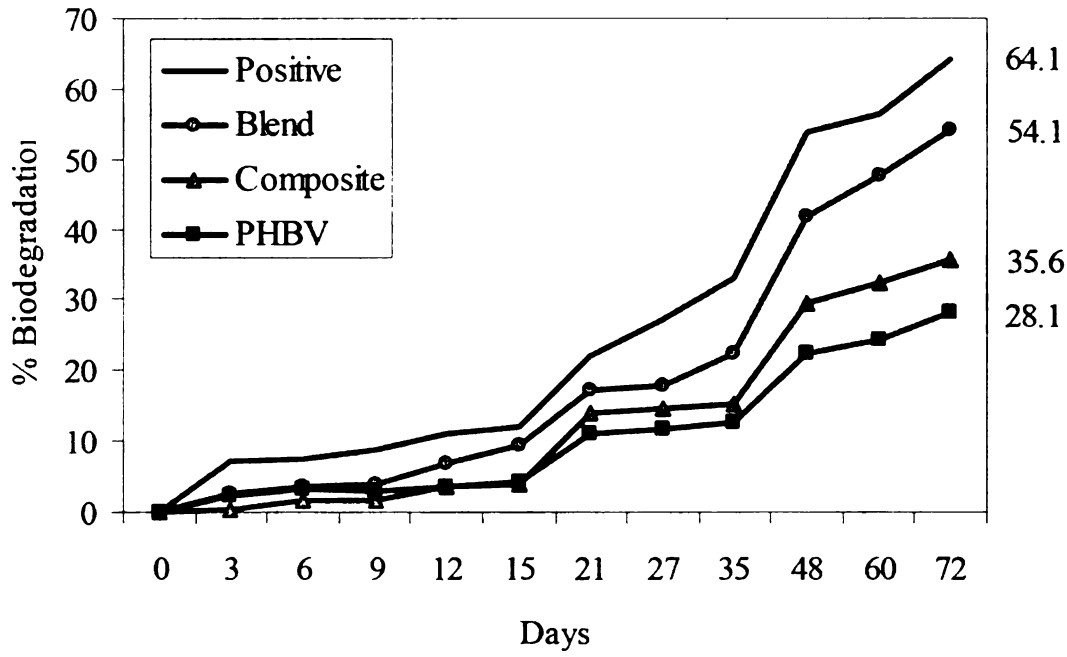

Figure 6.55: Aerobic Biodegradation of the PHBV-TPS and PHBV-TPS-talc composite with 5 wt. % talc.

6.6 Economic Analysis

From a commercial and industrial viewpoint, biopolymers can only be considered as replacements for conventional polymers if such substitutions are economically beneficial. The biopolymers of this work fall under two broad categories when considered for economic evaluation: materials based on renewable resources (Polyhydroxyalkanaotes, starch, glycerol, rubber) and secondly the materials based on petroleum resources (Polybutylene adipate-co-terephthalate).

Polymers based on renewable resources have for the past several years been looked at as potential substitutes for conventional polymers that are synthesized from petroleum. The main reasons behind this are the dwindling resources of petroleum and the ever-increasing cost of oil. Several countries and organizations are looking to bio-based polymers as an opportunity to decrease dependence on petroleum and ultimately stabilize material costs. A study undertaken by the Institute of Prospective Technological Studies in Europe looked at the maximum technical substitution potential of conventional polymers by bio-based polymers[81]. This study estimated a maximum possible substitution value of 33% of total polymers by bio-based polymers but this value was a combination of several uncertainties and factors and is more indicative than factual.

The main deterrence in the usage of bio-based polymers is their current high cost. Polymers from renewable resource are independent of fluctuating and ever-increasing petroleum prices yet have their own specific cost problem based on economies of scale. Renewable-resource based polymers lack a large market share and hence are synthesized

on a batch-scale. This batch-scale production cannot economically compete with the continuous production of conventional polymers.

Biodegradable synthetic polymers present significant environmental benefits yet are still linked to petroleum prices and thus have high cost[82]. Other obstacles to broader usage of biopolymers are the lack of critical mass and the cost of change. Converters and manufacturers cannot justify new processing equipment investments or capacity increases without the market achieving a critical mass. Also most manufacturers of finished products are not amenable to changing processing and converting conditions for a new class of polymers. All these factors combine to create an inflated cost for biopolymers and need to be addressed in order to make substitution of conventional polymers a reality.

Polyhydroxybutyrate, and the entire PHA family for that matter, has a huge potential market owing to excellent properties and attributes. PHA commercial production has been continuously investigated and developed by numerous companies such as ICI, Procter & Gamble, Monsanto, Dow, Biomer, Metabolix, etc. The initial price for PHA was 30 $/kg when it was launched by Zeneca. This price was still 10-20 € /kg (6- 12 $/lb) as recently as 2003, owing mainly to batch-scale production methods[81, 83]. However, Chinese suppliers are advertising capabilities to provide PHAs at 2.5-3.5 $/lb[84, 85]. Metabolix currently sells PHA for 2-3 $/lb and the company expects the price to drop below 1 $/lb by 2008-2010[86, 87]. PHA costs are related to two major factors; the raw material cost and the production scale. The raw material costs for PHAs are as high as 40-50 % of the total cost and the yields are only 10-25 % w/w. Thus the potential route to reduce costs is to use genetically modified plants with higher yields or recombinant

bacteria or lower cost carbon sources such as switch-grass. These routes are being investigated by researchers and should hopefully bring the price of PHAs down. For this work, the price of PHA is considered as 2 $/lb for the current time and 1 $/lb for the year 2010.

Starch is an inexpensive renewable-resource-based material and is abundantly available. The cost of starch is 0.09-0.95 $/lb depending on level of chemical modifications. This work uses corn starch with high-amylose content and is sold by National Starch and Chemical Company, NJ at 0.20 $/lb[88]. However current corn prices are driving this cost up and suppliers have announced 5-10% increase in prices for corn-based starches[89]. For this work, the price of corn starch is considered as 0.20 $/lb for the current time and 0.22 $/lb for the year 2010.

Glycerol, the plasticizer used for starch, can be produced from synthetic means as well as biobased resources. The upcoming soy-based biodiesel industry produces glycerol as a by-product and thus glycerol can be considered biobased. The current price of glycerol is 0.40-0.60 $/lb[59, 60]. However, as biodiesel production increases, the production of glycerol is also bound to increase and this is largely expected to decrease the cost of glycerol. The price of glycerol is estimated to drop to as low as 0.05 $/lb but a more conservative estimate is of $ 0.20 $/lb by the year 2010[90]. The price of glycerol is considered as 0.35 $/lb for the current time-frame and 0.20 $/lb for the year 2010.

Polybutylene adipate-co-terephthalate (PBAT) is sold by BASF corporation under the trade name Ecoflex®. PBAT prices have been fairly stable for some time and are currently at 1.85-1.95 $/lb[91]. These numbers are assumed to be constant through 2010.

Natural rubber costs between 0.97 and 1.25 $/lb and epoxidation adds a further 10-20% to the cost[92]. The epoxidized natural rubber price is thus considered to be 1.25 $/lb. The maleated rubber compatibilizer price is assumed to be the same as the modified rubber.

Montmorillonite Clay currently costs 6-7 $/lb and is expected to remain at these prices through 2010[93]. Talc price is also assumed to be constant through 2010 as 0.05 $/lb. The following tables give estimate costs for the materials developed in this research and comparison prices for conventional polymers that may be substituted.

Table 6.15: Cost estimates for toughened polyhydroxybutyrate blends and nanocomposites.

	PHA	Rubber	Compatibilizer	Clay	Total
Composition (wt. %)	*60*	*30*	*10*	-	*100*
2003 cost ($/lb)	1.20	0.375	0.125	-	**1.70**
2010 cost ($/lb)	0.60	0.375	0.125	-	**1.10**
Composition (wt. %)	*57*	*28.5*	*9.5*	*5*	*100*
2003 cost ($/lb)	1.14	0.356	0.118	0.325	**1.94**
2010 cost ($/lb)	0.57	0.356	0.118	0.325	**1.37**
TPO[94]					**0.80-1.35**
HIPS[94]					**1.10-1.36**

Table 6.16: Cost estimates for PHBV-TPS blends and composites.

	PHA	PBAT	Corn Starch	Glycerol	Talc	Total
Composition (wt.%)	*50*	*30*	*12*	*8*	-	*100*
2003 cost ($/lb)	1.00	0.55	0.024	0.028	-	**1.60**
2010 cost ($/lb)	0.50	0.55	0.0264	0.016	-	**1.09**
Composition (wt.%)	*47.5*	*28.5*	*11.4*	*7.6*	*5*	*100*
2003 cost ($/lb)	0.95	0.527	0.0228	0.0266	0.0025	**1.53**
2010 cost ($/lb)	0.475	0.527	0.02508	0.0152	0.0025	**1.04**
LDPE[94]						**0.70-0.82**
Nylon[94]						**1.72-1.95**

The above estimates are for materials only and further costs down the process such as production etc. are not considered. Thus one of the ways to decrease the cost of renewable-resource based polymers is to create applications for them thus increasing usage and consequently shift production from batch to continuous ways. This increased market-vale can also be achieved by improving the properties of the renewable-resource based polymers thus making them more attractive than conventional polymers.

6.7 References

1. J.L.Amos, J.L. McCurdy, O. R. McIntire, *Method of making Linear Interpolymers of Monovinly Aromatic Compounds and a Natural or Synthetic Rubber,* 1954, US Patent no. 2,694,692,

2. Z. Bartczak, A. S. Argon, R. E. Cohen and M. Weinberg, *Toughness mechanism in semi-crystalline polymer blends: I. High-density polyethylene toughened with rubbers*, Polymer, 1999, 40, 2331-2346

3. Z. Bartczak, A. S. Argon, R. E. Cohen and M. Weinberg, *Toughness mechanism in semi-crystalline polymer blends: II. High-density polyethylene toughened with calcium carbonate filler particles*, Polymer, 1999, 40, 2347–2365

4. J. Lu, G.Wei, H. Sue and J. Chu *Toughening Mechanisms in Commercial Thermoplastic Polyolefin Blends*, Journal of Applied Polymer Science, 2000, 76, 311-319

5. A. van der Wal, R. Nijhof and R. J. Gaymans, *Polypropylene Rubber Blends 1: The effect of matrix properties on the impact behaviour*, Polymer, 1998, 39, 6781-6787

6. A. van der Wal, R. Nijhof and R. J. Gaymans, *Polypropylene–rubber blends: 2. The effect of the rubber content on the deformation and impact behaviour*, Polymer, 1999, 40, 6031-6044.

7. Gaymans, A. van der Wal and R. J., *Polypropylene–rubber blends: 3. The effect of the test speed on the fracture behaviour*, Polymer, 1999, 40, 6045-6055

8. A. van der Wal, A. J. J. Verheul and R. J. Gaymans *Polypropylene–rubber blends: 4. The effect of the rubber particle size on the fracture behaviour at low and high test speed*, Polymer, 1999, 40, 6057-6065

9. I. Aravind, P.Albert, C. Ranganathaiah, J.V. Kurian and S.Thomas, *Compatibilizing effect of EPM-g-MA in EPDM/poly(trimethylene terephthalate) incompatible blends*, Polymer, 2004, 45, 4925-4937

10. W. M. Hess, C.R.Herd, P.C. Vegvari, *Characterization Of Immiscible Elastomer Blends*, Rubber Chemical Technology, 1993, 66, 329-346

11. H. K. Lee, J. Ismail, H. W. Kammer and M. A. Bakar, *Melt Reaction in Blends of Poly(3-hydroxybutyrate) (PHB) and Epoxidized Natural Rubber (ENR-50),* Journal of Applied Polymer Science, 2005, 95, 113-129

12. R. H. Marchessault, G. Yu *Crystallization and Material Properties of Polyhydroxyalkanoates*, in *Biopolymers* Y. Doi A. Steinbüchel, Editor. 2001, Wiley-VCH: Weinheim. pp. 157-200.

13. R. W. Lenz, R. H. Marchessault, *Bacterial Polyesters: Biosynthesis, Biodegradable Plastics and Biotechnology*, Biomacromolecules, 2005, 6, 1-8

14. N. Levin *Quality and Processing Aspects of Natural Rubber*, Natuurrubber, 1996, 5,

15. D. R. Paul, J. W. Barlow, *Polymer blends (or alloys)*, Journal of Macromolecular Science, Part C - Reviews in Macromolecular Chemistry, 1980, C18,

16. Takayanagi, M., *Mem. Fac. Eng. Kyushu Univ.*, 1963, 23

17. X. Shuai, Y. He, Y. Na and Y. Inoue, *Miscibility of block copolymers of poly(-caprolactone) and poly(ethylene glycol) with poly(3-hydroxybutyrate) as well as the compatibilizing effect of these copolymers in blends of poly(-caprolactone) and poly(3-hydroxybutyrate)*, Journal of Applied Polymer Science, 2001, 80, 2600-2608

18. S. Bloembergen, D. A. Holden, G. K. Hamer, T. L. Bluhm, R. H. Marchessault. , *Studies of composition and crystallinity of bacterial poly(P-hydroxybutyrate-co-p-hydroxyvalerate)*, Macromolecules, 1986, 19, 2865-2871

19. P. J. Barham, A. Keller, E. L. Otun, P. A. Holmes, *Crystallization and morphology of a bacterial thermoplastic: poly-3-hydroxybutyrate*, Journal of Material Science, 1984, 19, 2781-2794

20. R. B. Thompson, M. W. Matsen, *Effective interaction between monolayers of block copolymer compatiblizer in a polymer blend*, Journal of Chemical Physics, 2000, 112, 6863-6872

21. B. Guo, Y. Cao, D. Jia, Q. Qiu, *Thermoplastic Elastomers Derived from Scrap Rubber Powder/LLDPE Blend with LLDPE-graft-(Epoxidized Natural Rubber) Dual Compatibilizer*, Macromolecular Materials and Engineering, 2004, 289, 360-367

22. J. Zhang, X.Sun, *Mechanical Properties of Poly(lactic acid)/Starch Composites Compatibilized by Maleic Anhydride*, Biomacromolecules, 2004, 5, 1446-1451

23. A. Sanadi, D. Caulfield, R. Jacobson, and R. Rowell, *Renewable Agricultural Fibers as Reinforcing Fillers in Plastics: Mechanical Properties of Kenaf Fiber – Polypropylene Composites*, Industrial & Engineering Chemistry Research, 1995, 34, 1889-1896

24. A. A. Galuska, R. R. Poulter and K. O. McElrath, *Force Modulation AFM of Elastomer Blends : Morphology, Fillers and Cross-linking*, Surface and Interface Analysis, 1997, 25, 418-429

25. Y.Liu, M.Kontopoulou, *Mechanical Properties And Morphology Of PP And TPO / Nanosilica Nanocomposites*, ANTEC, Charlotte, NC, 2006.

26. D.H. Kim, P. D. Fasulo, W. R. Rodgers, D. R. Paul, *Structure and Properties of TPO-based Nanocomposites*, ANTEC, Charlotte, NC, 2006.

27. J. C. Dai, J.T. Huang, *Surface modification of clays and clay–rubber composite*, Applied Clay Science, 1999, 15, 51-65

28. N.N. Herrera, J. Letoffe, J.Putaux, L.David, E. Bourgeat-Lami, *Aqueous Dispersions of Silane-Functionalized Laponite Clay Platelets. A First Step toward the Elaboration of Water-Based Polymer/Clay Nanocomposites*, Langmuir, 2004, 20, 1564-1571

29. G. Berendsen, L. De Galan, *Preparation and chromatographi properties of some chemically bonded phases for reversed-phase chromatography*, Journal of Liquid Chromatography, 1978, 1, 561-569

30. Monte, S. J., *Kenrich Petrochemicals Reference manual and product literature*, 2007

31. Monte, S. J., *Neoalkoxy Titanate And Zirconate Coupling Agent Additives In Thermoplastics*, Polymers and Polymer Composites, 2002, 10, 1

32. C.J. Vanoss, R. F.Giese, *Surface modification of clays and related materials*, Journal of Dispersion Science and Technology, 2003, 24, 363-376

33. R. E. Ayala, E. Z. Casassa, G. D. Parfitt, *A study of the applicability of the capillary rise of aqueous solutions in the measurement of contact angles in powder systems*, Powder Techology, 1987, 51, 3-14

34. J. W. Gilman, T. Kashiwagi, J.D. Lichtenhan *Nanocomposites: a revolutionary new flame retardant approach*, 42nd International SAMPE Symposium, Anaheim, CA, 1997.

35. Giannelis, E. P., *Polymer Layered Silicate Nanocomposites*, Advanced Materials, 1996, 8, 29-35

36. Giannelis, E. P., *Polymer-Layered Silicate Nanocomposites: Synthesis, Properties and Applications*, Applied Organometallic Chemistry, 1998, 12, 675-680

37. E. P. Giannelis, R. Krishnamoorti, E. Manias, *Polymer-Silicate Nanocomposites: Model Systems for Confined Polymers and Polymer Brushes*, Advances in Polymer Science, 1999, 138, 107-147

38. S. Mehta, F. M. Mirabella, K. Rufener, A. Bafna, *Thermoplastic olefin/clay nanocomposites: Morphology and mechanical properties*, Journal of Applied Polymer Science, 2004, 92, 928-936

39. J. Zhao, A. B. Morgan, J. D. Harris, *Rheological characterization of polystyrene–clay nanocomposites to compare the degree of exfoliation and dispersion*, Polymer, 2005, 46, 8641-8660

40. Halpin, J. C., *Stiffness and expansion estimates for oriented short-fiber composites*, Journal of Composite Materials, 1969, 3, 732-734

41. Hill, R., *Theory of mechanical properties of fiber-strengthened materials: I Elastic behaviour*, Journal of the Mechanics and Physics of Solids, 1964, 12, 199-212

42. Es, M. Van, *Polymer-clay nanocomposites*, 2002, Ph.D. Thesis, Technical University of Delft, Delft

43. J. Mergaert, A. Webb, C. Anderson, A. Wouters, and J. Swings, *Microbial degradation of poly(3-hydroxybutyrate) and poly(3-hydroxybutyrate-co-3-hydroxyvalerate) in soils*, Applied Environmental Microbiology, 1993, 59, 3233-3238

44. Steinbüchel, K. Rose and A., *Biodegradation of Natural Rubber and Related Compounds: Recent Insights into a Hardly Understood Catabolic Capability of Microorganisms*, Applied and Environmental Microbiology, 2005, 71, 2803-2812

45. S.S. Ray, K. Yamada, M. Okamoto,K. Ueda, *Control of Biodegradability of Polylactide via Nanocomposite Technology*, Macromolecular Materials and Engineering, 2003, 288, 203-208

46. Liddell, J. M., *Biopol polyester: ICI's truly biodegradable polymer*, Special Publication - Royal Society of Chemistry (Chem. Ind.-Friend Environ.), 1992, 103, 10-25

47. I. Noda, R. H. Marchessault, M. Terada, *Poly(hydroxybutyrate)*, in *Polymer Data Handbook*. 1999, Oxford University Press: New York. pp. 586-597.

48. Avérous, L., *Biodegradable Multiphase Systems Based on Plasticized Starch: A Review*, Journal of Macromolecular Science—Part C, Polymer Reviews, 2004, C44, 231-274

49. L. Avérous , L. Moro, P. Dole , C. Fringant *Properties of thermoplastics blends: starch-polycaprolactone*, Polymer, 2000, 41, 4157-4167

50. L. Avérous, C. Fringant, *Association between plasticized starch and polyesters: processing and performances of injected biodegradable systems*, Polymer Engineering and Science, 2001, 41, 727-734

51. Narayan, R., *Starch Based Plastics*, in *Polymers from Biobased Materials*, H. L. Chum, Editor. 1991, Noyes Data Corporation: New Jersey. pp. 90-114.

52. C. Bastioli, R. Lombi, G. Del Tredici, I. Guanella, *Method for the preparation of destructured-starch-based compositions and compositions produced therby,* 1995, US Patent no. 5,462,982,

53. I. Koller, A. J. Owen, *Starch-Filled PHB and PHB/HV copolymer*, Polymer International, 1996, 39, 175-181

54. J.A. Ratto, P.J. Stenhouse, M. Auerbach, J. Mitchell, R. Farrell, *Processing, performance and biodegradability of a thermoplastic aliphatic polyester/starch system*, Polymer, 1999, 40, 6777-6788

55. Starch, National, *HYLON VII Technical Service Bulletin*, 2006

56. Russel, P.L., *Gelatinisation of starches of different amylose/ amylopectin content. A study by differential scanning calorimetry*, Journal of Cereal Science, 1987, 6, 133-145

57. R.L.Shogren, C.L. Swansom, A.R. Thompson, *Extrudates of cornstarch with urea and glycols: structure/mechanicals property relations,* , Starch, 1992, 44, 335-338

58. D.Coltrain, *Biodiesel: Is It Worth Considering?, Risk and Profit Conference*, 2002. Manhattan, Kansas, http://www.agmrc.org/NR/rdonlyres/513C6A14-28DE-4B54-A57E-EA7FE052E399/0/bdconsider.pdf, Accessed on April 17, 2007

59. Tyson, K. S., *Biodiesel R&D Potential, Montana Biodiesel Workshop*, 2003. Montana, http://leg.mt.gov/content/lepo/2003_2004/subcommittees/energy_group/staffmemos/bio_potential.pdf, Accessed on April 23 2007

60. Maneely, T., *Glycerin Production and Utilization, Biodiesel One-Day Course: From Field to Fuel*, 2006. Coeur d' Alene, Idaho, http://www.uidaho.edu/bioenergy/Feild2fuel_cda06/Tim_Glycerin%20biodiesel%20course%20061506_2.pdf, Accessed on April 23, 2007

61. Averous, E. Schwach and L., *Starch-based biodegradable blends: morphology and interface properties*, Polymer International, 2004, 53, 2115–2124

62. Selke, S.E., ed. *Biodegradation and Packaging*. 2nd ed. PIRA International Reviews of Packaging. 1996, Pira.

63. B. A. Ramsay, V. Langlade, P.J. Carreau, J. A. Ramsay, *Biodegradability and mechanical properties of poly(hydroxybutyrate-co-hydroxyvalerate)-starch blends*, Applied Environmental Microbiology, 1993, 59, 1242-1246

64. S. H. Imam, L. Chen, S. H. Gordon,R. L. Shogren, D. Weisleder nd R. V. Greene, *Biodegradation of Injection Molded Starch-Poly (3-hydroxybutyrate-c0-3-hydroxyvalerate) Blends in a Natural Compost Environment*, Journal of Environmental Polymer Degradation, 1998, 6, 91-98

65. L. H. Innocentini-Mei, J. R. Bartoli, R.C. Baltieri, *Mechanical and thermal properties of poly(3-hydroxybutyrate) blends with starch and starch derivatives*, Macromolecular Symposia, 2003, 197, 77-87

66. M. Huneault, H. Li, *Interfacial Modification of PLA/Thermoplastic Starch Blends*, International Degradable Plastics Symposium: Status Of Biobased And Synthetic Polymer Technology, Chicago, 2006.

67. L.H.Sperling, *Polymeric Multicomponent Materials: An Introduction*. 1997, New York: Wiley Interscience.

68. J. W. Barlow, D.R. Paul, *Polymer Alloys*, Annual Reviews Material Science, 1981, 11, 299-319

69. P.A.Small, *Some Factors Affecting the Solubility of Polymers*, Journal of Applied Chemistry, 1953, 3,

70. Sperling, L.H., *Polymeric Multicomponent Materials: An Introduction*. 1997, New York: Wiley Interscience.

71. E. L. Cussler, M. Mulski, W.R. Falla, *Estimating diffusion through flake-filled membranes*, Journal of Membrane Science, 1996, 119, 129-138

72. Rogers, C.E., *Permeation of Gases and Vapours in Polymers*, in *Polymer Permeability*, J. Comyn, Editor. 1985, Elsevier Applied Science: New York. pp. 11-74.

73. N. Grassie, E. J. Murray, P. A. Holmes, *The thermal degradation of poly(ß-hydroxybutyric acid): Part 2—Changes in molecular weight*, Polymer Degradation and Stability, 1984, 6, 95-103

74. M.E. Mackay, T. T. Dao, A. Tuteja, D. L. Ho, B. van Horn, H.-C. Kim, C. J. Hawker, *Nanoscale effects leading to non-Einstein-like decrease in viscosity*, Nature Materials, 2003, 2, 762-766

75. Tock, R.W., *Permeabilities and Water Vapor Transmission Rates for Commercial Polymer Films*, Advances in Polymer Technology, 1983, 3, 223-231

76. Keating, J. Z., *The role of talc and mica in natural fiber composites*, The Global Outlook for Natural Fiber and Advanced Wood Composites 2001.

77. Minerals, Mondo, *Technical Bulletin 1301: Talc in Plastics*, 2007, http://www.mondominerals.com/pdf/plastics.pdf Accessed on: March 2, 2007

78. F. Biddlestone, A. Harris, J. N. Hay, T. Hammond, *The Physical Ageing of Amorphous Poly(hydroxybutyrate)*, Polymer International, 1996, 39, 221-229

79. M. Scandola, M.L. Focarete, G. Adamus, W. Sikorska, I. Baranowska, S. Swierczek,M. Gnatowski, M. Kowalczuk, Z. Jedliski, *Polymer Blends of Natural Poly(3-hydroxybutyrate-co-3-hydroxyvalerate) and a Synthetic Atactic Poly(3-hydroxybutyrate). Characterization and Biodegradation Studies*, Macromolecules, 1997, 30, 2568 - 2574

80. Biomer, *Remarks on biodegradation*, 2007, http://biomer.de/BioabbauE.html, Accessed on: February 4, 2007

81. O. Wolf, M. Crank, M. Patel, F. Marscheider-Weidemann , J. Schleich, B. Hüsing, G. Angerer *Techno-economic Feasibility of Large-scale Production of Bio-based Polymers in Europe*, 2005, European Commission Joint Research Centre, http://www.biomatnet.org/publications/1944rep.pdf, Accessed on: March 12, 2007

82. Leaversuch, R., *Biodegradable Polyesters: Packaging Goes Green*, 2002, Plastics Technology, 66-79, September, http://www.ptonline.com/articles/200209fa3.html, Accessed on March 12, 2007

83. K. Petersen, P. V. Nielsen, G. Bertelsen, M. Lawther, M. B. Olsen, N. H. Nilsson, G. Mortensen, *Potential of biobased materials for food packaging*, Trends in Food Science & Technology, 1999, 10, 52-68

84. Chen, X., *Industrialization of PHBV in China,*, BEPS International Degradable Plastics Symposium: Status Of Biobased And Synthetic Polymer Technology., Chicago, IL, 2006.

85. Chen, Xuejun, Tianan Biologic Material Co., *E-mail Correspondence*, Y. Parulekar, 2007

86. Esposito, F., *Soaring resin prices help out bio-plastics*, 2005, Plastics News, 17, 38, http://www.plasticsnews.com/subscriber/printer.html?id=05112100901, Accessed on March 12, 2007

87. Esposito, F., *More bio-resins becoming commercially available*, 2005, Plastics News, November 16, http://www.plasticsnews.com/subscriber/arcshow.html?id=05112100902, Accessed on March 12, 2007

88. Raiti, K., National Starch, *E-mail correspondence*, Y. Parulekar, 2005

89. Starch, National, *Price Increases*, 2006, www.nationalstarch.com/NationalStarch/Price+Increases/, Accessed on: April 7, 2007

90. T. Werpy, G. Petersen, *Top Value Added Chemicals from Biomass Volume I—Results of Screening for Potential Candidates from Sugars and Synthesis Gas*, 2004, U.S. Department of Energy,

http://www1.eere.energy.gov/biomass/pdfs/35523.pdf, Accessed on: April 2, 2007

91. Edwards, K., BASF Corporation, *E-mail correspondence*, A.K. Mohanty, 2006

92. Board, Malaysian Rubber, *Daily rubber Prices*, 2007, http://www2.lgm.gov.my/mre/daily.aspx, Accessed on: 7 April, 2007

93. Simper, S., Southern Clay, *E-mail correspondence*, Y. Parulekar, 2005

94. *Plastics News Resin pricing Chart*, 2007, Plastics News, March 26, http://www.plasticsnews.com/subscriber/rprices.phtml, Accessed on March 12, 2007

7. CONCLUSION

7.1 Summary and Conclusions:

7.1.1 Elastomeric Toughening

Bacterial polyhydroxybutyrate (PHB) was successfully toughened by reactive extrusion with epoxidized natural rubber and using maleated rubber as the compatibilizer. The maleated rubber having high amount of maleic anhydride (MA) grafting and low molecular weight was found to be an effective compatibilizer where as the maleated rubber having low MA grafting and high molecular weight did not show any effect in improving the impact of the virgin PHB-rubber blend. Rheological, morphological and mechanical characterization substantiated these results. The experimental results matched Takayanagi model predictions of the blend moduli substantially. The toughened and compatiblized blends were found to have 440% better impact resistance and only 50% loss in modulus when compared to virgin PHB. These biobased and biodegradable materials thus show capability to replace toughened petroleum-derived polymers such as specific polyolefins (TPO) and High Impact Polystyrene.

7.1.2 Surface Modification of Clay

The design and synthesis of optimum nanocomposites rely on the ability of layered clays to intercalate and exfoliate in the polymer matrix. For this reason the

hydrophilic clay surface needs to be made organophilic and compatible with the organic polymer matrix. Successful surface modification of pristine montmorillonite clay was achieved using a titanate couping agent. Emphasis was placed on a characterizing and validating the surface modification by XPS, contact angle measurements and FTIR. By fine-tuning the surface characteristics (controlling the hydrophilicity) effective nanodispersion in polymers by intercalation or delamination can be accomplished. The titanate-coupling agent increased the water contact angle of the clay from 6 to 44° denoting significant decrease in hydrophilicity. Similarly XRD studies revealed the increased inter-gallery spacing from 9.8 to 12.7 Å. These results suggest compatibility with organic polymers can be accomplished by derivatizing the clays with alkyl-titanate complexes.

7.1.3 Nanocomposites

Toughening of polyhydroxybutyrate, PHB by functionalized elastomer and compatibilizer resulted in enhanced impact properties. The toughening by addition of the elastomeric components reduced the modulus as expected and this was regained to the permissible extent by the addition of organically modified nanoclay. Elemental analysis and contact angle measurements validated the successful surface modification of pristine montmorillonite clay using a titanate-coupling agent. Comparison with commercially available organically-modified clays having more that 30 wt. % of organic modifier on the clay showed significantly better impact properties while still improving modulus. This was achieved using organically-modified clays with only 11.4 wt. % modifier and shows economic as well as performance benefits. PHB-ENR compatiblized

nanocomposites with 5 wt % modified clay loading showed ~400% improvement in impact properties and only 40% reduction in modulus in comparison with pure PHB. The diffraction patterns and transmission electron microscopy images suggest exfoliation of the organically modified clays and this was further validated by melt rheological analysis. The mechanical properties of the nanocomposites were also correlated with modified Halpin-Tsai theoretical models and the predictions matched significantly with the experimental results.

7.1.4 Thermoplastic Starch -Polyhydroxyalkanoate Blends and Composites

Novel flexible materials were successfully developed from Polyhydroxyalkanoates by blending with thermoplastic starch utilizing extensive process engineering and composition optimization. Starch was plasticized with high glycerol content followed by blending with PHBV and PBAT. The starch phase was seen to be miscible with PHBV and PBAT phases independently thus performing the role of a compatibilizer in the PHBV-TPS system. The resulting material had 70% biobased content and yet showed excellent mechanical properties ideal for flexible packaging. Unmodified talc was incorporated at 2.5 wt.% and 5 wt.% into the PHBV-TPS blends using melt compounding and the resultant composites were extruded into cast films. The talc promoted disruptive mixing, homogeneity and ultimately reduced the droplet size of the minor component ultimately giving improvement in mechanical properties. The talc-filled films showed remarkable improvement in barrier properties and this was ascertained to be because of a combination of the tortuosity effect of the talc, the nucleating effect of the filler and the improved mixing. Ageing, an inherent problem

with starch-based materials as well as PHA-based materials, was effectively reduced in the composite films. This was ascertained by studying the mechanical properties, leaching and crystallization of the materials as a function of time under ambient conditions. The PHBV and PBAT as well as the platelet-shaped talc particles were able to control the moisture uptake of the starch component as well as hinder the glycerol from leaching out of the material. The secondary crystallization of the PHBV component was inhibited by the disruptive and intensive mixing and the compatibilizing effect of the starch phase. The developed PHBV-TPS composite films show promising potential as biodegradable flexible packaging materials owing to the excellent mechanical and barrier properties combined with the reduction in cost by using low-cost filler and low-cost starch.

7.2 Problems, Solutions and Proposals for the Future

While the above conclusions hold and have emphatically validated the concepts proposed in the initial part of this work, it is important also to recognize the areas that need to be addressed in future work. The theoretical modeling of the rubber-toughened nanocomposites was undertaken using *Halpin-Tsai* equations than gave an excellent correlation however this area can be expanded further. The individual effects of the components need to be studied using characterization techniques that may have been possibly ignored in this work. Theoretical models that can match experimental data, especially in nanocomposites, rely on a number of parameters that are intrinsic to the matrix. These parameters have been investigated and reported for conventional polymers

but are unavailable fro most biopolymers. Thus a better relation between predicted and actual data can be achieved by investigating and possibly proposing such intrinsic parameters.

The rubber-toughening mechanism relied on using a granular rubber and a liquid compatibilizer. It may be possible to further improve upon these results by using rubber latex and then vulcanizing the final blend. Since cross-linking of the rubber generally gives improvement in toughened systems, further work should address this issue by looking at different vulcanizing systems and conditions.

The PHA-TPS system, specifically the extruded films, showed excellent promise as a possible flexible packaging material. These films were made by cast film extrusion and it may be possible to further improve the properties by processing using blown film extrusion. This technique may impart further homogeneity as well as give improvements that are expected from the blown film process. Prior to this, the system's rheological characterization is necessary, especially extensional rheometry. Another area that may be investigated is increasing the filler loading combined with using other possible fillers such as specifically modified organoclay. Finally, it may be needed to characterize the PHA-TPS blends and composites using specific packaging-related tests such as heat-sealabilty, printability etc. in order to further develop this material as a potential flexible packaging material.

8. APPENDICES

8.1 Appendix A. Calibration curves for Capillary Wicking

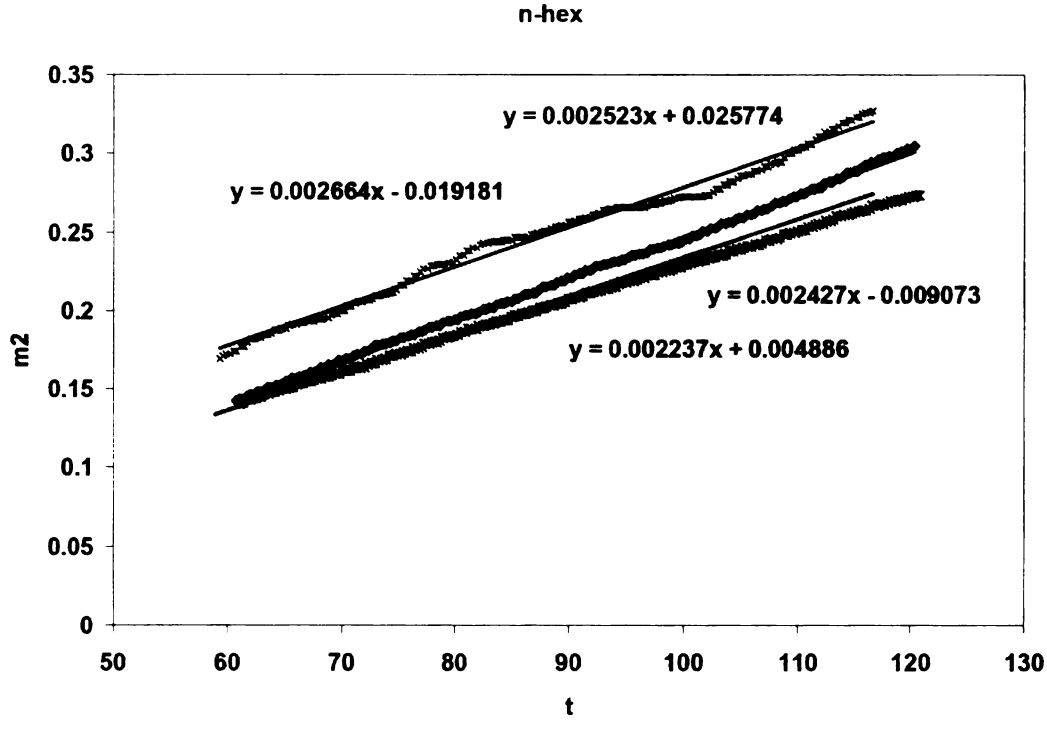

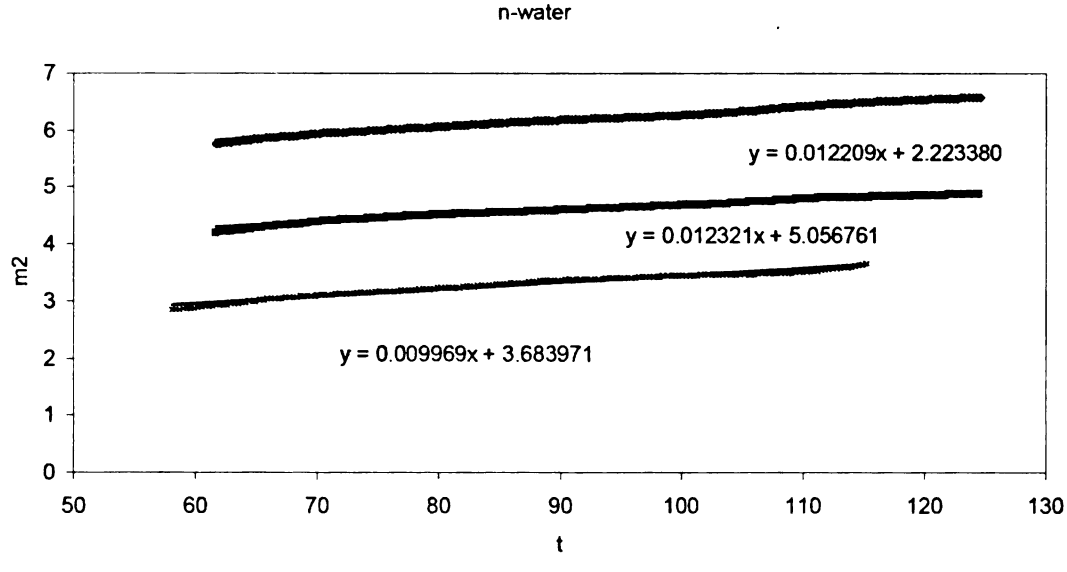

a-water

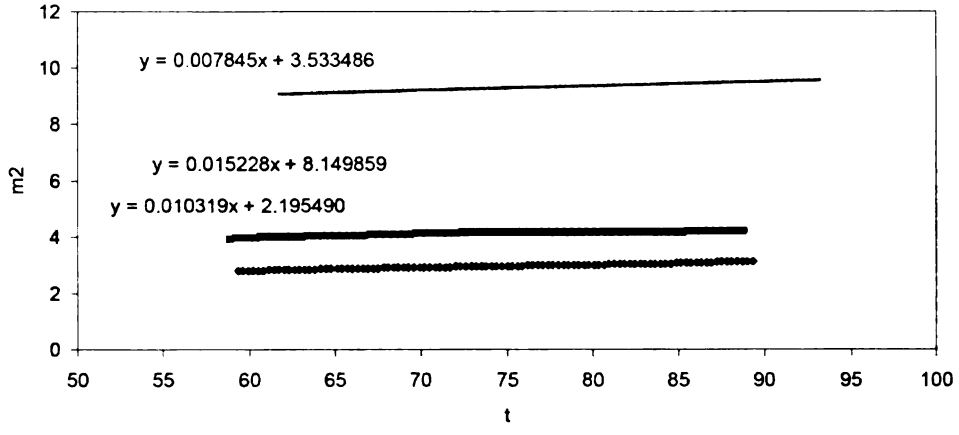
y = 0.007845x + 3.533486
y = 0.015228x + 8.149859
y = 0.010319x + 2.195490
m2
t
0
2
4
6
8
10
12
50
55
60
65
70
75
80
85
90
95
100

a-hex

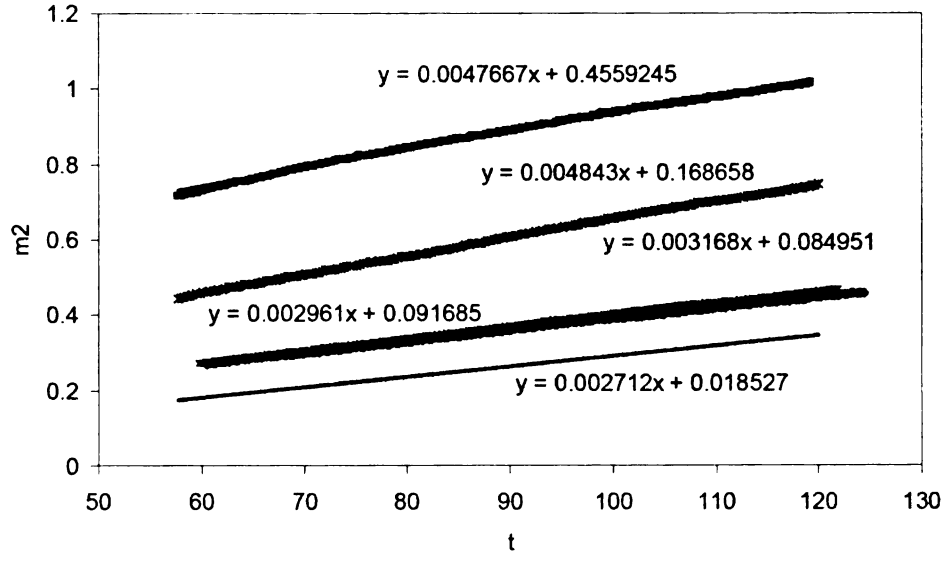
y = 0.0047667x + 0.4559245
y = 0.004843x + 0.168658
y = 0.003168x + 0.084951
y = 0.002961x + 0.091685
y = 0.002712x + 0.018527
m2
t
0
0.2
0.4
0.6
0.8
1
1.2
50
60
70
80
90
100
110
120
130

c-hex

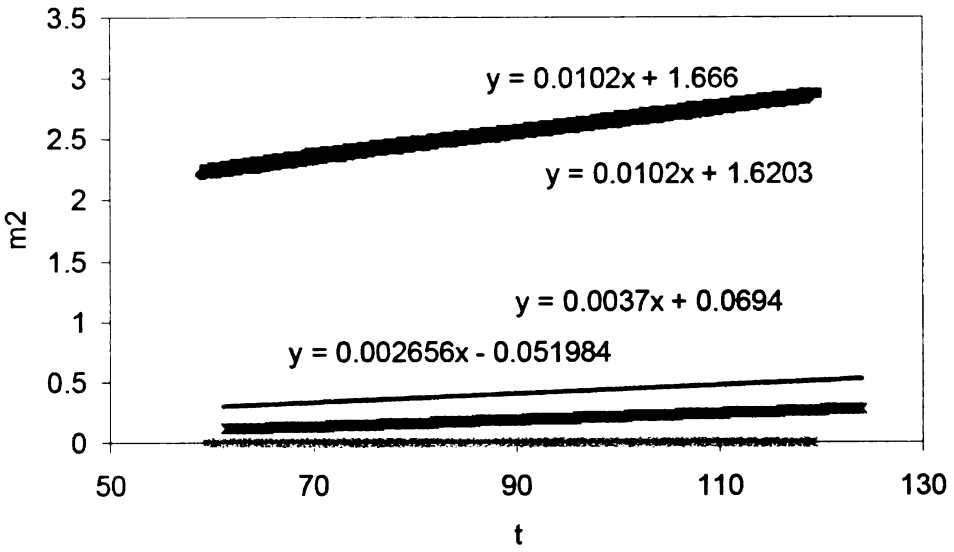
3.5
3
2.5
2
1.5
1
0.5
0
m2
y = 0.0102x + 1.666
y = 0.0102x + 1.6203
y = 0.0037x + 0.0694
y = 0.002656x - 0.051984
50
70
90
110
130
t

c-water

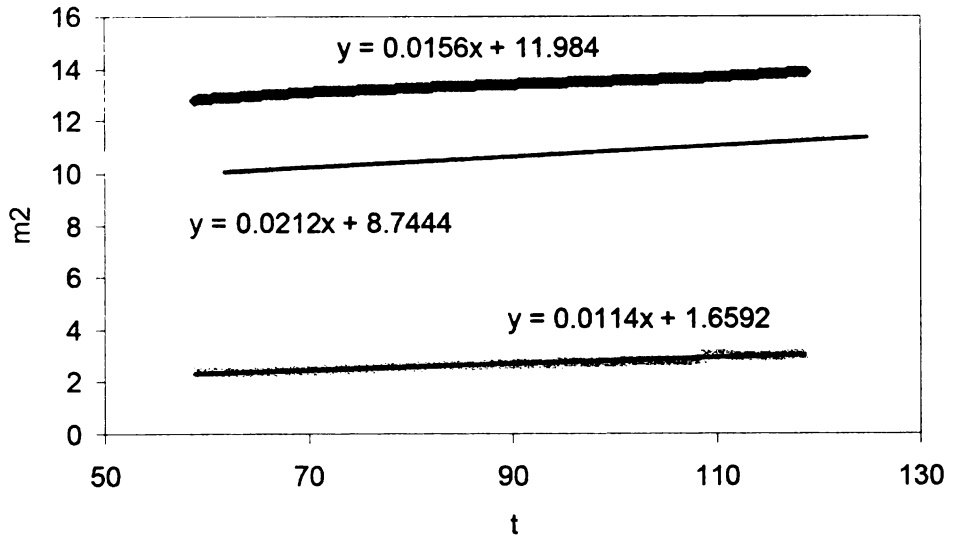
16
14
12
10
8
6
4
2
0
m2
y = 0.0156x + 11.984
y = 0.0212x + 8.7444
y = 0.0114x + 1.6592
50
70
90
110
130
t

From hexane, get m^2/t from slopes of lines;

Calculate material constant $C=[m^2/t] * [\eta/\rho^2 \cos\theta]$

$C_n=0.000101091$ $C_a=0.000161511$ $C_c=0.000274571$

From C values and water data,

$\text{Cos } \theta=[m^2/t] * [\eta/\rho^2 * C]$

8.2 Appendix B. Carbon Dioxide Emission in Respirometer

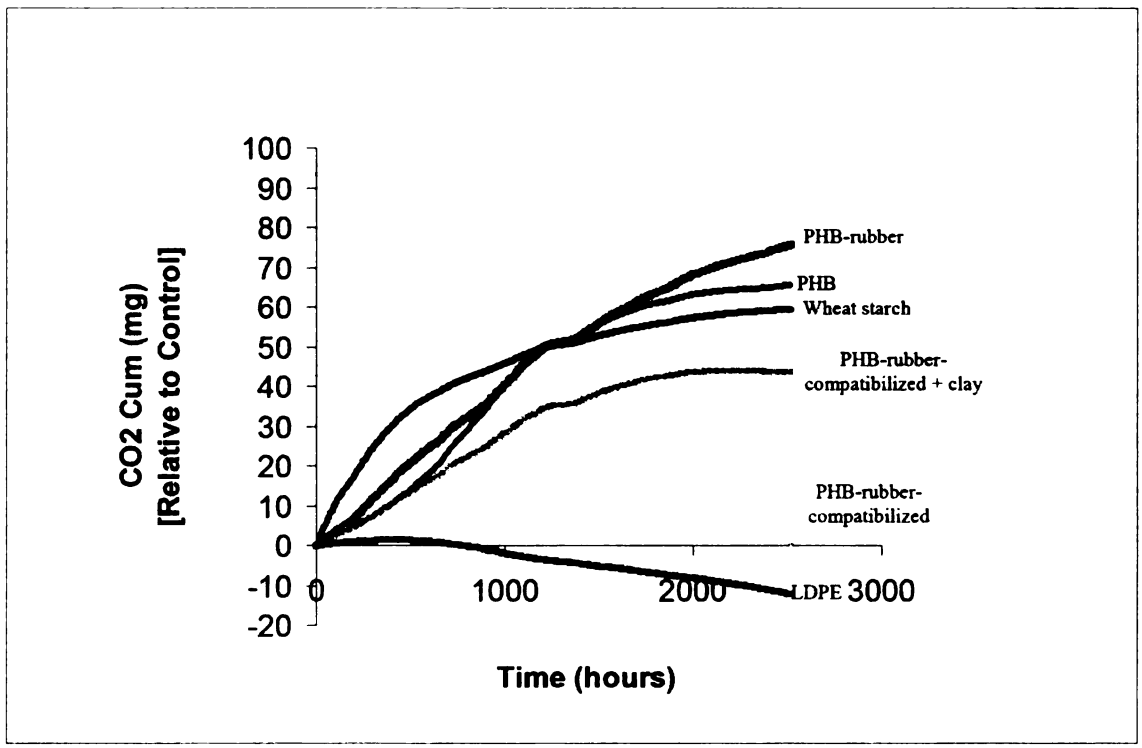

Material	C	H	N
PHB	55.65	6.18	0.35
PHB-40ENR	62.39	8.52	0.265
PHB-30ENR-10MR	60.43	8.1	0.24
PHB-30ENR-10MR-5TiClay	60.36	8.12	0.25

Appendix C. Aerobic biodegradation

C %	blend	composite	blank	positive	PHBV
1	55.08	52.74	29.13	40.17	
2	54.5	53.93	31.64	40.22	
avg	**54.79**	**53.335**	**30.385**	**40.195**	**60**
g of C	8.2185	8.00025	4.55775	6.02925	9
g of CO2	30.1345	29.33425	16.71175	22.10725	33